MICROFLUIDIC ENCAPSULATION OF CELLS FOR TRANSPLANTATION IN NEURODEGENERATIVE DISEASE

Victoria Workman

Thesis submitted for the degree of Doctor of Philosophy

September 2009

Engineering and Physical Sciences
Research Council

ProQuest LLC
789 East Eisenhower Parkway
P.O. Box 1346
Ann Arbor, MI 48106-1346

DECLARATION

This work has not previously been accepted in substance for any degree and is not concurrently submitted in candidature for any degree.

Signed ..... (candidate) Date 01.09.09

STATEMENT 1

This thesis is being submitted in partial fulfillment of the requirements for the degree of PhD.

Signed ..... (candidate) Date 01.09.09

STATEMENT 2

This thesis is the result of my own independent work/investigation, except where otherwise stated.
Other sources are acknowledged by explicit references.

Signed ..... (candidate) Date 01.09.09

STATEMENT 3

I hereby give consent for my thesis, if accepted, to be available for photocopying and for inter-library loan, and for the title and summary to be made available to outside organisations.

Signed ..... (candidate) Date 01.09.09

Acknowledgments

This study was financially supported by the Engineering and Physical Sciences Research Council and Q Chip. I would firstly like to thank my supervisors Dr. Peter Kille, Dr. Daniel Palmer and Prof. Stephen Dunnett for their continued guidance and encouragement throughout.

Many thanks Dan, for all your help and unwavering patience, and for driving me to be better than I ever thought possible.

Pete, I will always be grateful for the opportunities you have given me. Many thanks for allowing me to be part of your lab for so long!

Huge thanks go to Jo Daniels, if you hadn't driven me round Cardiff that day, I would never have got the chance to do this PhD.

I have met, and been lucky enough to work with, so many amazing scientists along the way, thanks go to them. Ed, I am indebted for all your help with the animal studies. To the Brain Repair Group, for all your support and encouragement: Ali, Anne-Marie, Becky, Claire, Emma, Gaynor, Ngoc-Nga, Sophie, Ulrike, Zubeyde. To members of the (extended) PK group, past and present, for being there for tea, moaning and cocktails: Chrissy, Jenny, Jodie, Tracey, Vega and Vikki.

A massive thanks to Jane for everything, words are not enough.

To Lata, for always being there with red wine and Black Books. Thank you so much for all your help, support and friendship. I couldn't have done this without you.

The Q Chip hardcore; Jo, Mark, Rich, Rob, thanks for all the drunken nights and all the help. A special thanks to Owen for making the chip diagrams in the Appendix look fab.

And finally, to Ezra, without whom none of this would have been possible.

This thesis is dedicated to Eric Workman, who unfortunately never saw my achievements.

Abstract

Polymer encapsulation is now an accepted route into cellular therapies *via* implantation of therapeutically active allogeneic and xenogeneic cells. Although many methods are currently used for encapsulation of cells, no single method is capable of producing large volumes of mono-disperse beads, containing cells completely covered by the polymer of choice. The overall aim of this project was to develop a microfluidic method to encapsulate dopamine releasing cells in an alginate matrix, determine their viability *in vitro* and investigate implantation into a rodent model of Parkinson's disease.

During the course of this study a novel microfluidic method was developed. Two cell types were encapsulated; a human test line and a therapeutic cell line derived from rat brain tumour cells (PC12). Cell viability, measured using an adapted trypan blue exclusion method, was observed to be minimally affected by the encapsulation process. Confocal images of cells encapsulated within alginate beads were collected in addition to long term viability data, up to 90 days post-encapsulation. Dopamine was still detected after PC12 cell encapsulation through use of an ELISA.

Modifications to the developed microfluidic method allowed beads of an appropriate size (<250μm in diameter) to be implantated into a rodent brain *via* a cannula. Upon implantation of alginate beads into rats' brains there was no evidence of beads after 7 days. Attempts were made to stabilise alginate beads further by addition of barium as a cross-linking agent and polycation secondary coating. Beads were observed to be more stable and remained visible within brain tissue for 14 days. Imaging of fluorescent alginate beads revealed that beads produced using the developed microfluidic method were homogeneous in nature.

The work presented here represents the first microfluidic method to be developed which is capable of encapsulating viable cells. Moreover, the viability measurements carried out were the first such experiments to be performed on cells encapsulated using microfluidic methods. Although the structure of alginate beads produced using more commonplace methods has been shown, this has not previously been reported for beads produced using a microfluidic technique.

Table of Contents

List of Abbreviations

APA	Alginate-PLL-alginate triple layer capsules
BBB	Blood-brain barrier
BDNF	Brain-derived neurotrophic factor
C2C12	Mouse myoblasts
CNTF	Ciliary neurotrophic factor
CNS	Central nervous system
CSF	Cerebrospinal fluid
CV	Coefficient of variation
DA	Dopamine
D-MEM/F12	Dulbecco's modified Eagle medium: Nutrient Mixture F12
EDTA	ethylenediaminetetraacetic acid
FBS	Foetal bovine serum
FITC	Fluorescein isothiocyanate
G	α-$_L$-guluronic acid
GDNF	Glial cell-derived neurotrophic factor
GDL	$_D$-Glucone-δ-lactone
GFP	Green fluorescent protein
HEK	Human embryonic kidney cells
HBSS	Hank's Buffered Saline Solution
Ig	Immunoglobulin
PBS	Phosphate buffered saline
PC12	Pheochromocytoma cells
PD	Parkinson's disease
PDMS	polydimethylsiloxane
PFA	processible fluoropolymer film
PLL	Poly-l-lysine
PLO	Poly-l-ornithine
poly(HEMA-MMA)	poly(hydroxyethyl methacrylate-co-methyl methacrylate)
PTFE	polytetrafluoroethylene
Re	Reynolds number
TBS	TRIS-buffered saline
TH	Tyrosine hydroxylase
LDH	lactate dehydrogenase
M	β-$_D$-mannuronic acid
MEL	Mouse erythroleukemia cells
MHC	Major histocompatibility complex
MIG	Microfluidic internal gelation
MTT	3-(4,5-Dimethylthiazol-2-yl)-2,5-diphenol tetrazolium bromide
MVG	Medium viscosity, high guluronate alginate
MVM	Medium viscosity, high mannuronate alginate
MWCO	Molecular weight cutoff
NA	Norepinephrine

Chapter 1. Introduction

1.1 ENCAPSULATION OF CELLS

Classical Mendelian disorders are curable by administration of a missing gene product, for example factor VIII or IX in patients with haemophilia (Liu *et al.*, 1993), or erythropoietin in sufferers of anaemia (Murua *et al.*, 2007). An ideal way to achieve this would be to introduce cells which express the missing gene product and integrate with the patient. Another class of disorders which could be cured by replacement of secretory cells are autoimmune diseases, such as Type I diabetes. In these cases, the immune system destroys a patients own cells, leading to loss of vital biochemical functions. Autoimmune disorders could be cured by replacement of destroyed cells. However, as with whole organ transplantation, immune reaction to cell transplantation is inevitable. A typical solution to immune rejection is treatment with immunosuppressive drugs. However, even with immunosuppression, many transplants are unsuccessful. For example, of the 267 patients receiving transplanted pancreatic islet cells between 1990 and 1999, only 12.4% (33 patients) experienced insulin independence for periods of more than one week, and only 8.2% (22 patients) for more than one year (Brendel *et al.*, 1999).

Transplantation of human or animals cells into a human patient requires immunosuppression to prevent rejection of the transplant. Rejection occurs when the body recognizes the cells as non-self and attempts to destroy them (Section 1.4). Immunosuppression has intolerable side-effect profiles and limited efficacy (Rang *et al.*, 2007). Skin cancer is a serious problem in immunosuppressed patients, this may be due to a general decrease in cancer surveillance due to immunosuppression, although specific drugs have been shown to sensitise DNA to ultraviolet A radiation (O'Donovan *et al.*, 2005). Some immunosuppressants, for example prednisone (Zeng *et al.*, 1993), induce diabetes, damage beta cells or induce peripheral insulin resistance. In these cases, the side effects exacerbate, or are worse than, the condition being treated.

Cell encapsulation was proposed as a means to immunoisolate transplanted cells (Chang, 1964). Through use of a semi-permeable membrane, the immune system is prevented from detecting or responding to foreign cells present within the device. The membrane is permeable to oxygen, nutrients and the therapeutic molecule(s).

Chang proposed using haemoglobin cross-linked with a diacid to form the cell-enclosing membrane. Whilst Chang has successfully developed red-blood-cell substitutes using cross-linked haemoglobin, cells were not effectively encapsulated until 1980. Lim and Sun pioneered the use of alginate and poly-l-lysine (PLL) in so called APA (alginate-PLL-alginate triple layer – Section 1.8.1) capsules to encapsulate cells (Lim and Sun, 1980). This is still the most widely used technique in research into cell encapsulation.

Three different sources of cells are available for cellular therapy; patients own cells (autologous), cells from another human (allogeneic) or cells from another species (xenogeneic). Autologous and allogeneic cells have limited availability and xenogeneic cells, although widely available, may transmit viruses to human hosts (Blusch *et al.*, 2002). Cell types from all three sources can be genetically modified to produce virtually any desired factor *in vivo*. A patient's cells can be removed, genetically engineered to produce the required factor and then re-implanted. Encapsulation is not necessary in this scenario as a patient will not attack their own (autologous) cells. However, as each treatment is patient-specific, costs would be high and scale up to treat multiple patients would be impossible (Gansbacher, 2002). A better solution might be to produce large batches of engineered human cells for use in any patient with the disease. Although banking of many different histocompatibility types has been postulated (Taylor *et al.*, 2005), a better approach may be cell encapsulation to overcome immune-mediated rejection of the allogenic graft.

1.2 PREVIOUS USE OF ENCAPSULATED CELLS FOR TREATMENT OF DIABETES

The most widely studied disease within the field of cell encapsulation is Type I diabetes. The World Health Organization (WHO) estimates that more than 170 million people worldwide suffer from diabetes, and this number is predicted to more than double by 2030 (Wild *et al.*, 2004). The National Diabetes Information Clearinghouse estimates that diabetes costs the United States $132 billion every year. The prospect of replacement of insulin-producing pancreatic islet beta cells has been described as "the ultimate treatment for Type I diabetes" (Shi and Cheng, 2004). The use of a bioartificial pancreas (providing immediate regulation of glucose levels *via* natural feedback mechanisms) is a seemingly simple way to cure Type I diabetes.

In spite of the proposed potential and massive research effort surrounding this area, researchers are apparently only slightly closer to the "ultimate cure" than in 1980 when Lim and Sun reversed diabetes in rats. Allotransplantation, in conjunction with encapsulation, is now routinely shown to be successful in treating diabetic rodents and canines (Soon-Shiong *et al.*, 1992; Calafiore *et al.*, 2004). Encapsulated allografts have been shown, in a Phase I clinical trial, to be successful in humans (Calafiore *et al.*, 2006). Encapsulated human pancreatic islets were transplanted into two patients, without immunosuppression, and decreased the need for exogenous insulin, although it was not completely withdrawn.

Encapsulated xenografts have been used to reverse diabetes in rodents (Duvivier-Kali *et al.*, 2004) and non-human primates (Sun *et al.*, 1996). There has been limited success with human patients. As part of a Phase I/II clinical trial in 1996, on an undisclosed number of patients, a diabetic patient received microencapsulated porcine islets. When followed-up in 2005, the xenotransplantation appeared to have had no deleterious effects on general health and dependence on insulin was reduced (Elliott *et al.*, 2007). Another clinical trial, consisting of 12 patients, reported 6 patients required a significantly reduced amount of insulin and two patients who were insulin-independent for several months (Valdes-Gonzalez *et al.*, 2005). Encapsulated islet cells, of human or porcine origin, have limited success when implanted, as shown by the low patient numbers "treated".

Although diabetes is most commonly investigated to model encapsulated cell systems, it will not be used within this study. Treatment of diabetes requires pancreatic islet cells, and although initial work has been carried out to immortalise pancreatic islet cells (Sinden *et al.*, 2007), these were not available for this study and so use of primary cells would have been necessary. As pancreatic islet cells and an animal model for diabetes were not available for use in this study an alternative model for investigation was required.

1.3 NEURODEGENERATIVE DISEASES AND PARKINSON'S DISEASE

Neurodegenerative diseases are caused by the degeneration of neurons within the brain. Cells within the brain are not readily regenerated (Cajal, 1928) and so these diseases worsen over time and commonly affect older people (Mayeux, 2003). Some of the more common neurodegenerative diseases include Alzheimer's disease,

Parkinson's disease, Huntington's disease, amyotrophic lateral sclerosis, spinal cord injury, cerebrovascular disease (associated with stroke) and epilepsy. In 2004, more than 15 million people in Europe were estimated to be affected by neurodegenerative disease, costing more than €60 billion (Andlin-Sobocki *et al.*, 2005).

Therapeutic strategies to treat neurodegenerative diseases are problematic as, although it is often known which molecules are required, neuroactive compounds are difficult to provide systemically. The difficulties arise as neuroactive molecules either have a short half life or the liver degrades them before they reach the brain. In addition, the blood-brain barrier (BBB), due to its low passive permeability (Rubin and Staddon, 1999), does not allow molecules to pass into the brain from the blood stream. Various delivery methods have been investigated (for example osmotic pumps (Olson *et al.*, 1991), sustained release polymer systems (McRae *et al.*, 1990) and direct gene therapy (Barsoum *et al.*, 2003)), but all have drawbacks limiting their use in patients.

Cellular therapy, as a treatment for neurodegeneration, allows cells to be used to deliver the therapeutic factor into the target area of the brain. Cellular therapy relies on *de novo* synthesis and release of missing molecule(s) by the introduced cells. This can be addressed in two ways; cell replacement by transplantation or polymer-encapsulated cell implantation. Functional reinnervation *via* cell-to-cell contact can be established through use of cell transplantation, whereas this is not possible with encapsulated cells. Although the primary purpose of cell encapsulation is immunoisolation of implanted cells from the host immune system, a secondary benefit might be to protect the host from any potential tumour formation by the implanted cells. Several beneficial cell lines for neurodegeneration are known to form tumours upon implantation (for example; PC12 cells (Jaeger, 1985)).

Through use of different cell types, various therapeutic molecules can be delivered to the brain for treatment of neurodegenerative diseases (Table 1.1). Parkinson's disease (PD) was chosen as a model to investigate cellular therapy through use of polymer encapsulated cells in this study. Simple animal models of Parkinsonism are available and well validated allowing *in vivo* testing to be carried out. The use of PD as a model was also advantageous as immortalised cell lines producing various neurotrophic factors are available. The various neurotrophic factors expressed are of different molecular weights and so allowed more flexibility in choice of molecule.

Cell type	Therapeutic expressed	MW (kDa)	Applicable disease
PC12	Dopamine	0.153	PD
Choroid plexus	Various neurotrophic factors		HD, stroke, spinal injuries
Neurosphere	Various neurotrophic factors		Stroke, spinal injuries
Engineered fibroblasts	BDNF	13.6	HD, PD, spinal injuries
Engineered Baby Hamster Kidney	CNTF	22	HD, PD
	GDNF	30	PD

PD: Parkinson's disease; HD: Huntington's disease; BDNF: Brain derived neurotrophic factor; CNTF: Ciliary neurotrophic factor; GDNF: Glial cell line-derived neurotrophic factor.

Table 1.1: Alternative therapeutic factors and cell types for encapsulation and treatment of a limited number of neurodegenerative diseases

PD is a disease of aging; typically age of onset is after 60. In order to be clinically diagnosed a patient must present with 3 out of 4 cardinal symptoms; tremor, slowness of movement (bradykinesia), rigidity (akinesia) and postural instability. The cause of symptoms is loss of dopaminergic neurons in the nigrostriatal pathway, which is responsible for the regulation of the forebrain centres controlling motor function. Up to 70% of dopaminergic neurons can be lost before symptoms become apparent; up to this point compensation within the system occurs (Bernheimer *et al.*, 1973). The cause of PD is unknown; some cases are caused by genetic factors, although this is not at all common (Polymeropoulos *et al.*, 1997). Prevalence of PD in the UK is 140 per 100,000, and 69% of these patients develop the disease after 65 years of age (Wickremaratchi *et al.*, 2009). Men are almost twice as likely to develop PD as women (Van Den Eeden *et al.*, 2003), although it is not clear why this is, it is possibly due to gender differences in exposure to chemicals, attitudes to smoking and employment history.

Cell transplantation has previously been used to treat PD in humans with variable success (for example, see Winkler *et al.*, 2005). Not only are there ethical and sourcing issues surrounding the use of the most promising cell type - midbrain foetal dopaminergic neurons - but the treatment is not an effective solution. In particular it remains unreliable even in the best centres, and results have not been entirely

consistent either between patients or research groups carrying out the surgery (Freed *et al.*, 2001; Olanow *et al.*, 2003; Piccini *et al.*, 2005; Mendez *et al.*, 2008). Use of polymer encapsulation allows many more cell sources to be exploited, as chemical immunosuppression is not required to protect allogeneic or xenogeneic cell types (as previously discussed regarding diabetes (Section 1.2)). Although various groups have attempted to use encapsulated cells to reverse Parkinsonism in animal models, there have been no studies carried out in humans.

1.4 HOST REACTIONS TO TRANSPLANTED CELLS

The immune system functions *via* three mechanisms: humoral immunity, cellular immunity and secretion of lymphokines. Humoral immunity relies on molecules in solution; these molecules are immunoglobulins, more commonly known as antibodies, which act by recognising non-self material. In cellular immunity, antibodies are attached to immune cells, known as T cells. The secretion of lymphokines stimulates humoral and cellular immunity as well as producing phagocytes; cells that kill, ingest and digest pathogens and any cell debris (Murphy *et al.*, 2007).

All cells in the body display a marker based on the major histocompatibility complex (MHC). Non-self material introduced into the body does not express the same MHC antigens as the host. T cells are produced which recognize non-self material, by direct contact with antigens on a foreign cell; CD8 T cells target peptides bound to MHC class I and CD4 T cells target MHC class II (Remes and Williams, 1992). When these T cells attach to foreign cells, many more T cells are clonally produced that are able to kill the foreign cells (Lombardi and Lechler, 1991).

Encapsulation of non-autologous cells prevents T cells from coming into direct contact with non-self antigens. However, any cells not entirely protected by the matrix can be attacked by T cells. Incomplete encapsulation is a major problem with current encapsulation techniques, as described below (Section 1.6.4). Cells fully encapsulated within a polymeric capsule must also be protected from antibodies in solution. The capsule material must have sufficiently low porosity such that immunoglobulin (Ig) antibody molecules cannot permeate. Immunoglobulin molecules range in size from IgG at around 150 kDa to IgM at around 950 kDa;

therefore any polymers used for encapsulation must have pore sizes below 17nm to prevent IgG entry (Saphire *et al.*, 2001).

The immune system also uses the complement system to detect pathogenic material. This is a biochemical cascade consisting of over 35 different proteins. The most important protein with regard to cell encapsulation is C3, as its activation does not rely upon pathogen-binding antibodies (Götze *et al.*, 1976). Therefore, encapsulated cells can still be attacked even if antibodies have not bound to and recognized them. C3 is cleaved into C3a and C3b by enzymes in the blood. C3b will bind to any pathogenic material within its vicinity. This binding starts a cascade of hydrolysis and cleavage, ultimately resulting in rapid pathogenic cell lysis (Liszewski *et al.*, 1996). Part of the function of this cascade is to initiate a positive-feedback mechanism that produces even more C3b (Sim and Tsiftsoglou, 2004). C3b is an example of an opsonin, in that it acts as a binding enhancer for the process of phagocytosis (Hart *et al.*, 1986). *In vivo*, exposed antigens on a foreign cell are bound by antibodies and complement proteins. This enhances phagocyte binding to the foreign cell as phagocytic cells express receptors which bind opsonin molecules (Ezekowitz *et al.*, 1984). Without opsonin binding, most phagocytic binding would not occur. As C3b is a small (181 kDa) protein, it is likely to be able to diffuse through the capsule membrane, thus allowing complement system activation.

The mammalian brain does not have any true lymphatic vessels and the presence of the BBB isolates it from the circulatory system. For these reasons the brain was historically thought of as an "immuno-privileged" site (Barker and Billingham, 1977). However, this assumption has recently been dispelled. Lymphatic drainage from the brain is thought to occur (Knopf *et al.*, 1995), thus allowing naïve T cells to be activated in the cervical lymph nodes through indirect antigen presentation. Microglia within the brain can act as antigen presenting cells and interact with activated T cells, which can cross the BBB (Aloisi, 2001). In addition, the BBB is necessarily disrupted by surgery required for grafting; the immune response thus generated keeps the BBB open. In conclusion, the seemingly simple task of preventing immune rejection of foreign cells is actually exceedingly complex.

Although there are reports of allogeneic (Borlongan *et al.*, 2008) and xenogeneic (Kordower *et al.*, 1995; Veng *et al.*, 2002) transplantation into rodent models for human neurodegenerative diseases, it is important to remember that rodents react less aggressively to transplantation than humans. For instance, in

rodents, invaders such as parasites can be separated from the host systems *via* production of dense fibrous tissue, which is not observed in humans (Veng *et al.*, 2002).

1.5 IMMUNOISOLATION DEVICES

Immunoisolation devices are typically divided into two categories; macrocapsules and microcapsules. Each of these approaches makes use of different geometries, imparting distinct advantages and disadvantages. The characterizing differences are size of device and number of cells encapsulated.

Macroencapsulation employs large macroscopic devices (0.5-6mm in diameter, 0.5-10cm in length (Gentile *et al.*, 1995)), originally derived from microdialysis tubing, filled with thousands, often millions, of cells. The membrane is usually prepared prior to filling with cells and so synthetic polymers (Section 1.7.1) can be employed more easily than when manufacturing microcapsules, without harming encapsulated cells. Use of synthetic polymers and manufacture prior to filling with cells allows for the permeability, together with various other advantageous properties of the device, to be easily tuned. Macroencapsulated cells are easily retrievable and devices are often mechanically strong. However, implantation of these devices can be invasive, and, due to their small surface area to volume ratio, problems with oxygen transfer are common. For this reason macroencapsulated cells often have lower viability than microencapsulated cells, and so, many more cells are required (Kordower *et al.*, 1995).

Microencapsulation allows small numbers of cells to be immobilized in spherical beads <1mm (but more commonly <450μm) in diameter. Microencapsulation offers many advantages over macroencapsulation. Due to higher surface area to volume ratio and hence enhanced oxygen transfer, microencapsulated cells often have higher viability. As microcapsules are smaller then macrocapsules, a greater number of suitable implantation sites are available. The smaller size is also advantageous as it allows simple and precise stereotaxic positioning within the brain, which removes the need for major invasive surgery. Moreover, in contrast to macrocapsules, if one microcapsule breaks the whole graft is not lost. However, microcapsules are more difficult to retrieve after implantation than macrocapsules.

The major limitations of microencapsulation are fibrotic overgrowth of beads and low stability (de Vos *et al.*, 2006).

1.6 REQUIREMENTS OF ENCAPSULATED CELL SYSTEMS

Depending on the function of the cell line encapsulated, for cell encapsulation to be successful there are several essential capsule and cell requirements. These are:

- Diffusion of materials to and from cells
- Stability – both mechanical and chemical
- Small size (<350μm in diameter) and narrow size distribution
- Complete coverage of cells
- Capsule production needs to harness simple and non-toxic procedures
- Biocompatible encapsulation material – non-toxic to both cells and host

1.6.1 Diffusion

Cells need a constant supply of oxygen and nutrients to survive. The encapsulation material in use must allow efficient diffusion of oxygen and nutrients into capsules and allow noxious materials and therapuetic products out again. The permeability of a molecule through a polymer matrix is dependant upon the molecular weight cut off of the polymer and the rate of diffusion of the molecule. The rate of diffusion is determined by the size, shape and charge of the molecule; the charge of the polymer is also important. Changing porosity affects diffusion rates of molecules into and out of capsules. Hence, the porosity of the capsule matrix must be tailored to fit the requirements of the system. To prevent immune rejection of encapsulated cells, the porosity must be low enough to exclude antibodies and other immune molecules (Section 1.4).

Due to ineffective diffusion of oxygen, nutrients and waste products, cell necrosis frequently occurs at the centre of large capsules (>500μm), when implanted (De Vos *et al.*, 1999). Ogbonna *et al.* (1991) calculated that capsules, in a stirred bioreactor, should be no more than 300μm in diameter to ensure effective diffusion and hence cell survival. Many polymer-encapsulation techniques fail to produce capsules of sufficiently small diameter (to be discussed in Section 1.10.4).

1.6.2 Stability

Mechanical stability is important in the production and handling of capsules. Capsules must remain intact throughout surgical procedures and be able to withstand any pressure or stress at the site of implantation. In cases where the implanted cells are intended to serve as long-term replacements for endogenous cells, it is clear that the capsules must stay intact after implantation. Degradation of capsules due to chemical changes is undesirable, as again, capsules will lose integrity and the graft will be lost. However, for other applications, slow predictable solubility of the capsule may allow timed delivery of compounds over periods of weeks or months prior to cell exposure and shut down. *In vitro* testing of beads is often carried out minus encapsulated cells, however, the addition of cells has been shown to decrease the mechanical strength of alginate beads (Rokstad *et al.*, 2003). It is therefore important that complete encapsulated cell systems are measured for mechanical strength, not merely polymeric capsules.

The mechanical strength required of capsules is dependant upon the site of implantation. The most commonly used site for encapsulated cell implantation is the peritoneal cavity. It has been shown that alginate capsules break down faster in the peritoneal cavity than in the striatum or subcutaneous space (Thanos *et al.*, 2007). Distributions of capsules within each of these implantation sites are different, as are forces exerted upon the capsules. For example, capsules are implanted into the brain in a cylindrical tract arrangement. Although some surfaces of some capsules are not exposed to the surrounding tissues, the forces exerted by the neighbouring tissue has been posited to be able to cause physical damage (Thanos *et al.*, 2007).

In humans, intracranial pressure has been measured to be 7-15mmHg when lying down, which falls to -10mmHg when standing (Steiner and Andrews, 2006). As the brain is incompressible and the volume within the skull is fixed, blood, cerebrospinal fluid and brain tissue are in a state of volume equilibrium (Monro, 1783; Kelly, 1824). Hence, intracranial pressure can be extrapolated to pressure exerted within the brain tissue. Converting to kPa, the pressure exerted within brain tissue is -1.3kPa to 1.9kPa. Alginate gels (2%, M:G = 1.67) have been shown to withstand compression forces of up to 10kPa (LeRoux *et al.*, 1999). Hence, the pressure exerted by surrounding brain tissue should not be enough to cause damage to implanted beads.

1.6.3 Small size and narrow size distribution

According to Robitaille *et al.* (1999), small capsules (<350μm) show increased biocompatibility when compared to capsules with a diameter of 1250μm. It is not clear why this should be the case, though it has also been observed in another study (Omer *et al.*, 2005). Ross and Chang (2002) showed that smaller APA (Section 1.8.1) capsules have higher mechanical strength than larger ones. As discussed previously (Section 1.6.1), smaller size capsules allow enhanced oxygen transfer (Ogbonna *et al.*, 1991). Many properties of capsules are dependant upon size, therefore a narrow size distribution is important to ensure a homologous population of beads which will all respond in the same manner (Strand *et al.*, 2002).

1.6.4 Complete covering of cells

Cells protruding from the bead matrix through incomplete covering are susceptible to attack by the immune system. This not only compromises the individual bead concerned, but also exposes the whole graft to immune attack (King *et al.*, 2001b). Through exposure to a few cells which are not encapsulated, the immune system becomes sensitised to the encapsulated cells and increased levels of antibody are produced, causing the entire graft to be destroyed. Several studies by de Vos *et al.* into encapsulated islets have found that physical irregularities such as tails, craters and protruding islets decrease the stability of beads, leading to bead breakage as well as fibrotic overgrowth (de Vos *et al.*, 1994). Decreasing bead diameter from 800μm to 500μm increased the likelihood fourfold of islets protruding (De Vos *et al.*, 1996). An increased fibrotic reaction was observed with islets encapsulated in beads 500μm in diameter compared with beads 800μm in diameter (De Vos *et al.*, 1996).

1.6.5 Non-harmful procedures

It is clear that the encapsulation procedure should not adversely affect the viability of the cells to be encapsulated, i.e. ensuring maximum cell viability at the end of an encapsulation procedure is of paramount importance. Current procedures have limitations in this regard. For example, the encapsulation method (such as interfacial polymerisation) may involve organic solvents (Sefton *et al.*, 1987; Desmangles *et al.*, 2001) or expose the cells to high shear forces, (i.e. any production method which forces cells in solution through a narrow aperture at high velocities or involves an impeller (Section 1.9)), both of which may be harmful.

1.6.6 Biocompatible encapsulation material

Biocompatibility has many definitions, not all of them useful. The Williams definition of biocompatibility is "the ability of a material to perform with an appropriate host response in a specific application" (Williams, 1987). This definition allows interaction between the host and the implant to be taken into account. In the context of encapsulated cells, the encapsulation material should not irritate the tissues surrounding the implant, provoke an inflammatory response nor incite allergic reactions. It is preferable that the polymeric material should not be cytotoxic or mutagenic, either to the encapsulated cells or to the host. The immune system should not attack the material and no changes in the material's properties should occur when in a biological environment.

1.7 ENCAPSULATION MATRICES

Most cell encapsulation is "polymeric", i.e. it makes use of polymers. Polymers are molecules made up of repeating units (monomers), which can be naturally occurring or synthetically produced. Monomers are connected together by covalent chemical bonds into repeating chains by the process of polymerisation. The term homopolymer describes a polymer chain where all the monomers are identical; in contrast, a copolymer consists of a mixture of monomers. Polymer chains can be linear or branched and are joined together by various cross-linking mechanisms. Cross-linked polymers often have very different properties from their pre-cross-linked counterparts. Take for example polyacrylamide; used in gel electrophoresis. This homopolymer is made up of acrylamide monomers (Fig 1.1).

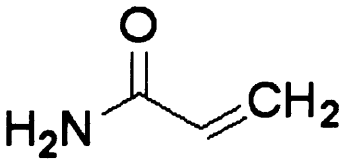

Figure 1.1: Chemical structure of acrylamide

Many hundreds of thousands of monomers are polymerized to form long chains of polyacrylamide. These chains are not attached to each other and can move freely. Upon addition of a cross-linking agent (for example, bisacrylamide in the case of gel electrophoresis), the chains become linked to each other. The resulting cross-

linked polymer is a gel capable of absorbing many times its own mass in water (Fig 1.2).

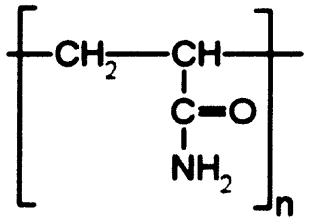

Figure 1.2: Cross-linking of polyacrylamide

1.7.1 Synthetic encapsulation matrices

Use of synthetic polymers for cell encapsulation is advantageous as they can, in principle, be designed to meet specific requirements and reproducibly manufactured. Many synthetic polymers do not permit cell adhesion (Folkman and Moscona, 1978), but can be made more suitable for cell attachment (Chinn *et al.*, 1989). For example, cell adhesion has been enhanced within beads by manufacturing polymers incorporating arginine–glycine–aspartic acid (RGD) peptides (reviewed in Hersel *et al.*, 2003). Other disadvantages to the use of synthetic polymers are issues with toxicity. Polymerisation often requires the use of conditions that affect encapsulated cell viability, for instance, organic solvents or high temperatures. In addition, low molecular weight components of the polymer, such as unreacted monomers, plasticizers or catalysts, are able to leach from the device upon implantation and cause harm (Taylor *et al.*, 1994).

Due to the detrimental effects of polymerisation, synthetic polymers have most often been used in conjunction with macroencapsulation devices (Section 1.5). As the device is manufactured prior to filling with cells, cells are not exposed to conditions required for device formation. Numerous synthetic polymers have been used for the microencapsulation of cells including; an amphiphilic poly(ethylene glycol)-conjugated phospholid derivative (Teramura and Iwata, 2009), poly(ethylene glycol)-*co*-poly(glycolic acid) (Bencherif *et al.*, 2009) and Poly(ethylene glycol)-poly(propylene glycol) block copolymers (Cellesi and Tirelli, 2005). However, due to the concerns of long-term safety, naturally occurring polymers are used in preference to synthetic polymers.

1.7.2 Alginate

The most commonly used polymer in cell encapsulation is alginate (salt of alginic acid), a naturally occurring hydrogel. Hydrogels are hydrophilic polymers which can consist of up to 99% water. Their high water content and hydrophilic nature prevents damage through friction to tissues when implanted. The aqueous environment can also protect encapsulated cells and allow transport of nutrients to cells. Alginic acid has properties which make it ideal for cell encapsulation. For example, alginate forms a gel under very mild, physiological conditions (Smidsrod and Skjakbraek, 1990), very rapidly, and it is both biocompatible and biodegradable (Orive *et al.*, 2004).

1.7.2.1 Structure

Alginate is obtained relatively easily from seaweed, although extraction and purification techniques must be extensive to prevent an immune response upon implantation (Zimmermann *et al.*, 2005). This naturally occurring polysaccharide is a block copolymer comprised of β-$_D$-mannuronic (M) acid and α-$_L$-guluronic (G) acid residues (Figure 1.3).

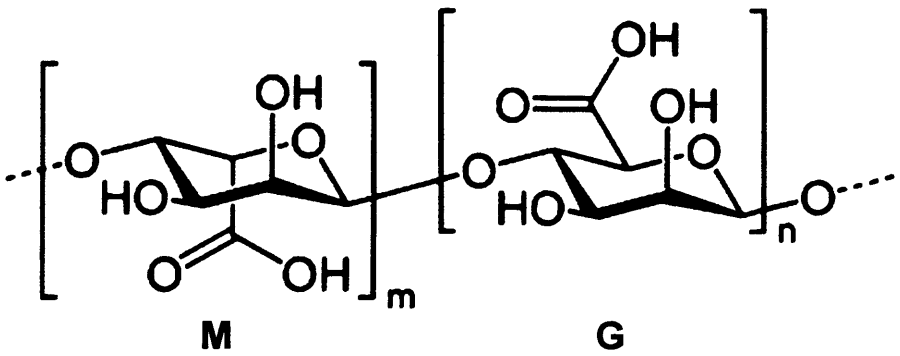

Figure 1.3: Chemical structure of alginate. Ring conformation of β-$_D$-mannuronic acid (M) and α-$_L$-guluronic acid (G)

The residues can form into four types of diad: MM, GG, MG and GM. These diads can then form into three types of block: homopolymeric M- and G-blocks and alternating MG-blocks (Gaserod *et al.*, 1998). The percentage and sequence of the block is unique to each algal species it is extracted from. Alginic acid extracted from *Laminaria hyperborea* has a high percentage of G residues, whereas alginic acids extracted from *Durvillea antartica*, *Ascophyllum nodosum*, *Laminaria digitata* and *Macrocystis pyrifera* have a high percentage of M residues (Smidsrod and

Skjakbraek, 1990). Gels formed from these different alginic acids have varying pore sizes, degradation rates, mechanical stability and diffusion kinetics (Smidsrod, 1974; Martinsen *et al.*, 1989; Stokke *et al.*, 1991).

The carboxyl groups on alginate residues have a strong affinity for divalent and trivalent cations such as Ca^{2+}, Sr^{2+}, Al^{3+} or Ba^{2+}. The affinity of alginate chains for alkaline earth metals decreases thus; $Ba^{2+} > Sr^{2+} > Ca^{2+} >> Mg^{2+}$ (Smidsrod and Skjakbraek, 1990). The selective binding of divalent and trivalent cations leads to ionotropic gel formation. Ca^{2+} is the most widely used ion to form alginate gels for cell encapsulation, as it is non-toxic at the low concentrations used and selectively binds G-blocks. Two alginate chains are thought to form helical structures around Ca^{2+} ions (Figure 1.4), this is often referred to as the "egg-box model" (Braccini and Perez, 2001).

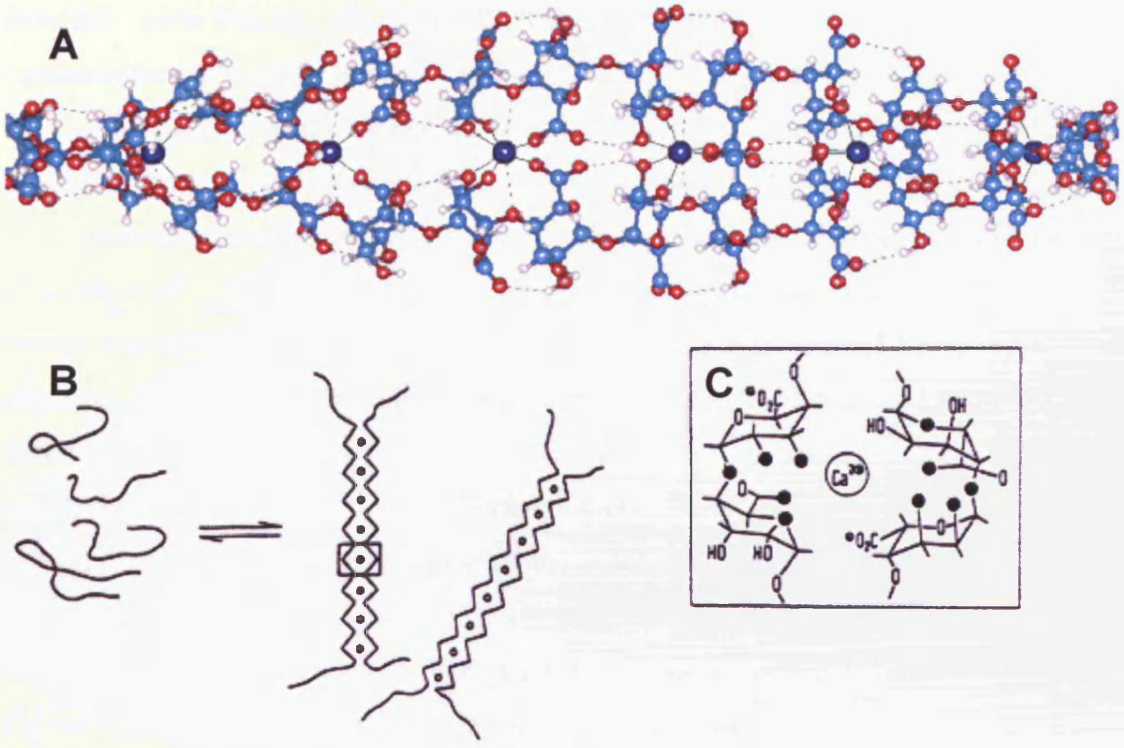

Figure 1.4: Representations of cross-linked alginate 3D structure. A) Ball and stick representation of poly-L-guluronate sequences of alginate cross-linked by calcium ions. B) Conversion of random coils to buckled ribbon-like structures which contain arrays of Ca^{2+} ions. C) Schematic of the proposed stereochemistry of Ca^{2+} ion complexation. The oxygen atoms involved in the coordination sphere are shown as filled circles. From Wee and Gombotz (1998)

Anions with the ability to chelate Ca^{2+}, such as citrate, phosphate or EDTA will destabilise ionically cross-linked alginate gels, causing the 3D matrix to dissolve (Smidsrod and Skjakbraek, 1990). Ca^{2+} ions can also be displaced by other cations

such as sodium and magnesium, so high concentrations of these cations can also dissolve alginate gels. This example of ion-exchange occurs *via* diffusion of ions into the cross-linked structure. LeRoux *et al.* (1999) found that 60% of the mechanical strength of an alginate bead is lost within 15 hours of exposure to biological buffers. Destabilisation is bought about by a combination of ion-exchange of Ca^{2+} with sodium, and calcium chelation by phosphate.

1.7.2.2 Internal and External cross-linking

The most common method for producing alginate beads is droplet formation with subsequent ionic cross-linking occurring in a setting bath containing a calcium (II) ion solution (Section 1.9). This is termed "external gelation", as Ca^{2+} ions are external to the droplets of dissolved alginate. Alginate chains within the fluid droplet diffuse to the interface of the droplet where the Ca^{2+} concentration is highest, thus forming an alginate gradient within the cross-linked alginate beads. Beads formed *via* external cross-linking are termed "non-homogeneous" as there is a higher concentration of alginate and Ca^{2+} at the surface than the core (Quong *et al.*, 1998).

Internal cross-linking occurs when Ca^{2+} ions are liberated, within an alginate droplet, from an insoluble or inactive form. The only cells to be encapsulated thus far using internal cross-linking were *Lactococcus lactis*, an acid-loving bacterial species (Larisch *et al.*, 1994), based on a method described by Lencki *et al.* (1989). Calcium citrate was used as the insoluble calcium source. This was dispersed in a solution of alginate, which was emulsified in vegetable oil. Acetic acid in vegetable oil was subsequently added to the emulsion. Liberation of Ca^{2+} occurs upon reaction of calcium citrate with H^+, from the dilute solution of acetic acid. Thus, Ca^{2+} ions were released within the dispersed phase of the emulsion, thereby initiating ionic cross-linking of alginate chains.

In 1995, Poncelet *et al.* replaced calcium citrate with calcium carbonate (see Figure 1.5). As calcium carbonate releases Ca^{2+} at a higher pH than calcium citrate, the cross-linking reaction is almost instantaneous. Equation 1.1 shows the reaction that occurs; the by-products from this reaction are water and carbon dioxide. With modifications, such as the addition of chitosan, this method has subsequently been widely used to encapsulate biological macromolecules, such as haemoglobin (Ribeiro *et al.*, 2005) and DNA (Quong *et al.*, 1998). Internal cross-linking of alginate is most commonly used in conjunction with an emulsion formation method (Section 1.9.3).

Alginate beads formed using internal cross-linking methods typically have a homogeneous concentration of alginate and calcium throughout. As the calcium source is homogeneously dispersed throughout the fluid alginate droplets, a gradient of alginate chains is prevented from forming.

$$CaCO_3 + 2H^+ \rightarrow Ca^{2+} + CO_2 + H_2O \qquad \textbf{Equation 1.1}$$

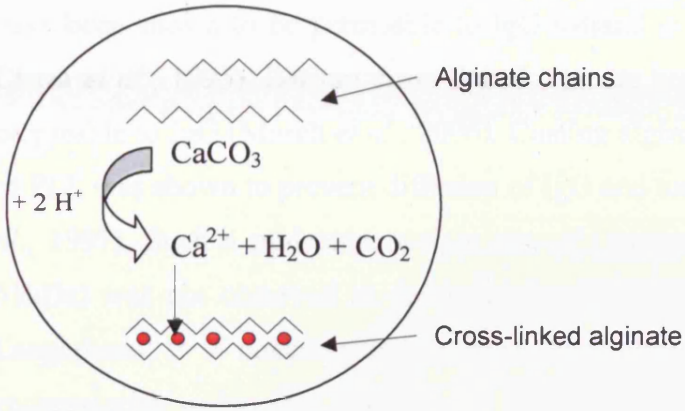

Figure 1.5: Schematic diagram illustrating internal gelation. Ca^{2+} is released from calcium carbonate upon addition of acid, inside a liquid alginate droplet. Chains of alginate become cross-linked by free Ca^{2+} (red circles)

Although the cross-linking reaction of alginate by calcium is often thought of as "mild" and occurs under physiological conditions, both external and internal cross-linking methods can be toxic to cells. Calcium at high concentrations is known to be toxic to cells (Choi, 1992; Barros *et al.*, 2002; Burek *et al.*, 2003). There is a danger with both methods that excess calcium which is not used in the cross-linking reaction may harm encapsulated cells. The acidic conditions required by the internal cross-linking method, coupled with the extended (20 minute) exposure required when using emulsion formation techniques (Section 1.9.3) to fully cross-link the alginate, are also extremely toxic to cells. Indeed, this may explain why only acid-loving bacterial species have previously been encapsulated using internal cross-linking.

1.7.2.3 Porosity

Pore sizes range widely from 50 – 200nm in calcium cross-linked alginate gels (Smidsrod and Skjakbraek, 1990). Increasing alginate concentration has the effect of decreasing the matrix porosity (Martinsen *et al.*, 1992). Gels formed from alginates high in M-residues have a more flexible structure and a lower porosity than alginate high in G-residues (Martinsen *et al.*, 1989). This is due to G-blocks forming more

rigid tertiary structures than M-blocks upon cross-linking, as Ca^{2+} preferentially binds G-residues. Homogeneous beads have a higher porosity than non-homogeneous beads (Section 1.7.2.2) as the increased concentration of alginate at the surface of non-homogeneous beads reduces diffusion of molecules (Martinsen *et al.*, 1992).

As the primary function of an immobilisation matrix is to prevent encapsulated cells being attacked by the immune system, it should be impermeable to antibodies and complement species (Section 1.4). Calcium cross-linked alginate beads have been shown to be permeable to IgG (Strand *et al.*, 2002) and C3 (Section 1.4, Lanza *et al.*, 1995). Barium cross-linked alginate beads have also been shown to be permeable to IgG (Morch *et al.*, 2006). Coating alginate beads with a secondary layer of PLL was shown to prevent diffusion of IgG and tumour necrosis factor (Kulseng *et al.*, 1997). Such a molecular weight cut-off (tumour necrosis factor has a MW of 51kDa) was not observed to detrimentally affect viability of encapsulated islets of Langerhans. It is conceivable, however, that other cell types may be affected by encapsulation within such a membrane.

1.7.2.4 Mechanical strength

Encapsulated cells should have sufficient mechanical strength to be able to withstand forces exerted during administration and *in vivo* (Section 1.6.2). The rigidity of alginate gels increases with the affinity for the cross-linking ion, thus; $Ba^{2+} > Sr^{2+} > Ca^{2+} >> Mg^{2+}$ (Smidsrod, 1974). So, barium cross-linked alginate gels are mechanically stronger than calcium cross-linked alginate gels due to the stronger affinity of alginate residues for Ba^{2+} than Ca^{2+}.

As stated in Section 1.7.2.1, exposure of calcium cross-linked alginate to biological buffers leads to significant loss of mechanical strength. As Ba^{2+} has a stronger affinity for alginate, barium cross-linked alginate is expected not to undergo ion-exchange with monovalent ions, or smaller divalent ions. Addition of small amounts of barium (1mM) during cross-linking was shown to reduce the swelling of alginate beads, as well as increase gel strength (Morch *et al.*, 2006). Another method of stabilising alginate beads is to apply a secondary polycation layer; this will be discussed in Section 1.8.

Rokstad *et al.* (2006) have pioneered an alternative approach to producing stronger gels. By introducing photo-cross-linkable methacrylate groups onto M-residues of alginate chains, beads could be produced using ionic and covalent cross-

linking. Hence, beads were produced using conventional cross-linking methods (Section 1.9), and subsequently photo-cross-linked by methacrylates, initiated by Eosin Y and white light. The resultant beads were found to be more mechanically stable than barium cross-linked alginate beads. HEK (Human Embryonic Kidney), C2C12 (mouse myoblasts) and pancreatic islet cells were successfully encapsulated and showed excellent initial viability. However, only slow growing C2C12 cells and islet cells continued to be viable for longer than 13 days. HEK cells did not proliferate in the photo-cross-linked beads. Increased cross-linking density was thought to make the beads more solid, hence preventing the fast growing HEK cells from expanding.

1.7.3 Alternative, naturally occurring encapsulation polymers

Temperature sensitive gels, such as agarose (Sakai *et al.*, 2005), have also been utilised for cell encapsulation. Agarose is soluble in hot water and forms a reversible hydrogel upon cooling. Due to its inherent hysteresis (the difference between its melting and gelling temperatures) it melts at a very high temperature (80-95°C) and gels at 32-45°C. Other examples of this kind of temperature sensitive gel are agar and κ-carrageenan (Prakash and Bhathena, 2008). Agarose gels are highly porous and have previously been used as extracellular matrices. Lahooti and Sefton (2000) incorporated agarose cores into poly(hydroxyethyl methacrylate-co-methyl methacrylate) (poly(HEMA-MMA)) capsules in order to promote cell growth. They observed that HEK cells suspended within agarose cores surrounded by poly(HEMA-MMA) capsules showed decreased cellular aggregation, and increased viability over time. An overproliferation of cells was also reported, with subsequent capsule rupture.

1.8 COATING

An additional coating layer can be used to improve the characteristics of encapsulated cell systems. For instance, additional coating may improve mechanical stability (Section 1.7.2.4), as well as reducing matrix porosity (Section 1.7.2.3). By reducing matrix porosity, it is less likely that elements of the immune system will be able to enter the encapsulated system by diffusion. Also, if any cells protrude from the polymeric matrix, an additional coating layer may prevent them from coming into contact with immune cells and antibodies (Section 1.6.4).

Commonly, coating is performed using a two-step process. Polymeric beads are formed using an entrapment technique, as described below (Section 1.9), and then

treated with a solution of the appropriate coating species. Coated beads are removed from the solution after an empirically determined time and washed to remove unbound coating material. The original bead material may also be re-dissolved, to leave cells in a liquid centred capsule surrounded by a polymer shell (Lim and Sun, 1980; Kampf, 2002).

Coating materials must be similar in characteristics to the encapsulation matrix materials, namely; non-toxic to cells, appropriate porosity, mechanical stability and biocompatibility. Alginates are negatively charged polymers, and as such form strong complexes with polycations (positively charged polymers). Several forms of polycation have been used to stabilise alginate beads and reduce their porosity. The following sections discuss the most commonly used polycations for coating alginate beads.

1.8.1 Poly-L-lysine

Poly-L-lysine (PLL, Figure 1.6) is the most commonly employed coating material used in conjunction with alginate. The use of this polycation and the method for producing PLL-coated alginate beads was pioneered by Lim and Sun (1980).

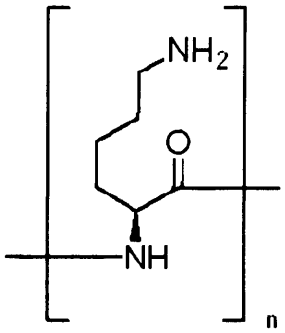

Figure 1.6: Chemical structure of poly-L-lysine

Although there was initial enthusiasm for PLL coating, it has since been shown that PLL attracts inflammatory cells, and fibrotic overgrowth often occurs in implanted capsules of this type (Vandenbossche *et al.*, 1993). Fibrotic overgrowth is undesirable as it leads to a decrease in transfer of oxygen, nutrients and metabolites and ultimately cell death. To prevent fibrotic overgrowth, PLL capsules are additionally treated with an external second coat of alginate. The resulting capsules are known as alginate-PLL-alginate (APA) capsules. It was thought that the additional

alginate layer prevented the PLL from coming into contact with cells at the implantation site, thus reducing the immune response. However, it has recently come to light that there is no distinct outer alginate layer in APA beads. Tam *et al.* (2005) have shown, using high performance techniques (such as attenuated total reflectance Fourier transform infrared spectroscopy, X-ray photoelectron spectroscopy, and time-of-flight secondary ion mass spectrometry) that APA beads consist of an alginate core surrounded by a single layer of alginate and poly-L-lysine complexes. This could explain observations that immune responses are still evoked by these beads (King *et al.*, 2001a).

Calcium cross-linked alginate beads swell when placed in solutions which do not contain calcium, but do contain Na^+ (Morch *et al.*, 2006); this is due to ion exchange of Na^+ for Ca^{2+}, which destabilises the gel. In an attempt to prevent destabilisation and swelling, a semi-permeable membrane of PLL has been used. Ideally the PLL membrane would be elastic and flexible enough to counteract the increased osmotic pressure caused by influx of water. If the osmotic pressure becomes too high or the elasticity of the membrane is too low the capsule will burst. To test the ability of beads or capsules to withstand osmotic pressure they are exposed to solutions of different osmolarities, the most extreme being distilled water. The so-called osmotic pressure test (Van Raamsdonk and Chang, 2001) and explosion assay (distilled water only, Thu *et al.*, 1996a) have allowed investigations to be carried out to improve the mechanical stability of APA capsules.

It has been shown that APA capsules with a membrane more resistant to osmotic pressure can be produced by increasing the exposure time of alginate beads to PLL, and also by increasing the concentration and decreasing the MW of PLL (Thu *et al.*, 1996a). The same study also found that PLL binding is proportional to the content of M residues present within the alginate, and that this is irrespective of alginate gradient.

1.8.2 Poly-L-ornithine

Poly-L-ornithine (PLO, Figure 1.7) has been used as an alternative coating material to PLL. As PLO is similar to PLL, i.e. a positively charged polypeptide, additional coating with alginate is required to prevent a strong immune reaction and fibrotic overgrowth. PLO has been shown to reduce swelling observed with PLL coated alginate beads, resulting in increased stability as well as reduced permeability

(Darrabie *et al.*, 2005). It was postulated that the improved performance of PLO-coated alginate beads were due to more efficient binding of PLO to alginate than PLL, brought about by its more compact structure (Darrabie *et al.*, 2005). As can be seen by comparing Figure 1.6 to Figure 1.7, PLO is shorter in structure than PLL by one methylene group.

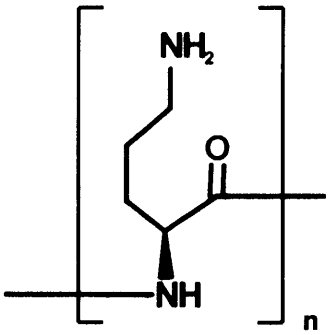

Figure1.7: Chemical structure of poly-L-ornithine

Despite improved *in vitro* properties, PLO-coated alginate beads were observed to elicit an even larger immune response *in vivo* than PLL-coated alginate beads (Ponce *et al.*, 2006). Although some enhanced properties have been observed, the improvements are minor and do not represent significant advantages over PLL.

1.8.3 Chitosan

Chitosan (Figure 1.8) is a naturally occurring polymer, prepared by *N*-deacetylation of chitin occurring in crustacean exoskeletons. It is biocompatible and has a low toxicity. Chitosan is soluble in acidic conditions, but insoluble at neutral pH.

Riberio *et al.* (2005) compared chitosan-coated alginate beads, made using two different methods, to non-coated alginate beads. In all methods, alginate beads were formed using emulsification (Section 1.9.3) and internal gelation (Section 1.7.2.2). In the one-step coating method, chitosan was added to the oil phase in an acidified state. In the two-step method, beads were isolated, washed, and then transferred to an aqueous solution of chitosan. Beads coated *via* the two-step method showed decreased porosity compared to both uncoated beads and coated beads produced *via* the one-step method. These beads were also found to be more mechanically stable than beads coated using the one-step method (Gaserod *et al.*, 1999).

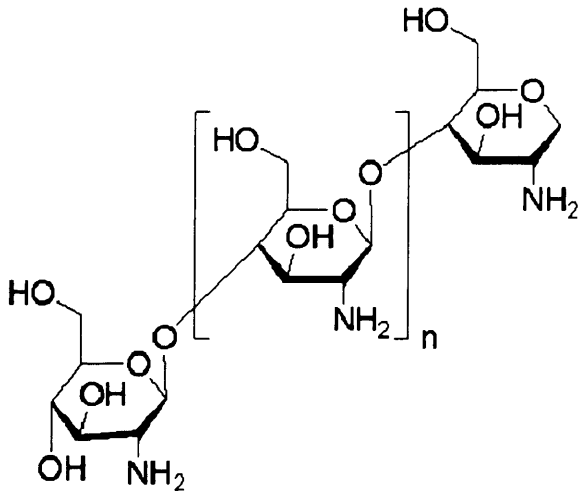

Figure 1.8: Chemical structure of chitosan

Gaserod *et al.* (1998) carried out a comprehensive investigation of the interaction between alginate and chitosan. By changing various factors related to the alginate bead composition, method of production and the chitosan coating it was found that binding of chitosan to alginate could be increased. Increased binding of chitosan to alginate decreased the permeability of the bead and increased stability (Gaserod *et al.*, 1999).

Hepatocytes have been successfully encapsulated, using the two-step method, in alginate-chitosan capsules (Haque *et al.*, 2005). However, viability was reduced when compared to APA capsules. Reduced viability was thought to be due to the longer coating time (30 minutes compared to 10 minutes for PLL) required for chitosan, although it is more likely to have been caused by the acidic pH (pH 5.2) required to dissolve chitosan.

1.9 CURRENT ENCAPSULATION METHODS

Numerous methods for encapsulating cells in alginate are described in the literature, which are outlined below. All methods employ a two step process; production of fluid alginate droplets containing cells, followed by Ca^{2+} cross-linking to form solid beads. Beads can be maintained in a solid state, or, with the application of additional coating layer/s, be converted into capsules (Section 1.8). Beads are solid

throughout their cross-section, whereas capsules have a liquid centre with a layer of polymer forming a peripheral shell (Kampf, 2002).

The main difference between the current encapsulation methods is one of droplet generation. Once droplets are formed, cross-linking is always achieved by dropping into a collection bath. The collection bath contains $CaCl_2$, which allows diffusion of Ca^{2+} into droplets to form beads. This mode of forming alginate beads is termed external gelation, as the Ca^{2+} source is outside the alginate droplet (Section 1.7.2.2). The most commonly used techniques are discussed briefly below. A more detailed discussion of the advantages and disadvantages of the methods, with emphasis on key requirements, will follow in Section 1.10

1.9.1 Extrusion through a needle

A narrow stream of polymer (containing cells) is pumped through a small needle/nozzle, whereupon it breaks up into droplets, due to the phenomenon known as Rayleigh break-up (Rayleigh, 1879). The described break-up only occurs if there is sufficient distance between the nozzle and the collecting bath. Extrusion is the simplest of all the described methods and uses readily available equipment. Very large beads are produced using this method and users have little control over the diameter and size distribution of beads produced (For example, see Fundueanu *et al.*, 1999, mean diameter 1.2mm, CV = 16%). For this reason many groups utilize one of the modifications discussed below (Sections 1.9.1.1 – 1.9.1.3).

1.9.1.1 Coaxial air or liquid flow

The needle extrusion method is most commonly modified by allowing a fluid (for example, air (Tagalakis *et al.*, 2005) or hexadecane (Sefton *et al.*, 1987)) to flow around the polymer stream. The liquid stream break-up is thus enhanced and smaller beads can be produced. Once the flows of fluid and distance of the nozzle from the collecting bath have been empirically determined, this procedure is straightforward.

1.9.1.2 Electrostatic

Another modification of the needle extrusion method establishes an electrostatic potential of 1-20kV between the needle and the collection bath, thus enhancing droplet formation by drawing the droplet towards the collection bath. Another consequence of an electrostatic potential is to disperse droplets as they fall into the collection bath (Serp *et al.*, 2000; Koch *et al.*, 2003). Thus, beads do not

coalesce upon falling into the collection bath and the polydispersity of the beads is reduced. By altering the needle diameter and alginate flow rate, varying bead diameters can be achieved.

1.9.1.3 Vibrating jet break-up

In this adaptation of the needle extrusion method, harmonic vibrations are applied to the needle thus aiding droplet formation (Seifert and Phillips, 1997). This method is difficult to reproduce in a laboratory-made device and is more commonly employed in commercial encapsulation devices, such as those manufactured by Nisco (Zurich, Switzerland). An electrostatic potential can be additionally applied to further enhance bead formation (Serp *et al.*, 2000).

1.9.2 Rotating jet break-up

Polymer solutions containing cells are forced out of nozzles to form fluid jets. Droplets are generated by cutting the continuous jet of fluid with rotating wires, which are angled to prevent "spraying loss" (Pruβe *et al.*, 1998). The cylinders of fluid produced form into droplets due to surface tension. As this technique does not rely upon Rayleigh break-up to produce droplets, it is uniquely compatible with highly viscous fluids.

1.9.3 Emulsion formation

An aqueous polymer solution containing cells is rapidly stirred with an immiscible phase to form small, spherical droplets of one phase within the other. The polymer is referred to as the dispersed phase; the immiscible fluid is referred to as the continuous phase. Surfactants are often used to enhance emulsion formation. Both internal and external gelation approaches (Section 1.7.2.2) can be used in conjunction with emulsion formation. If external gelation is employed, an appropriate cross-linking agent is added to the continuous phase and polymer cross-linking occurs in the dispersed polymer phase. Alternatively, an immobilised or inactivated cross-linking agent can be added to the dispersed polymer phase and then activated by addition of a chemical or photochemical trigger. Although all of the above methods (Section 1.9) can also be used in combination with internal gelation, oil-in-water emulsion formation is most suitable and frequently used with internal gelation (Poncelet *et al.*, 1992).

1.10 REQUIREMENTS OF A CELL ENCAPSULATION METHOD

Based upon a review of current cell encapsulation devices and platforms, the following points have been identified as being critical to further development in this field.

- Sterile
- Not harmful to cells
- Able to produce many beads – requiring scale-up
- Small diameter of beads with a narrow size distribution
- Short production time

The methods outlined in Section 1.9 have various advantages and disadvantages; each method has one or more major disadvantage which makes its use for cell encapsulation problematic. Each requirement will be discussed, highlighting any disadvantages of the described methods.

1.10.1 Sterile production method

Sterility is defined as the complete absence of all viable microorganisms (Akers *et al.*, 2002). Sterility is paramount when beads are prepared for clinical use and this can often be problematic with many of the discussed methods. All parts of the device which come into contact with alginate solutions, cells and beads should be capable of being autoclaved, to ensure sterility of product. Many non-commercial encapsulation devices are small enough to be operated within a sterile hood, thus bypassing the need for further modifications to ensure sterility.

All of the methods discussed above (Section 1.9) utilise devices which are constructed from components which can be autoclaved. Devices which operate on the basis of electrostatic and vibrating jet break-up comprise a sealed collection unit, which removes the need to operate the devices within a sterile flow hood. The only method which cannot be operated within a sterile environment is the rotating jet cutter (Section 1.9.2). The fluid containing the material to be encapsulated has to be accelerated to maintain a jet. The droplets thus produced travel at high velocity. Upon entering the collection bath droplets travelling at these high velocities deform and do not produce spherical beads. To avoid droplet deformation, droplets are pre-gelled by spraying with $CaCl_2$ whilst travelling down a 5m long spraying tunnel (Nedovic and Willaert, 2004). The spraying tunnel used is not sterile; despite this cells have been encapsulated and shown good viability (Schwinger *et al.*, 2002).

1.10.2 Non-toxic encapsulation process

Cytotoxic process steps reduce cell viability and therefore therapeutic productivity. The process of cross-linking alginate is considered to be "gentle" as it is carried out at neutral pH and does not require the use of organic solvents. As has previously been discussed (Section 1.7.2.2) high concentrations of Ca^{2+} can be toxic to cells and therefore must be limited. It is important that droplet generation methods do not involve high shear forces as these are harmful to cells. Although a high shear stress is inflicted upon cells suspended in droplets produced using rotating jet break-up (Section 1.9.2), murine fibroblasts were successfully encapsulated and shown to be viable and able to proliferate up to 6 weeks post-encapsulation (Schwinger *et al.*, 2002). All other "dropping" techniques have been used to successfully encapsulate viable cells (coaxial fluid flow (Fiszman *et al.*, 2002), electrostatic (Zhou *et al.*, 2005), and vibrating jet break-up (Coward *et al.*, 2005)). Emulsion formation (Section 1.9.3) is not regularly used with mammalian cells due to issues of cell viability. The use of an oil phase is essential for emulsion formation, but many cell types cannot be exposed to oil for prolonged periods of time (Kim *et al.*, 2009).

1.10.3 Production of large volumes of encapsulated cells in a short time period

Production of large quantities (50ml per patient (Calafiore *et al.*, 2006)) of mono-disperse beads required for clinical applications is problematic with many of the methods discussed above (Section 1.9). Whilst the majority of the methods are easy to establish within a laboratory setting, few can be used to produce batches larger than 20ml, which may be insufficient for treatment of even a single patient. The exception to this is rotating jet technology, which is capable of producing 2L/hour of 600 μm diameter beads (Prüße *et al.*, 2000). The solution to producing larger batches is to produce devices consisting of multiple parallel nozzles. For example, a device using the principles of laminar jet break-up (Section 1.9.1.1) was designed with 13 nozzles, which were supplied from a common reservoir (Brandenberger and Widmer, 1998). The 13 nozzle device was used to produce 1L of beads 560μm in diameter in 12 minutes. In contrast, a device based upon electrostatic principles with 20 needles, took much longer (1.5 hours) to produce an equivalent volume of 400μm diameter beads (Poncelet *et al.*, 1994).

Although scaled-up devices can produce large beads at high production rates, this is more problematic for small beads. Not only is the production of narrow

aperture nozzles problematic, blockage is more likely to occur than with larger nozzles and operating pressures become high. The number of needles required to maintain flow rate for production of small diameter beads is inversely proportional to the bead volume. Reduction of bead diameters to 100μm, or even 500μm, requires several hundreds or thousands of needles working in parallel to maintain required flow rates (Poncelet *et al.*, 1992). Seifert and Phillips (1997) calculated that 250μm diameter beads took nearly four times as long to manufacture using a vibrating jet method as an equivalent amount of beads 500μm in diameter. The increased production time is due to an inability to maintain high frequencies required for droplet formation. With rotating jet technology, reduction of bead diameters to 200μm reduces production time to 80ml/h (Prüβe *et al.*, 2000).

1.10.4 Small diameter beads with a narrow size distribution

More implantation sites are available through the use of beads with small diameters (Robitaille *et al.*, 1999), and bead samples with a narrow size distribution are required for reproducibility between experiments and groups (Strand *et al.*, 2002). However, many of the methods discussed above have only recently been optimised to allow beads with a diameter less than 400μm to be produced and size distributions remain large and uncontrollable. This is typically exacerbated by attempts to scale-up production. Issues with variability in nozzle manufacture and other physical parameters involved mean that multiple devices (nozzles) run in parallel each produce a slightly different bead diameter and size distribution (Brandenberger and Widmer, 1998). Size distribution is often described using the coefficient of variation (CV), which is defined as the ratio of the standard deviation to the mean and expressed as a percentage.

The major limitation of all non-commercial devices based upon needle extrusion (Section 1.9.1) is the nozzle size, which is restricted by the size of needles available commercially. As the narrowest needle available has an outer diameter of 250μm it is not possible to reproducibly manufacture beads smaller than this. Another problem is that of size distribution. Satellite droplets much smaller than the parent droplets are commonly produced with any method utilising nozzles (Figure 1.9). It is reported that satellite droplets produced using coaxial air flow droplet break-up (Section 1.9.1.1) are roughly 1% of the volume of the parent droplets (Zhang, 1999). Thus a bi-, or even, poly-modal size distribution are often obtained.

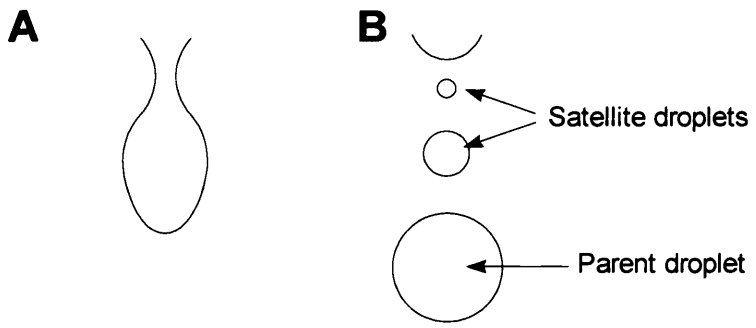

Figure 1.9: Satellite droplet formation from a needle. A) Fluid extruded from a needle begins to form a droplet. B) A parent droplet is formed as well as satellite droplets from the neck of the droplet

Needle extrusion (Fundueanu *et al.*, 1999), coaxial fluid flow (Fiszman *et al.*, 2002; Koch *et al.*, 2003) and electrostatic jet break-up (Strand *et al.*, 2002; Zhou *et al.*, 2005) are not suitable methods for producing small beads with a size distribution of less than 5% CV. Vibrating (Seifert and Phillips, 1997; Serp *et al.*, 2000) and rotating (Schwinger *et al.*, 2002) jet break-up methods are capable of consistently producing small beads with a CV of less than 5%. Large quantities of small beads are easily produced using emulsion formation; however, product size distribution is the largest of all the techniques discussed here. For example, Silva *et al.* report the smallest diameter beads generated using this method as 25μm with a CV of 47% (2005). Poncelet (2001) posited that a size dispersion of less than 30% of the mean bead size was not achievable using present emulsion techniques.

The information discussed above is summarised in Table 1.2.

Technique	Product bead diameter	CV	Possibility of scale-up?	Length of time to produce 1L of beads	Maximum batch size	No. of batches to make 1L of beads	Sterility	Toxicity
Needle extrusion	Very large (1-5mm)	>5%	30 nozzles	Slow	Small		Hood	None
Coaxial fluid flow	Small (200µm)	>5%	4 nozzles	100 hours (500µm beads, 4 nozzles)	50ml	20	Hood	None
	Large (700µm)	<5%						
Electrostatic	Small (160µm)	>5%	20 needles	31 hours (160µm, single needle)	20ml	50	Sealed unit	None
	Large (700µm)	<5%		1.5 hours (400µm, 20 needles)	1L	1		
Vibrating jet break up	Small (300µm)	<5%	13 nozzles	4 hours (200µm, single nozzle)	20ml	50	Sealed unit	None
	Large (700µm)	<5%		12 minutes (560µm, 13 nozzles)	1L	1		
Rotating jet	Small (<300µm)	<5%	48 wires, 4 jets	6 hours (200µm, 48 wires, 1 jet)	1L	1	No	None
	Large (3mm)	<5%		1.5 hours (200µm, 48 wires, 4 jets)				
Emulsion	Any	Large	Yes	20 minutes, any size	>10L	1	Hood	Possibly

Table 1.2: A summary of methods used for encapsulating cells discussed in Section 1.9. CV is calculated as standard deviation divided by mean diameter and expressed as a percentage. Parameters which fall outside optimal conditions are highlighted with red lettering, parameters which are ideal are highlighted with green lettering and sub-optimal parameters are highlighted with orange lettering

1.11 LIMITATIONS OF CURRENT CELL ENCAPSULATION SYSTEMS

Although extensive research has been carried out over the last 25 years on encapsulated cell systems, a "perfect" capsule is only slightly closer to being realised (Lacik, 2006). Several reasons for this failure have been suggested, including those discussed in Sections 1.6 and 1.10. Some progress has been made with issues such as biocompatibility of polymers, where use of highly purified alginate has reduced immune reactions to implanted beads (see Section 1.7.2.1 and De Vos *et al.*, 1997; Zimmermann *et al.*, 2005). Even if problems with encapsulation systems were solved, a major issue yet to be overcome is that of cell availability. For instance, 8 donors were required to provide the 678,000 encapsulated islet equivalents implanted into one patient, at half the optimal therapeutic dose (Soon-Shiong *et al.*, 1994).

The major limitation to progress in the field of cell encapsulation appears to be one of reproducibility. Currently results cannot be replicated between different labs, using differing protocols or even between batches of encapsulated cells. Much of the published data is conflicting, with little agreement between research groups; this is thought to be due to a lack of workable definitions and incomplete reporting of encapsulation protocols concealing differences between groups (Orive *et al.*, 2003). Any new encapsulation procedure must (at least) address the issue of reproducibility to prevent these problems arising.

1.12 MICROFLUIDIC TECHNOLOGY

Microfluidics is the study and use of fluid flows in micrometer scale channels (i.e. less than 1mm, Stone *et al.*, 2004; Atencia and Beebe, 2005). At this scale, viscosity, surface tension and diffusion have a larger effect on fluid flow than the forces of gravity and inertia, which influence the macro-world. At macro-scale, liquids flowing through pipes do so in a turbulent fashion, i.e. flow is chaotic and unpredictable (the position, within a fluid stream, of a particle cannot be predicted as a function of time, Beebe *et al.*, 2002). In micrometer scale channels, fluids flow in a laminar fashion due to a low Reynolds number (Re), which is defined as:

$$\mathrm{Re} = \frac{L v_s \rho}{\mu} \qquad \textbf{Equation 1.2}$$

Where L = most relevant length scale,

μ = viscosity,

ρ = fluid density,

v_s = average velocity of the flow.

For circular microchannels, L = 4A/P, where A = cross sectional area of channel and P = wetted perimeter of channel. For rectangular microchannels, L = 2 a b/ (a + b), where a = height of channel and b = width of channel.

As the cross-sectional area is small, the Reynolds number is decreased, usually to below 100. Therefore, viscous forces (denominator in Equation 1.2) dominate in this scenario, resulting in smooth, constant fluid flow. As a result, mixing between fluids in microchannels occurs *via* interfacial diffusion not turbulent agitation (Brody *et al.*, 1996). The transition from laminar to turbulent flow generally occurs in the range of Re = 2000. A corollary of the above equation is that only one dimension of the channel needs to be micro-scale (<1mm) to harness these properties.

The science of microfluidics has expanded rapidly in the past two decades. Part of the reason for this is advancement in microfabrication techniques, allowing microfluidic structures to be manufactured more easily. Since its inception in the mid 1990's, many different fields have used this science in a multitude of ways, for example; electrophoresis in biology (Yu *et al.*, 2007), chemical transformations (Palmieri *et al.*, 2009) and miniature fuel cells in electrical engineering (Brushett *et*

al., 2009). Not only do the uses of microfluidic science cross many different fields, it is itself also a multi-disciplinary field, linking engineering and physics with chemistry and biotechnology.

1.12.1 Use of microfluidic principles to form linear emulsions

Fluid flow in microfluidic channels is typically laminar (Re < 2000), this means that two fluid streams brought into contact in a microchannel will flow side-by-side, with mixing occurring *via* interfacial diffusion (see Figure 1.10A). Miscible fluids will always flow in this fashion, independent of microchannel geometry. Immiscible fluids will only flow in a laminar manner in a straight channel, due to low Reynolds number. However, this is only true for short periods of time, after which droplets of one liquid spontaneously form within the other. Certain channel geometries, i.e. cross-junctions (see Figure 1.10B) or T-junctions (see Figure 1.10C) enhance this effect, which is termed segmentation. Thorsen *et al.* (2001) were the first group to report incorporating segmented flow into a microfluidic chip.

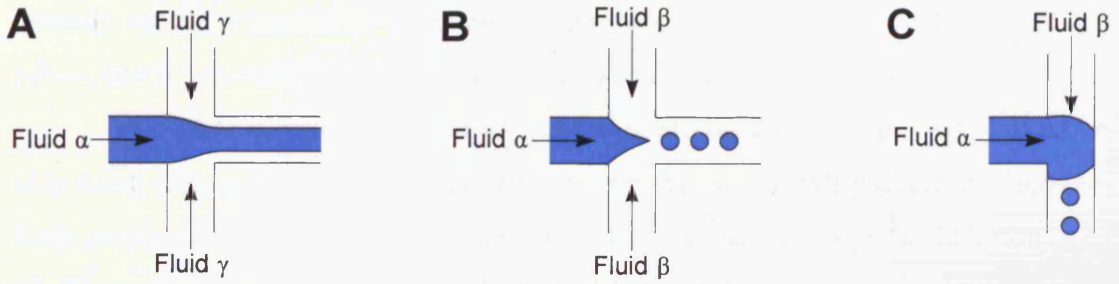

Figure 1.10: Schematic representations of laminar and segmented flow within microchannels. A) Schematic showing laminar flow between two miscible fluids. B) Schematic showing segmented flow of two immiscible fluids in a microfluidic cross-junction. C) Schematic showing segmented flow in a microfluidic T-junction

In conventional emulsion formation, the fluid which forms droplets is termed the dispersed phase, with the immiscible fluid being termed the continuous phase (Section 1.9.3). This is also true in microfluidic circuits. The fluid which forms droplets (Fluid α in Figure 1.10) is also called the functional fluid, and the immiscible fluid (Fluid β in Figure 1.10) is called the carrier fluid. Channel properties, such as surface energy, contact angle and hydrophobicity, influence which fluid forms droplets. Hydrophobic channels repel aqueous flows; hence aqueous droplets are formed within an organic continuous phase. Conversely, hydrophilic

surfaces attract aqueous flows, thereby coating (termed wetting) the channel walls and forcing the immiscible (organic) phase to form droplets. In both cases, segmented flow occurs and linear emulsions are formed. In the latter scenario a reverse emulsion is produced i.e. oil droplets in a continuous water phase (Shinohara *et al.*, 2008).

1.12.2 Use of microfluidic devices for alginate bead production

Several attempts have been made since the beginning of this project, by other groups, to produce alginate beads using microfluidic systems. The work presented within this thesis was carried out prior to or concurrently with the work discussed in the next sections. Both internal and external cross-linking methods have been employed, as have ionic cross-linking occurring on- and off-chip. Huang *et al.* (2006) first demonstrated that liquid alginate solutions could be segmented using a cross-junction microchannel to generate droplets of liquid alginate. These droplets were transported, with the oil used for segmentation, into a beaker containing a calcium (II) ion solution. Beads were produced with a diameter of 200±5μm and a CV of 2.5%. These beads were ionically cross-linked off-chip *via* external gelation. Yeh *et al.* have recently used a microfluidic T-junction to produce alginate droplets, which were also subsequently ionically cross-linked off-chip *via* external gelation (2009).

Two groups have attempted to make alginate beads ionically cross-linked on-chip using external gelation and collision of droplets, with varying degrees of success. Both groups produced separate droplets of $CaCl_2$ solution and alginate solution using oil. These two sets of droplets were then collided, within the system, to produce solid alginate beads. Neither of these methods produced spherical beads; Liu *et al.* (2006) produced disk-like and thread-like structures and Shintaku *et al.* (2007) produced tooth-shaped structures. As the kinetics of alginate gel formation are extremely fast, the reaction was complete before the two droplets had fully merged to form a spherical droplet.

Various other attempts have been made to use external gelation to ionically cross-link alginate on-chip. The most successful of these produced beads with a diameter of 70μm and a CV of 1.1% (Choi *et al.*, 2007). This is by far the best size distribution achieved to date; however, this method was unsuitable for use with cells, as hexadecane was used to segment the alginate solution. Kim *et al.* (2009) produced externally cross-linked alginate beads on-chip by using a flow focussing device

(Section 3.2). The oil used for segmentation contained a small amount of $CaCl_2$ thus allowing cross-linking of alginate chains.

Several groups have adapted internal gelation methods pioneered by Poncelet *et al.* (1992) and Ribeiro *et al.* (2005) for use in microfluidic systems. Huang *et al.* (2007) segmented liquid alginate solutions containing $CaCO_3$ using oil in a cross-junction microchannel. The emulsion generated was dripped into a beaker containing oil, Tween80 and acetic acid. Alginate chains became ionically cross-linked when droplets containing $CaCO_3$ came into contact with acetic acid. Zhang *et al.* (2007) proposed adding acetic acid to the fluid used for segmentation, in a similar system to the one described above. They were unable to collect any solid beads from this endeavour, although partially gelled beads were produced. Tan and Takeuchi (2007) used a T-junction to produce droplets of fluid alginate solutions containing $CaCO_3$ nanoparticles. Downstream of the junction used to produce droplets, corn oil containing acetic acid was introduced. Solid alginate beads were produced and collected. The work presented in this thesis was carried out and published concurrently with these studies.

The use of microfluidic techniques to produce alginate beads is summarised in the following table (Table 1.3).

Study	Carrier fluid	Cross-linking method	Channel dimensions	Size of product bead	CV
Huang *et al.* (2006)	Sunflower oil	External – dripped into bath	400μm cross-junction	200±5μm	2.5%
Liu *et al.* (2006)	Soybean oil	External – collision of droplets	60μm cross-junction	Threads and discs	
Zhang *et al.* (2006)	Undecanol	External	100μm flow focussing device	30-320μm	2.2%
Shintaku *et al.* (2007)	Food oil	External – collision of droplets	105μm flow focussing device	129μm (not spherical)	6.4%
Choi *et al.* (2007)	Hexadecane	External – mixing prior to segmentation	90μm modified T-junction	~70μm	1.1%
Huang *et al.* (2007)	Sunflower oil	Internal – dripped into bath	200μm cross-junction	180±10μm	5.5%
Zhang *et al.* (2007)	Soybean oil	Internal	100μm flow focussing device	60-110μm	1.5-2%
Tan and Takeuchi (2007)	Corn oil	Internal	50μm T-junction	94-150μm	2.8%-3.6%
Yeh *et al.* (2009)	Sunflower oil	External – dripped into bath	200μm T-junction	70-220μm	<10%
Kim *et al.* (2009)	Oleic acid	External	Unreported flow focussing device	96-195μm	11-13%

Table 1.3: Summary of attempts to use microfluidic devices to produce alginate beads

1.12.3 Advantages of microfluidic technology for cell encapsulation

The requirements of a production method for encapsulating cells were discussed previously (Section 1.10). The use of microfluidic techniques to encapsulate cells will be considered as compared to these requirements.

1.12.3.1 Small diameter beads with a narrow size distribution

Most importantly for the present application, linear emulsions of droplets with diameters ranging from 60-320μm have been reported with size distributions of <3% CV formed using microfluidic devices (Table 1.3). Production of bead samples with size distributions less than 3% are the very best that non-microfluidic techniques can achieve (Section 1.10.4). As discussed previously (Section 1.10.4), beads produced *via* emulsification methods typically have a large size distribution (~30%). Within microfabricated devices, the size of produced droplets can be varied both by the dimension of the channels and by the speed of fluid flows. By decreasing channel sizes to below 50μm and increasing flow rates, droplets with diameters (10-30μm) approaching that of cells have been produced (Chabert and Viovy, 2008; Edd *et al.*, 2008). Droplets of such a small diameter are useful for encapsulating single cells, which in this case were then sorted for down-stream applications. Encapsulated single cells may be useful for implantation as the diffusion barrier created by the matrix would be greatly reduced. Data summarised in Table 1.3 shows that all of the methods which can produce spherical beads can produce bead samples with size distributions <5.5% CV, typically <2.5% CV.

1.12.3.2 Production of large volumes of encapsulated cells in a short time period

In comparison to previously described nozzle-based methods (Section 1.9), size distribution of produced beads does not increase when microfluidic systems are scaled up as circuits are identical, merely run in parallel. The ability of microfluidic devices to be run in parallel has been illustrated by Nisisako and Torii (2008); their 128-circuit device was capable of producing acrylate beads with a diameter of 96μm and a CV of 1.3%. Beads were produced at a rate of 320 ml/h, proving that microfluidic devices are suitable for generating large batches of small, monodisperse beads. Using Nisisako and Torii's device, 1L of beads would take 3 hours to produce. None of the methods discussed previously (Section 1.9) were seen to be capable of producing beads of this diameter. The smallest bead size produced was 160μm in

diameter, using electrostatic jet break-up (Table 1.2, Section 1.10.4). It would take 31 hours to produce 1L of beads this size.

1.12.3.3 Sterile production method

Devices incorporating microfluidic channels are necessarily sealed, therefore they are easily kept sterile. Many materials used in the production of microfluidic devices can be sterilised, for example polydimethylsiloxane (PDMS) can be sonicated in ethanol and then exposed to UV (Gomez *et al.*, 2007). Most microfluidic devices are small; even the multichannel device (previously described) with 128 circuits running in parallel only measures $4cm^3$ (Nisisako and Torii, 2008). Devices of this scale can easily be operated inside a sterile hood, thus removing the need for additional modifications to ensure sterility. By incorporating filters into microfluidic devices, solutions can be sterilised on-chip (Mohamed *et al.*, 2004; Crowley and Pizziconi, 2005; VanDelinder and Groisman, 2006; VanDelinder and Groisman, 2007).

1.12.3.4 Non-toxic encapsulation process

As most encapsulation polymers are aqueous in nature, a non-aqueous carrier fluid is required to promote segmented flow and thus produce droplets. Oils and organic solvents are often used as carrier fluids. As previously stated (Section 1.10.2) many oils and organic solvents are toxic to mammalian cells. However, the use of microfluidic processes can help to overcome the deleterious effects of the carrier fluids chosen. As each droplet is produced individually and transported along the same circuit, each undergoes the same chemical treatment for the same length of time. These features can be exploited to ensure that droplets, and hence cells within them, are exposed to chemicals for equivalent, minimal periods. Nonetheless, successful encapsulation of viable cells through use of microfluidic techniques has been reported rarely. Those that have will be discussed in the following section (Section 1.12.4).

1.12.4 Use of microfluidic devices to encapsulate cells

Prior to this study, microfluidic devices had been used to encapsulate cells within liquid droplets. He *et al.* (2005) encapsulated cells and single organelles into picolitre- and femtolitre-volume droplets using microfluidic circuits. However, these droplets were not hardened to make beads and maintaining cell viability was not their aim; rather they sought to carry out further analytical tests on the cells/organelles after

lysing them within their droplet. Tan *et al.* (2006a) also used microfluidic devices to encapsulate cells and proteins, this time within lipid vesicles. Viability of HeLa cells was shown for over two hours, but no further time points were reported. The produced lipid vesicles were reported to be stable for more than 26 days.

Of the methods discussed in the previous section (Section 1.12.2); very few groups have successfully encapsulated live cells. Shintaku *et al.* (2007) encapsulated mouse erythroleukemia (MEL) cells in alginate, but presented no viability data. Choi *et al.* (2007) successfully encapsulated GFP-expressing yeast cells in alginate, which were shown to still express GFP after encapsulation, but no long term viability study was carried out. GFP expression is not the most accurate or reliable way of demonstrating cell viability as GFP can still be observed in dead, fixed samples (Chalfie *et al.*, 1994). Given its cytotoxicity, it is doubtful that cells encapsulated using hexadecane would survive. Tan and Takeuchi (2007) encapsulated viable Jurkat cells using internal gelation of alginate, but no long term viability data was reported. Kim *et al.* (2009) successfully encapsulated mouse stem cells (P19 EC), HepG2, and human breast cancer cells (MCF-7) in alginate beads and reported viability 0, 3 and 7 days after encapsulation. It should be noted that all of these reports were published after the start of this project.

1.12.5 Microfluidic experiments performed with a MicroPlant™

This project makes use of a unique platform allowing rapid evaluation of microfluidic circuits and junctions. The microfluidic device used was developed by Q Chip (Cardiff, UK), based on a patent by Professor David Barrow (Barrow *et al.*, 2002). In contrast to many other microfluidic systems, polytetrafluoroethylene (PTFE), a rigid and hydrophobic plastic, is utilised for microfluidic chip synthesis. PDMS is the substrate of choice for many groups fabricating microfluidic devices. This is due, in part, to its favourable hydrophobic properties, its relatively low cost and standardisation of the soft-lithography technique utilised to produce microchannels in this substrate. However, synthesis of such devices takes a minimum of eight hours (Zhao *et al.*, 2003). In addition, as the devices are permanently sealed, any blockage of channels (which can occur rapidly after commencement of an experiment) results in unusable devices.

Through use of PTFE as a material for microfabrication of devices, the multi-step lithography process can thus be avoided, and substituted by a single, automated

micro-machining operation. This method allows microfluidic features composed of microchannels with square or rectangular cross-sections. Microchannels with dimensions of 100μm or greater can be produced. Typically, a microfluidic device of this kind, containing multiple parallel circuits can be produced within sixty minutes. In addition, by avoiding a permanently sealed cover, a compression-sealed PTFE device may be dismantled, cleaned and reassembled as required. This is particularly useful in cases of accidental experimental failure (e.g., channel blockage due to unwanted polymer cross-linking), allowing rapid recovery during testing and optimisation of conditions, which would be impossible in PDMS/PMMA/glass devices.

In 2005, the microfluidic evaluation platform used in this project had previously been used for the generation of cross-linked hydrogel beads, composed of PVA (polyvinyl alcohol), PEGDM (poly(ethylene glycol) dimethacrylate) or HEMA (hydroxyethyl methacrylate). All these hydrogel beads were formed *via* a photochemical cross-linking method. A photo-initiator is added to the polymer solution, which is then segemented to produce droplets. When the droplets are illuminated with UV light (~350nm), the photoinitiator undergoes homolytic cleavage, which produces two radical-bearing intermediates, these go on to initiate the cross-linking reaction and crosslink the polymer within the droplet. Exposure of cells to UV light is inappropriate and so the developed methods were not applicable to encapsulation of cells. A purpose-made microfluidic device for ionotropic gelation, or manipulation of polysaccharides or cells was not available and thus, this project was established to develop a microfluidic method for cell encapsulation.

1.13 AIMS

Currently there is much interest surrounding encapsulated cells. Alginate has emerged as the polymer of choice, for several reasons; alginate is biocompatible and biodegradable, as well as requiring an innocuous cross-linking reaction. However, challenges remain to be solved before a satisfactory production method is found. For example; cells must be completely covered by the polymeric matrix, the capsules produced must be consistently small and in large volumes. Although there are currently many production techniques for encapsulating cells, no single method can solve these challenges.

The overall aim of this project was to develop a microfluidic method to encapsulate dopamine releasing cells in an alginate matrix, determine their viability *in vitro* and investigate implantation into a rodent model of Parkinson's disease. This process took part in several stages:

AIM 1: to develop a microfluidic process to generate alginate beads encapsulating cells and to evaluate the short and long term impact of this process on cell viability.
Prior to this study alginate solutions were segmented using microfabricated arrays within a macro-scale device (Sugiura *et al.*, 2001) but there were no methods using microfluidic devices to encapsulate cells. Several viability methods were investigated to determine their suitability for use with encapsulated cell systems. The acute and long term effects of the developed microfluidic encapsulation process on cells were examined.

AIM 2: to validate the encapsulation process with therapeutically relevant cells (PC12) and determine dopamine release.
Initial encapsulation experiments were carried out with a rapidly dividing epithelial cell line; Human Embryonic Kidney 293 (HEK293). Upon successful development of a microfluidic encapsulation protocol using HEK293 cells, a therapeutic cell line, PC12, was encapsulated. Measurement of the levels of the therapeutic molecule dopamine, produced by PC12 cells, ensured that the developed microfluidic encapsulation method did not adversely affect cells.

AIM 3: to modify the microfluidic method developed in the previous steps to produce smaller beads suitable for cannula implantation and determine their *in vivo* stability.
Use of encapsulated PC12 cells in a rodent model of Parkinson's disease required that beads were small enough to be implanted through a cannula with a 300μm inner diameter. To manufacture beads <200μm in diameter, modifications were made to the developed microfluidic system and cell processing. Stabilisation of the resultant beads was investigated to ensure beads would persist in the brain for more than 6 weeks. Stabilisation was carried out by i) barium cross-linking and ii) secondary coating with polycations. The resultant beads were implanted into rats to investigate *in vivo* stability. The internal structure of alginate beads produced using the developed microfluidic method was also elucidated.

Chapter 2. Materials and Methods

2.1 MATERIALS

2.1.1 Alginate

Pronova UltraPure alginate was purchased from NovaMatrix™ (Drammen, Norway). This medical grade alginate is ultrapure with low endotoxin levels and low protein contamination. Viscosity can be controlled by changing the molecular weight of the alginate used. Pronova UltraPure medium viscosity, high mannuronate (UP MVM) alginate has a molecular weight of 200,000 – 300,000 g/mol and was composed of 57% mannuronate units with a viscosity of 254 mPa·s at 20°C. Pronova UltraPure medium viscosity, high guluronate (UP MVG) alginate has a molecular weight of 200,000 – 300,000 g/mol and was composed of 31% mannuronate units with a viscosity of 318 mPa·s at 20°C.

2.1.2 Carrier fluid

High oleic acid sunflower oil was used in all experiments as it is inexpensive to obtain in large quantities, from a batch traceable source (Statfold, Staffordshire, UK). Sunflower oil can also be sterilised using heat.

2.1.3 Cross-linker

Microcrystalline precipitated calcium carbonate (a gift from Specialty Minerals, Birmingham, UK); with an average particle size of 0.07μm (Figure 2.1) was used in all experiments.

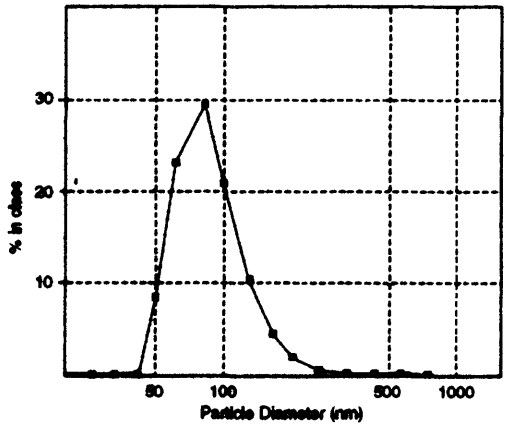

Figure 2.1: Particle size distribution of microcrystalline precipitated calcium carbonate. Supplied by Specialty Minerals, Birmingham, UK

Supplier	Reagent
Autogen Bioclear, Wiltshire, UK	Foetal bovine serum
Greiner, Stonehouse, UK	Culture flasks/dishes and disposable plastics
Biotech-IgG, Winslow, UK	Dopamine research EIA (ELISA kit)
Invitrogen, Paisley, UK	LIVE/DEAD viability assay RPMI medium D-MEM/F12 0.05% Trypsin/EDTA Donor Horse serum (Heat inactivated) 10,000U/ml Penicillin & 10,000µg/ml Streptomycin in 85% saline alamarBlue™
Sigma Chemicals, Dorset, UK	0.4% Trypan blue MTT assay Flouresceinamine ($C_{20}H_{13}NO_3$, mixed isomers) Poly-L-ornithine hydobromide (MW 5-15 kDa) Poly-l-lysine hydrobromide (MW 4-15 kDa) FITC-labelled Poly-l-lysine (MW 30-70 kDa (high MW) or 15-30 kDa (low MW)) Procion Blue 4 Rhodamine B All other chemicals
AbCellute, Cardiff, UK	Hepatocytes
Lonza, Cambridge, UK	Phosphate Buffered Saline
Partec, Kent, UK	CellTrics® (30 and 150µm)
BD Biosciences, Oxford, UK	Cell Strainers (100µm)
Medicell, London, UK	Dialysis membranes (12-14 kDa)

2.1.4 Solutions

2.1.4.1 Artificial cerebrospinal fluid (CSF)

Solution A

Compound	g/L
NaCl	17.32
KCl	0.448
$CaCl_2 \cdot 2H_20$	0.412
$MgCl_2 \cdot 6H_20$	0.326

Solution B

Compound	g/L
$Na_2HPO_4 \cdot 7H_20$	0.214
$NaH_2PO_4 \cdot H_20$	0.027

Solutions were autoclaved separately and then combined in 1:1 ratio. Electrolyte concentrations of the resultant solution are shown in Table 2.1.

Ion/Compound	Cerebrospinal fluid (mM)*	Artificial CSF (mM)
Na	154	150
K	3.0	3.0
Ca	1.4	1.4
Mg	0.9	0.8
P	0.4	1.0
Cl	136	155
HCO_3	24.1	N/A

* Concentrations are an average of values for human, dog, cat and rabbit taken from an average of data listed in Davson (1967) and Altman and Dittmer (1974)

Table 2.1: Comparison of real and artificial CSF electrolyte concentrations

2.1.4.2 TRIS-buffered saline

Compound	g/L
Trizma base	48
NaCl	36

pH was adjusted to 7.4 using hydrochloric acid.

2.1.4.3 Cresyl violet

Compound	
Cresyl violet	5g in 600ml distilled water
1M sodium acetate	600ml
Glacial acetic acid	340ml

2.2 BEAD-BASED METHODS

2.2.1 Microfluidic experiments

The microfluidic device used in all experiments (MicroPlant™) consists of a 316 stainless steel manifold into which HPLC fluid connectors (Anachem, Bedfordshire, UK) are introduced equatorially. Vertical through holes were sealed with nitrile rubber O-rings (Sealmasters, Cardiff, UK), allowing fluid to flow to the top surface of a virgin PTFE disc (50mm diameter x 3mm thickness) located on the manifold. A circular PFA gasket (250μm thickness; Polyflon, Staffordshire, UK) was placed in between the PTFE chip (Polyflon, Staffordshire, UK) and a borosilicate glass disc cover (50mm diameter x 5mm thickness; H Baumbach, Suffolk, UK). A 316 stainless steel clamping piece was bolted to the fluidic manifold, allowing the entire laminated assembly to be compression sealed. Fluids were introduced into the microfluidic circuit *via* sterile $1/16^{th}$ inch inner diameter Teflon-FEP tubing (Anachem, Bedfordshire, UK) using syringe drivers (KD Scientific - Linton Instrumentation, Norfolk, UK).

The development of a microfluidic method for production of alginate beads is described and discussed in detail in Chapter 3. As the main aim of this thesis was the development of the microfluidic process it was felt that this was a more appropriate location than this chapter. Specific details for encapsulation of cells using the chosen microfluidic method can be found in Section 3.3.3.

In all cell encapsulation experiments, the stainless steel manifold, glass, gasket, fittings and PTFE chip were autoclaved and then air dried in an oven at 50°C. Syringe drivers were cleaned with bactericidal wipes before being placed in a Class II hood to maintain sterility. All cell encapsulation experiments were carried out in a Class II hood.

2.2.2 Manufacturing microfluidic chips

Microchannels were machined into virgin PTFE discs using a Computer Numerical Controlled milling machine (Roland, Swansea, UK). An example of a milled chip is shown in Figure 2.2A. Microfluidic circuit diagrams (an example is shown in Figure 2.2B) used to mill each chip are presented in Appendix 1 along with details of channel geometry.

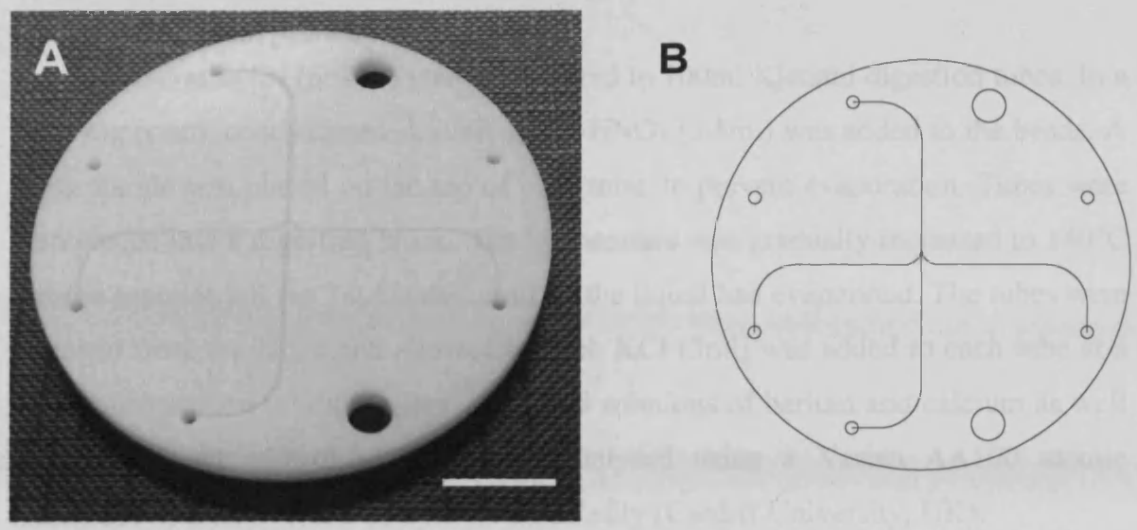

Figure 2.2: A PTFE chip with a milled microfluidic circuit. A) Photograph of an example microfluidic chip. Scale bar represents 1cm. B) Circuit diagram of the microfluidic chip shown in A

2.2.3 Measuring bead diameter

Beads were measured from a representative sample of each bead type. Beads from all experiments were not measured so there is no indication of batch to batch variability. A small volume of beads were placed on a microscope slide with sufficient buffer to form a single layer. Photographs of beads were taken using a light microscope equipped with a camera (Motic, Microscopes Plus Limited, London, UK). Sphere diameters were measured using calibrated Motic software tools. The coefficient of variation (CV) was calculated as shown in Equation 2.1.

$$CV = \frac{\text{standard deviation}}{\text{mean diameter}} \times 100 \qquad \textbf{Equation 2.1}$$

2.2.4 Viscosity measurement

Viscosity was measured using a vibrational viscometer (SV-10, Patterson Scientific, Cambridge, UK). The device has two gold plated paddle-shaped sensors which were immersed into the sample to be measured (35-45ml depending upon viscosity). The paddles vibrate at a constant frequency when stimulated by an electromagnetic drive. Constant amplitude is maintained by the electromagnetic drive in response to the amplitude of vibration. The vibration is dampened by the viscosity of the sample. The current required to maintain the vibration amplitude is monitored and converted to viscosity at a given temperature.

2.2.5 Atomic absorption spectroscopy

Bead samples (n=450) were transferred to 100ml Kjedahl digestion tubes. In a fume cupboard, concentrated AnalaR-grade HNO_3 (3.5ml) was added to the beads. A glass marble was placed on the top of each tube, to prevent evaporation. Tubes were then placed into a digestion block. The temperature was gradually increased to 140°C and the samples left for 2-2.5 hours until all the liquid had evaporated. The tubes were removed from the block and allowed to cool. KCl (3ml) was added to each tube at a final concentration of 2000µg/cm^3. Standard solutions of barium and calcium as well as samples and control samples were analysed using a Varian AA100 atomic absorption spectrophotometer by Mr M. O'Reilly (Cardiff University, UK).

2.2.6 Secondary coating of alginate beads with polycations

Calcium cross-linked alginate beads were produced using the microfluidic internal gelation method (Section 3.3.3). Poly-L-lysine (PLL) and poly-L-ornithine (PLO) solutions (0.05% w/v) were prepared in PBS; alginate solutions (0.15% w/v) were prepared with D-MEM/F12 medium. PLL or PLO solution (twice bead volume) was added to beads for 10 minutes with agitation. Beads were added to 100µm filters; Phosphate Buffered Saline (PBS, 10ml) was added four times to wash off excess coating solution. A secondary coat of alginate was added by placing beads into alginate solution (twice bead volume) for 5 minutes. Washes were again carried out four times by washing PBS (10ml) over beads placed on 100µm filters.

2.2.7 Determination of pH of carrier phase

Carrier phase (2ml sunflower oil, Section 2.1.2) was mixed with an equal volume of HBSS (Hank's Buffered Saline Solution). An approximate pH of the medium was gained using narrow-range pH paper (pH 3-7).

2.2.8 Fluorescently labelled alginate

Alginate was labelled with the fluorochrome fluoresceinamine using a method adapted from Strand *et al.* (2003). Briefly, sodium alginate was dissolved in PBS (pH 7.2 – 7.4) to give ~90mM carboxylic groups. 1-Ethyl-3-(3-imethylaminopropyl) carbodiimide hydrochloride (EDC) and N-hydroxysulfosuccinimide sodium salt (Sulfo-NHS) were then added to give 9mM of each. The solution was stirred for 2 hours at room temperature. Fluoresceinamine was added to give a final concentration of 0.6mM and the solution was stirred, protected from light, at room temperature for 18 hours. To remove fluoresceinamine which had not reacted, the solution was

transferred to dialysis membranes (MWCO 12,000-14,000) and dialyzed against ion-free water overnight at 4°C (1 shift). The solution was then dialyzed against 1M NaCl for 24 hours (3 shifts) and finally against ion-free water until the water was no longer yellow (~5 shifts). The solution was adjusted to pH 7.4 before being freeze-dried. Fluorescence labelled alginate was kept at 4°C, protected from light until use.

2.2.9 Confocal microscopy

A Leica DM6000B upright confocal microscope was used for all confocal microscopy experiments.

2.2.9.1 Analysis of fluorescent beads with confocal microscopy

An argon 488nm laser was used for excitation of the fluorescein-labelled alginate and FITC-labelled PLL, and emission light between 505 and 530nm was detected. Beads were scanned through the equator. The images were taken at constant laser power, and were optimised to the dynamic range of the detectors used.

2.2.10 Production of alginate beads with air-assisted droplet break-up

A method for the production of alginate beads cross-linked using external gelation was adapted from Fiszman *et al.* (2002). Briefly, a 21 gauge needle was adapted by making the end blunt and removing the plastic hub. A T-shaped fluid connector was used to hold the adapted 21 gauge needle in place. A liquid alginate solution (2% w/v) was pumped through the needle using a syringe driver (20ml/h). Air was forced through the remaining arm of the T-shaped fluid connector and past the needle (Figure 2.3). The airflow was empirically determined as it could not be measured with the equipment used. A beaker containing $CaCl_2$ (50mM) collecting solution was placed 6cm below the tip of the needle.

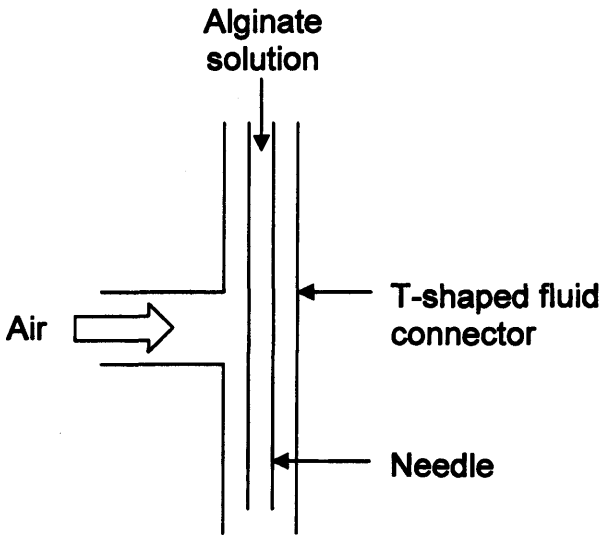

Figure 2.3: Schematic of homemade device for producing alginate beads *via* air-assisted droplet break-up. A cross-section through the homemade device, showing the needle position. Alginate solution (2% w/v) was pumped through the needle and air was forced to flow around it

2.3 *IN VITRO* METHODS

2.3.1 Cell culture methods

2.3.1.1 Maintenance of cell lines in culture

Routine cell culture work was carried out under laminar flow in a Class II hood (MDH, Andover, Hampshire, UK). Cells were maintained at 37°C in a hydrated atmosphere of 5% CO_2 and air in appropriate medium. Human Embryonic Kidney (HEK293) cells (American Type Culture Collection, CRL-1573) were maintained in Dulbecco's modified Eagle medium: Nutrient Mixture F12 (D-MEM/F12) supplemented with 10% foetal bovine serum (FBS). PC12 (ATCC, CRL-1721, a gift from Dr Jack Ham at the Centre for Endocrine and Diabetes Sciences, Cardiff University, UK) were grown in D-MEM/F12 supplemented with 5% foetal calf serum and 10% heat-inactivated horse serum. Serum was supplied heat inactivated (to inactivate complement) and was of foetal origin so that levels of antibodies (which may bind to human cells) would be low. Penicillin (10,000 units per ml) and streptomycin (10,000 μg per ml) were also added to all medium. All medium was stored at 4°C until use, when it was warmed to 37°C to prevent temperature shock of cells.

2.3.1.2 Sub-culturing of cells

The cell line HEK293 was routinely passaged weekly when growth had achieved confluence using 0.02% trypsin/0.05% EDTA in PBS. Culture medium was removed and cells rinsed with pre-warmed (37°C) trypsin/EDTA (0.5ml). This was removed and further enzyme (1ml) added to the flask. Cells were incubated for 2-3 minutes at 37°C to allow detachment of cells into a single-cell suspension. After incubation, enzymatic action was terminated through the addition of serum-containing medium (3ml). Gentle pipetting was used to disperse any clumps of cells and cells were then divided at a ratio of approximately 1:8 into new T-75 flasks before media was replenished (final volume 25ml).

The PC12 cell line was routinely passaged when growth had achieved confluence by scraping cells from the flask surface with a cell scraper. Approximately 1/3 to 1/2 of the cell suspension was removed and discarded. New medium was added to a final volume of 25ml.

2.3.1.3 Freezing and thawing cells

To preserve stocks of cells, samples were harvested (see Section 2.3.1.2), pelleted by centrifugation at 100 x g, washed and resuspended in foetal bovine serum with 10% sterile DMSO at a concentration of 10^6 cells/ml (calculated as described in Section 2.3.1.4). The DMSO added interacts with plasma membranes and reduces cell lysis upon freezing. Cell suspensions (1ml) were pipetted into a cryovial (Fisher, Leicestershire, UK) and then frozen to –70°C in a container filled with isopropanol, which is specially designed to cool at a rate of less than 1°C per minute (Fisher, Leicestershire, UK). Once frozen (overnight) cell vials were placed into liquid nitrogen and stored until required.

Recovery of cells was achieved by removing a vial of cells stored in liquid nitrogen, which were then warmed rapidly by placing in a 37°C water bath. Cells were then diluted into culture medium prewarmed to 37°C, doubling the volume every 4 minutes until the volume was increased to 20ml. Cells were pelleted by centrifugation at 100 x g, resuspended into medium (2ml), placed into a $25cm^2$ flask and cultured for at least 24 hours at 37°C in a hydrated atmosphere of 5% CO_2 and air.

2.3.1.4 Counting of total cell numbers and number of viable cells

After enzyme disaggregation, cell suspensions were counted using a haemocytometer. Haemocytometer counting allowed not only the counting of cells in suspension under phase contrast microscopy, but the percentage of viable (intact) cells to be determined using the dye exclusion method (described below).

A haemocytometer is a modified microscope slide comprising two polished surfaces, each of which displays a precisely ruled, sub-divided grid (Figure 2.4). The grid consists of nine primary squares, each measuring 1mm on each side (area $1mm^2$) and limited by three closely spaced lines (2.5μm apart). Each of the primary squares is further divided into secondary squares, each measuring 0.2mm on each side (area $0.04mm^2$). The plane of the grid rests 0.1mm below two ridges that support a sturdy coverslip. There are bevelled edges at both sides of each polished surface where cell suspension is added which is subsequently drawn across the grid by capillary action.

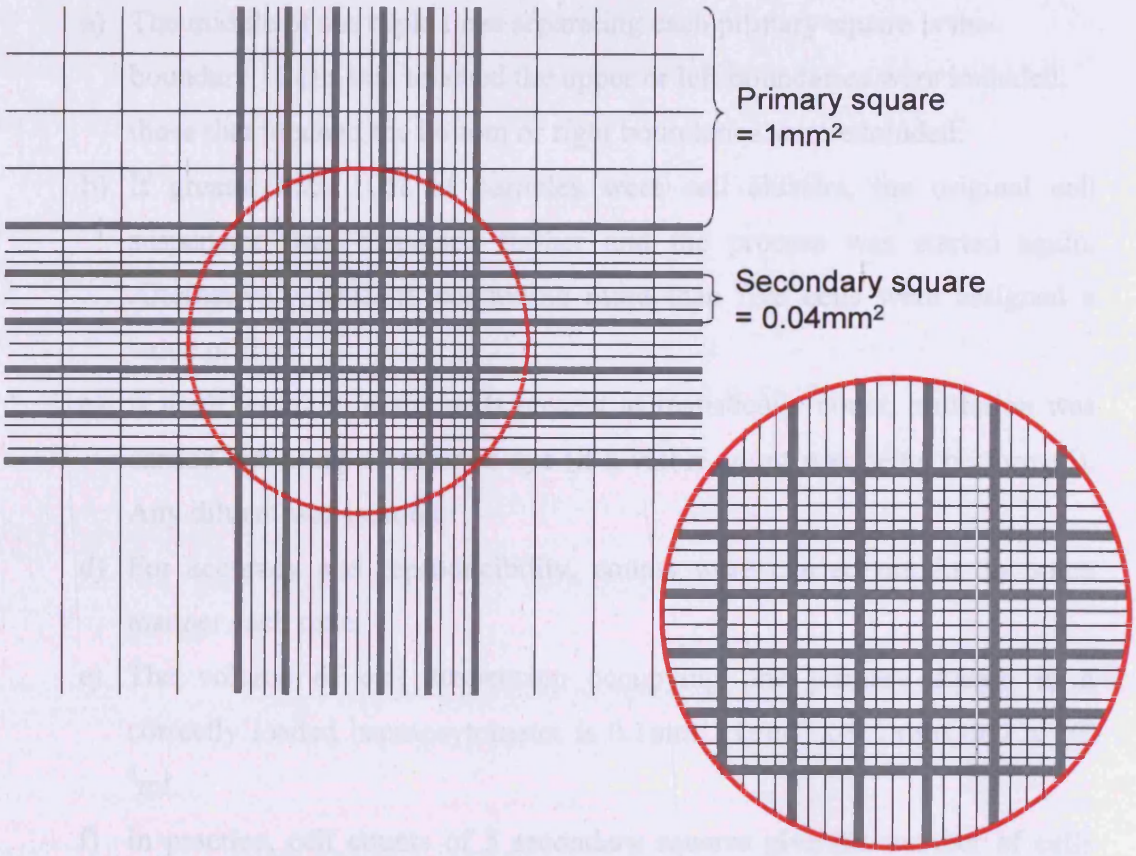

Figure 2.4: Grid patterns of Neubauer ruled haemocytometer. The figure shows the size of primary and secondary squares, with the inset showing an enlargement of the secondary squares. The number of cells in 5 secondary squares is counted

To carry out a total cell count, cells were trypsinsed as described in Section 2.3.1.2. Cells were pelleted by centrifugation at 100 x g for 5 minutes at room temperature and resuspended in an appropriate volume of medium ensuring a unicellular suspension. The haemocytometer and cover slip were then cleaned using 70% ethanol and the coverslip placed squarely on top of the haemocytometer, lightly moistening the polished surface of the slide before pressing the coverslip into position. Cells were gently redistributed throughout the medium as before and a small sample of cells taken up into the pipette. The haemocytometer was loaded so that the fluid entirely covered the polished surface of each chamber. Care was taken not to overload the counting chambers. Any accidental overloading was rectified by carefully removing any excess fluid from the groove using filter paper. Using the 20X objective of the microscope, the upper left primary square of each grid was located. The number of cells in 5 secondary squares were counted using the following conventions:

a) The middle of the triple lines separating each primary square is the boundary. Cells that touched the upper or left boundaries were included, those that touched the bottom or right boundaries were excluded.
b) If greater than 10% of particles were cell clusters, the original cell suspension was dispersed further and the process was started again. Alternatively, clusters containing more than five cells were assigned a value of five.
c) If there were too many cells present to realistically count, a dilution was carried out using a buffer or dye (if a viable count was being performed). Any diluent was isotonic.
d) For accuracy and reproducibility, counts were carried out in the same manner each time.
e) The volume of cell suspension occupying one primary square in a correctly loaded haemocytometer is $0.1mm^3$ ($1mm^2$ x 0.1mm) or 1×10^{-4}ml.
f) In practice, cell counts of 5 secondary squares give the number of cells within $0.02mm^3$ ($5 \times 0.004\ mm^3$) or 2×10^{-5}ml. Total cell concentration in the original suspension (in cells/ml) is then:

Cells/ml = total count x 50,000 x dilution factor

To determine the approximate number of viable cells by dye exclusion, an aliquot of cells was mixed with a volume of buffer or balanced saline containing a water-soluble (membrane lipid-insoluble) dye (e.g. trypan blue) which is visible when it leaks into cells that have damaged plasma membranes.

An aliquot (5µl) of cell suspension was mixed with trypan blue solution (5µl). The haemocytometer was prepared and loaded as previously described in this section. Unstained (viable) cells and stained (non-viable) cells were counted using the conventions listed above and the following equation:

$$\text{Percentage viable cells} = \frac{\text{number of unstained cells counted}}{\text{total cell count}} \times 100 \qquad \textbf{Equation 2.2}$$

2.3.2 Reactivating hepatocytes

Hepatocytes and all solutions were supplied in 100mm Petri dishes by AbCellute (Cardiff, UK). Reactivation medium (3ml) was added to each Petri dish, which was then incubated for 20 minutes in a humidified 37°C incubator without CO_2. When cells were freely in suspension, they were transferred into sterile 50ml centrifuge tubes. Wash medium (2ml) was added to each Petri dish, which was then manually rocked from side to side to release any residual cells. This wash solution was added to cells in the centrifuge tubes. The suspension was centrifuged at 100 x g for 4 minutes. The supernatant was removed without touching the cell pellets. Cells were washed using wash medium and resuspended by gentle pipetting through a 5ml pipette tip. The cells were re-pelleted and resuspended in hepatocyte medium ready for use.

2.3.3 Cytotoxicity testing

Cells were harvested, washed and counted as described in Sections 2.3.1.2 and 2.3.1.4. Cells were pipetted into an appropriate number of tubes and pelleted by centrifugation at 100 x g. Medium was removed and replaced with the substance to be tested, into which cells were gently resuspended. At timed intervals as stated in the relevant sections, aliquots (20µl) were removed from tubes and mixed with trypan blue (20µl), then counted as described in Section 2.3.1.4. If oil was the substance being tested, trypan blue (20µl), medium (20µl) and oil plus cells (20µl) were added to a separate eppendorf and mixed. The cells moved into the aqueous phase, which was then added to the haemocytometer and counted.

2.3.4 Viability methods

2.3.4.1 Use of MTT (3-(4,5-Dimethylthiazol-2-yl)-2,5-diphenol tetrazolium bromide) for viability testing

MTT (3-(4,5-Dimethylthiazol-2-yl)-2,5-diphenol tetrazolium bromide) assay was purchased from Sigma and used according to the manufacturers' instructions. Briefly, each vial of MTT (15mg) was resuspended in culture medium (3ml). Reconstituted MTT (10% of culture volume) was added to cells or beads and incubated for 2 hours at 37°C, 5% CO_2. Formazan crystals were dissolved by adding MTT Solubilization Solution (at a 1:1 ratio with original culture volume). Absorbance was subsequently measured at a wavelength of 570 nm. Absorbance was used to compare rates of cell growth.

2.3.4.2 Use of lactate dehydrogenase (LDH) for viability testing

A lactate dehydrogenase (LDH) based *in vitro* toxicology assay kit (Sigma) was used to estimate LDH released by dead cells. Briefly, cells were harvested, washed and counted as described in Sections 2.3.1.2. and 2.3.1.4. A standard curve of cells was prepared by 2-fold dilution between 1 x 10^6 cells/ml and 7.81 x 10^4 cells/ml in 100µl of medium in a 96-well plate. LDH Assay Lysis Solution (10µl) was added to each well in the prepared standard curve and the plate returned to the incubator for 45 minutes. Cells were pelleted by centrifugation at 100 x g for 4 minutes. Medium (50µl) was removed from each well containing the standard curve and transferred to a fresh 96-well plate. An equal amount of LDH assay substrate, cofactor and dye solutions were mixed together and added to each well of the plate (final volume of 150µl). The plate was left at room temperature, protected from the light for 30 minutes. Absorbance was measured at a wavelength of 490nm, with background at 690nm subtracted.

2.3.4.3 Use of alamarBlue™ for viability testing

The assay was purchased from Invitrogen and carried out according to manufacturers' instructions. Briefly, varying numbers of beads were counted into separate wells of a 96-well plate in 100µl of medium. Each well received 10µl of alamarBlue™. The plate containing beads and alamarBlue™ was incubated for 24 hours at 37°C, 5% CO_2. Samples were taken from the plate at 0, 2, 4, 6, 8, 16 and 24 hours, added to a separate plate from which spectrophotometric readings (at 540nm

and reference at 620nm) were taken. A correction factor (R_O) was calculated, as shown in Equation 2.3, as the filters used were slightly different to those suggested (570nm and reference at 600nm). However, as this is a common issue, the manufacturers recommend a correction factor to calculate the percentage of reduced alamarBlue™ present (Equation 2.4).

$$R_O = AO_{540} / AO_{620} \qquad \textbf{Equation 2.3}$$

$$AR_{540} = A_{540} - (A_{620} \times R_O) \times 100 \qquad \textbf{Equation 2.4}$$

Where R_O = correction factor, AO_{540} = absorbance of oxidised alamarBlue™ at 540nm, AO_{620} = absorbance of oxidised alamarBlue™ at 620nm, AR_{540} = percentage of reduced alamarBlue™, A_{540} = absorbance at 540 nm, and A_{620} = absorbance at 620nm.

2.3.4.4 LIVE/DEAD® viability/cytotoxicity kit

Cells were detached from culture flasks using trypsin, washed and counted as described in Sections 2.3.1.2. and 2.3.1.4. Cells were passed through a 30μm CellTrics strainer to remove any clumps of cells or large debris and resuspended at a cell count of between 0.1 to 5 x 10^6 cells/ml in D-MEM/F12 (1ml). Beads were removed from medium by passing through a 30μm CellTrics strainer. As serum contains esterases, which can interfere with this analytical method; any remaining serum was removed by washing, and replaced with medium. Calcein AM stock solution (supplied at 4mM in DMSO by Invitrogen) was diluted to 50μM in DMSO. Diluted calcein AM (2μl, final concentration 2μM) and ethidium homodimer-1 stock solution (4μl, supplied at 2mM in DMSO by Invitrogen, final concentration 4μM) were added to cells (1ml) or bead samples and mixed by gentle inversion. Cells or bead samples were incubated for 20 minutes at room temperature, then analysed. Calcein fluoresces green (479nm excitation and 517nm emission) and ethidium homodimer-1 fluoresces bright red (528nm excitation and 617nm emission, Figure 2.5).

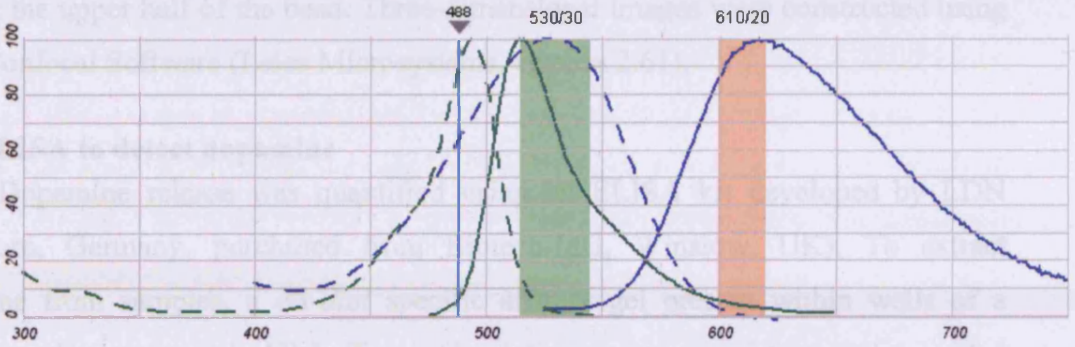

Figure 2.5: Absorption and fluorescence emission spectra of dyes used in LIVE/DEAD® staining. Green lines show absorption and fluorescence emission spectra of calcein in pH 9.0 buffer and dark blue lines show absorption and fluorescence emission spectra of ethidium homodimer-1 bound to DNA. The light blue line marked 488 represents the excitation wavelength of the laser (488nm). Green shading represents the 530nm bandpass filter used to collect fluorescence from calcein and the light orange shading represents the 610/20nm longpass filter used to collect fluorescence from ethidium homodimer-1

2.3.4.5 Flow cytometry to detect and quantify cell numbers

Cell samples were analysed using a FACSCanto flow cytometer (Beckton Dickinson, Oxford, UK); where they were focussed into a fluid stream one cell wide. Cells then passed through a laser one at a time. Voltage fluctuations caused by cells passing through the laser beam were converted to digital form and analysed automatically *via* computer to generate dot-plot displays indicating the fluorescent characteristics of the cell sample being analysed. Output data from the flow cytometer was analysed using Win MDI software which presents data as dot plots and histograms and permits calculation of the mean fluorescent intensity of the cells.

To analyse the stained cells, 30,000 events were captured for each sample using a FACSCanto flow cytometer. Constant machine settings were maintained during each experiment. An argon 488nm laser was used for excitation. Green fluorescence emission for calcein (530/30nm bandpass filter) and red fluorescence emission for ethidium homodimer-1 (610/20nm longpass filter) was measured. The data was transferred to a computer with the Win MDI software.

2.3.4.6 Analysis of LIVE/DEAD stained cells with confocal microscopy

An argon 488nm laser was used for excitation of calcein and emission light between 505 and 530nm was detected. A HeNe 543nm laser was used for excitation of Ethidium homodimer-1 and emission light over 650nm detected. Due to limited passage of fluorescent light through the alginate beads, optical sections were taken

through the upper half of the bead. Three-dimensional images were constructed using Leica Confocal Software (Leica Microsystems, version 2.61).

2.3.5 ELISA to detect dopamine

Dopamine release was quantified using an ELISA kit developed by LDN (Nordhorn, Germany, purchased from Biotech-IgG, Winslow, UK). To extract dopamine from samples, a *cis-diol* specific affinity gel present within wells of a microtitre plate was used. All buffers and solutions were proprietary and provided with the kit. Sample (100µl), standards (10µl) and controls (10µl) were added to wells containing *cis-diol* specific affinity gel. All wells were made up to a final volume of 100µl with distilled water. Assay (25µl) and extraction buffers (25µl) were added to the wells. The microtitre plate was covered and incubated whilst shaking (600rpm) for 30 minutes at room temperature. The wells were washed twice with wash buffer (300µl). Acylation of dopamine to N-acyldopamine was carried out by adding acylation buffer (150µl) and reagent (10µl) to the wells. The acylation reaction was allowed to proceed for 15 minutes with shaking (600rpm) at room temperature. The wells were washed twice with wash buffer (300µl). Dopamine was eluted from the wells using hydrochloric acid (0.025M, 50µl). Eluate (40µl) was removed from the wells after 10 minutes incubation at room temperature with shaking (600rpm) and used in the dopamine enzyme immunoassay.

Dopamine was bound to the solid phase of the provided microtitre plate. Enzyme solution (containing the enzyme catechol-O-methyltransferase and coenzyme S-adenosyl-methionine, 25µl) and extracted samples, controls and standards (40µl each) were added to the microtitre plate. During a 30 minute incubation, with shaking (600rpm), at room temperature the N-acyldopamine was converted to N-acyl-3-methoxytyramine. Acylated dopamine from the sample and solid phase bound dopamine competed for a fixed number of antiserum binding sites introduced by adding dopamine antiserum (50µl) and antiserum buffer (50µl). After incubating the microtitre plate for 2 hours at room temperature with shaking (600rpm), any free antigen and free antigen-antiserum complexes were removed by washing three times with wash buffer (300µl). The antibody bound to the solid phase dopamine was detected using an anti-rabbit IgG-peroxidase conjugate (100µl) using TMB (tetramethyl benzidine, 100µl) as a substrate. After 1 hour incubation at room temperature with shaking (600rpm), stop solution (100µl) was added. Absorbance of

the solutions in the wells was read using a microplate reader set to 450nm with a reference wavelength of 630nm. The amount of antibody bound to the solid phase dopamine was inversely proportional to the amount of dopamine present in the sample. The amount of dopamine was calibrated from a standard curve based on standards provided in the kit.

2.4 *IN VIVO* METHODS

2.4.1 Animal care

All animal experiments were performed in full compliance with local ethical guidelines and approved animal care according to the UK animals (Scientific Precodures) Act 1986 and its subsequent amendments. Adult, female Sprague-Dawley rats, typically weighing 200-250g at the start of experiments, were used. They were housed in cages of 4, in a natural light-dark cycle, with access to food and water *ad libitum.*

All surgery was performed under isoflurane anaesthesia. Anaesthesia was induced in an induction box with isoflurane and oxygen, and maintained by passive inhalation of isoflurane and a mixture of oxygen and nitrous oxide. Animals were allowed to recover in a warmed recovery chamber and received analgesia through paracetamol dissolved in drinking water (2mg/ml) for 3 days subsequent to surgery.

2.4.2 Bead injections into rat brain

Unilateral striatal injections of empty alginate beads without cells were carried out by Dr E. Torres using a standard protocol (Torres *et al.*, 2005). Briefly, beads were suspended in 0.9% sterile saline and injected into striatum using a 30-gauge cannula connected to a 10µl Hamilton syringe in a micropump driver set to deliver 1µl/minute. The stereotaxic coordinates for injection were: A=+0.6 from bregma, L=±3.0 from midline, V=-4.5 below dura. Beads were suspended in 3µl of saline and so injections therefore took three minutes. The micropump driver was stopped after three minutes, a further three minutes passed to allow diffusion of saline, before the cannula was slowly withdrawn from the brain. Control injections of 3µl artificial cerebrospinal fluid (Section 2.1.4.1) were carried out over three minutes, with a further three minutes to allow diffusion. Cleaning, closure and suturing of the wound was then carried out.

2.4.3 Histopathology

Animals were terminally anaesthetised using a standard protocol (Torres *et al.*, 2005). Briefly, sodium pentobarbitone (200mg/kg) was injected intraperitoneally, followed by transcardial perfusion with PBS at pH 7.4 (100ml) and then 4% paraformaldehyde in PBS (250ml) over a 5 minute period. After brains were removed, they were post-fixed by immersion in the same fixative solution for 4 hours, and then transferred to 25% sucrose in PBS for equilibration. Coronal sections of 40μm thickness were cut on a freezing stage sledge microtome into 0.1M TRIS-buffered saline pH 7.4 (TBS, Section 2.1.4.2) and stored at +4°C prior to staining. Alternatively, coronal sections were cut on a cryostat and collected onto microscope slides coated with 1% gelatin.

The nissl stain, cresyl fast violet (Section 2.1.4.3) was used to stain neuronal cells using a standard protocol (Torres *et al.*, 2006) as follows. Sections were mounted onto gelatine coated microscope slides and dried at room temperature overnight. Dehydration was carried out in an ascending series of alcohol solutions (70%, 95% and 100% ethanol), and slides were immersed in 50/50 (v/v) chloroform/ethanol mix for 30 minutes. Slides were immersed (with agitation) in 95%, 70% ethanol and then distilled water for 5 minutes each to re-equilibrate. Slides were immersed in cresyl fast violet solution (5% in 0.1M sodium acetate buffer, pH 3.5) for 5 minutes. Again slides were dehydrated in ascending alcohol solutions (see above), cleared in xylene, and a coverslip applied using DPX mounting medium (Thermo Scientific, Leicestershire, UK).

2.4.4 Magnetic Resonance Imaging (MRI)

Rats were imaged using a Bruker Biospec Avance 9.4T (400 mHz) MRI system, equipped with an S116 gradient set (EMRIC, Cardiff University). Each rat was operated upon (Section 2.4.2) and whilst still anaesthetised, positioned inside a 72-mm ID linear polarised birdcage volume coil coupled with a quaderature combined rat head surface coil. Anaesthesia was maintained with ~2% isoflurane and body temperature and breathing were monitored. Gradient-echo pilot scans were performed at the beginning of each imaging session for accurate positioning of the animal inside the magnet bore. For each animal a series of FLASH images (flip angle α =30°, 15 slices, 0.5-mm thickness) were acquired in axial orientation. T2*-weighted data sets were acquired using gradient-echo sequence with the following acquisition

parameters: repetition time=300 ms, echo time=8.5 ms, field of view=1.92x1.92 cm^2 and image matrix=192x192.

Chapter 3. Development of a microfluidic system to generate ionically cross-linked alginate beads

3.1 INTRODUCTION

Although several methods for the production of alginate beads containing cells already exist, there was no precedent for the use of microfluidics-based devices in continuous alginate bead production at the initiation of this project. Continuous microfluidic synthesis of alginate microbeads can be described as emulsification followed by on-chip cross-linking of alginate. Of these processes, the latter step is the most problematic to achieve in a microfluidic system. Polymer cross-linking on-chip is challenging as it must be prevented from occurring at the fluidic junction. Premature ionic cross-linking at the junction results in uncontrolled gel formation within the channel, which prevents further emulsion formation (i.e. a blockage). Therefore, although microfabricated devices had previously been employed to generate droplets of various liquids, some of which contained cells (He *et al.*, 2005; Sakai *et al.*, 2005; Sugiura *et al.*, 2005), *in situ* cross-linking of alginate droplets was not reported prior to 2005. Continuous microfluidic synthesis is desirable as the need for further processing steps after bead collection can be eliminated.

In this study, continuous microfluidic synthesis was achieved through custom design of microfabricated circuits consisting of milled microchannels to form microemulsions of aqueous alginate solutions *via* segmented flow. Subsequently, various approaches to promote polymer cross-linking were investigated, and both internal and external gelation approaches were tested. Product beads were examined to ensure stable, spherical morphology; size and dispersity were measured. The target size of product beads produced by this prototype system was <500μm in diameter.

3.2 EMULSION FORMATION IN MICROFLUIDIC DEVICES

Microfabricated devices consist of microchannels arranged in specific, user-defined geometries to exploit specific microfluidic phenomena. Such arrangements are termed fluidic circuits. Originally, fluidic circuits were manufactured from silicon, although soft lithography of polydimethylsiloxane (PDMS) is now the most commonly used microfabrication method as it is easier, cheaper, quicker, requires less

specialised knowledge and reduces the number of steps used in the manufacturing process. Typically devices are permanently sealed, with external connections through which fluids are introduced.

For this study a novel microfluidics-based device, termed a MicroPlant™ (described in Section 2.2.1), was used. The system, developed by Q Chip (Cardiff, UK), was designed to enable rapid evaluation of fluidic circuits. In comparison with traditionally fabricated microfabricated devices, MicroPlants™ are not permanently sealed and so can be assembled and disassembled rapidly. In addition, instead of the laborious processes used to produce circuits in PDMS (taking a minimum of 8 hours (Zhao *et al.*, 2003)), a single milling operation is employed, making the production of a circuit much quicker and easier. The use of a MicroPlant™ thus allowed ideas to be rapidly converted into testable circuits. Design iterations were also quick and easy to investigate.

Microfluidic circuits are machined into blank polytetrafluoroethylene (PTFE) chips, and as such are hydrophobic and rigid. The microfluidic circuits consist of microchannels, which are rectangular in cross-section. A Computer Numerical Controlled (CNC) milling machine is used to create the microchannels in the PTFE surface (Section 2.2.2). Microchannels, by definition, must be less than 1mm and can be made any size, to a minimum of 100μm, which represents the limit of the micromilling method.

The completed, milled PTFE chip is located onto a 316 stainless steel fluid distribution manifold, into which high performance liquid chromatography fluid connectors are introduced equatorially. Fluids can then be loaded into disposable syringes which are connected *via* narrow bore tubing to the device. Before fluids can flow through the channels a transparent borosilicate disc is placed over the chip, thus allowing observation of fluid flows in microchannels. As borosilicate is hydrophilic, a hydrophobic gasket (PFA film, 250μm thick) is inserted between it and the chip. Finally, a stainless steel clamping piece is bolted to the fluidic manifold, allowing the entire laminated assembly to be compression sealed. The device is illustrated schematically and pictorially in Figure 3.1.

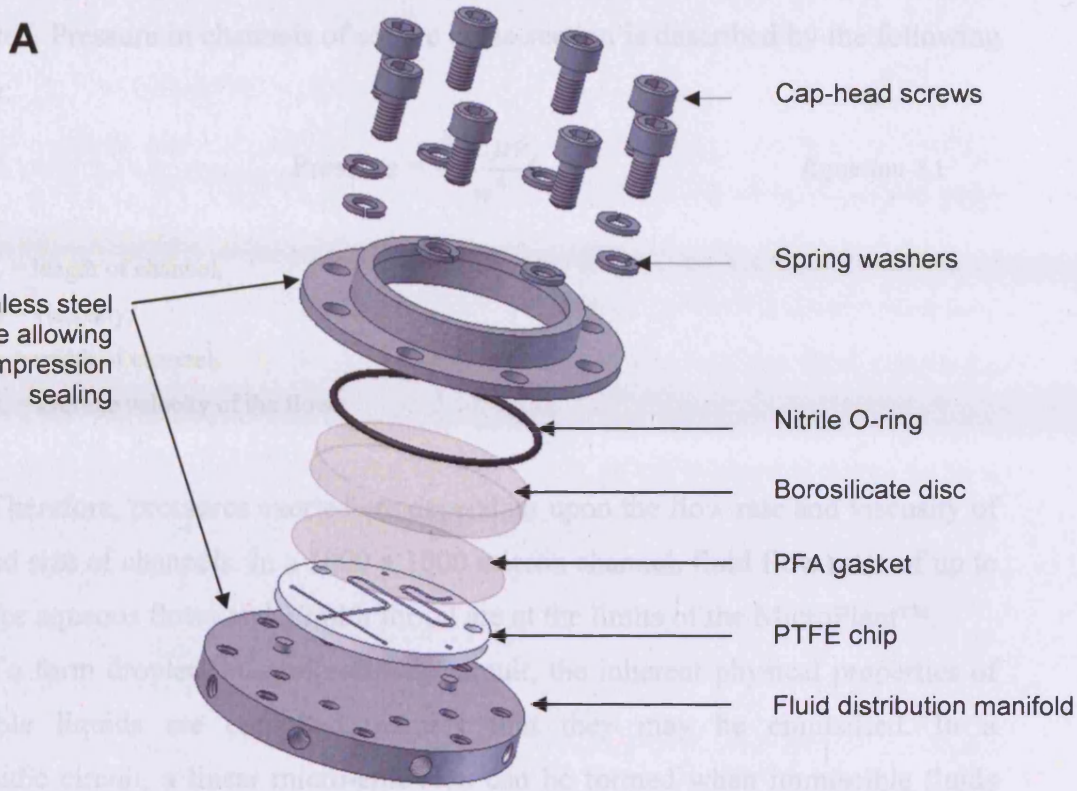

Figure 3.1: The microfluidic evaluation platform (MicroPlant™) used in all microfluidic experiments. A) Expanded schematic showing the components of the microfluidic evaluation rig. B) Photograph showing evaluation device sealed, with a microfluidic chip inserted and fluid connectors

Fluids enter the fluid distribution manifold and flow *via* vertical through holes (sealed with nitrile rubber O-rings) to the top of a chip located on it. Fluids are

pumped using syringe drivers, however any pulseless, pressure driven device may be substituted. Pressure in channels of square cross-section is described by the following equation:

$$\text{Pressure} = \frac{32L\mu v_s}{w^4} \qquad \textbf{Equation 3.1}$$

Where L = length of channel,
μ = viscosity,
w = width of channel,
v_s = average velocity of the flow.

Therefore, pressures exerted are dependant upon the flow rate and viscosity of fluids and size of channels. In a 1000 x 1000 micron channel, fluid flow rates of up to 60ml/h for aqueous flows and 30ml/h for oil are at the limits of the MicroPlant™.

To form droplets in a microfluidic circuit, the inherent physical properties of immiscible liquids are exploited, namely that they may be emulsified. In a microfluidic circuit, a linear micro-emulsion can be formed when immiscible fluids flow together into a microfluidic junction. The simplest of these is the T-junction, illustrated in Figure 3.2A. Fluid flowing in one channel is sheared by a second immiscible phase, flowing in the cross-channel (Thorsen *et al.*, 2001). Co-flowing streams can also be used to generate emulsions, these can take the form of cross-junctions (Figure 3.2B, Tan *et al.*, 2008) or flow focusing devices (Figure 3.2C, Anna *et al.*, 2003).

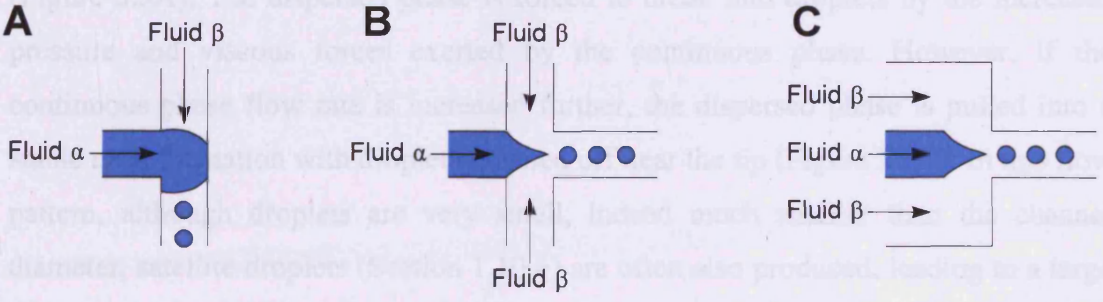

Figure 3.2: Schematic representations of microfluidic junctions. A) Emulsion formation in a T-junction, B) cross-junction, or C) flow focussing device. Orientation of flow is specified by arrows

In conventional emulsion formation, the fluid which forms droplets is termed the dispersed phase, and the immiscible fluid is termed the continuous phase. This is

also true in microfluidic circuits, however the fluid which forms droplets (Fluid α in Figure 3.2) is also called the functional fluid, and the immiscible fluid (Fluid β in Figure 3.2) is also called the carrier fluid.

Channel properties, such as contact angle, surface energy and hydrophobicity, influence which liquid forms droplets. Aqueous alginate solutions are repelled from the hydrophobic PTFE chip surface used in the MicroPlant™. A fluid which is immiscible with an aqueous alginate solution is required to form a linear emulsion. The nature of a linear emulsion is dependant on the surface tensions (and interfacial tension) of the component fluids, as well as the energies of the microchannel surfaces. The particular characteristics of a linear emulsion, e.g. droplet size, size variance, and droplet production frequency are strongly dependant upon fluid flow rate and microchannel architecture. As the interfacial surface tension is constant for a given pair of fluids at a given temperature, variations in relative flow rates are used to produce different flow patterns.

At slow fluid flow rates, plug formation occurs, rather than spherical droplet formation (Figure 3.3B). A plug is defined as a droplet large enough to fill the cross-section of a channel, with its length in the direction of fluid flow greater than its width (Christopher and Anna, 2007). Plugs are surrounded by a thin layer of continuous phase and so do not come into contact with the channel walls. Upon passing into a channel with a greater cross-sectional area, liquid plugs form spheres due to surface tension forces.

By increasing the continuous fluid flow rate, droplet formation is favoured (Figure 3.3A). The dispersed phase is forced to break into droplets by the increased pressure and viscous forces exerted by the continuous phase. However, if the continuous phase flow rate is increased further, the dispersed phase is pulled into a stable neck formation with droplets pinched off near the tip (Figure 3.3C). In this flow pattern, although droplets are very small, indeed much smaller than the channel diameter, satellite droplets (Section 1.10.4) are often also produced, leading to a large observed dispersity (Cramer *et al.*, 2004). Flow rates were empirically determined in all experiments to bring about stable segmentation, as opposed to plug or unstable droplet formation.

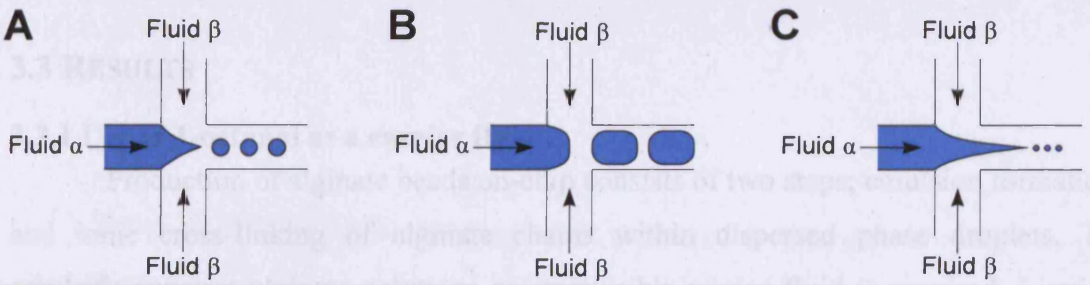

Figure 3.3: Flow patterns produced in a microfluidic cross-junction. A) Droplet formation, B) plug formation and C) stable neck formation. Orientation of flow is specified by arrows

3.3 RESULTS

3.3.1 Use of 1-octanol as a carrier fluid

Production of alginate beads on-chip consists of two steps; emulsion formation and ionic cross-linking of alginate chains within dispersed phase droplets. To emulsify aqueous alginate solutions an immiscible carrier fluid is required. Liquids which are immiscible with aqueous alginate solutions are necessarily non-polar, i.e. an organic solvent such as hexadecane or sunflower oil. Ionic cross-linking of alginate chains is bought about by divalent cations, the most commonly used being Ca^{2+}. Calcium is described as a hard ion in the Lewis definition of acids and bases (Lewis, 1923). As such, calcium (II) salts are easier to dissolve in polar solvents (high dielectric constant) such as water than in non-polar solvents (low dielectric constant).

The properties required for each step in alginate bead production are opposed. A non-polar solvent is required to form an emulsion of alginate droplets in a microfluidics-based circuit; however, the calcium ions required to cross-link alginate molecules have low solubility in such liquids. Either the calcium ions required for cross-linking must be supplied in the non-polar carrier fluid or in an additional aqueous flow. Both of these methods were investigated.

The solvent initially chosen as a carrier fluid was 1-octanol, which belongs to a class of chemicals known as fatty or aliphatic alcohols. These chemicals are amphiphatic in nature, meaning they are soluble in both water and organic solvents. 1-Octanol is immiscible with water, but still polar enough to dissolve calcium salts to a certain extent (dielectric constant = 10.34, compared with water = 80). Initially 1-octanol was saturated with $CaCl_2$ by heating 1-octanol and excess $CaCl_2$.

1-Octanol was demonstrated to be a suitable carrier fluid to produce a linear emulsion with alginate solution (1% w/v) as droplets of alginate were observed after segmentation by utilising a classical microfluidic cross-junction (as illustrated in Figure 3.4, circuit diagram shown in Appendix 1).

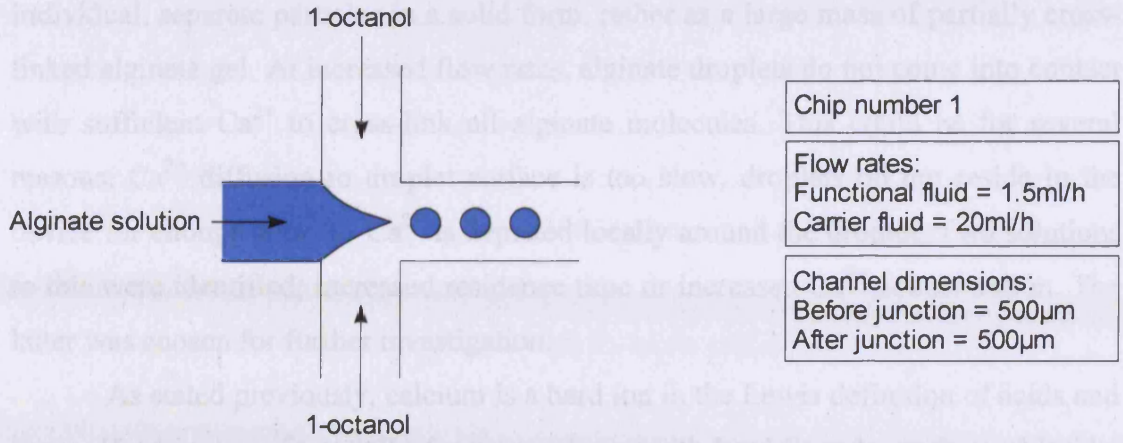

Figure 3.4: Schematic illustrating a classical microfluidic cross-junction. Functional fluid was composed of alginate solution (1% w/v) with carrier fluid composed of 1-octanol. Flow rates and channel dimensions are shown. Orientation of flow is specified by arrows

The experiment was repeated with 1-octanol saturated with $CaCl_2$; however, stable segmentation could not be achieved. Alginate chains are very rapidly cross-linked by Ca^{2+}, and even the small amount of calcium present was enough to cause immediate gelation at the junction where the liquid interface is largest (Figure 3.5). Cross-linked alginate chains occluded the junction causing all flows to decelerate and eventually cease. Hence, direct exposure of the emerging alginate solution to free Ca^{2+} results in immediate gelation and channel blockage.

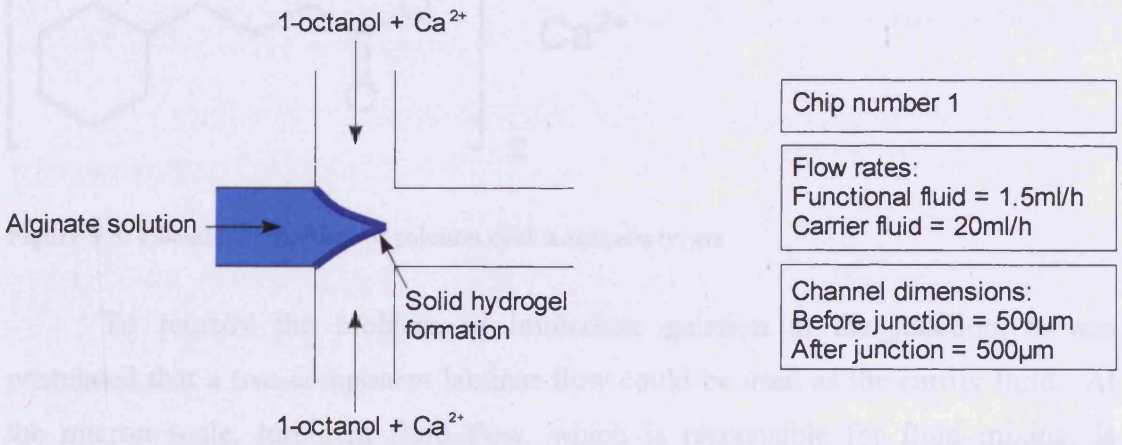

Figure 3.5: Schematic showing immediate interfacial hydrogel formation in a classical microfluidic cross-junction. Functional fluid was composed of alginate solution (1% w/v) with carrier fluid composed of 1-octanol saturated with $CaCl_2$. Alginate molecules react rapidly with Ca^{2+} dissolved in the carrier fluid. The cross-linked alginate chains form solid hydrogel at the junction. Flow rates and channel dimensions are shown. Orientation of flow is specified by arrows

A linear emulsion of alginate solution was generated at increased flow rates (60ml/h and 4ml/h for carrier fluid and functional fluid, respectively). However, alginate droplets did not become fully cross-linked and did not exit from the device as

individual, separate particles in a solid form, rather as a large mass of partially cross-linked alginate gel. At increased flow rates, alginate droplets do not come into contact with sufficient Ca^{2+} to cross-link all alginate molecules. This could be for several reasons; Ca^{2+} diffusion to droplet surface is too slow, droplets do not reside in the device for enough time, or Ca^{2+} is depleted locally around the droplet. Two solutions to this were identified; increased residence time or increased Ca^{2+} concentration. The latter was chosen for further investigation.

As stated previously, calcium is a hard ion in the Lewis definition of acids and bases. Hard ions preferentially form complexes with hard ligands, such as chloride, and bind less favourably to soft ligands. It was postulated that the Ca^{2+} concentration could be increased by utilising a soft, organic anion as opposed to a hard counter-ion such a Cl^-. In this way Ca^{2+} is poorly bound to the ligand and more likely to dissolve in the solvent. A mixture of calcium cyclohexanebutyrate (Figure 3.6) and calcium nitrate allowed Ca^{2+} to be dissolved into 1-octanol at a concentration of 40mM. However, even at high flow rates (60ml/h and 4ml/h for carrier fluid and functional fluid respectively) stable segmentation was not possible due to the immediate reaction between alginate moieties and Ca^{2+} at the junction.

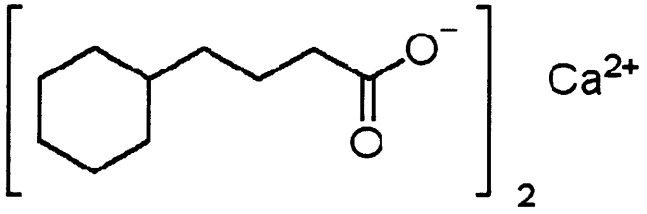

Figure 3.5: Chemical structure of calcium cyclohexanebutyrate

To remedy the problem of immediate gelation at the junction, it was postulated that a two-component laminar flow could be used as the carrier fluid. At the micron scale, turbulent fluid flow, which is responsible for fluid mixing, is constrained and replaced by laminar flow (Section 1.12.1). Under these conditions, fluids move in planes, and with the exception of slow interfacial diffusion, do not undergo mixing. Therefore, it is possible to create a laminar flow of two miscible liquids, and maintain separation of the two for some considerable time.

The microfluidic circuit was enhanced to include an additional fluid flow; into which pure 1-octanol was introduced. Hence, the carrier fluid can be thought of as a

reactive stream of Ca^{2+} dissolved in 1-octanol, containing a stripe of inert, unmodified 1-octanol; hereafter referred to as the "shielding" flow (shown in red in Figure 3.7). The two-phase laminar flows were created at microfluidic T-junctions, and approached the aqueous alginate mixture from either side, at an angle of 90°. The fluid flows were oriented such that the non-reactive shielding flows contacted the aqueous alginate flow at the junction. However, the 1-octanol containing Ca^{2+} did not come into contact with the emerging aqueous droplets at the junction.

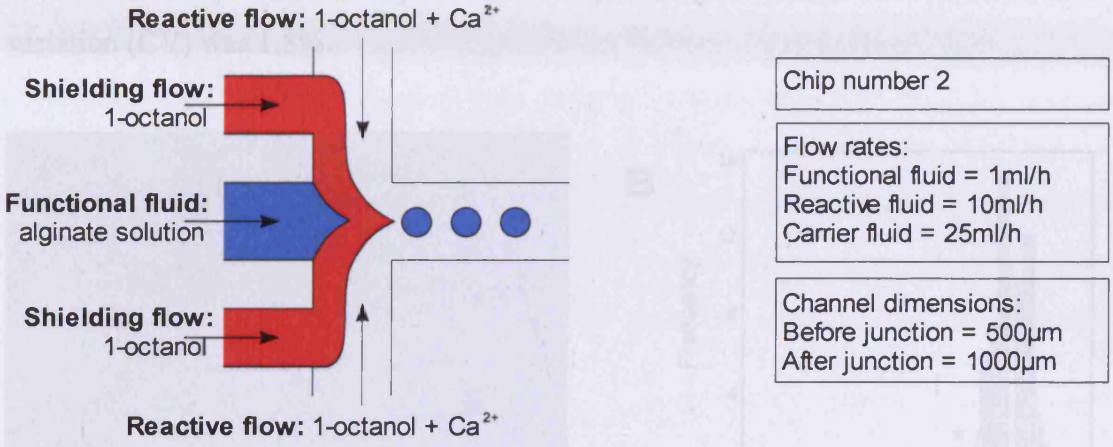

Figure 3.7: Schematic of novel shielding junction design incorporating additional fluid flows to provide a non-reactive shielding flow. Functional fluid (shown in blue) was composed of alginate solution (1% w/v), shielding flow (shown in red) was composed of 1-octanol and reactive flow (no shading) was composed of 1-octanol containing Ca^{2+} at a final concentration of 40mM, by dissolving calcium cyclohexanebutyrate and calcium nitrate into 1-octanol. Flow rates and channel dimensions are shown. Orientation of flow is specified by arrows

This modification allowed the problem of immediate gelation at the junction to be overcome. The emerging droplets were insulated from the fraction of the carrier phase containing Ca^{2+} by a layer of the shielding fluid. Spherical droplets of alginate solution were successfully generated at the junction, and these proceeded through the reactor channel. As the droplets were carried through the circuit, Ca^{2+} gradually diffused through the shielding layer surrounding them. The eventual reaction between calcium and alginate chains was seen to be more controllable; since the relative flow rates (and consequently the thicknesses) of the two components of the laminar flow could be entirely independently controlled. Hence, by varying the relative proportion of the shielding fluid within the carrier phase, the rate of alginate bead gelation could be adjusted. This novel method has been described in patent application number GB0525951.0 (Davies *et al.*, 2005).

Solid calcium cross-linked alginate beads were successfully produced when 1-octanol was used as a carrier fluid in conjunction with the novel shielding junction developed (Figure 3.7). For this experiment only, sodium alginate (1% w/v) from Sigma-Aldrich was used. Sodium alginate from this source is known to be of lower quality than the NovaMatrix sodium alginate used throughout the rest of this thesis. As the alginate solution was not filtered insoluble particles can be seen in the beads (Figure 3.8A). The average diameter of blank beads (n=50) made using this method was measured (Section 2.2.3) to be 277±5μm (Figure 3.8B). The coefficient of variation (CV) was 1.8%.

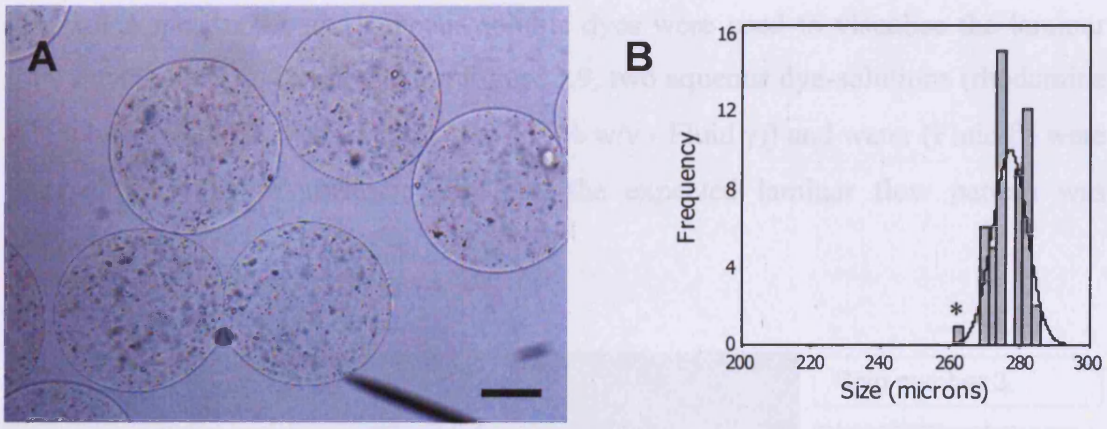

Figure 3.8: Calcium cross-linked alginate beads produced using 1-octanol as a carrier fluid. A) A representative calcium alginate bead population produced using 1-octanol as carrier fluid to segment alginate solution (1% w/v) using a shielded microfluidic junction (as shown in Figure 3.7). Insoluble particles are present due to use of low purity alginate. Scale bar represents 100μm, B) histogram of beads represented in A; grey bars show measured data, with black line representing normal distribution. Mean bead diameter was 277±5μm. Distribution was considered not normal (A^2=1.37, $p < 0.005$), with an outlier at 263μm, represented by an asterisk (*)

3.3.2 Use of an aqueous shielding flow

As explained in the previous section, a liquid which is immiscible with aqueous alginate solutions is required to enable segmentation. The method arrived at in the previous section (Section 3.3.1) utilised an organic solvent; however oils are also suitable for use as a carrier fluid to segment alginate, as they are non-polar. The dielectric constant (k; a measure of a solvent's ability to decrease the force with which two oppositely charged ions attract each other) is even lower in oleic acid (k = 2.5) than in 1-octanol (k = 10.34), both of which are much lower than water (k = 80). Whereas a small amount of Ca^{2+} can be dissolved in organic solvents, such as 1-

octanol, virtually none can be dissolved in oils. As such, oils are not suitable for undertaking external gelation of alginate solutions.

A further attempt to use external gelation to cross-link alginate droplets was made. As Ca^{2+} cannot be provided in the continuous oil phase, an additional aqueous flow containing Ca^{2+} was proposed as an alternative. As seen previously (Section 3.3.1), allowing aqueous alginate solutions and Ca^{2+} ions to combine prior to segmentation causes cross-linking of alginate chains and subsequent occlusion of the junction. It was postulated that an aqueous shielding flow could be used as a barrier to prevent Ca^{2+} diffusing from an aqueous $CaCl_2$ solution to an alginate solution.

To test this theory, a chip was designed and milled (Section 2.2.2, circuit diagram Appendix 1), and aqueous soluble dyes were used to visualise the laminar flow established. As can be seen in Figure 3.9, two aqueous dye-solutions (rhodamine B (1% w/v - Fluid α) and procion blue 4 (1% w/v - Fluid γ)) and water (Fluid β) were pumped into this microfluidic chip and the expected laminar flow pattern was demonstrated.

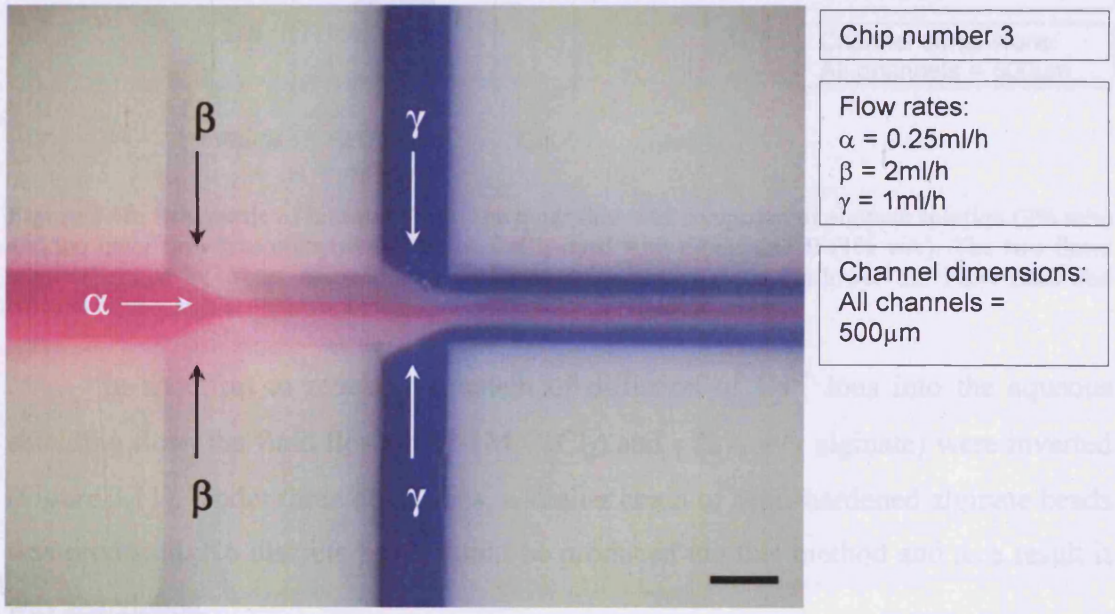

Figure 3.9: Laminar flow in a microfluidic circuit. Aqueous soluble dyes, rhodamine B (1% w/v - Fluid α) and procion blue 4 (1% w/v - Fluid γ), have been used to differentiate between the laminar fluid streams. Fluid β consisted of water. Flow rates and channel dimensions are shown. Orientation of flow is specified by arrows. Scale bar represents 500μm

Flow γ in Figure 3.9 was replaced with sodium alginate solution (2% w/v), with no perturbation to the laminar flow regime. The aqueous rhodamine and alginate

solutions were successfully segmented with oil (flow rate = 20ml/h, not shown on diagram). Mixing between the dyed water and alginate solution occurred inside the droplet after segmentation.

The replacement of Flow α in Figure 3.9 with an aqueous solution of 0.1M $CaCl_2$ containing rhodamine B (1% w/v) as shown schematically in Figure 3.10, caused turbulent flow between the shielding water and $CaCl_2$ to occur. Upon segmentation, a chain of semi-hardened alginate beads linked by a thread of cross-linked alginate was produced. A possible explanation for this phenomenon is partial cross-linking of alginate chains *via* the disrupted shielding flow prior to segmentation, leading to an increase in viscosity which had an adverse effect upon segmentation.

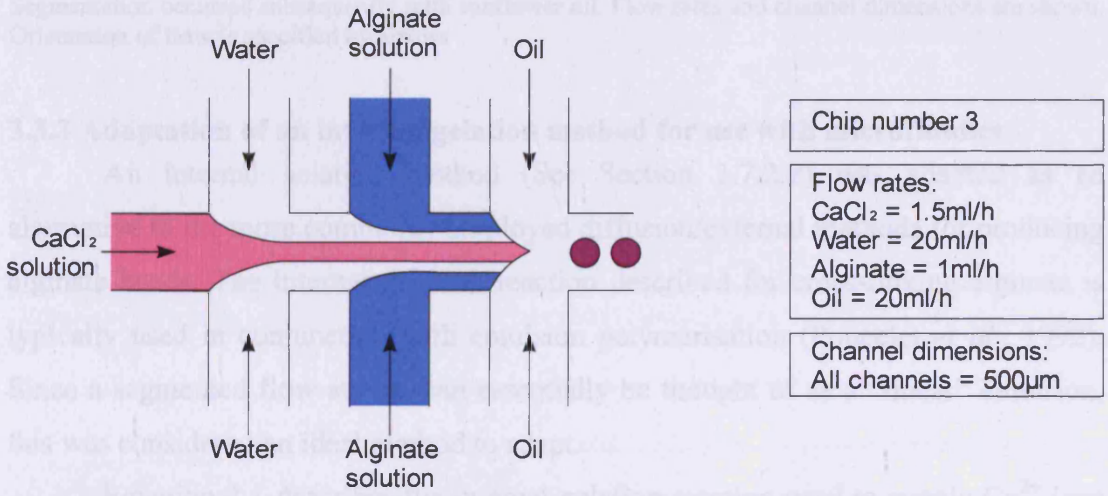

Figure 3.10: Schematic of laminar flow. The outer flow was composed of alginate solution (2% w/v) and the inner flow was composed of 0.1M $CaCl_2$ dyed with rhodamine B (1% w/v). The two flows were separated by water. Segmentation occurred subsequently with sunflower oil. Flow rates and channel dimensions are shown. Orientation of flow is specified by arrows

In an effort to reduce the extent of diffusion of Ca^{2+} ions into the aqueous shielding flow, the fluid flows α (0.1M $CaCl_2$) and γ (2% w/v alginate) were inverted (Figure 3.11). Under these conditions, a similar chain of semi-hardened alginate beads was produced. No discrete beads could be produced *via* this method and as a result it was abandoned.

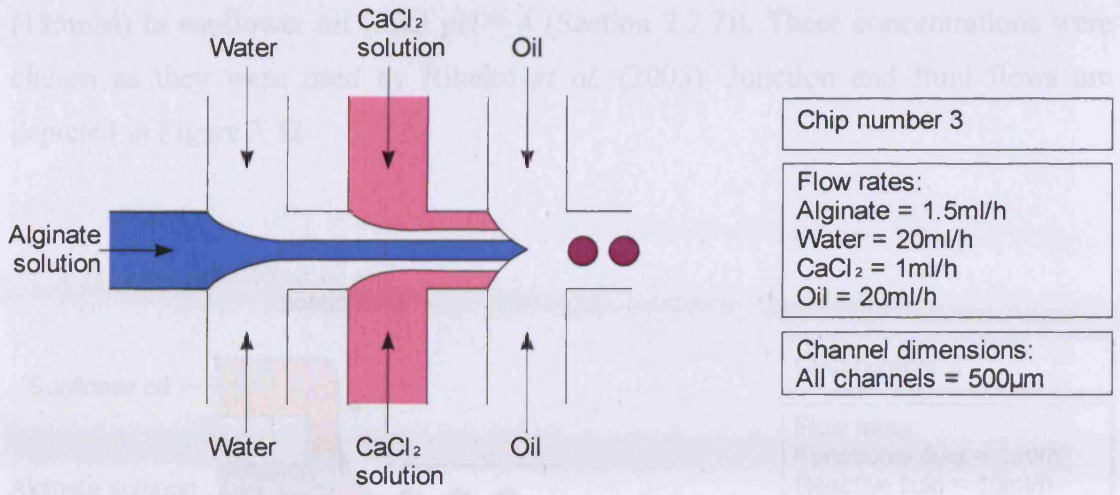

Figure 3.11: Schematic of laminar flow. The outer flow was composed of 0.1M $CaCl_2$ and the inner flow was composed of alginate solution (2% w/v). The two flows were separated by water. Segmentation occurred subsequently with sunflower oil. Flow rates and channel dimensions are shown. Orientation of flow is specified by arrows

3.3.3 Adaptation of an internal gelation method for use with microfluidics

An internal gelation method (See Section 1.7.2.2) was adapted as an alternative to the more commonly employed diffusion/external methods for producing alginate beads. The internal gelation reaction described for cross-linking alginate is typically used in conjunction with emulsion polymerisation (Poncelet *et al.*, 1992). Since a segmented flow stream can essentially be thought of as a "linear" emulsion, this was considered an ideal method to adapt.

Equation 3.1 describes the internal gelation reaction used to supply Ca^{2+} ions for cross-linking alginate chains. Calcium carbonate was used as the insoluble calcium salt, with dilute acetic acid providing protons.

$$CaCO_{3\,(s)} + 2H^{+}_{\,(aq)} \rightarrow Ca^{2+}_{\,(aq)} + CO_{2\,(g)} + H_2O_{\,(l)} \qquad \textbf{Equation 3.1}$$

As in previous experiments (Section 3.3.1), use of a classic microfluidic cross junction was inappropriate for this application due to alginate chains prematurely cross-linking at the junction. To prevent immediate reaction of alginate molecules and free Ca^{2+}, $CaCO_3$ suspended in the alginate solution must be protected from a decrease in pH. The shielding junction, described previously (Section 3.3.1), was used to prevent this problem. Nanocrystalline calcium carbonate (Section 2.1.3, 400mM) suspended in alginate solution (2% w/v) was used as the functional fluid with sunflower oil used as the shielding flow. The reactive flow consisted of acetic acid

(125mM) in sunflower oil (final pH = 4 (Section 2.2.7)). These concentrations were chosen as they were used by Ribeiro *et al.* (2005). Junction and fluid flows are depicted in Figure 3.12.

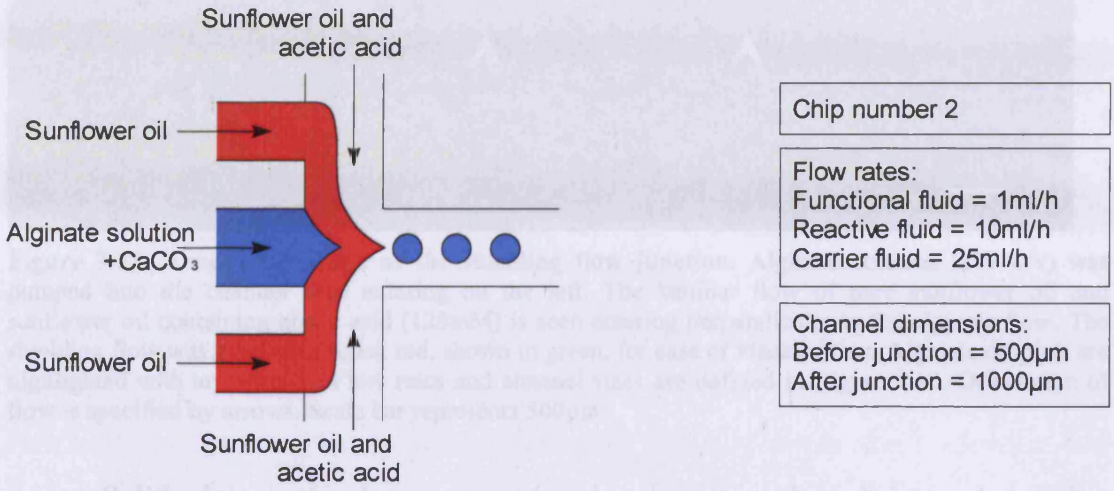

Figure 3.12: Schematic diagram showing the shielded junction and its use for producing calcium alginate beads *via* internal gelation. Functional fluid (shown in blue) was composed of alginate solution (2% w/v) containing $CaCO_3$ (400mM), shielding flow (shown in red) was composed of sunflower oil and reactive flow (no shading) was composed of sunflower oil containing acetic acid (125mM). Flow rates and channel dimensions are shown. Orientation of flow is specified by arrows

Under these conditions, alginate droplets containing dispersed $CaCO_3$ were formed. Acetic acid in the reactive flow reacted with $CaCO_3$ present at the interface between the droplets' surface and the oil, whereupon Ca^{2+}, H_2O and CO_2 were produced. Alginate chains present in a droplet became cross-linked upon exposure to the free Ca^{2+} present. $CaCO_3$ throughout the droplet reacted to produce free Ca^{2+} and the alginate chains became completely cross-linked. A shielding flow of pure sunflower oil was employed to prevent $CaCO_3$ suspended in the alginate solution from coming into contact with the reactive flow containing acetic acid. The shielding and reactive flows remained laminar until the junction (Figure 3.13). The emerging alginate droplet disrupted this laminar stream and newly formed droplets almost immediately came into contact with the reactive flow.

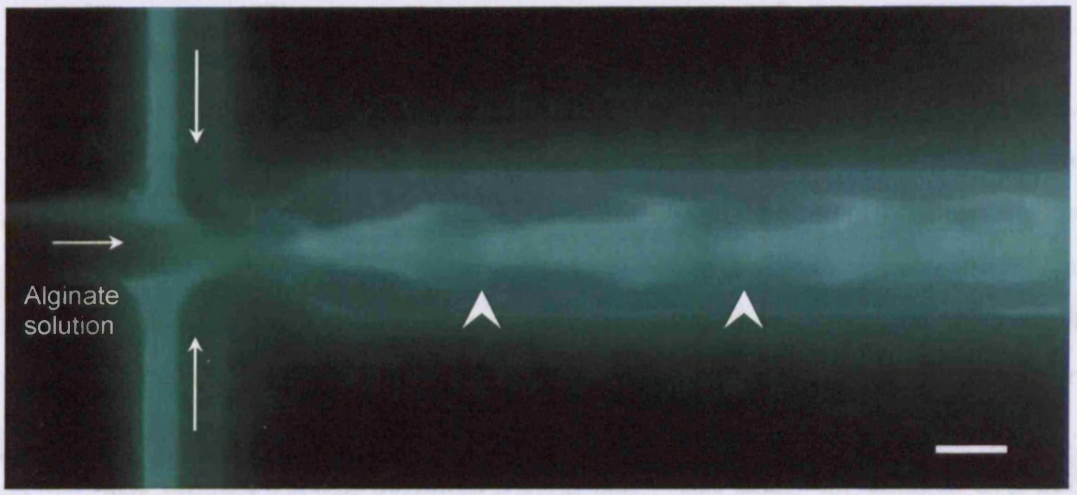

Figure 3.13: A negative image of the shielding flow junction. Alginate solution (2% w/v) was pumped into the channel seen entering on the left. The laminar flow of pure sunflower oil and sunflower oil containing acetic acid (125mM) is seen entering perpendicular to the alginate flow. The shielding flow was dyed with sudan red, shown in green, for ease of visualization. Alginate droplets are highlighted with arrowheads. Flow rates and channel sizes are defined in Figure 3.10. Orientation of flow is specified by arrows. Scale bar represents 500μm

Solid alginate beads were produced using the adapted internal gelation method. As can be seen in Figure 3.14A, beads appeared opaque due to remaining, unreacted, insoluble $CaCO_3$. The average diameter of blank beads (n=20) made using this method was measured (Section 2.2.3) to be 269±4μm (Figure 3.14B). The coefficient of variation (CV) was 1.6%.

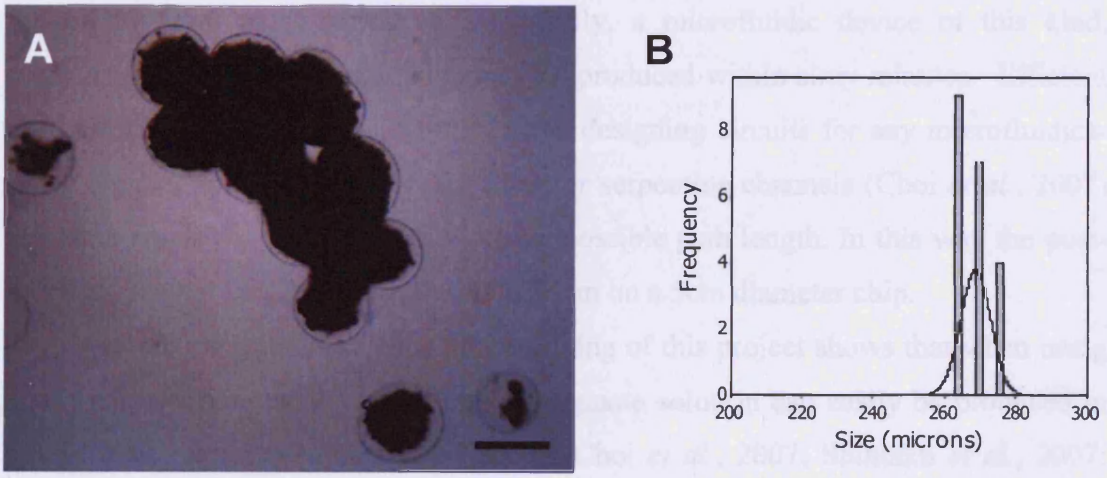

Figure 3.14: Calcium cross-linked alginate beads produced using the adapted internal gelation method. A) A representative calcium alginate (2% w/v) bead population produced using an adapted internal gelation method utilizing $CaCO_3$ (400mM) as an inert calcium source and a shielded microfluidic junction (as shown in Figure 3.12). Scale bar represents 250μm. B) Histogram of beads represented in A; grey bars show measured data, with black line representing normal distribution. Mean bead diameter was 269±4μm. Distribution was considered not normal (A^2=1.76, $p < 0.005$)

3.4 DISCUSSION

Three different approaches were employed to develop microfluidic methods for producing alginate beads. Both internal and external gelation methods were adapted for use in a microfluidics-based device. The development of a novel circuit design allowed calcium cross-linked alginate beads to be produced *via* internal and external gelation. Beads thus produced were collected upon exiting the microreactor without requiring further processing steps. The novel circuit has been described in a patent application (Davies *et al.*, 2005).

The unique, custom-designed MicroPlant™ has many advantages over more commonly used PDMS microdevices. By avoiding a permanently sealed cover, a compression-sealed PTFE device may be dismantled, cleaned and reassembled as required. This is particularly useful in cases of accidental failure (e.g., channel blockage due to unwanted gelation), allowing rapid recovery during testing and optimisation of conditions. Synthesising a microfluidic device *via* the multi-stage soft-lithography, PDMS casting, oven-curing and plasma cleaning process has been reported to take a minimum of eight hours (Zhao *et al.*, 2003). By using PTFE as a starting material for microfluidic chip synthesis, the multi-step lithography process is avoided, and substituted by a single, automated micro-machining operation. This allows microfluidic features consisting of microchannels with cross-sections of 100μm to 1mm to be produced. Typically, a microfluidic device of this kind, containing multiple parallel circuits may be produced within sixty minutes. Efficient use of space is a major consideration when designing circuits for any microfluidics-based device. Spiral (Zourob *et al.*, 2006) or serpentine channels (Choi *et al.*, 2007) are often employed to produce the longest possible path length. In this way the post-junction channel length was increased to 14cm on a 5cm diameter chip.

Literature published since the beginning of this project shows that when using an organic continuous phase, droplets of alginate solution can easily be produced in microfluidic circuits (Sugiura *et al.*, 2005; Choi *et al.*, 2007; Shintaku *et al.*, 2007; Zhang *et al.*, 2007). Varying approaches have been explored to generate hydrogel beads (for example agarose (Sakai *et al.*, 2005), Dextran-hydroxyethyl methacrylate (De Geest *et al.*, 2005), chitosan (Yang *et al.*, 2007) and Puramatrix (Um *et al.*, 2008)), however only alginate microparticles will be discussed here. Various groups have investigated both internal and external gelation approaches to produce calcium

cross-linked alginate beads. Each approach has been combined with alginate ionotropic cross-linking on- and off-chip.

Huang *et al.* (2006) first demonstrated that alginate solutions can be segmented using a cross-junction microchannel. Droplets of aqueous alginate were generated, and then transported, along with the continuous oil phase, into a beaker containing a calcium (II) ion solution, thus producing beads off-chip *via* external gelation. In an adaptation of Poncelet's internal gelation method, the same group segmented alginate solutions containing $CaCO_3$ using oil in a cross-junction microchannel (Huang *et al.*, 2007). The emulsion generated was dripped into a beaker containing oil, Tween80 and acetic acid. When droplets containing $CaCO_3$ came into contact with acetic acid, Ca^{2+} ions were produced causing polymer gelation. Thus, beads were produced off-chip *via* internal gelation. Thus, transportation off-chip for subsequent cross-linking has been shown to be possible but difficult to achieve, as droplets have a tendency to coalesce prior to exiting the device, which is a major drawback. This tendency for droplet coalescence prior to cross-linking leads to an increased size distribution of product beads produced using off-chip ionic cross-linking. For these reasons cross-linking of alginate droplets prior to exiting a microfluidics-based device is preferable and ionic cross-linking off-chip is rarely reported.

Continuous microfluidic fabrication of alginate beads requires polymer gelation on-chip. However, ionic cross-linking must be prevented from occurring at the junction where excess cross-linked polymer prevents emulsion formation. The most obvious, though least successful, technique to combine Ca^{2+} with aqueous alginate solutions in microfabricated devices is to emulate conventional production methods and introduce aqueous $CaCl_2$ solutions. As outlined above, attempts during this study to separate aqueous alginate and $CaCl_2$ flows with an aqueous shielding flow stream were unsuccessful. This approach has not been reported in combination with alginate solutions, but a modified circuit design has been shown to be effective at separating reactive chemicals over short distances (Song *et al.*, 2003). To improve the use of an aqueous barrier, decreasing the contact time between laminar flows is of paramount importance. Decreasing contact time can be achieved by decreasing the channel length and thus time available for Ca^{2+} to diffuse into the alginate flow.

The need for additional aqueous barriers has been disposed of altogether by a few groups. An aqueous alginate solution emanating from a central flow bought into

contact with two flanking $CaCl_2$ streams immediately prior to segmentation was observed not to segment into droplets. Instead, "the resulting thread" was observed to form into "nodules" (Zhang *et al.*, 2006). This was observed at a wide range of continuous phase flow rates. Premature polymer cross-linking prevented emulsion formation rendering this method unsuitable for alginate bead production. A modified T-junction was more successfully employed to combine aqueous $CaCl_2$ and alginate flows (Choi *et al.*, 2007, junction design illustrated in Figure 3.15). Aqueous $CaCl_2$ and alginate solutions were bought into contact at the junction where segmentation with a carrier fluid produced droplets which became cross-linked whilst moving down the microchannel.

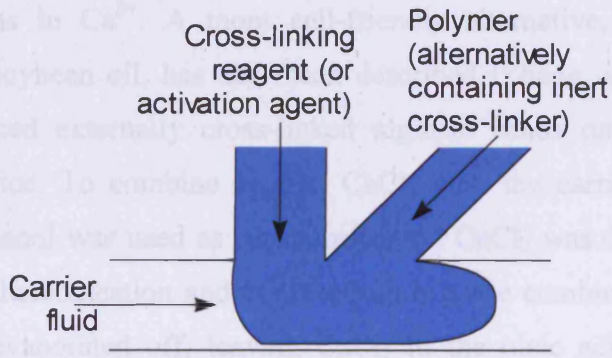

Figure 3.15: Schematic showing a modified T-junction. A classical T-junction was modified by addition of a channel at 45° to the junction. Mixing between the cross-linking reagent and polymer is prevented by this junction design until a droplet is formed, whereupon rapid mixing and thus bead formation occurs

Several groups have attempted to effect alginate cross-linking on-chip *via* coalescence of aqueous $CaCl_2$ and alginate droplets, with varying degrees of success. Separate populations of small $CaCl_2$ droplets and larger alginate droplets were produced using oil. The $CaCl_2$ droplets were produced at a higher frequency than alginate droplets. The two resulting sets of droplets were then collided, within the system, to produce solid alginate beads. Liu *et al.* (2006) employed two fluid focussing devices to produce the two separate populations of droplets. Circular chambers were used to induce changes in velocity gradients forcing one alginate droplet to fuse with one $CaCl_2$ droplet. This succeeded in producing disk-like and thread-like structures, but no discernable spherical beads. Shintaku *et al.* (2007) also used a flow focusing device to form larger alginate droplets, but, instead used a T-junction to produce the increased number of smaller diameter $CaCl_2$ droplets required. The alginate and $CaCl_2$ droplets were observed to spontaneously coalesce due to

velocity differences bought about by the discrepancies in droplet volume. The particles produced in this way were solid but non-spherical. Although alginate chains were cross-linked using both of these methods, spherical beads were not made. Whilst there may be applications where non-spherical products are desirable, the aim of this project was to produce spherical beads.

Experiments combining Ca^{2+} in the continuous phase have also been described in the literature published since this project began. Zhang *et al.* (2006) reproduced the experiment described above (Section 3.3.1), replacing 1-octanol to segment alginate solution in a cross-junction with undecanol containing CaI_2. This was more successful than the attempt outlined in this study (Section 3.3.1) as capsules with a distinct outer shell were produced. The thickness of the shell was a function of exposure time of alginate chains to Ca^{2+}. A more cell-friendly alternative, using calcium acetate dispersed in soybean oil, has also been described (Zhang *et al.*, 2007). Kim *et al.* (2009) produced externally cross-linked alginate beads on-chip by using a flow focussing device. To combine enough $CaCl_2$ with the carrier fluid (oleic acid) 2-methyl-1-propanol was used as an intermediary. $CaCl_2$ was dissolved in 2-methyl-1-propanol by ultrasonication and the resulting mixture combined with oleic acid. The alcohol was evaporated off, leaving $CaCl_2$ in the oleic acid. As the oil used for segmentation contained a small amount of $CaCl_2$, cross-linking of alginate chains occurred.

Zhang *et al.* (2007) also proposed adapting Poncelet's internal gelation method by adding acetic acid to the continuous phase. As this experiment was carried out in a cross-junction microchannel this group experienced the same difficulties observed in this study and were unable to collect solid calcium cross-linked alginate beads from this endeavour. Although partially gelled beads were produced, they did not remain spherical upon exiting the microfluidic circuit. The most successful alternative described again employs a modified T-junction (see above and Figure 3.15). A mixture of aqueous alginate solution and $CaCO_3$ was supplied *via* the 45° arm, with hydrolysed D-Glucone-δ-lactone (GDL) flowing in the perpendicular arm (Amici *et al.*, 2008). The two flows were combined at the junction and segmented with sunflower oil. GDL, being weakly acidic, reacts with $CaCO_3$ to release Ca^{2+} thus effecting alginate chain cross-linking. Tan and Takeuchi (2007) have also successfully converted internal gelation with a shielding flow for use with

microfluidic devices. Their circuit design only differs from the work presented here in the placement of the additional stream of acidified oil.

Of the methods discussed, only four successfully produce spherical calcium cross-linked alginate beads, cross-linked *in situ* (Choi *et al.*, 2007; Tan and Takeuchi, 2007; Zhang *et al.*, 2007; Kim *et al.*, 2009). Each method is unique and novel, with no replication of the techniques presented in this thesis. Previously, microfluidic laminar flows have been used to create chemical gradients and to perform liquid-liquid extractions (Surmeian *et al.*, 2002; Maruyama *et al.*, 2004; Atencia and Beebe, 2005). These reported experiments involved combinations of miscible fluids or stratified flows containing an immiscible "membrane" flow. However, their use has not been applied to the problem of premature alginate cross-linking within microfluidic circuits before.

Two of the methods developed in this chapter were used to produce solid calcium cross-linked alginate beads on-chip. In both cases bead diameters were <280μm with CV <2%. This is within the range of reported literature (Table 1.3, Section 1.12.2). By far the best size distribution of alginate beads produced using a microfluidic circuit reported to date is a CV of 1.1% (mean bead diameter = 79μm, Choi *et al.*, 2007). These beads were produced using hexadecane as the continuous phase. It was acknowledged that use of an organic solvent may not be compatible with cell viability. The next section of work will deal with the issue of toxicity of the developed processes.

Chapter 4. Toxicity of microfluidic encapsulation processes and selection of viability estimation method

4.1 INTRODUCTION

Two microfluidic methods were developed to manufacture solid alginate beads. The first method employed external gelation of alginate droplets formed *via* segmentation with 1-octanol, an organic solvent. The second method was an adapted internal gelation method utilising $CaCO_3$ as an inert cross-linker, acetic acid to liberate Ca^{2+} and sunflower oil to create droplets *via* segmented flow. Whilst there was evidence that solid alginate beads of an appropriate size and narrow size distribution were produced using both methods, no attempt was made to incorporate cells within the hydrogel matrix.

It was necessary to investigate the suitability of each method for cell encapsulation. The method chosen to encapsulate cells was required to not harm cells (cytotoxic) and, ideally, minimally decrease cell viability. Each of the developed encapsulation methods was assessed to evaluate potential cytotoxic effects. Adaptations were implemented in order to decrease any observed cytotoxicity and ensure maximal viability of encapsulated cells. The long term effects of encapsulation upon cell viability were also investigated.

Various commercially available viability estimation methods have been described to estimate cell viability in adherent or suspension mammalian cell culture. To use these methods to measure viability of encapsulated cells, cells must first be removed from the surrounding polymer. This adds an additional step which in itself may compromise cell viability, acting as a potential source of experimental error. Therefore it was important to assess the suitability of several commercially available viability methods for use with encapsulated cells. An ideal method is rapid, cost effective and accurate, and would preferably be a simple assay, which does not require cells to be removed from beads and allows analysis of multiple samples simultaneously. The methods chosen for investigation were; trypan blue exclusion, MTT (3-(4,5-Dimethylthiazol-2-yl)-2,5-diphenol tetrazolium bromide), lactate dehydrogenase (LDH), alamarBlue™, and LIVE/DEAD® staining. The chosen procedures were tested for their compatibility with encapsulated cells. Alterations to the recommended procedures are discussed in the following sections.

4.2 RESULTS

4.2.1 Comparison of methods for estimating viability of encapsulated cells

4.2.1.1 Adapted trypan blue

Trypan blue is a vital stain bearing two azo chromophores. As these chromophores are negatively charged they do not interact with intact cell membranes and so live cells remain unstained (Strober, 2001). When a cell is dead and the plasma membrane is compromised the stain is no longer excluded, and so it enters the cell, causing the development of a blue pigmentation. It is a relatively straightforward task to count the number of stained and unstained cells observed, by employing a haemocytometer (Section 2.3.1.4). The percentage of viable cells present was calculated using the following equation:

$$\text{Percentage viable cells} = \frac{\text{number of unstained cells counted}}{\text{total cell count}} \times 100 \qquad \textbf{Equation 4.1}$$

In initial experiments, trypan blue was added directly to beads on a microscope slide. The dye permeated the outer layer of alginate gel, but did not diffuse completely to the bead centre. For this reason, results gained were not repeatable, reliable or accurate.

Both EDTA and citrate ions have a high affinity for Ca^{2+} and so can be used to sequester Ca^{2+} from solid calcium cross-linked alginate gels. For the trypan blue method to be effective, cells needed to be released from the beads. EDTA and sodium citrate solutions were tested to find the most appropriate chemical to re-dissolve beads. Upon ion-exchange with sodium citrate or sodium EDTA, alginate chains re-dissolve to produce sodium alginate solution; hence cells are freed from beads. As cell culture medium contains metal ions (which are also chelated by these ligands), beads were removed from medium before chelating agents were added.

As EDTA and citrate ions are cytotoxic (Amaral *et al.*, 2007), minimum exposure was required. Trypsin/EDTA solution containing 0.53mM EDTA, EDTA solution (125mM) and sodium citrate (55mM) were each added to alginate beads (100µl). Alginate beads did not dissolve upon addition of EDTA solution or Trypsin/EDTA, whereas treatment with sodium citrate (55mM) resulted in dissolution of the alginate matrix. As an equivalent concentration of sodium citrate is routinely

used to liquefy PLL-coated alginate beads (Lim and Sun, 1980), and the encapsulated cells are exposed to it for much longer (~5 minutes) than in the adapted method described below, the toxic effects of citrate were not considered further.

Based upon these findings, cells in individual beads were counted using a slightly adapted method based upon trypan blue exclusion. A single bead was placed on each half of a haemocytometer and as much medium as possible was removed. Sodium citrate (55mM, 5µl) was added to each bead followed by trypan blue (5µl). After 10 seconds a coverslip was placed over the beads, which had dissolved to give a cell suspension. Total cell and viability counts were carried out as described (Section 2.3.1.4). Using this method, cell viability and total cell numbers could be measured for each individual bead.

4.2.1.2 MTT

MTT (3-(4,5-Dimethylthiazol-2-yl)-2,5-diphenol tetrazolium bromide) is a yellow dye, which is reduced to insoluble purple formazan crystals in the presence of mitochondrial reductase enzymes. The resulting intracellular purple formazan can be solubilised and quantified colourimetrically. As mitochondrial reductase enzymes are only active in viable cells, this conversion can be used as a direct measurement of viable cell numbers (Mosmann, 1983).

Reconstituted MTT was added to adherent HEK293 cell cultures or bead samples as described in Section 2.3.4.1. Solubilisation of formazan using the solubilisation solution provided in the kit used (consisting of 10% Triton X-100 plus 0.1M HCl in anhydrous isopropanol; Sigma, UK) was successful for adherent cell cultures. However, once formazan had been formed by encapsulated cells, it remained trapped within the beads and could not be dissolved by the solubilisation solution provided. Other groups have bypassed this issue by applying DMSO to solubilise formazan instead (Rollan *et al.*, 1996; Rokstad *et al.*, 2002). This modification makes it necessary to introduce washing steps into the protocol. Whilst washing was not problematic for large beads, this proved extremely difficult when combined with the smaller beads produced by the microfluidic methods. It was found that smaller beads were easily lost whilst carrying out necessary washes with a micropipette. Also, sufficient formazan to produce a colour change was not present until 7 days after encapsulation, as low numbers of cells were present within the beads. Early stage viability could therefore not be obtained using this method.

4.2.1.3 LDH

The presence of lactate dehydrogenase (LDH) can be used to estimate the number of dead cells present in a given population. Upon cell death, LDH is released into surrounding medium, where it converts pyruvate to lactate, thus reducing NAD to NADH (Decker and Lohmannmatthes, 1988; Legrand *et al.*, 1992). The reduced NADH stoichiometrically converts a tetrazolium dye, thus producing a measurable colour change at 490nm.

To test this assay, encapsulated cells (40 beads) were added to medium (100µl) in a 96-well plate. This was carried out in quadruplicate. Beads and medium were incubated for 24 hours. The assay was then carried out on medium taken from encapsulated cells and medium taken from a serial dilution of cells, which had been killed by addition of LDH assay lysis solution (Section 2.3.4.2). The standard curve produced using the serial dilution of cells was linear between 7.8 x 10^4 and 2.5 x 10^6 cells per ml (Figure 4.1). A linear best fit line was fitted between these points (y=0.3747x + 0.0809). The R^2 value was 0.987. The slope of this line gives the relationship between cell concentration and absorbance reading. The number of cells present in the unknown samples was then calculated from absorbance.

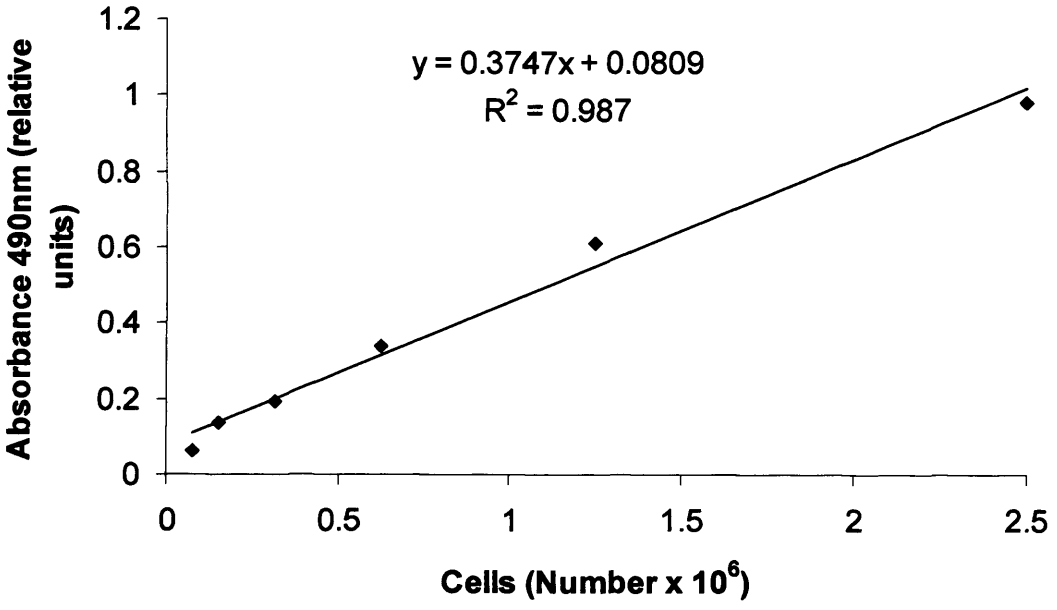

Figure 4.1: Graphical representation of absorbance obtained with varying cell numbers. LDH assay was carried out after 24 hour incubation of HEK293 cells with medium. Absorbance readings were taken at 490nm, background was subtracted at 690nm

The assay was carried out over 7 days after encapsulation of 4 separate cell populations (Figure 4.2). The standard deviation of the four replicates was large and the results gained were inconsistent. Hence this method was deemed to be of limited use.

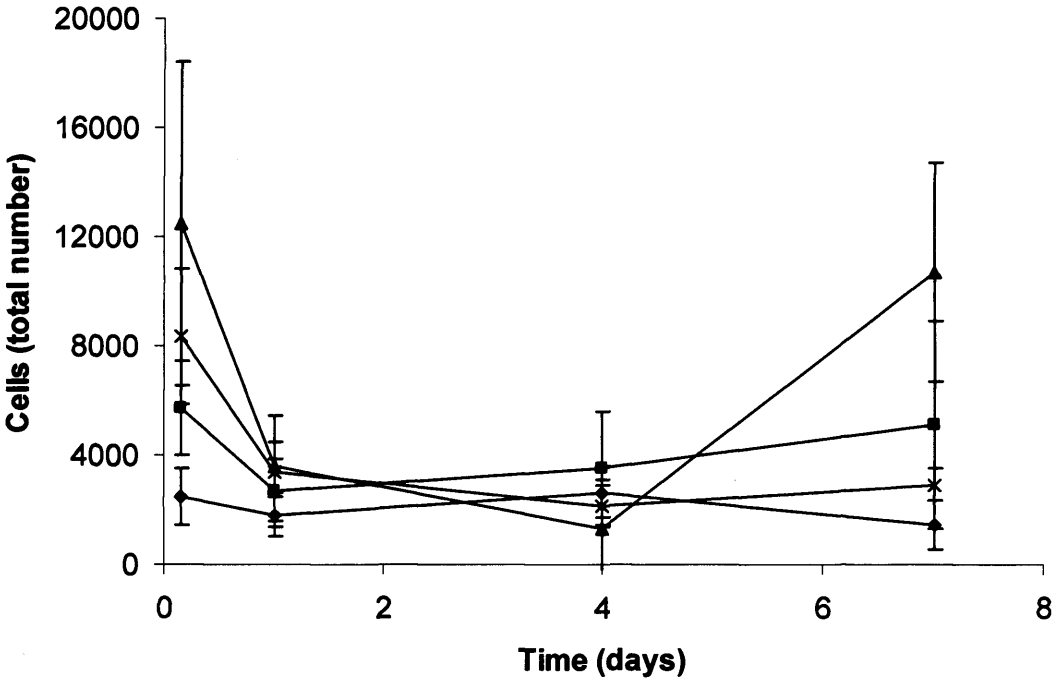

Figure 4.2: Graph showing number of dead cells estimated using LDH assay over time. Each point is from four replicate assay readings. Error bars show standard deviation

4.2.1.4 alamarBlue™

The alamarBlue™ assay contains a proprietary REDOX indicator, which is soluble and stable in cell culture medium and non-toxic to cells, thus allowing cells to be continuously monitored in cell culture medium (Ahmed *et al.*, 1994). AlamarBlue™ is reduced from its oxidised, blue form (absorbance peak at 600nm) to its reduced red form (absorbance peak at 570nm) after cellular uptake and metabolic activity. The resulting colour change from reduction of alamarBlue™ by living cells can be monitored using a spectrophotometer.

To test this assay with encapsulated cells, varying bead numbers were added to a 96-well plate. Approximately 50 beads were counted in quadruplicate into separate wells. As this proved to be very time consuming, for the remaining trial varying amounts of medium containing beads were measured volumetrically into wells. Flasks containing beads and medium were agitated to obtain a dispersed

mixture. Medium containing beads was pipetted in quadruplicate into separate wells of a 96-well plate. Different pipettor tips were chosen to investigate the reproducibility of this technique and to attempt to measure different volumes of encapsulated cells. In the first instance, 100µl of medium containing beads was pipetted with a 200µl pipettor tip. In the second instance, 200µl of medium containing beads was measured with a 1000µl pipettor tip. The assay was carried out on encapsulated cells as described (Section 2.3.4.3). A change in peak absorbance was observed over time (Figure 4.3). This correlates to a reduction of alamarBlue™, and thus cell proliferation. Samples containing the highest numbers of beads did not show an additional increase in absorbance between 16 and 24 hours. For comparison, fully reduced alamarBlue™ was obtained by autoclaving alamarBlue™ solution (10% v/v) according to the manufacturers' protocol (Section 2.3.4.3).

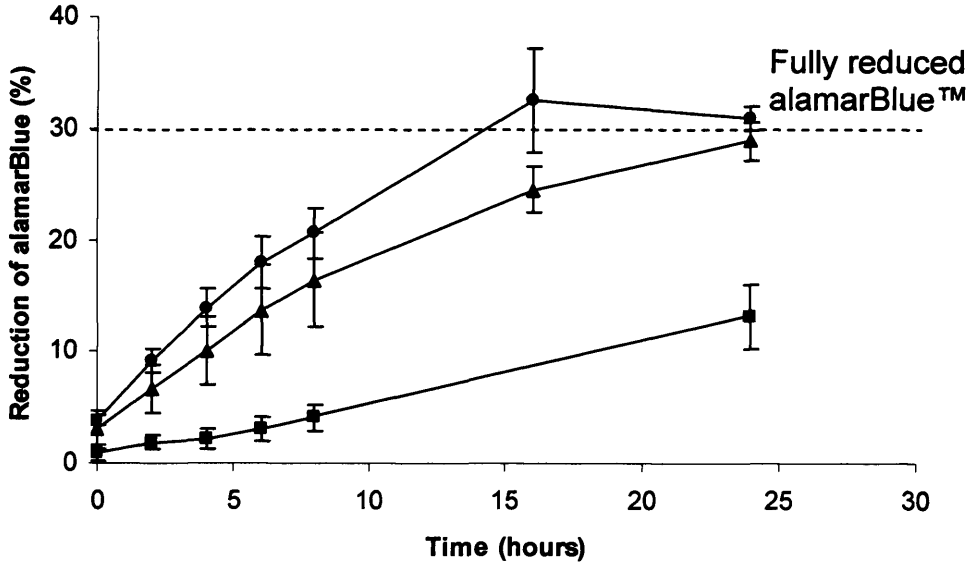

Figure 4.3: Graph showing percentage reduction of alamarBlue™ over time. Fifty beads (■), 100µl of beads (▲) and 200µl of beads (●) were present per well. All bead samples were incubated with alamarBlue™ (10%) in medium. Dashed line at 30% represents fully reduced alamarBlue™ obtained by autoclaving alamarBlue™ solution (10% v/v). Error bars show standard deviation of 4 replicates

4.2.1.5 LIVE/DEAD® staining

The commercially available LIVE/DEAD® Viability/Cytotoxicity Kit for mammalian cells (Molecular Probes, Paisley, UK) allows live and dead cells to be detected *via* fluorescent probes. Calcein AM is non-fluorescent and cell-permeant. It is converted to the highly fluorescent calcein by intracellular esterase activity. Calcein

is retained within living cells giving an intense green fluorescence (479nm excitation and 517nm emission). Ethidium homodimer-1 binds to nucleic acids, but is excluded by living cell membranes. When bound to DNA of cells with damaged membranes, ethidium homodimer-1 fluoresces bright red (528nm excitation and 617nm emission). The dual fluorescence can be detected by fluorescent microscopy, multiwell plate scanners, and flow cytometers. In this investigation, flow cytometery and microscopy (both fluorescent and confocal) were evaluated as potential platforms to quantify relative cell viability.

4.2.1.5 a) Microscopic quantification

Dyes were added directly onto encapsulated cells, in medium without serum, in 96-well U-bottom plates (Section 2.3.4.4). Use of a haemocytometer or 384-well plate was not possible with the available microscope. Small volume U-bottom plates were deemed most suitable for observation of single beads. Although cells were observed to glow green and red, cell counting was unreliable and inaccurate due to weak overall fluorescence from individual cells. Photographs could not be taken using this method as the microscope was not equipped with a camera and so counting had to be carried out rapidly at the microscope.

4.2.1.5 b) Confocal microscopy

Beads were observed using confocal microscopy (Leica DM600B upright microscope) after LIVE/DEAD® staining (Figure 4.4). Again, stains were added directly to beads in medium without serum (Section 2.3.4.4). As the fluorescent signal became attenuated by passing through more than 200μm of cross-linked alginate, beads were not imaged in their entirety; instead imaging began at the top of the bead and was continued until the fluorescent signal could no longer be collected. Therefore images shown are representative of the uppermost 200μm area of bead.

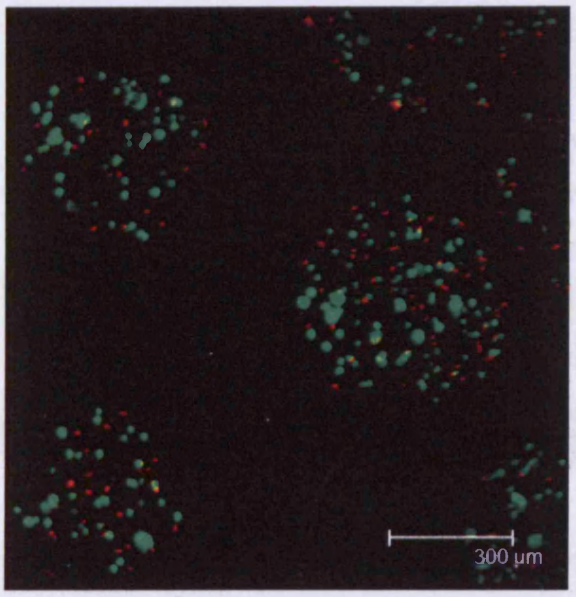

Figure 4.4: Confocal image of encapsulated HEK293 cells stained with LIVE/DEAD® stain. Image shows distribution of live and dead HEK293 cells encapsulated within alginate microcapsules, 1 day after encapsulation. Green fluorescence is emitted from intracellular esterase-converted calcein in live cells, whereas red fluorescence is emitted from ethidium homodimer present in the nuclei of dead cells. Scale bar represents 300µm

4.2.1.5 c) Flow cytometry

Flow cytometry is a technique where a stream of cells is forced to flow in a restricted fluid channel, thus allowing characteristics of an individual cell to be assessed. In modern flow cytometers, laminar flow systems are used so that a focussed flow of cells can be achieved without blocking the flow cytometer nozzle. Cell detection is by fluorescent emissions and light scatter from the cells following laser excitation. Light scatter, which occurs with all particles passing through the flow cytometer allows the size and density of the cell to be measured. Forward (or low angle scatter) increases with cell size, whilst side (or high angle) scatter increases with cell density and granularity. In addition to the scatter characteristics, if the cells are labelled with fluorescent probes (such as antibodies conjugated to fluorochromes), laser excitation of the probes results in emissions of specific wavelengths, which are captured through one set of collection lenses, separated according to wavelength by dichroic mirrors, individually amplified and detected by photomultiplier tubes.

As encapsulated cells were too large to pass through the cytometer nozzle, cells had to be released from beads before this technique could be used. Sodium citrate (55mM, 1ml) was used to dissolve beads (1ml) after medium had been removed. Beads and sodium citrate were incubated for 10 minutes at 37°C. Cells

liberated in this way were washed in D/MEM-F12, counted as described in Section 2.3.1.4 and then resuspended at a concentration between 0.1 and $5x10^6$ cells per ml in D-MEM/F12 (1ml). Cells from culture were trypsinised (Section 2.3.1.2), and washed. Dyes were added to cells, both from culture and released from beads, as described (Section 2.3.4.4) and detected using FACScanto (488 nm excitation and measuring green fluorescence emission for calcein (530/30 bandpass filter) and red fluorescence emission for ethidium homodimer-1 (670 longpass filter)). As can be seen from Figure 4.5 and Table 4.1, live and dead cells could be detected from both populations of cells.

	Number of live cells	Number of dead cells	Cells alive (%)
Cells	13010	5613	69.9
Cells from beads	5908	7741	43.3

Table 4.1: Summary of data collected using flow cytometry

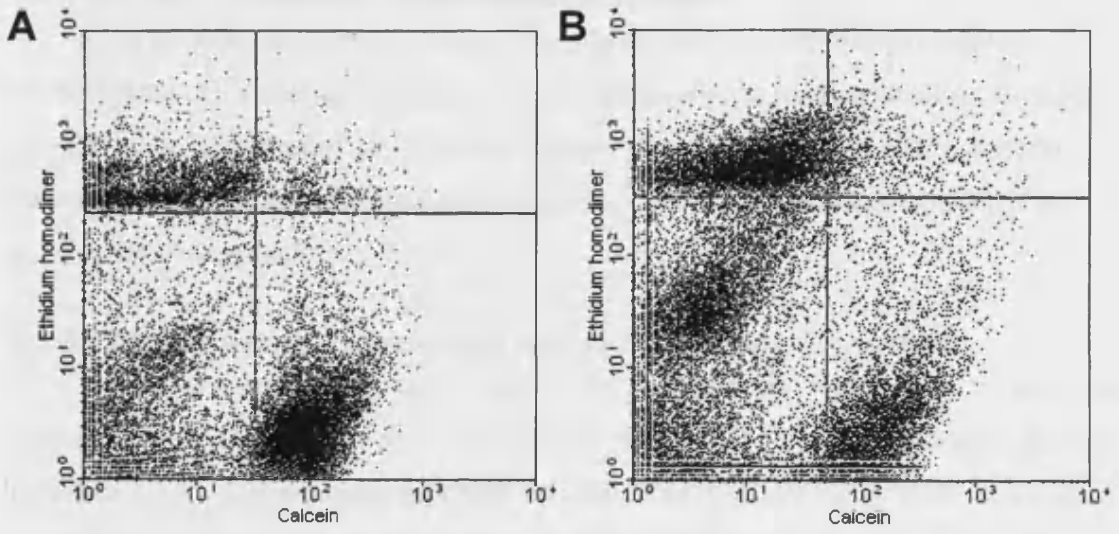

Figure 4.5: Diagram showing fluorescence of HEK293 cells stained with ethidium homodimer and calcein. A) HEK cells from culture and B) HEK cells released from beads. Green fluorescence is emitted from intracellular esterase-converted calcein in live cells, whereas red fluorescence is emitted from ethidium homodimer present in the nuclei of dead cells. Fluorescence was detected using FACScanto (488 nm excitation and measuring green fluorescence emission for calcein (530/30 bandpass filter) and red fluorescence emission for ethidium homodimer-1 (670 longpass filter)). Each dot represents one cell

Comparison of trypan blue exclusion and flow cytometry

Cell populations used above were counted using trypan blue exclusion (Section 2.3.1.4) to estimate the number of cells to stain using LIVE/DEAD® staining. Live and dead cells were analysed using flow cytometry (Table 4.1). Cells from culture had a viability of 68% when counted using trypan blue exclusion, compared with 70% when using flow cytometry. The viability of the cells used for this experiment was lower than that seen in previous experiments (for example, see Section 4.2.2.1). The reason for this reduced viability was not clear. Cells from beads had a viability of 52% when counted using trypan blue exclusion, compared with 43% when using flow cytometry.

As a result of the above experiments, trypan blue was used to estimate cell viability in all subsequent experiments. The adapted trypan blue method was used to obtain estimates of encapsulated cell viability at regular time points throughout experiments, with observations of encapsulated cells carried out visually using a light microscope. At key time points, for example, when clusters began to form, viability was estimated using LIVE/DEAD® staining and detected using a confocal microscope.

4.2.2 Toxicity of developed encapsulation procedures

As an appropriate combination of methods had been developed to assess encapsulated cell viability, the cytotoxicity of each developed encapsulation method could now be investigated. As previously stated (Sections 4.1 and 1.6) the method chosen to encapsulate cells should not be cytotoxic and cell viability should not be substantially decreased.

4.2.2.1 Toxicity testing of components used in external gelation method

For this experiment only, reactivated hepatocytes were used to test the cytotoxicity of the components used in the microfluidic external gelation method (Section 3.3.1). Hepatocytes supplied by Abcellute (Cardiff, UK) were reactivated according to the manufacturers' instructions, outlined in Section 2.3.2. Reactivated hepatocytes were resuspended at a cell concentration of 4.4×10^6 cells per ml. Cell viability prior to any testing was carried out using trypan blue exclusion (Section 2.3.1.4).

An aliquot (1ml) of hepatocytes in suitable medium was split in half, with one half placed in a humidified 5% CO_2 incubator at 37°C for the duration of the

experiment as a control. The remaining cells in medium were used to test the effect of transit through the MicroPlant™. This was repeated using cells resuspended in alginate solution (2% w/v). A final sample of cells was encapsulated using the microfluidic method developed using 1-octanol as a carrier fluid. After each process cell viability was estimated again using trypan blue. Viability was expressed as the percentage of cells surviving each process, as shown in Figure 4.6.

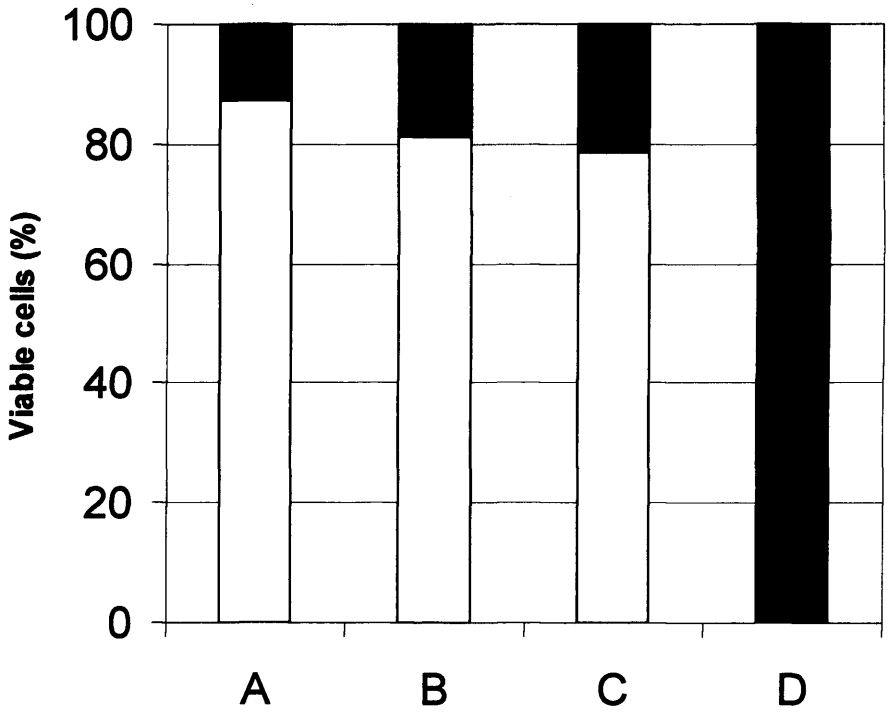

Figure 4.6: Stack diagram showing percentages of cells alive and dead from varying components of the encapsulation process. A represents control cells in medium placed in an incubator for the duration of the experiment, B represents cells transported through the MicroPlant™ in medium, C represents cells transported through the MicroPlant™ in alginate (2% w/v) and D represents cells encapsulated using the microfluidic method developed using 1-octanol as a carrier fluid. Viability was estimated using trypan blue exclusion

Passage through the microfluidic device was not harmful, in medium or alginate solution. This also showed that alginate solution was not harmful to the cells. Use of 1-octanol however was extremely detrimental to cell viability, with no cells surviving the encapsulation process.

Figure 4.7A shows dead hepatocytes encapsulated within alginate beads produced *via* the microfluidic external gelation method. Product beads containing cells (n=40) had a slightly smaller mean diameter (249±4μm, with a CV of 1.6%; Figure 4.7B) than plain alginate beads produced previously using this method

(Section 3.3.1; 277±5μm; t_{87} = -29.30, $p < 0.005$). This method was rejected due to the observed cytotoxic effects of 1-octanol.

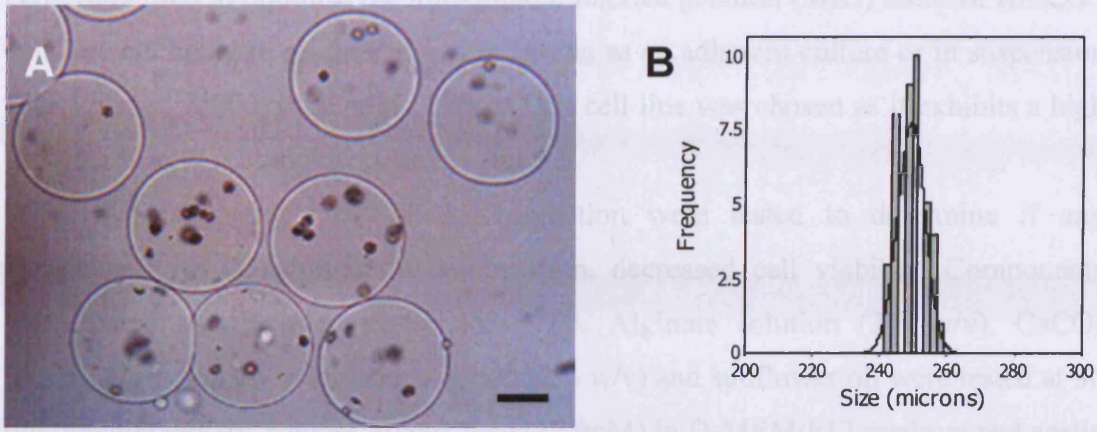

Figure 4.7: Rat hepatocytes encapsulated in alginate beads. A) A representative bead population containing rat hepatocytes produced by segmenting alginate with 1-octanol using a shielded microfluidic junction, as shown in Figure 3.7. Scale bar represents 100μm. B) Histogram of beads represented in A; grey bars show measured data, with black line representing normal distribution. Mean bead diameter was 249±4μm. Distribution was considered not normal (A^2=0.84, $p < 0.028$)

4.2.2.2 Toxicity testing of components used in the internal gelation method

From this point onwards in this chapter Human Embryonic Kidney (HEK293) cells were used to optimise the microfluidic internal gelation (MIG) method. HEK293 cells are epithelial in origin and can be grown as an adherent culture or in suspension (Parekh *et al.*, 2000; Park *et al.*, 2006). This cell line was chosen as it exhibits a high growth rate and is straightforward to culture.

All components of the MIG reaction were tested to determine if any components, in isolation or in combination, decreased cell viability. Components were tested as described in Section 2.3.3. Alginate solution (2% w/v), $CaCO_3$ (400mM) suspended in alginate solution (2% w/v) and sunflower oil were tested at 30 minute intervals for 5 hours. Acetic acid (125mM) in D-MEM/F12 medium and acetic acid (125mM) in sunflower oil were tested at 1, 5 and 10 minute periods. All samples were stored in a sterile hood between testing points, with the exception of cells in control medium which were stored in a humidified 5% CO_2 incubator at 37°C.

Alginate solution, calcium carbonate and oil were shown to be non-toxic over 5 hours (Figure 4.8). However, acetic acid at the concentration used, was shown to have a negative effect upon viability after one minute and was fatal to cells after 10 minutes (Figure 4.9). The addition of oil to acetic acid appeared to ameliorate the toxic effect observed, as after 10 minutes of exposure cell mortality had reduced by 50%. HEK293 cells did not survive encapsulation with components at stated concentrations.

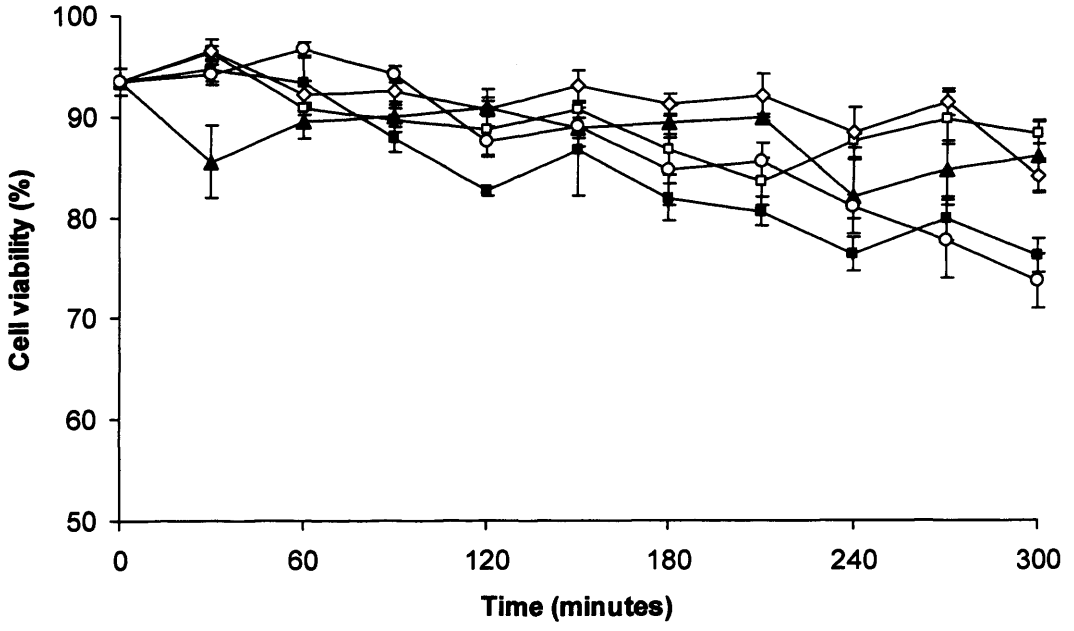

Figure 4.8: Viability of HEK293 cells exposed to components of the MIG method over 5 hours. Cytotoxic effect of alginate (2% w/v ◊), alginate and calcium carbonate (400mM▲) and oil (○) on cells over 5 hours. Medium kept in an incubator (■) and medium kept in the hood (□) for the duration of the experiment are included as control points. Viability was estimated using trypan blue exclusion. Error bars show standard error of the mean of 3 replicate samples

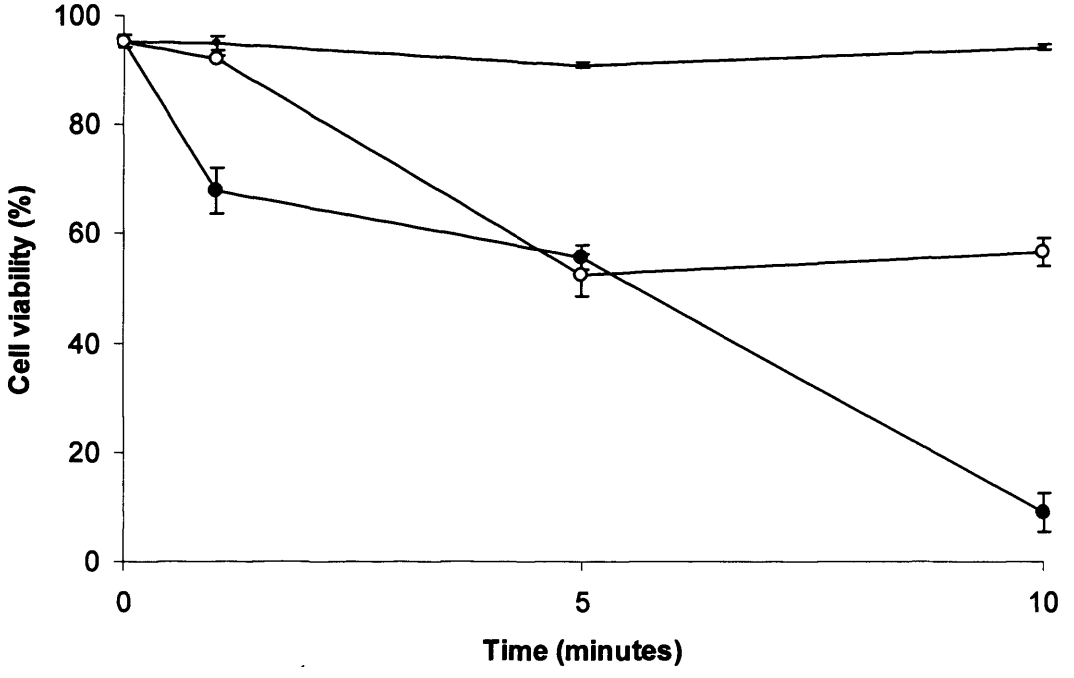

Figure 4.9: Viability of HEK293 cells exposed to components of the MIG method for 10minutes. The effect on cell viability of acetic acid (125mM●) and acetic acid (125mM) plus oil (○), over 10 minutes. Medium kept in the hood (·) for the duration of the experiment is included as a control. Viability was estimated using trypan blue exclusion. Error bars show standard error of the mean of 3 replicate samples

4.2.2.3 Optimising concentration of components used in the internal gelation method

Although acetic acid was shown to be toxic to cells at the concentration used (125mM in medium), this effect was ameliorated in the presence of sunflower oil. Thus, the presence of acetic acid did not, in isolation, account for the toxic effect the entire process had on cells. It was observed that excess $CaCO_3$ was present in beads produced using the MIG method (Section 3.3.3). As solid beads were produced, there was obviously sufficient Ca^{2+} liberated to cross-link all alginate chains present within a droplet. Hence, it was concluded that, since a surfeit of $CaCO_3$ was present, the concentration used could be reduced. From Equation 1.1 (Section 1.7.2.2) stoichiometric amounts of $CaCO_3$ and acetic acid react to form Ca^{2+}. If $CaCO_3$ concentrations can be reduced, then a concomitant decrease in acetic acid concentration can occur.

Concentrations of $CaCO_3$ and acetic acid were reduced as shown in Table 4.2. Reaction components at these concentrations were used in the microfluidic circuit shown in Figure 3.10, as previously described (Section 3.3.3). Beads produced thus were observed *via* a light microscope and photographs were taken (Table 4.2). Size was determined (Section 2.2.3) and diameters calculated (n=20). $CaCO_3$ concentrations of less than 50mM resulted in non-spherical, unstable beads. A distinct interface between beads and the aqueous medium was not observed using a light microscope. Upon reducing acetic acid concentrations to 50mM (pH = 4.5, Section 2.2.7), solid beads were produced. Hence, acetic acid and calcium carbonate concentrations of 50mM were used in all subsequent experiments with HEK293 cells.

Concentration of $CaCO_3$	Concentration of acetic acid	Solid beads?	Average diameter ± SD (μm)	CV%	Photograph
400mM	125mM	Yes	268±4.2	1.6	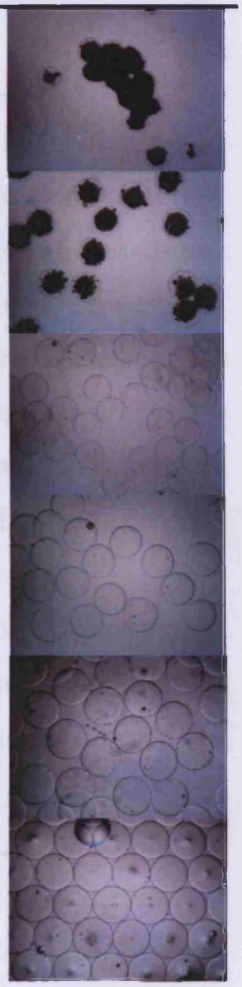
300mM	125mM	Yes	298.4±4.9	1.6	
200mM	125mM	Yes	275.6±6.6	2.4	
100mM	125mM	Yes	329.8±11.1	3.4	
50mM	125mM	Yes	378.9±8.9	2.4	
50mM	50mM	Yes	377.3±7.6	2.0	
25mM	50mM	No			

Table 4.2: Formation of alginate beads using differing concentrations of calcium carbonate and acetic acid. Beads were made using 2% alginate

4.2.3 Extended viability measurements

Using the concentrations determined above, four independent bead replicates (numbered sequentially from 1 to 4 in order of encapsulation) were generated from four separate flasks of HEK293 cells. Each flask of cells was trypsinised (Section 2.3.1.2), washed and counted (Section 2.3.1.4) immediately prior to encapsulation. Cells were encapsulated at a concentration of $2x10^7$ cells per ml. Beads were collected from the MicroPlant™ in the carrier fluid. The following steps were carried out on beads collected over a 5 minute period, with each encapsulation experiment lasting 20 minutes. Medium was added to beads in carrier fluid and the mixture subsequently

centrifuged to remove beads into medium. Beads were then transferred to a T25 flask with D-MEM/F12 supplemented with serum (25ml). Roughly 500µl of beads were produced in each encapsulation experiment. To maintain cell viability, medium was changed twice a week.

The adapted trypan blue method (described in Section 4.2.1.1) was used to establish any effects of encapsulation on long-term viability of the four encapsulated cell replicates. For each time point, four beads from each replicate were taken and viable cells counted (Figure 4.10). Time point zero represents cell viability measured after cells were trypsinised, prior to addition of $CaCO_3$ and alginate mixture and subsequent encapsulation. An initial decrease in cell viability was observed, the decrease in cell viability continued until 14 days post-encapsulation, after which time cell viability was seen to increase to near pre-encapsulation levels. The increase in cell viability was coincident with the appearance of cells growing in aggregates (Figure 4.11).

Although initial cell counts were easy to perform using the adapted trypan blue exclusion method, as cell numbers increased, counts became more problematic. Initially, low cell numbers were present and cells were observed to be discrete and randomly distributed throughout each bead. Subsequently, as cell aggregates grew, cells were very difficult to count accurately. Viability counts were continued until no beads remained for each replicate. Replicate 4 showed a much larger decrease in viability than any of the other three replicates. After 14 days it was decided that as so few cells were alive further viability measurements would be discontinued.

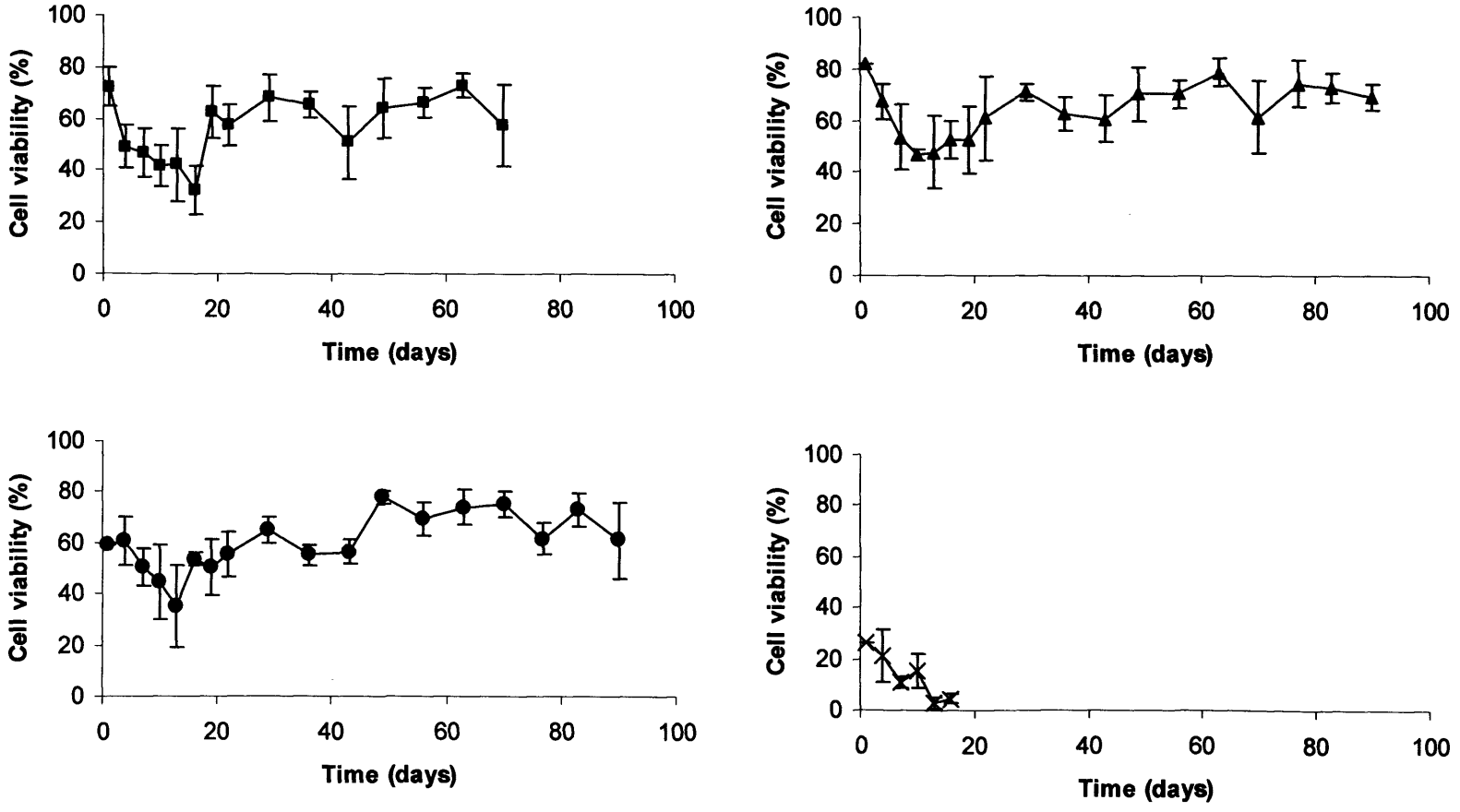

Figure 4.10: Graph showing percentage cell viability of four replicates of encapsulated cells. Each replicate of cells, Replicate 1 (■), Replicate 2 (▲), Replicate 3 (●) and Replicate 4 (X), was taken from a separate flask and encapsulated individually. Pre-encapsulation viability was 96% for Replicates 1 and 3 and 97% for Replicate 2 and 4. Viability was estimated using the adapted trypan blue method. Error bars show standard deviation of 4 individual beads

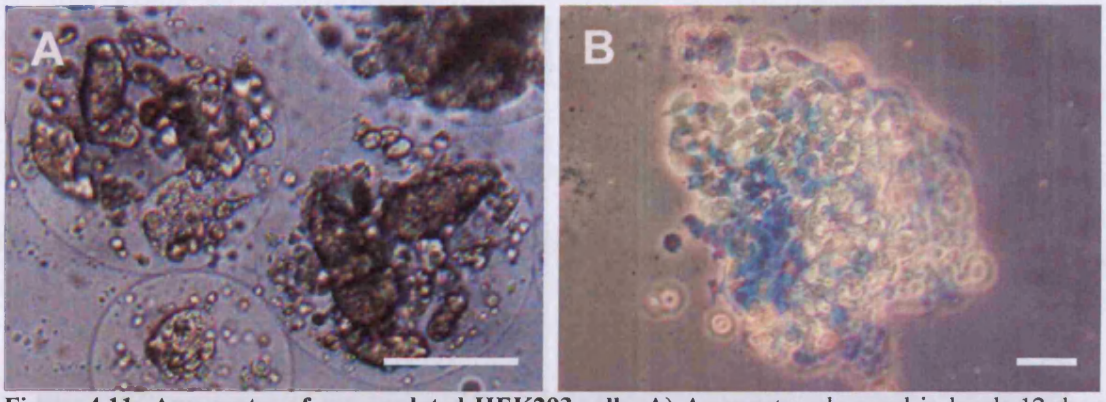

Figure 4.11: Aggregates of encapsulated HEK293 cells. A) Aggregates observed in beads 12 days after encapsulation. Scale bar represents 250μm. B) Aggregates observed on a haemocytometer after alginate bead dissociation and trypan blue staining. Scale bar represents 50μm

Encapsulated cells were also observed using LIVE/DEAD® staining and confocal microscopy (Section 4.2.1.5 b) at 1, 5, 12 and 20 days post-encapsulation (Figure 4.12). Both live and dead cells were detected at all time points. Cells were seen to be separate and individual at 1 and 5 days post-encapsulation (Figure 4.12A-C). When beads were observed 5 days after encapsulation, a proportion contained cells which appeared to be swollen in comparison to cells in other beads (Figure 4.12B – normal compared with C – swollen). By 12 days after encapsulation, aggregates of cells were observed inside beads, which had not been present prior to this time point (Figure 4.12D). By increasing the magnification, individual cells within the aggregates could be seen (Figure 4.12E). These aggregates of cells continued to expand and were much larger by day 20 (Figure 4.12F).

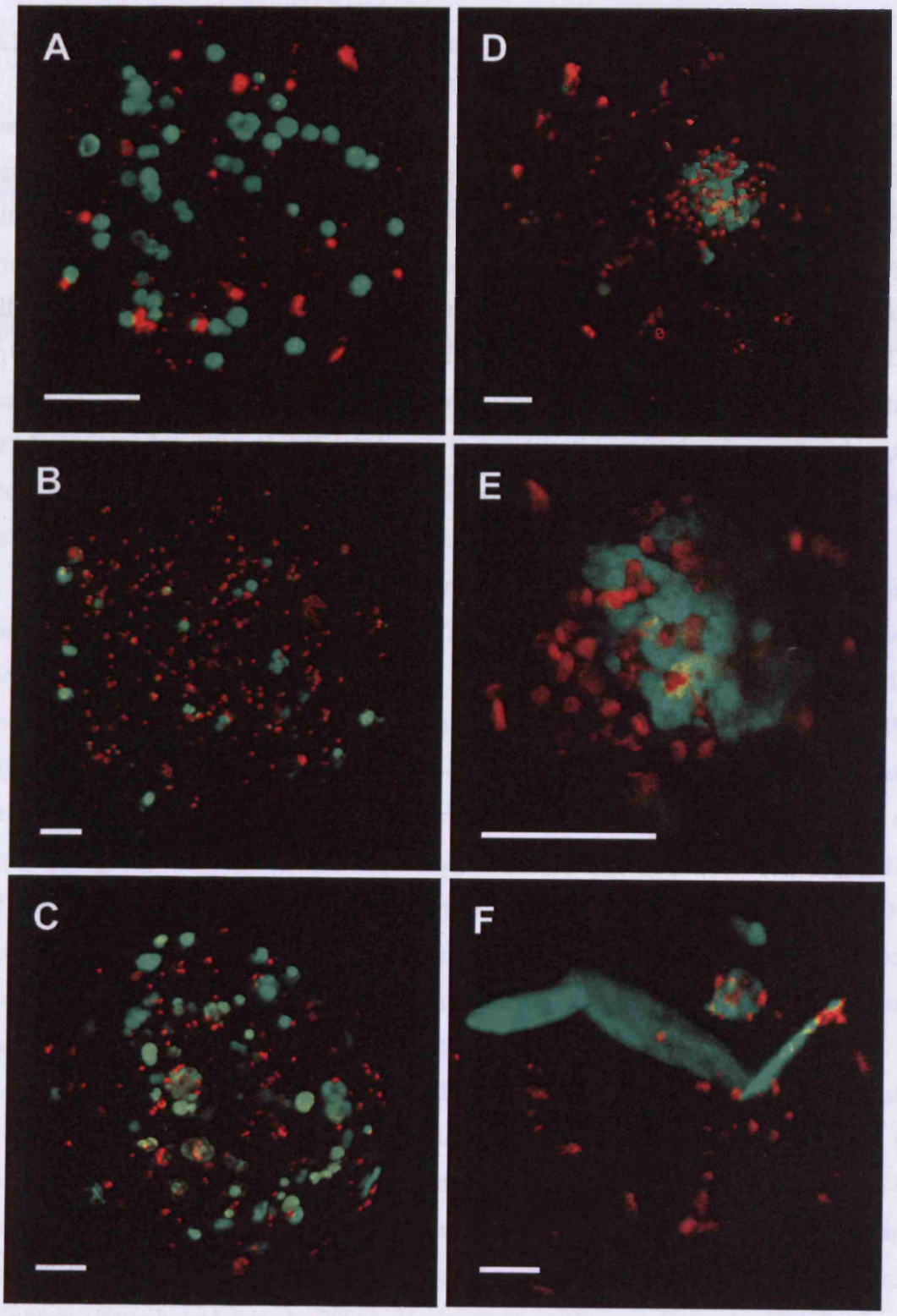

Figure 4.12: Confocal images of encapsulated HEK293 cells. Images show distribution of live and dead HEK293 cells encapsulated within alginate microcapsules, 1 day (A), 5 days (B,C), 12 days (D,E) and 20 days (F) after encapsulation. Swollen cells can be observed in C when compared with B. A-D and F represent all cells within the top hemisphere of an individual bead. E represents Aggregates of cells present in D magnified. Green fluorescence is emitted from intracellular esterase-converted calcein in live cells, whereas red fluorescence is emitted from ethidium homodimer present in the nuclei of dead cells. Scale bars represent 100μm

4.3 DISCUSSION

4.3.1 Comparison of cell viability methods

Methods were investigated to assess their suitability for estimating viability of encapsulated cells. It was essential that the method ultimately chosen gave an accurate estimate of cell viability and was quick and easy to carry out. It would be useful, although not necessary, for the chosen method to consist of minimal steps, allow multiple samples to be analysed simultaneously and cells to remain *in situ*. Although all the methods investigated have been successfully utilised by other groups investigating encapsulated cells (e.g. MTT (Roberts *et al.*, 1996), LIVE/DEAD® staining (Choi *et al.*, 2006), alamarBlue™ (McGuigan *et al.*, 2008) and LDH (Khattak *et al.*, 2006)), they proved difficult to use in combination with beads produced using the MIG method. There were several issues arising from the use of beads produced using the MIG method, which will be discussed below.

To ensure comparability, an equal number of beads must be measured at each time point and in each replicate sample. This is not problematic if beads are much larger than the inner diameter of a pipette tip, such as those produced *via* commonly used droplet production methods (Section 1.9). As beads are too large to enter the pipette tip they are held on to it by suction, thus allowing manipulation. In contrast, beads generated *via* MIG are of a diameter slightly smaller than the inner diameter of a pipette tip. This means beads are too small to be manipulated *via* suction on the tip of a pipette. For this reason it is difficult to count beads produced using the MIG method accurately and quickly. So, although MTT, LDH and alamarBlue™ have been shown to be suitable for use with traditionally generated beads, problems were encountered when used in conjunction with beads produced using the MIG method.

Another problem arising from bead size is that washing steps were extremely difficult to carry out. MTT has been used extensively to estimate cell viability in encapsulated cell populations. Modifications are extremely common, although this is not surprising, as even when used with un-encapsulated cell lines, modifications are needed to solubilise the formazan produced, as it is not fully soluble in aqueous solutions (Kwack and Lynch, 2000). Various alternatives to isopropanol have been suggested, for example: acidified sodium dodecyl sulphate (Tada *et al.*, 1986) or DMSO (Sladowski *et al.*, 1993; Uludag and Sefton, 1993; Roberts *et al.*, 1996). Stevens and Olsen (1993) propose that MTT is inappropriate and that XTT (2,3-bis[2-

Methoxy-4-nitro-5-sulfophenyl]-2H-tetrazolium-5-carboxanilide) is preferable as water soluble formazan is produced by its conversion. All of the discussed adapted MTT protocols require wash steps and whilst this has not been reported as problematic for large beads, smaller beads were easily lost whilst carrying out necessary washes with a micropipette. As more care is required when washing smaller beads, washing steps take longer to carry out and any advantages conferred with respect to time are lost. Accuracy also decreases if beads are lost as samples are no longer equivalent. Thus, all the advantages of the MTT method, that is, rapid, one-step, *in situ* viability estimates, were lost with the addition of washing steps.

The LDH assay did not prove to be a consistent method for determining numbers of dead cells. Also, due to upregulation of per cell function of several proteins due to encapsulation (Selden *et al.*, 1999), it may be problematic to compare LDH release from monolayer cells to LDH release from encapsulated cells. A better comparison would be to compose a standard curve from different numbers of beads (Khattak *et al.*, 2006).

MTT, LDH and alamarBlue™ assays are relatively easy and quick to carry out. LDH and alamarBlue™ are simple, one-step assays. Initial steps of the MTT assay can be carried out and then stored to enable multiple samples to be analysed together (Rokstad *et al.*, 2002). All of these protocols require beads to be counted as an initial step.

Few measurements can be performed in a given time using trypan blue to estimate cell viability, as counts have to be performed sequentially. This makes it one of the more time consuming methods investigated. Although staining cells using the LIVE/DEAD® protocol is rapid and easily carried out, downstream steps i.e. microscopy and flow cytometry, require optimisation and care to be taken. Confocal microscopy and analysis *via* flow cytometry are more time consuming for this reason. As counting must be carried out immediately after trypan blue or LIVE/DEAD® staining, samples cannot be stored or analysed in parallel. This adds to the time taken to estimate cell viability.

All tested methods are cytotoxic or destructive apart from alamarBlue™ and LDH. Thus, it is theoretically possible to re-introduce beads into the culture flask after using alamarBlue™ and LDH assays leaving the population undiminished. Unfortunately, as plates containing beads are read without a lid, in a

spectrophotometer, sterility is not ensured. Consequently the observed readings may be due to micro-organism contamination.

As the only method tested which allows measurements to be taken of individual beads, trypan blue does not require as many beads to estimate cell viability as the other methods. Trypan blue is also the only method tested which allows individual bead measurements to be taken as opposed to average values from multiple beads. Due to the many data points collected, flow cytometry is statistically better than any other method investigated. However, the disadvantage of this is that many encapsulated cells are needed for each time point. Three times more beads than can be produced in a single encapsulation experiment are required for *each* time point. This means that to produce data for 20 time points, 60 encapsulation experiments are required. LDH assay also required many more beads at each time point than those tested. The numbers of cells present in the 40 beads taken for each replicate were at the lower limit of detection for the assay. To give readings within the linear range of the LDH assay, 4000 beads should be taken for each time point. This is roughly half the beads produced in one encapsulation experiment.

The most appropriate detection method tested in combination with LIVE/DEAD® staining was confocal microscopy. Unfortunately, this detection method is extremely expensive as specialised equipment and personnel are required. For this reason, it was only used to take limited measurements. As trypan blue is very cheap, it was used more often to give estimates of viability. This compromise was deemed the most accurate method for estimating viability.

Difficulties in quantifying cells in aggregates were encountered when using methods requiring visual counts, i.e. trypan blue and LIVE/DEAD® staining. Although cell morphology is retained when LIVE/DEAD® staining is used in conjunction with confocal imaging, this is not true of trypan blue counts. Not only is cell cluster morphology unobservable when using trypan blue, large numbers of cells may be compressed when covered with a coverslip. This leads to an overestimation of dead cells and a decrease in estimated overall cell viability. However, it was observed that trypan blue diffused to the centre of aggregates, thus enabling accurate estimates to be made. Use of an o-ring to raise the coverslip would allow counts to be carried out without compressing the encapsulated cells, and thus more accurate counts would be obtained.

Analysis *via* flow cytometry requires filtering steps which unavoidably exclude cell clusters. To remove the cells from beads, harsh pipetting steps are required which may cause dead cells to disintegrate or indeed kill fragile cells. This may help to explain the observation that percentage viability of encapsulated cells appeared lower when estimated using flow cytometry than with trypan blue (Section 4.2.1.5 c). Other methods tested, with the exception of trypan blue, do not require beads to be dissolved prior to analysis and would hopefully be more accurate than FACs or trypan blue.

In summary, although the methods investigated have been used by other groups analyzing encapsulated cells produced using common techniques, only trypan blue and LIVE/DEAD® staining were appropriate for use with cells encapsulated using the MIG method. This was due to difficulties encountered when counting and washing smaller beads. In addition, there were various problems specific to each method. In these investigations the LDH assay was extremely unreliable and difficult to carry out. This is probably due to difficulties in counting beads. AlamarBlue™ was found to be inaccurate as microbial contamination is difficult to avoid and so any observed reduction may be due to micro-organism contamination.

Of all the methods tested, the adapted trypan blue exclusion method developed was deemed most suitable, as it proved to be both simple and rapid to carry out. There were difficulties accurately counting cell clusters at later time points. As cells became ruptured by the pressure applied with the coverslip, dye was able to pass inside. This led to possible overestimation of dead cell numbers. Encapsulated cells were labelled using LIVE/DEAD® stain and observed using confocal microscopy at various key time points. This allowed 3D cell morphology to be seen, which was impossible with trypan blue exclusion. Using both methods in conjunction allowed encapsulated cell viability to be estimated for extended time periods, cheaply and easily. This approach has also been employed by Choi *et al.* (2006).

4.3.2 Toxicity of developed encapsulation methods

Although two microfluidic methods were developed which produced alginate beads, only one was deemed suitable for encapsulating cells. The external gelation method utilising 1-octanol for segmentation was extremely toxic to cells. Two groups have successfully used organic solvents in microfluidic circuits to produce calcium cross-linked alginate beads. Choi *et al.* (2007) observed GFP expression in alginate

encapsulated yeast cells after encapsulation using hexadecane. GFP expression is not the most accurate or reliable way of demonstrating cell viability as GFP protein can still be seen in dead, fixed samples (Chalfie *et al.*, 1994). No further methods were used to establish cell viability, nor was viability shown for extended periods of time. Zhang *et al.* (2006) did not attempt to encapsulate cells using the previously discussed method (Section 3.4) utilising CaI_2 in undecanol, indeed their next publication utilised soybean oil as an alternative to undecanol (Zhang *et al.*, 2007).

Viable cells could not initially be encapsulated using the MIG method. Upon testing, acetic acid was the only component used in the MIG method found to be cytotoxic. However, when sunflower oil was also present, this toxic effect was lessened. Therefore the presence of acetic acid, in isolation, could not completely explain why the encapsulation process should cause total cell death. In addition, acetic acid was seen to be toxic after five minutes of exposure, whereas, cells are exposed to acetic acid in sunflower oil for approximately 30 seconds whilst in the MicroPlant™. This short exposure is unlikely to result in complete cell death, as a 5 minute exposure to acetic acid in sunflower oil was shown to reduce viability by 50%.

It was proposed that excess Ca^{2+}, produced from excess $CaCO_3$ and acetic acid, was responsible for the extreme toxicity of the MIG process. As only a finite number of cross-linking points are present in a given sample of alginate, only a finite amount of Ca^{2+} can be utilised for cross-linking. Once Ca^{2+}, liberated from the $CaCO_3$ by acetic acid, has been sequestered by all available alginate chains any excess will serve to increase the extracellular Ca^{2+} concentration. Excess Ca^{2+} influx into cells is known to trigger apoptosis (Burek *et al.*, 2003), thus causing cell death. A reduction in acetic acid and $CaCO_3$ concentrations allowed solid alginate beads to be produced. These concentrations were also suitable for encapsulating HEK293 cells with little loss of observed viability. This represents the first successful synthesis of calcium alginate beads containing live mammalian cells in a microfluidic chip (Workman *et al.*, 2007; Workman *et al.*, 2008).

The MIG method with reduced concentrations of $CaCO_3$ and acetic acid was used to encapsulate four separate populations of HEK293 cells. All populations, except one, showed an initial decrease in viability followed by recovery and an increase in viability. In contrast, population 4, did not increase in viability, but continued to decrease. Population 4 was encapsulated last, but as all encapsulation experiments were carried out immediately following trypsinisation of cell populations

all cells were exposed to alginate and $CaCO_3$ for the same length of time. The microfabricated device was not taken apart and cleaned between each encapsulation experiment, this may have affected the operation and hence the viability of this encapsulated cell population.

During this experiment some encapsulated cells appeared swollen in comparison to cells in other beads. This apparent swelling was not observed at all time points. Swelling of cells occurs in response to changes in osmotic pressure (Macknight, 1988). Changes in osmotic pressure bought about by the encapsulation process would be expected to cause cells to swell almost immediately after encapsulation. As the apparent swelling was observed 5 days after encapsulation it is unlikely to have been due to the encapsulation process. A more likely explanation is that cells were beginning to form the aggregates observed at later time points. These aggregates appeared to be groups of daughter cells produced by division and contained by the matrix near their parent cells. The increase in observed viability can be explained by this cell division producing increased numbers of viable cells.

Microfluidics-based devices have previously been used to encapsulate cells in lipid vesicles (Tan *et al.*, 2006a) and droplets (He *et al.*, 2005). However, these systems are more commonly used for analytical testing of cells/organelles or on-chip cell culture (Clausell-Tormos *et al.*, 2008; Koester *et al.*, 2008). Various micro-systems have been developed to encapsulate cells in alternative hydrogels (for example; puramtrix (Um *et al.*, 2008) and chitosan (Yang *et al.*, 2007)). Of the methods discussed previously (Section 3.4), very few groups successfully encapsulated live cells. Shintaku *et al.* (2007) encapsulated murine erythroleukemia cells, but presented no short- or long-term viability data. Tan and Takeuchi (2008) encapsulated viable Jurkat cells using a similar internal gelation technique as outlined in this thesis. Kim *et al* (2009) successfully encapsulated mouse stem cells (P19 EC), HepG2, and human breast cancer cells (MCF-7) in alginate beads and reported viability 0, 3 and 7 days after encapsulation. As such the MIG method is the only microfluidics-based continuous alginate bead production technique that has been shown to allow viable cell encapsulation with extensive viability data.

Chapter 5. Encapsulation of a therapeutic cell line

5.1 INTRODUCTION

HEK293 cells were successfully encapsulated using the microfluidic internal gelation (MIG) method developed in Chapter 3. After optimisation of component concentrations, minor adverse effects were observed upon cell viability. Although, HEK293 is a very robust, adherent cell line, it has no clinical significance. A cell line which expresses a therapeutic product was required to move closer to the goal of treating Parkinsonism in a rodent model.

The application of cell replacement to cure CNS disorders, such as Huntington's and Parkinson's disease, has largely been focussed upon the use of primary cells. Although there has been some success with tissue obtained from human foetuses (for example, Lindvall *et al.*, 1992), the ethical and practical considerations concerning use of this cell source are restrictive. Use of immortalised cell lines is preferable for several reasons, including; unlimited supply, ease of maintenance, and precisely defined genotype and phenotype.

The clonal cell line PC12 was derived from a rat pheochromocytoma; a vascular tumour of chromaffin tissue, of the adrenal medulla (Greene and Tischler, 1976). This cell-line synthesizes, stores and secretes clinically useful catecholamines, including dopamine (DA) and norepinephrine (NA) (Greene and Rein, 1977). Secretion of NA and DA by PC12 cells is bought about by depolarizing concentrations of K^+ by similar mechanisms to those in normal chromaffin cells (Greene and Rein, 1977). PC12 cells transplanted into the brains of Sprague Dawley rats stained intensely for tyrosine hydroxylase (TH), the first enzyme in the biosynthesis of dopamine (Levitt *et al.*, 1965), thus proving that dopamine is still expressed (Jaeger, 1985).

Although immortalised cell lines are preferable to primary cells, the major disadvantage to their use is tumour formation. PC12 cells are no exception and have been observed to form tumours after transplantation into the brains of Sprague Dawley rats (Jaeger, 1985). Grafts grew up to 60 times their original size within two months of transplantation. This effect was seen only when large pellets (1.5 – 3mm) of cells were transplanted as opposed to cell suspensions. PC12 cells were observed to be destroyed when transplanted without encapsulation or immunosuppression into guinea pig brain (Aebischer *et al.*, 1991a).

It has been proposed that undesirable cell division could be controlled by pre-treatment with mitotic inhibitors (Gash *et al.*, 1986) or by integration of temperature sensitive Large T antigen of SV40, which halts cell division at 37°C (Lundberg *et al.*, 1996). Polymer encapsulation has also been suggested as a means to prevent cell line overgrowth (Winn *et al.*, 1991). Encapsulation of PC12 cells for implantation into the brain has been investigated with both hollow fibre-based technology, so called macroencapsulation (Aebischer *et al.*, 1991b), and microencapsulation within small polymer microspheres (for example, Roberts *et al.*, 1996).

The MIG method was used to encapsulate PC12 cells in calcium cross-linked alginate beads. Maximal viability of the cells was paramount and long term effects of encapsulation were investigated. Levels of the therapeutic molecule dopamine were measured to ensure encapsulation did not adversely affect PC12 cells ability to release dopamine and that the bead structure did not prevent dopamine from diffusing out of the beads.

5.2 RESULTS

5.2.1 Optimisation of the MIG method for encapsulation of PC12 cells

PC12 cells were encapsulated using the previously developed method (Section 3.3.3), which was non-cytotoxic to HEK293 cells (Section 4.2.2.2). As PC12 cells grow in small aggregates, trituration was required to obtain a single cell suspension.

The functional fluid was composed of 50mM $CaCO_3$ suspended in sodium alginate solution (2% w/v). Following trituration, PC12 cells were resuspended in the previously prepared functional fluid. The reactive fluid was composed of acetic acid (50mM) dissolved in sunflower oil and the shielding flow was composed of sunflower oil. After encapsulation using these conditions >90% of the encapsulated PC12 cells were observed to be dead when stained with trypan blue (Section 4.2.1.4).

Cytotoxicity testing was carried out as described in Section 2.3.3, to investigate the effect of the components used in the encapsulation protocol. PC12 cells were triturated and split into three, with one third being resuspended in D-MEM/F12 medium as a control, one third resuspended in 50mM acetic acid in sunflower oil, and the remaining third resuspended in 50mM acetic acid in D-MEM/F12 medium. Samples were taken at 1, 5 and 10 minute intervals and viability was estimated using trypan blue exclusion (Section 4.2.1.4). Viability estimates are shown in Figure 5.1.

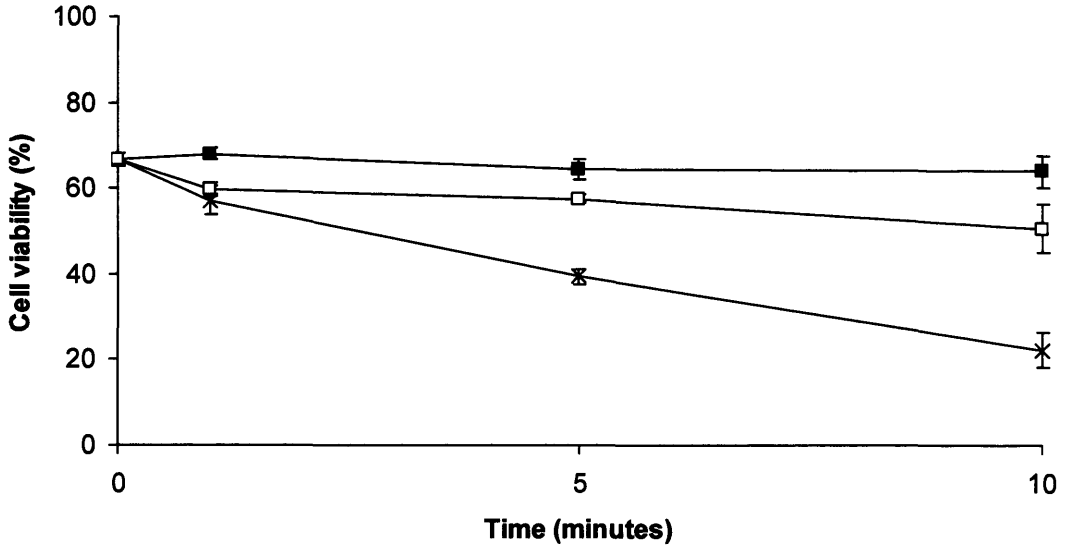

Figure 5.1: Viability of PC12 cells exposed to components of the MIG method. Graph showing effect upon viability of PC12 cells exposed to medium (■), 50mM acetic acid (□) and 50mM acetic acid in sunflower oil (X). Viability was estimated using trypan blue exclusion. Error bars show standard error of the mean of 3 replicate samples

In a separate experiment, triturated PC12 cells were observed to survive for 2 hours in alginate solution (2% w/v) with 50mM $CaCO_3$. Further time points were not tested as it was not expected that cells would be exposed to the functional fluid for longer than the duration of an encapsulation experiment, i.e. ~ 20 minutes.

PC12 cells showed a 13 percentage point decrease in viability upon exposure to acetic acid in medium, and a 42 percentage point decrease in viability upon exposure to acetic acid dissolved in sunflower oil. Cells were exposed to acidified oil for approximately 30 seconds in the MicroPlant™. Upon exiting the MicroPlant™, encapsulated cells remained in the acidified oil for a further 5 minutes prior to removal into medium. It was postulated that prolonged exposure to acidified oil after exiting the MicroPlant™ might account for the reduced viability of encapsulated cells observed.

In order to increase PC12 viability upon encapsulation, the acid concentration needed to be decreased and product beads needed to be rapidly removed from acidified oil. A new chip was designed to transfer product beads into medium on-chip. Two new channels were introduced *via* two T-junctions at right angles to the exit channel. Medium was introduced *via* these two additional channels. At sufficiently high flow rates (>50ml/h) alternating segmentation of the oil occurred (Figure 5.2). At these high flow rates, hydrogel spheres overcame the surface tension of the oil and broke through into the aqueous medium. The additional flow of medium was referred to as the flushing flow.

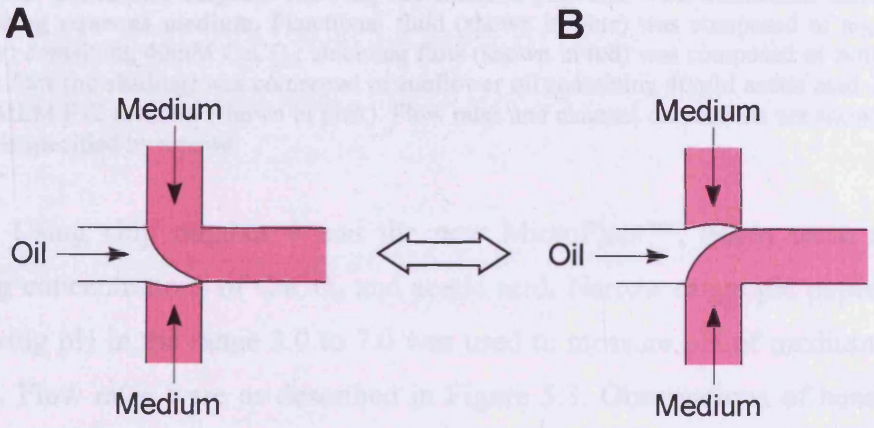

Figure 5.2: Schematic diagram representing alternating segmentation at double T-junction. Flushing flow is represented in pink. Orientation of flow is specified by arrows

As the new design required more fluid inputs than were available with the MicroPlant™ used thus far, a new MicroPlant™ was designed by Q Chip. The new MicroPlant™ was rectangular as opposed to circular, and incorporated the same features as those described for the circular MicroPlant™ (Section 2.2.1). A rectangular shape was chosen to allow a longer straight channel to be incorporated into circuit designs (Appendix 2). The surface area of the rectangular MicroPlant™ was 7.6 times greater than the circular MicroPlant™. This allowed a longer channel length after the junction; 3900mm for the rectangular as opposed to 160mm for the circular MicroPlant™ (compare Chip 1 to Chip 3 in Appendix 1). The new flows were introduced after 2840mm, 1060mm before the exit. The new chip is shown schematically in Figure 5.3, with the actual circuit diagram shown in Appendix 1.

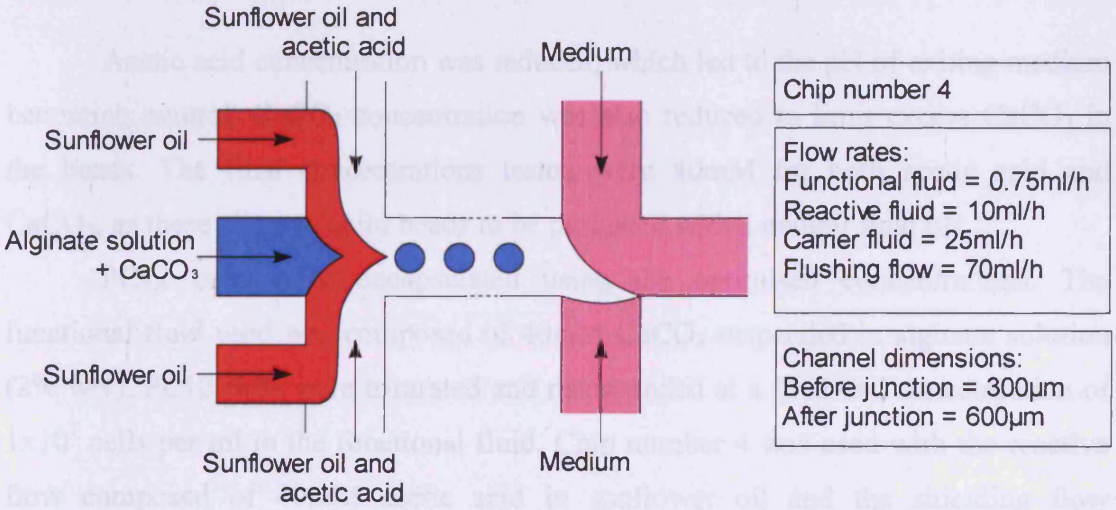

Figure 5.3: Schematic diagram showing the shielded junction with additional flushing flow for introducing aqueous medium. Functional fluid (shown in blue) was composed of alginate solution (2% w/v) containing 40mM $CaCO_3$, shielding flow (shown in red) was composed of sunflower oil and reactive flow (no shading) was composed of sunflower oil containing 40mM acetic acid. Flushing flow was D-MEM/F12 medium (shown in pink). Flow rates and channel dimensions are shown. Orientation of flow is specified by arrows

Using chip number 4 and the new MicroPlant™, beads were made using varying concentrations of $CaCO_3$ and acetic acid. Narrow range pH paper capable of measuring pH in the range 3.0 to 7.0 was used to measure pH of medium exiting the device. Flow rates were as described in Figure 5.3. Observations of beads produced using differing concentrations of acetic acid and $CaCO_3$ are shown, along with pH of exiting medium, in Table 5.1.

Concentration of $CaCO_3$ (mM)	Concentration of acetic acid (mM)	Observations	pH of exiting medium
50	50	Solid beads	6.0
50	45	Solid beads	7.0
50	40	Beads were opaque due to excess $CaCO_3$	7.0
40	40	Solid beads	7.0
50	20	Beads not solid	Not measured

Table 5.1: Optimisation of components used to encapsulate PC12 cells. Beads were produced using 2% (w/v) alginate. pH was measured using narrow range pH paper

Acetic acid concentration was reduced, which led to the pH of exiting medium becoming neutral. $CaCO_3$ concentration was also reduced to limit excess $CaCO_3$ in the beads. The final concentrations tested were 40mM for both acetic acid and $CaCO_3$, as these allowed solid beads to be produced with a neutral final pH.

PC12 cells were encapsulated using the optimised concentrations. The functional fluid used was composed of 40mM $CaCO_3$ suspended in alginate solution (2% w/v). PC12 cells were triturated and resuspended at a final cell concentration of $1x10^7$ cells per ml in the functional fluid. Chip number 4 was used with the reactive flow composed of 40mM acetic acid in sunflower oil and the shielding flow composed of sunflower oil. D-MEM/F12 medium was introduced *via* the flushing flow. Viable PC12 cells were encapsulated using the optimised component concentrations and the new chip design incorporating a flushing flow (Figure 5.4A). Cells were not successfully triturated to a single cell suspension as cell aggregates can be seen in the product beads. The average diameter of these beads (n=10) was measured to be 378±10μm (Figure 5.4B). The CV was 2.8%.

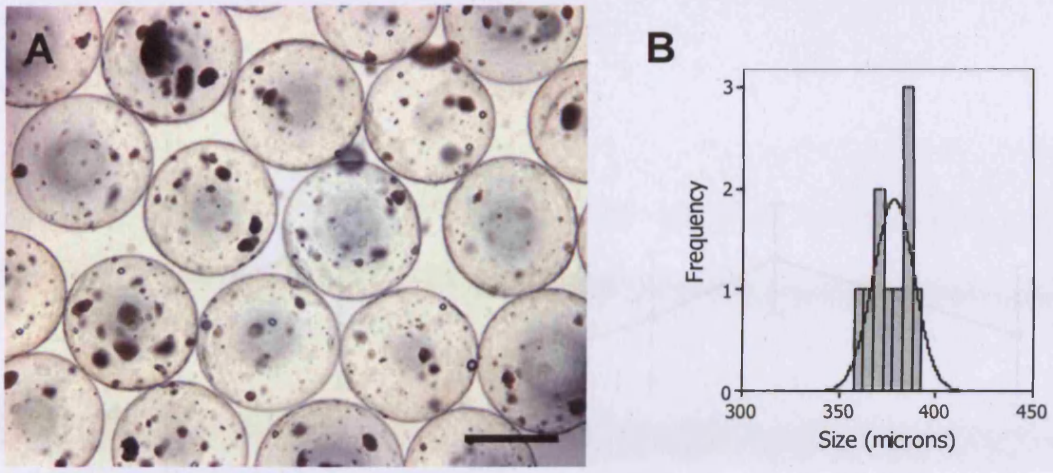

Figure 5.4: PC12 cells encapsulated in calcium cross-linked alginate beads. A) A light microscope image of encapsulated PC12 cells in calcium cross-linked alginate beads. It is possible to observe small cell aggregates present within the ionically cross-linked beads. Scale bar represents 250μm. B) Histogram of beads represented in A; grey bars show measured data, with black line representing normal distribution. Mean bead diameter was 378±10μm. Distribution was considered to be approximately normal (A^2=0.39, $p > 0.303$)

The viability of produced encapsulated cells was estimated using the adapted trypan blue exclusion method (Section 4.2.1.1) over a 50 day period (Figure 5.5). Percentage viability was seen to decrease gradually between encapsulation and day 21, after which point a gradual increase was observed. A substantial decrease in viability was observed between day 35 and the next time point at day 50. As there were a limited number of beads, no further time points were tested between these two.

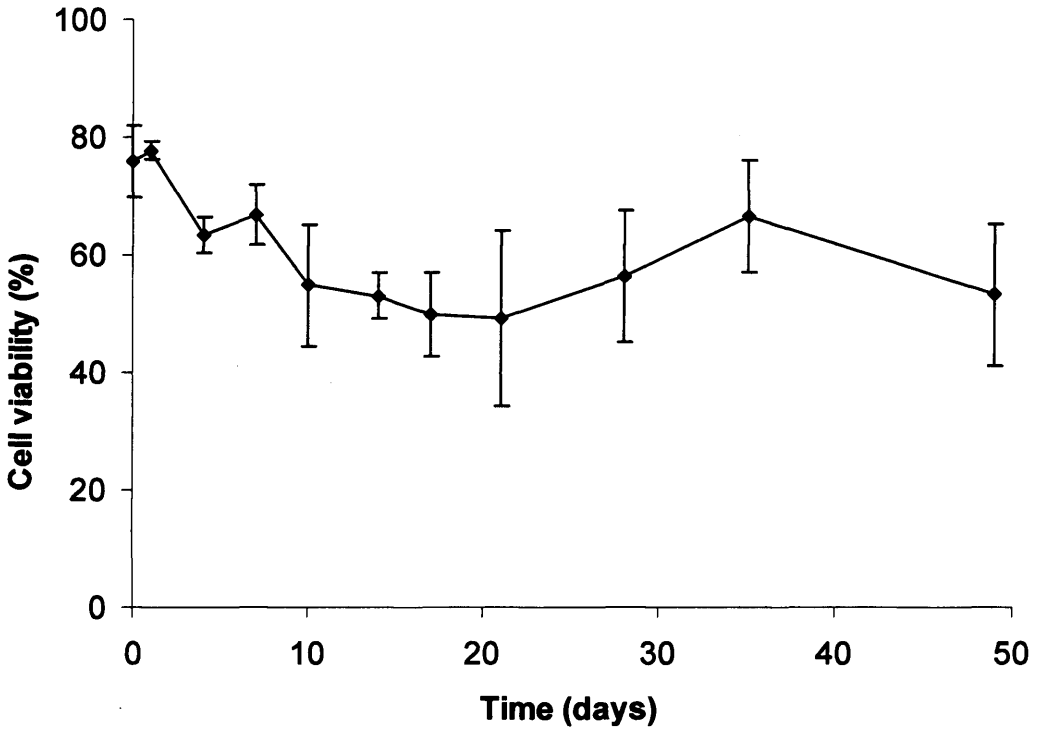

Figure 5.5: Graph showing percentage viability of encapsulated PC12 cells. Pre-encapsulation viability was 74%. Viability was estimated using the adapted trypan blue method. Error bars show standard deviation of 4 individual beads

Confocal images were taken of the encapsulated PC12 cells after LIVE/DEAD® staining 24 hours, 21 days and 60 days after encapsulation (Figure 5.6). Cell clusters were observed at 24 hours and 21 days. By 60 days, flattened discs of cells could be seen. Viability, when estimated using trypan blue exclusion, was seen to be lower than that estimated from confocal images. As can be seen from confocal images, encapsulated cells showed good viability at all time points tested. However, cell proliferation was limited and cell numbers were not observed to increase substantially.

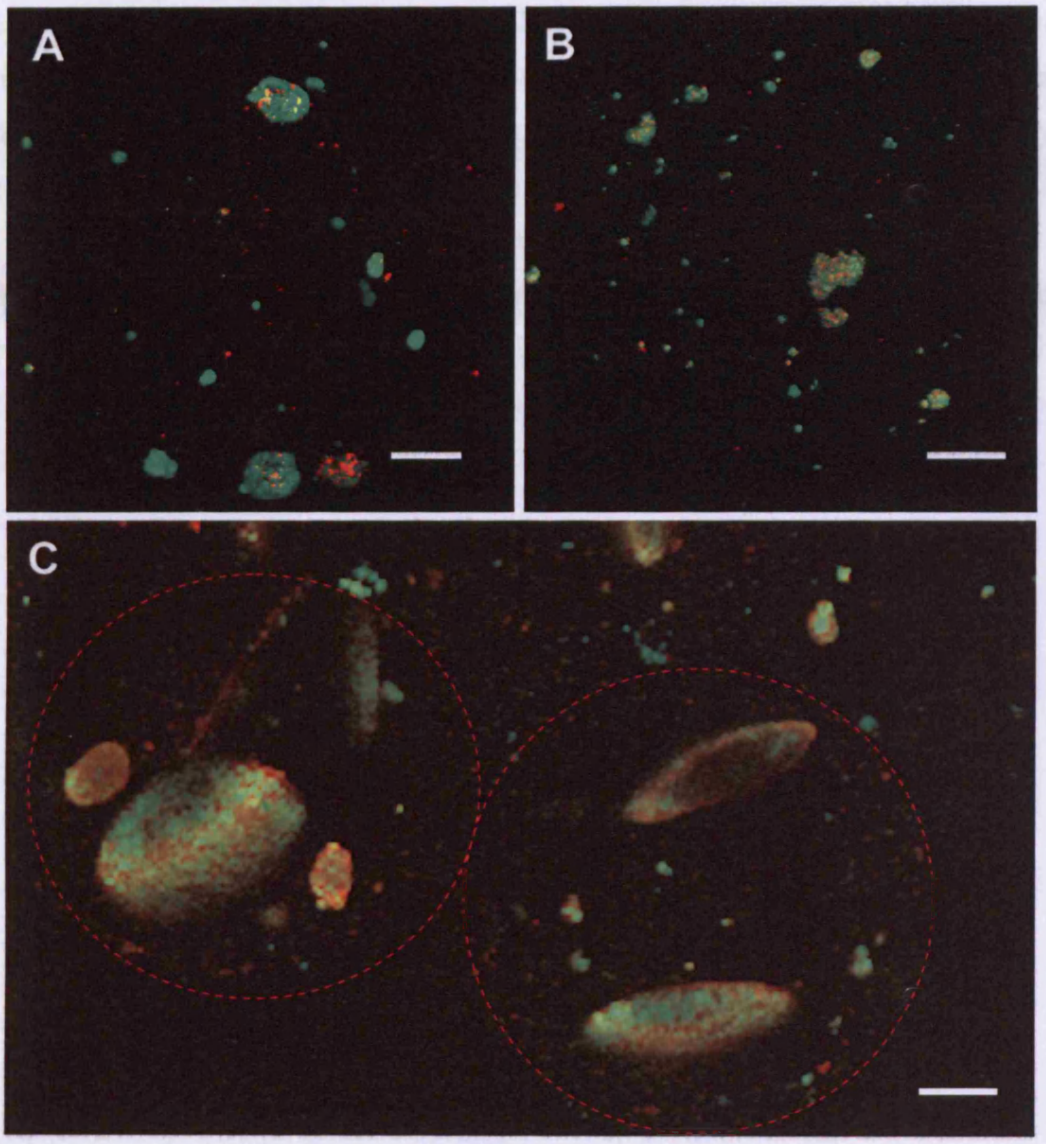

Figure 5.6: Confocal images showing encapsulated PC12 cells after LIVE/DEAD® staining. A) 24 hours after encapsulation, B) 21 days after encapsulation, C) 60 days after encapsulation (dotted red lines show bead boundary). Green fluorescence is emitted from intracellular esterase-converted calcein in live cells, whereas red fluorescence is emitted from ethidium homodimer present in the nuclei of dead cells. Scale bars represent 100μm

5.2.2 Optimisation of cell concentration

It was hypothesised that changes to initial cell concentration at the time of encapsulation may affect cell proliferation. To investigate this hypothesis, varying cell concentrations were encapsulated: $1x10^7$ cells per ml (referred to as low initial density, Figure 5.7A-C), $2x10^7$ cells per ml (referred to as medium initial density, Figure 5.7D-F) and $4x10^7$ cells per ml (referred to as high initial density, Figure 5.7G-I). Viability was estimated using trypan blue prior to encapsulation, and at 1, 7, 10 and 14 days after encapsulation. Viability was observed to remain high and consistent over time (Figure 5.8). However, the low initial density population showed a slight decrease in viability which increased to a similar level to the other encapsulated populations after 10 days.

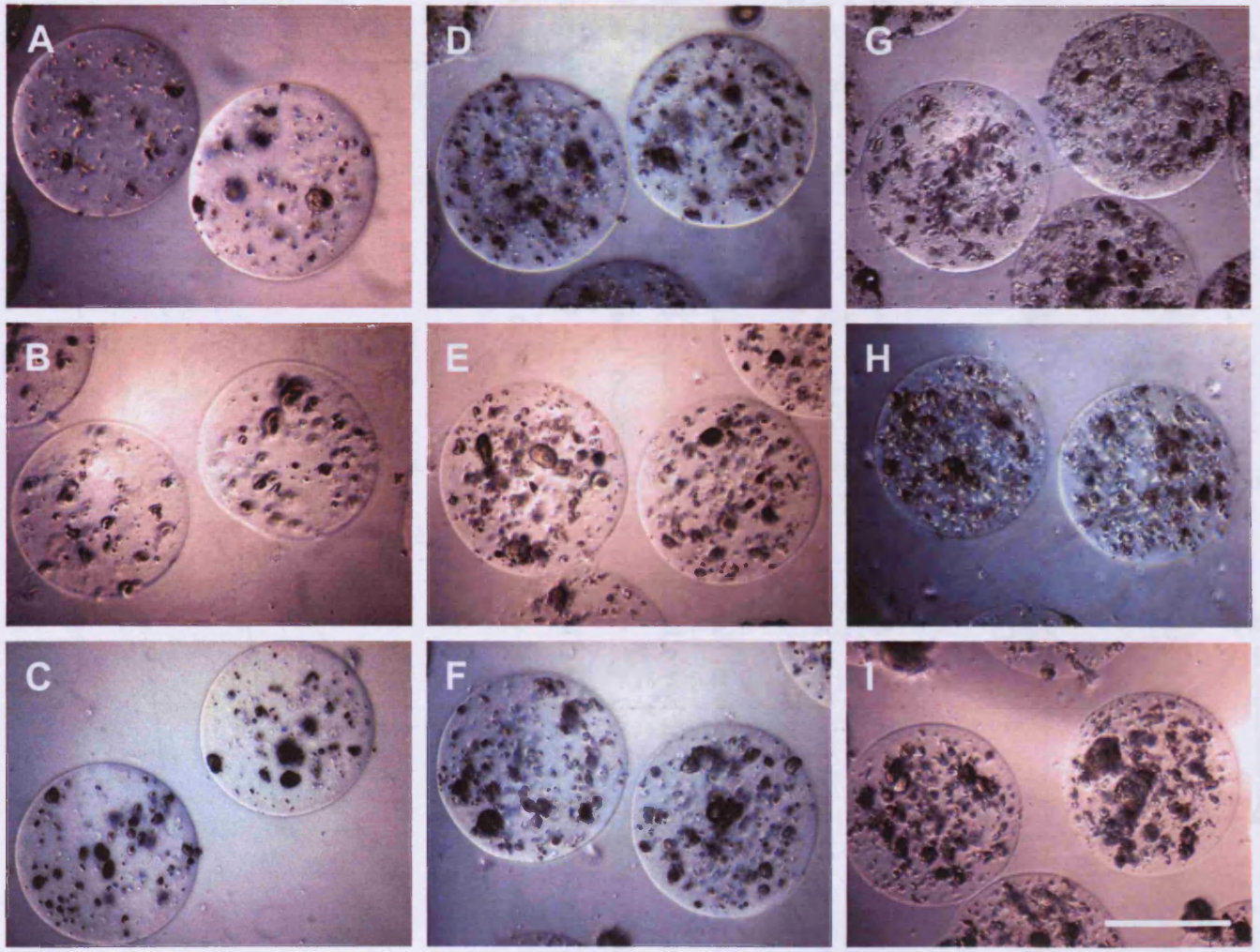

Figure 5.7: Encapsulated PC12 cell populations. A-C: Low initial cell density, D-F: medium initial cell density, G-I: high initial cell density. A, D and G: Day of encapsulation, B, E and H: 7 days after encapsulation, C, F and I: 14 days after encapsulation. Scale bar represents 250μm

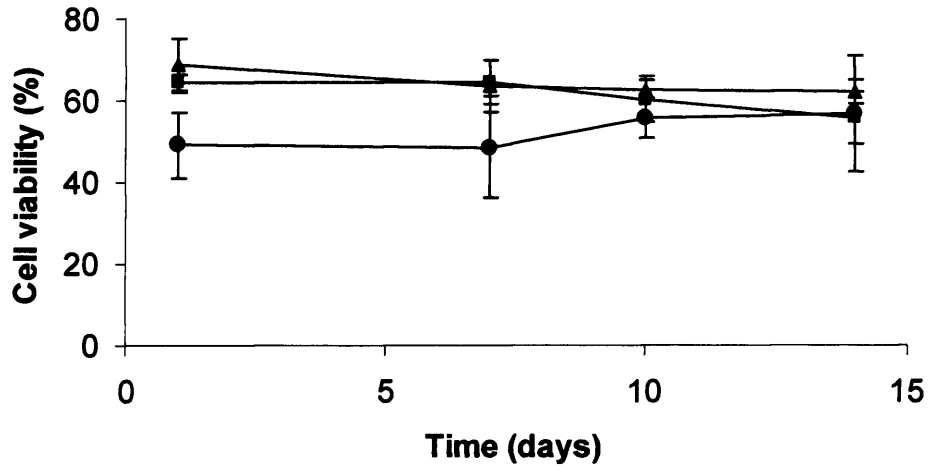

Figure 5.8: Graph showing effect upon encapsulated PC12 cell viability as a function of initial cell concentration. Initial cell concentrations were $1x10^7$ (•), $2x10^7$ (■) and $4x10^7$ (▲) cells/ml. Pre-encapsulation viability was 68%. Viability was estimated using the adapted trypan blue method. Error bars show standard deviation of 4 individual beads

Although cell proliferation was observed in all three encapsulated populations (Figure 5.9), higher initial concentrations of cells allowed increased cell expansion. The rate of increase in cell numbers was similar for the two higher initial cell concentrations (medium = 41.6 and high = 47.6 cells per day), whereas the rate of increase was lower (18.9 cells per day) for the low initial cell concentration (Table 5.2).

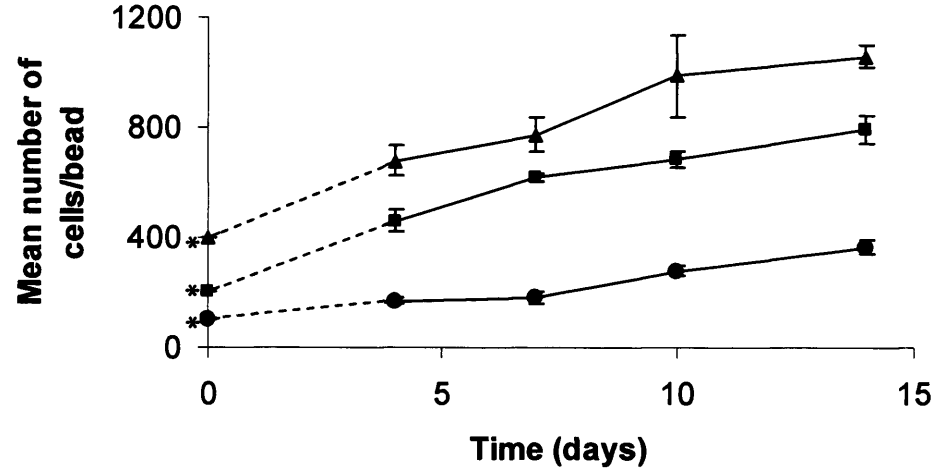

Figure 5.9: Graph showing increasing numbers of PC12 cells over time. Differing initial cell concentrations were encapsulated, $1x10^7$ (•), $2x10^7$ (■) and $4x10^7$ (▲) cells/ml. Viability was estimated using the adapted trypan blue method. Mean number of cells from 4 beads was calculated and error bars show standard error of the mean. Asterisks (*) denote estimated data from cell concentration and bead diameter

Initial cell concentration (cell/ml)	Rate of increase of cell numbers (cells/day)
Low ($1x10^7$)	18.9
Medium ($2x10^7$)	41.6
High ($4x10^7$)	47.6

Table 5.2: Rate of cell increase for three different cell encapsulation concentrations. Values calculated from linear fit of plot of cell numbers against days after encapsulation. R^2 values in all cases > 0.94

5.2.3 Dopamine expression

An ELISA to detect dopamine was carried out on the above populations (Section 5.2.2) and single cell suspensions of PC12 cells. After 14 days in culture, 50 beads were taken from each population and incubated for 2 hours with D-MEM/F12 medium (600µl), as were single cell suspensions. All medium was removed and wells were washed with Hank's balanced saline solution (HBSS). To detect basal expression HBSS (600µl) was added to wells. To detect induced expression HBSS with 56mM KCl (600µl) was added. Beads and medium or cells and medium were incubated for 45 minutes, after which time medium was removed and frozen. An ELISA to detect dopamine was carried out according to the manufacturer's instructions (Section 2.3.5) on 100µl of defrosted medium and standard dopamine samples provided by the manufacturer. Technical replicates (two) were carried out for each sample and standard. Absorbance of the wells was measured at 450nm with background subtraction at 630nm.

The standard curve produced was linear between 100 and 6400 pg of dopamine (Figure 5.10). A linear best fit line was fitted between these points ($y=-0.3587x + 1.8924$). The R^2 value was 0.9682. The slope of this line gives the relationship between log dopamine concentration and absorbance reading. Dopamine concentration of unknown samples was then calculated from absorbance.

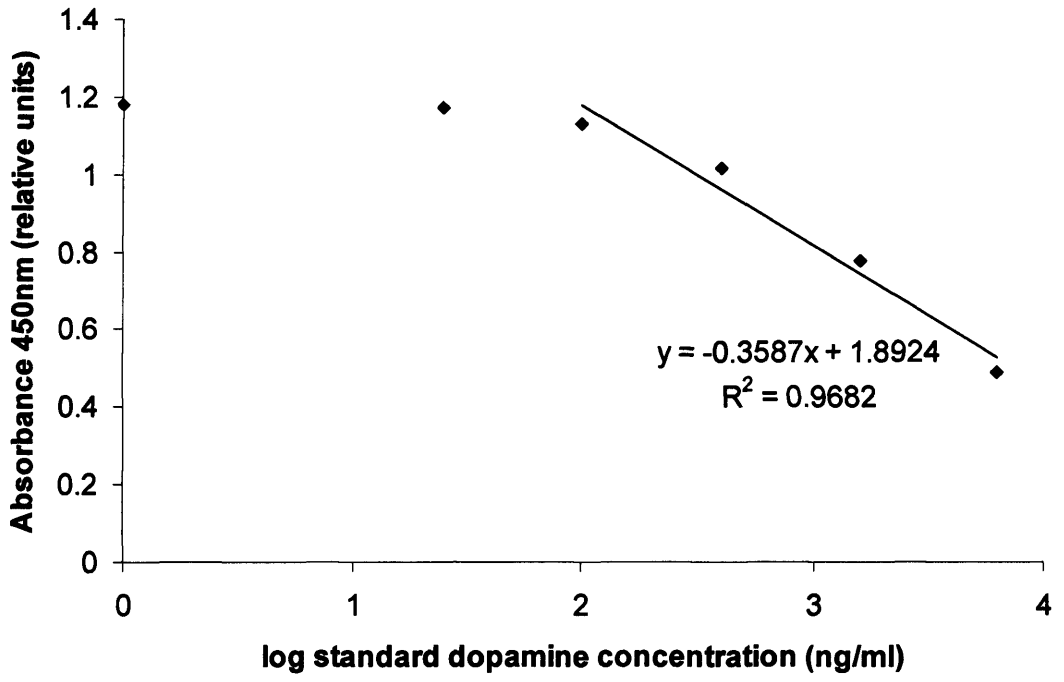

Figure 5.10: Graph showing absorbance obtained with standard concentrations of dopamine. Dopamine ELISA was carried out on standards provided by the manufacturer. Absorbance readings were taken at 450nm with background subtraction at 630nm

Basal dopamine secretion was undetectable from the samples taken both from beads and single cell suspensions. After potassium induction, dopamine was detectable in all bead samples (Table 5.3), but not from cell suspensions. The measured values all fell within the range of the standard curve.

Initial cell concentration (cell/ml)	Number of cells present ± SD (day 14)	Dopamine secretion (pg/bead/45minutes)
Low ($1x10^7$)	366±51	10.5±1.0
Medium ($2x10^7$)	793±108	12.4±1.2
High ($4x10^7$)	1058±79	12.7±1.2

Table 5.3: Amount of dopamine, secreted per bead, for three different initial encapsulation concentrations. Cells were allowed to grow within beads for 14 days before measurements were taken. Mean number of cells per bead for 4 beads was counted. Beads were incubated for 45 minutes before ELISA to detect dopamine secretion was carried out in duplicate. Confidence interval of dopamine secretion reported is error of ELISA assay as quoted by manufacturer (10%)

5.3 DISCUSSION

As PC12 cells grow slowly (doubling time is ~92 hours (Greene and Tischler, 1976) compared with HEK293 at ~26 hours (Schwarz *et al.*, 2006)), it takes a long time to expand enough cells to work with. Consequently, smaller scale experiments were carried out than those utilising HEK293. In addition, as more cells were encapsulated cell counts took much longer and were less accurate as trypan blue is taken up by viable, as well as non-viable cells, after prolonged exposure.

5.3.1 Optimisation of microfluidic encapsulation of PC12 cells

Initial attempts to encapsulate PC12 cells using the MIG method previously described (Section 3.3.3) were unsuccessful as cells were not viable after the process. Viable PC12 cells were successfully encapsulated after optimisation of the method. Cytotoxicity testing showed that acetic acid in combination with sunflower oil was toxic to PC12 cells (42 percentage point decrease in viability), whereas acetic acid in isolation did not have such a pronounced effect (13 percentage point decrease in viability). Sunflower oil may affect PC12 cell membranes making cells more susceptible to acetic acid. Toxicity may have been decreased by using different types of acid and oil, but it was decided to investigate reducing cell exposure to acid.

The effects of acidified oil upon PC12 cells were observed after 10 minutes of exposure during cytotoxic testing. Although cells were exposed to acidified oil for less than 30 seconds within the MicroPlant™, encapsulated cells were collected in the acidified oil for a further 5 minutes prior to transfer into medium. It appears that this time period is too long for cells to remain viable, as under these conditions encapsulation was fatal to cells.

Estimation of pH of exiting medium in this experiment was estimated using narrow range pH paper, range 3-7. It is acknowledged that this was not the most accurate range to choose and that pH paper in the range 6.8-8.2 would have been more appropriate for the physiological experiments carried out. Obviously, use of a pH meter would give even more accurate results. However, the amounts of medium exiting from the device were too small to be measured in this way.

To enable encapsulation of viable PC12 cells the exposure of cells to acidified oil needed to be reduced. This was achieved by decreasing the acid concentration utilised in the MIG method and reducing the amount of time prior to transferring

beads into medium. A new circuit was designed to rapidly remove encapsulated cells from the acidified continuous phase into medium, on-chip.

An additional flow of medium, termed the flushing flow, was introduced into the circuit *via* two T-junctions at right angles to the exit channel. At empirically determined, rapid flow rates (>50ml/h), segmentation between the continuous phase and the flushing phase occurred. Upon coming into contact with another fluid stream liquid droplets will coalesce with the introduced stream. To prevent coalescence of liquid alginate droplets with the flushing flow, the additional T-junctions were positioned such that solid calcium cross-linked alginate beads had formed prior to coming into contact with the aqueous phase. After the introduction of the flushing flow, solid calcium cross-linked alginate beads were observed to overcome the surface tension of the oil phase and thus enter the aqueous fluid segments.

In combination with the new circuit design, the minimum acid concentration that permitted production of solid beads with no excess $CaCO_3$ present was 40mM. It is interesting to note that alterations to the microfluidic circuit require modifications to the acetic acid and $CaCO_3$ concentrations. Although conditions required for a chemical reaction are known/constant at the macro scale, this is obviously different at the micro scale. Both the reduction in acetic acid concentration and the modified chip design allowed viable PC12 cells to be encapsulated within alginate beads using a microfabricated device.

5.3.2 Behaviour of encapsulated PC12 cells

Under culture conditions PC12 cells grow in small clumps (Greene and Tischler, 1976). This is also observed in encapsulated cell populations, and is consistent across a number of investigated polymers, including alginate (Winn *et al.*, 1991; Zielinski and Aebischer, 1994), agarose/Poly(styrene sulfonic acid) (Miyoshi *et al.*, 1996) and hydroxyethyl methacrylate-methyl methacrylate copolymer (HEMA-MMA) (Roberts *et al.*, 1996). PC12 cells encapsulated using the MIG method also formed small clusters and eventually grew to form disc-like structures.

All the above groups, except one (Miyoshi *et al.*, 1996), observed cell necrosis within encapsulated cell clusters after two weeks of encapsulation. Cell necrosis was observed with PC12 cells encapsulated using the MIG method after 60 days of culture. Necrosis is thought to occur at the centre of cell clusters due to limited

exchange of nutrients and waste products when cell aggregates reach >200μm in diameter (Uludag *et al.*, 1993).

The group (Miyoshi *et al.*, 1996) which did not observe cell necrosis within encapsulated cell clusters investigated beads with much smaller (300 - 600μm) diameters than other groups (>600μm). Beads produced using the MIG method were also smaller (~370μm) than those produced by alternative methods. As beads become larger the matrix hinders diffusion of nutrients and waste materials (Ogbonna *et al.*, 1991). Smaller beads are seen to be advantageous as diffusion can still occur and cells remain viable for longer.

Initial observations of PC12 cells encapsulated using the MIG method showed that although viability was consistent over time, cell numbers did not substantially increase. Confocal images taken of beads stained with LIVE/DEAD® reagents at 1 and 21 days after encapsulation are virtually indistinguishable. Cell clusters did not appear to increase in size between encapsulation and 21 days later. PC12 cells encapsulated at $1x10^7$ cells per ml did not form the large cell aggregates observed with encapsulated HEK293 cells (Section 4.2.3).

There is evidence that microstructure within beads effects cell growth and expression of biomolecules (Stabler *et al.*, 2001). Increased osmotic pressure is known to decrease cell growth rate and affect protein expression in batch culture of baby hamster kidney cells (Yi *et al.*, 2004). Mouse insulinoma cells exhibited decreased growth rates when encapsulated in high G content alginate beads, and solid core beads reduced growth rates more than liquid core beads (Constantinidis *et al.*, 1999). Only G residues in alginate form bonds with divalent ions, and the strength of the interaction increases with frequency and length of G blocks (Section 1.7.2.1). Thus, high G content alginate beads are stronger and more rigid than beads composed of high M content alginate. The increased rigidity of high G content alginate leads to increased stress or pressure exerted on encapsulated cells. Decreased growth rate occurs when cells are encapsulated in alginate beads with enhanced stability, specifically Ba^{2+} treated or those constructed of alginate epimerised to increase the G content (Rokstad *et al.*, 2003). Conditions within beads produced using the MIG method must be unsuitable for PC12 cells to proliferate at low cell concentrations. The internal structure of beads produced using the MIG method will be investigated in the following chapter.

It was postulated that increasing initial cell density may increase subsequent cell proliferation, as Roberts *et al.* observed such an effect with PC12 cells encapsulated in HEMA-MMA capsules. High ($4x10^6$ cells per ml) and low ($4x10^5$ cells per ml) initial cell densities were encapsulated and cell numbers estimated using MTT at various time periods over 28 days. Both encapsulated cell populations exhibited an initial decrease in viable cell numbers. Viable cell numbers were observed to increase in the high density population from day 3 until a plateau at day 14. In contrast, the low density population entered a quiescent period from day 7 to day 21, followed by an increase in cell numbers from day 21 to day 28 (Roberts *et al.*, 1996).

Similar effects were observed in PC12 cells encapsulated using the MIG method. An increase in the rate of cell proliferation was observed when initial cell density was doubled from $1x10^7$ to $2x10^7$ cells per ml. However, the rate of cell proliferation did not increase substantially when the initial cell density was doubled from $2x10^7$ to $4x10^7$ cells per ml. Again, conditions within the beads may not be conducive to enhanced cell growth or cells may have reached their proliferation limit. Beads with low initial cell concentrations ($1x10^7$, Section 5.2.2) were observed to decrease in cell viability until 21 days, in agreement with Roberts *et al.* (1996).

PC12 cells are known to form tumours (Jaeger, 1985); therefore, decreased cell division may be advantageous in preventing uncontrolled growth and tumour formation. However, the rate of cell proliferation is not the most important factor when encapsulated PC12 cells are used to treat neurodegenerative diseases, rather that the cells must continue to secrete dopamine.

Dopamine secretion was observed after PC12 cells were encapsulated using the MIG method. However, no dopamine secretion was detected in suspensions of PC12 cells. Thus, this encapsulation method does not affect PC12's ability to secrete dopamine and the encapsulation matrix does not prevent dopamine from diffusing from the beads. In addition, encapsulation and subsequent aggregate formation enhances dopamine secretion compared with growing cells in a monolayer.

A summary of studies discussed above (Table 5.4) shows that researchers detect varying amounts of dopamine secreted from encapsulated cells. An order of magnitude difference was reported between the lowest amount of dopamine released (4.3 pg/capsule/15 minutes) and the highest (1.5 ng/capsule/15 minutes). This is most probably due to the differing cell numbers present in the capsules produced and the

diverse range of matrix materials employed. It is interesting to note that the group which reported the lowest dopamine release did not observe large cell aggregates or necrotic areas (Miyoshi *et al.*, 1996).

Although PC12 cells encapsulated using the MIG method secreted dopamine after encapsulation, the release observed is roughly in line with the lower reported values (Table 5.4). This may be due to smaller cell aggregates forming than those observed in studies where more dopamine was observed. Tyrosine hydroxylase (TH) is the first and rate-limiting enzyme in the biosynthesis of dopamine (Levitt *et al.*, 1965). Growing PC2 cells at high densities ($>10^5$ cells/cm^2) increases TH activity and specific cell contact between PC12 cells is required for this effect to be seen (Lucas *et al.*, 1979). In addition, aggregation enhances catecholamine secretion in cultured cells (Baldwin and Saltzman, 2001). Larger aggregates (16,600±700μm^2) produce more dopamine, in a shorter time period (6 days), than smaller aggregates (2800±50μm^2, taking 10-12 days). Secretion of dopamine appears to be independent of cell number and instead is related to aggregate size. In this study, there was no significant increase in dopamine secretion between medium and high initial cell concentration populations. The level of cell aggregation may have been similar between the two populations even though cell numbers were different.

Cell-binding domains have been used to enhance cell binding to biomaterials. Increased PC12 cell growth and dopamine secretion was observed when cells were encapsulated in polymers incorporating the pentapeptide Gly-Arg-Gly-Asp-Ser (Park *et al.*, 2004) or Arg-Gly-Asp (Park and Yun, 2004; Orive *et al.*, 2009). Further investigation into extra-cellular matrices to enhance cell attachment or encapsulation of pre-formed aggregates may help to improve dopamine secretion from encapsulated PC12 cells.

In human patients with Parkinson's disease, the daily dose of L-dopa is roughly 1g, although, as less than 1% penetrates the CNS due to limited bioavailability (Gilman, 2001), only 10mg of DA is required daily. This would require implantation of ~37,000 beads produced using the MIG method (~2.4ml in volume). A standard amount of dopamine required to see behavioural effects in a rodent model of Parkinson's disease has not been reported. Only two of the studies discussed above implanted encapsulated PC12 cells into rodents, but both observed behavioural effects. Winn *et al.* (1991) implanted 7 beads into rats which secreted 0.18μg of dopamine/24 hours. An equivalent amount of dopamine would be provided

by 700 beads produced using the MIG method (45μl in volume). Aebischer *et al.* (1991b) implanted 14 beads into rats which secreted 0.053μg of dopamine/24 hours. An equivalent amount of dopamine would be provided by 200 beads produced using the MIG method (13μl in volume).

	Bead matrix	Encapsulated cell concentration (cell/ml)	No of cells/bead (at encapsulation)	Bead diameter (μm)	Dopamine release	
					Basal	K^+ induced
Ehringer and Hornykiewicz	Post mortem dopamine levels in the caudate nucleus				Range 2.7-5.5 μg/g Mean 3.5 μg/g	
Winn *et al.*	APA	$1x10^6$	300-500	560±65	100 pg/capsule/hour[1]	270 pg/capsule/15minutes[2]
Zielinski and Aebischer	APA	$1x10^7$			ND	1.5 ng/capsule/15minutes[1]
Miyoshi *et al.*	Agarose/PSSa	$3x10^5$	300	300-600	2.27±0.18 pg/capsule/15minutes[3]	4.30±0.35 pg/capsule/15minutes[3]
Roberts *et al.*	HEMA-MMA	$4x10^5$	270	660±44	ND	110 pg/capsule/hour[1]
		$4x10^6$	2700	660±44	ND	856 pg/capsule/hour[1]
Current study	Alginate	$1x10^7$	100*	370±10	ND	10.5±1.0 pg/bead/45minutes[1]
		$2x10^7$	200*	370±10	ND	12.4±1.2 pg/bead/45minutes[1]
		$4x10^7$	400*	370±10	ND	12.7±1.2 pg/bead/45minutes[1]

[1] 2 weeks after encapsulation
[2] Peak dopamine expression at 2 days after encapsulation
[3] 3 weeks after encapsulation
* Cell numbers estimated from cell concentration and bead diameter

APA = alginate-PLL-alginate
PSSa = poly(styrene sulfonic acid)
HEMA-MMA = Hydroxyethyl methacrylate-methyl methacrylate
ND = not detectable

Table 5.4: Summary of studies examining encapsulated PC12 cells and dopamine expression

Chapter 6. Production of alginate beads suitable for implantation into the central nervous system

6.1 INTRODUCTION

Implantation of cells into the brain has been carried out in an attempt to treat several diseases, for example; CNS disorders, such as Huntington's disease (Borlongan *et al.*, 2008), Parkinson's disease (Ando *et al.*, 2007), and brain tumours (Kuijlen *et al.*, 2006). Stereotactic surgery is used to implant cell suspensions, small cell aggregates or encapsulated cells in precisely defined areas of the brain through use of three-dimensional coordinates. Provided that a small cannula (<2.5mm outer diameter) is used to introduce the cellular material, this technique is minimally invasive. Smaller cannulae (50-70μm outer diameter) have been shown to cause less damage than large cannulae (500μm outer diameter) (Nikkhah *et al.*, 1994).

It has been found that beads with a diameter smaller than 200μm are needed to ensure efficient loading of a 500μm inner diameter cannula (Ross and Chang, 2002). Only a few of the groups implanting encapsulated cells into animal brains utilise beads of this size, however, those that do report superior properties for smaller beads. For example, Ross and Chang (2002) reported an increased packing density of small beads (100-200μm in diameter) compared with medium-sized beads (500-700μm in diameter), which resulted in an increased number of cells and more protein expression per volume of beads. The same beads were also found to be more resistant to osmotic pressure. Other studies have found small beads to be more biocompatible (Robitaille *et al.*, 1999), have improved oxygen transport properties (Ogbonna *et al.*, 1991) and reduced response time of encapsulated islets to glucose (Chicheportiche and Reach, 1988).

An important property for therapeutically useful encapsulated cells is their ability to survive after implantation. Calcium cross-linked alginate beads are known to be unstable in biological environments (LeRoux *et al.*, 1999, Section 1.7.2.1). In physiological solutions, ion-exchange of Ca^{2+} with Na^{+} occurs, as well as calcium sequestration by various species, such as phosphate, both of which lead to bead dissolution. Additionally, bead properties may alter through processes such as ion-exchange, which causes osmotic swelling and leads to larger pore sizes (Thu *et al.*, 1996b).

Various approaches have been employed to stabilise alginate beads prior to implantation (Sections 1.7.2.4 and 1.8). The simplest of these is use of barium as an alternative cross-linking ion. Barium ions have a stronger affinity for alginate than calcium ions, and as such form stronger bonds and more rigid gels (Smidsrod, 1974). High concentrations of barium are cytotoxic, as K^+ channels are inhibited. However, protein biosynthesis is not affected at concentrations of barium below 10mM (Howell and Tyhurst, 1976) and so concentrations below this level are preferred.

The most commonly investigated technique for producing stabilised alginate beads is production of a polycation/alginate complex membrane around the beads. Since its inception in 1980 by Lim and Sun, the most extensively studied polycation for this purpose is poly-L-lysine (PLL). As most polycations are cytotoxic and immunogenic, an additional alginate layer is applied to the beads, generating alginate-PLL-alginate (APA) capsules, to prevent tissue fibrosis. Although APA capsules are resistant to destabilisation in biological systems, as the liquefied core is contained by a membrane, the mechanical stability is decreased due to increases in osmotic pressure (Thu *et al.*, 1996a).

Investigations into the concentration of alginate present within individual beads led to the proposal of two alternative structures for alginate beads; homogeneous and non-homogeneous (Skjakbraek *et al.*, 1989). Homogeneous beads are characterised by an equal concentration of alginate throughout the bead (equal alginate density), whereas non-homogeneous beads have a higher concentration of alginate near the surface of the bead (variable alginate density, Figure 6.1). Non-homogeneous beads are formed as alginate molecules diffuse towards the droplet surface where the concentration of calcium ions is highest. Homogeneous beads are formed by disrupting diffusion of alginate molecules to the surface by addition of non-gelling ions, such as sodium. External gelation (Section 1.7.2.2) typically forms non-homogeneous beads, whereas homogeneous beads are typically formed through internal gelation (Section 1.7.2.2). Non-homogeneous beads are deemed more suitable for implantation as they have a lower porosity and increased stability (Thu *et al.*, 1996a) compared to homogeneous beads.

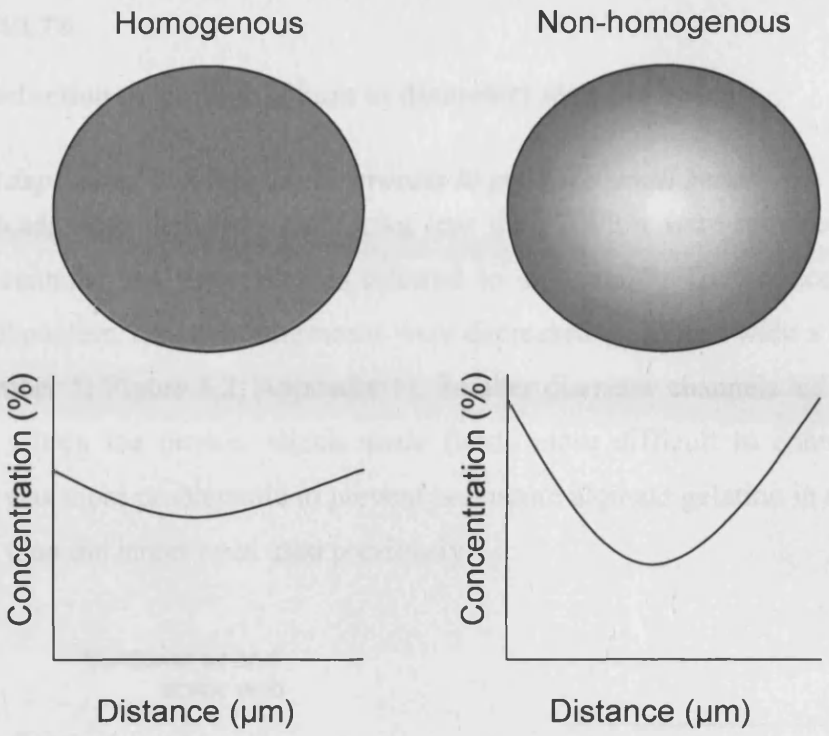

Figure 6.1: Comparison of alginate gradient in homogeneous and non-homogeneous alginate beads. Homogeneous beads are characterised by an equal concentration of alginate throughout, whereas non-homogeneous beads are characterised by a higher concentration of alginate at the surface, with a decreasing alginate concentration towards the centre. Note that homogeneous beads have a lower concentration of alginate at the surface than non-homogeneous beads for beads made with the same concentration of alginate. Adapted from Uludag *et al.* (2000)

Adaptations to the method previously developed (Section 3.3.3) were made to enable smaller beads to be manufactured using a microfabricated device. The inner diameter of the cannula used for implantation into rats' brains was 300μm, requiring beads with diameters of 100-250μm. After some method development the robust, test cell line HEK293 and the therapeutic cell line PC12 were encapsulated to show that the method developed to decrease the size of beads was suitable for encapsulating cells.

Barium cross-linking and polycation secondary coatings were investigated in an attempt to stabilise calcium cross-linked alginate beads produced using the MIG method. The effect of barium on encapsulated cells was evaluated by observing cell viability. The internal structure of beads produced using the MIG method was observed *via* confocal microscopy. Adaptations to the production method were investigated to produce small, stabilised alginate beads. The small, stabilised alginate beads produced were implanted into rats' brains to investigate *in vivo* stability.

6.2 RESULTS

6.2.1 Production of small (<200μm in diameter) alginate beads

6.2.1.1 Adaptations to microfluidic process to produce small beads

Beads with diameters measuring less than 200μm were required to implant using a cannula; the target size is referred to as "small". To produce beads with smaller diameters, channel dimensions were decreased to 200μm wide x 100μm deep (chip number 5; Figure 6.2, Appendix 1). Smaller diameter channels led to increased pressure within the device, which made fluids more difficult to control. For this reason it was more problematic to prevent premature alginate gelation in these smaller channels than the larger ones used previously.

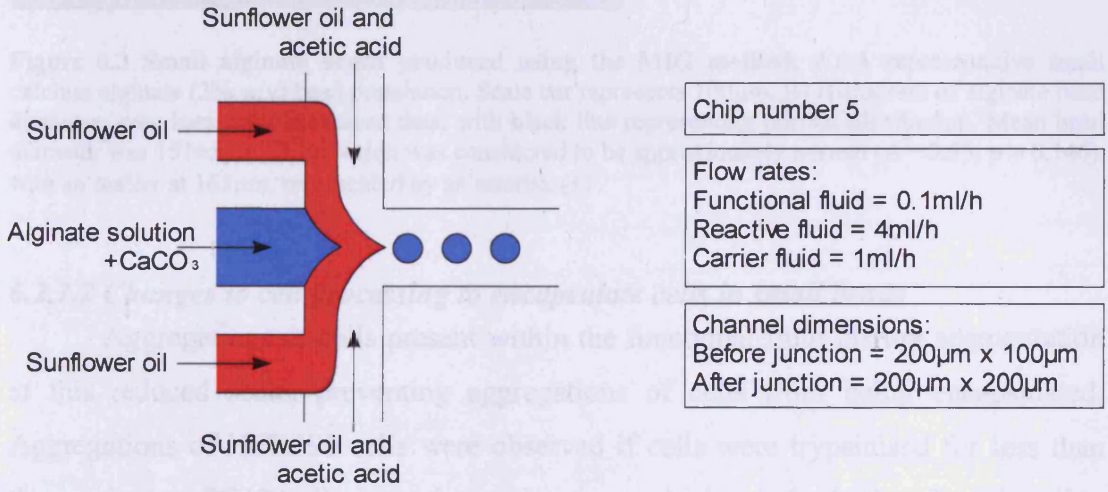

Figure 6.2: Schematic diagram showing the shielded junction and its use for producing calcium alginate beads *via* internal gelation. Functional fluid (shown in blue) was composed of alginate solution (2% w/v) containing 40mM $CaCO_3$, shielding flow (shown in red) was composed of sunflower oil and reactive flow (no shading) was composed of sunflower oil containing 40mM acetic acid. Flow rates and channel dimensions are shown. Orientation of flow is specified by arrows

By constricting the channels through which the continuous phase entered and decreasing the dimensions of the channel through which the functional fluid was introduced, oil was prevented from flowing into the channel containing the functional fluid. In this way premature cross-linking of the functional fluid was prevented. In addition, the reactive flow was not introduced into the device until stable segmentation between the dispersed and continuous phases had been established. As smaller channels were utilised, flow rates were very much reduced (Figure 6.2). Unacceptable leakage of continuous phase occurred when a PFA gasket was used to

seal the device. Nescofilm was instead used to seal the device, this prevented leakage of the reactive fluid, thus averting it flowing back into the functional fluid channel and causing premature cross-linking. Product beads (n=30) were measured (Section 2.2.3) and found to have a mean diameter of 151±5µm with a CV of 3% (Figure 6.3).

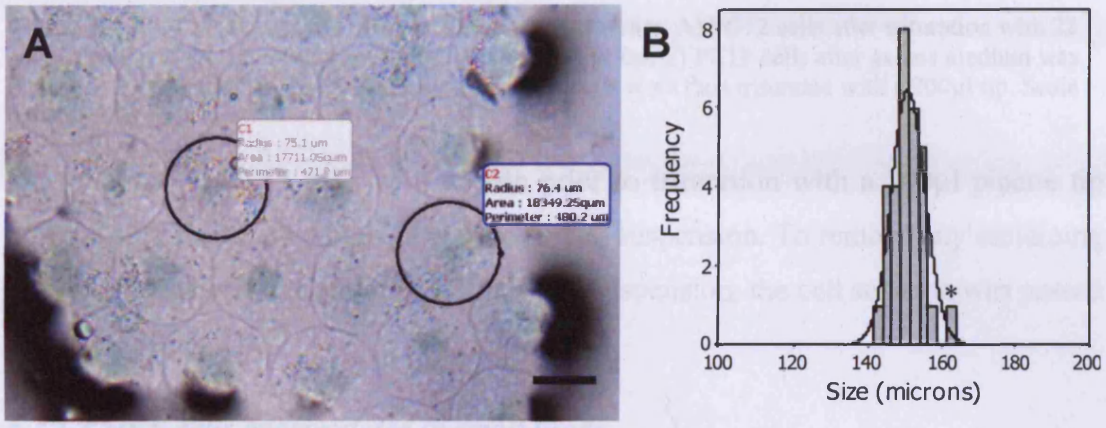

Figure 6.3 Small alginate beads produced using the MIG method. A) A representative small calcium alginate (2% w/v) bead population. Scale bar represents 100µm. B) Histogram of alginate bead diameter; grey bars show measured data, with black line representing normal distribution. Mean bead diameter was 151±5µm. Distribution was considered to be approximately normal (A^2=0.55, p > 0.146), with an outlier at 163µm, represented by an asterisk (*)

6.2.1.2 Changes to cell processing to encapsulate cells in small beads

Aggregations of cells present within the functional fluid disrupt segmentation at this reduced scale, preventing aggregations of cells from being encapsulated. Aggregations of HEK293 cells were observed if cells were trypsinised for less than three minutes. PC12 cells grow in aggregations which can be broken by trituration (production of a homogeneous mixture). Varying methods for triturating PC12 cells were investigated. A sample of cells were triturated with a 22 gauge needle (Figure 6.4A), another sample was triturated using a 200µl pipette tip (Figure 6.4B), and a final sample was triturated with a 200µl pipette tip after 2 minute exposure to trypsin (Figure 6.4C).

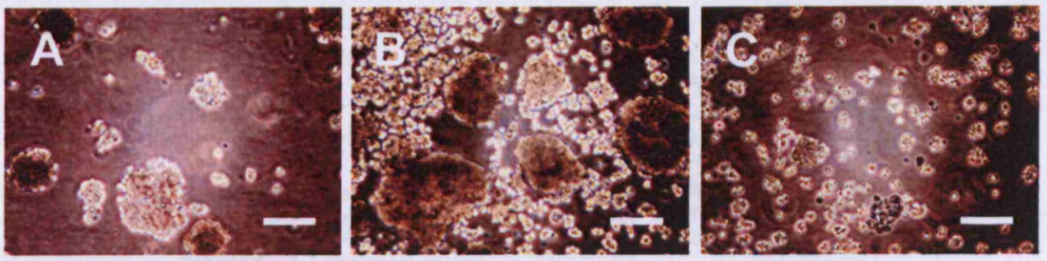

Figure 6.4: PC12 cells after varying trituration treatments. A) PC12 cells after trituration with 22 gauge needle, B) PC12 cells after trituration with a 200µl tip, C) PC12 cells after excess medium was removed, 200µl trypsin added and left for 2 minutes, cells were then triturated with a 200µl tip. Scale bars represent 500µm

Treating PC12 cells with trypsin prior to trituration with a 200µl pipette tip was the only treatment which gave a single cell suspension. To remove any remaining clumps of cells and thus produce a single cell suspension, the cell solution was passed through a 30µm filter.

6.2.1.3 HEK cells encapsulated in small beads

As viability of encapsulated cells was seen to improve after rapid transfer into medium on-chip, an additional chip was designed combining small channels with a flushing flow (chip number 6; Figure 6.5, Appendix 1). Beads consisting of MVM and MVG alginate without cells were produced using chip number 6. MVM alginate beads were 233±10µm (n=20) in diameter and MVG alginate beads were 232±10µm (n=20) in diameter (Figure 6.6).

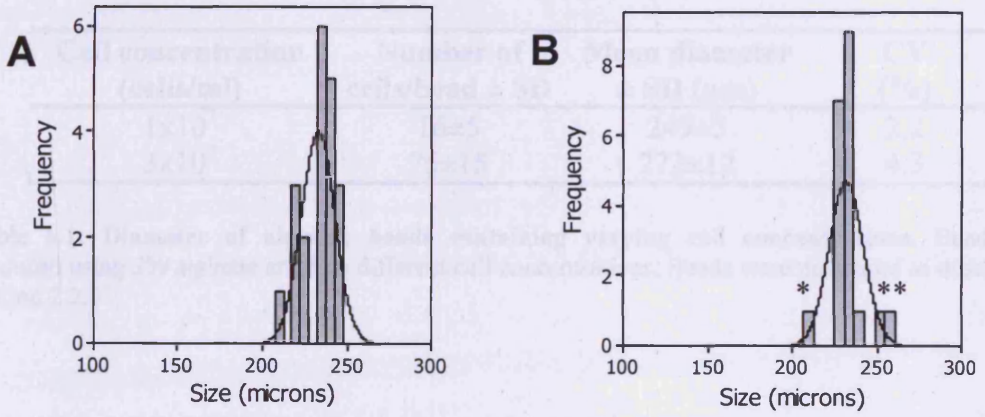

Figure 6.5: Histograms of MVM and MVG alginate beads. A) Histogram of MVM alginate beads; grey bars show measured data, with black line representing normal distribution. Mean bead diameter was 233±10µm. Distribution was considered to be approximately normal (A^2=0.62, p > 0.091). B) Histogram of MVG alginate beads; grey bars show measured data, with black line representing normal distribution. Mean bead diameter was 232±10µm. Distribution was considered not normal (A^2=1.80, p > 0.005), with outliers at 212µm, 253µm and 260µm represented by asterisks (*)

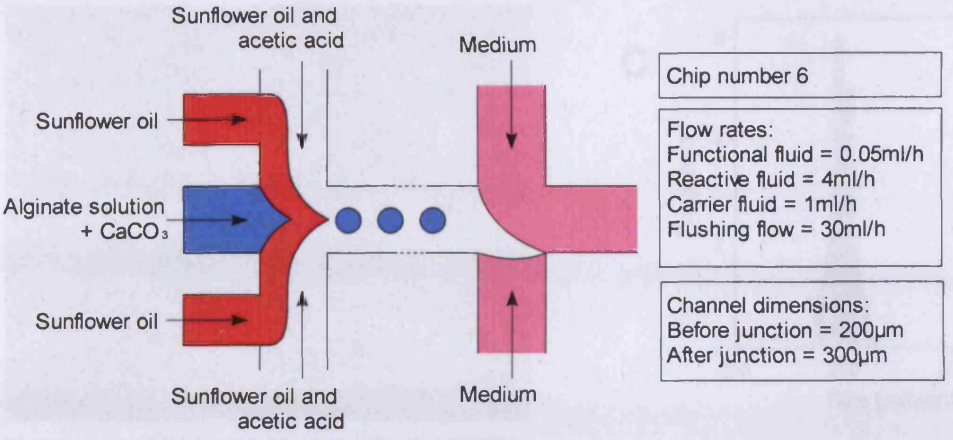

Figure 6.6: Schematic diagram showing the shielded junction with additional flushing flow for introducing aqueous medium. Functional fluid (shown in blue) was composed of alginate solution (2% w/v) containing 40mM $CaCO_3$, shielding flow (shown in red) was composed of sunflower oil and reactive flow (no shading) was composed of sunflower oil containing 40mM acetic acid. Flushing flow was D-MEM/F12 medium (shown in pink). Flow rates and channel dimensions are shown. Orientation of flow is specified by arrows

Using chip number 6, HEK293 cells were successfully encapsulated in small MVM alginate beads. The encapsulation experiment was repeated twice with two different cell concentrations; $1x10^7$ and $3x10^7$ cells per ml. The number of cells per bead was counted (n=45) and the diameter was measured (n=22, Section 2.2.3). These data are summarised in Table 6.1 and Figure 6.7. Both bead samples produced were larger than alginate beads without cells (233±10µm) and were too large to fit inside the implantation cannula.

Cell concentration (cells/ml)	Number of cells/bead ± SD	Mean diameter ± SD (µm)	CV (%)
$1x10^7$	16±5	249±5	2.2
$3x10^7$	75±15	272±12	4.3

Table 6.1: Diameter of alginate beads containing varying cell concentrations. Beads were produced using 2% alginate and two different cell concentrations. Beads were measured as described in Section 2.2.3

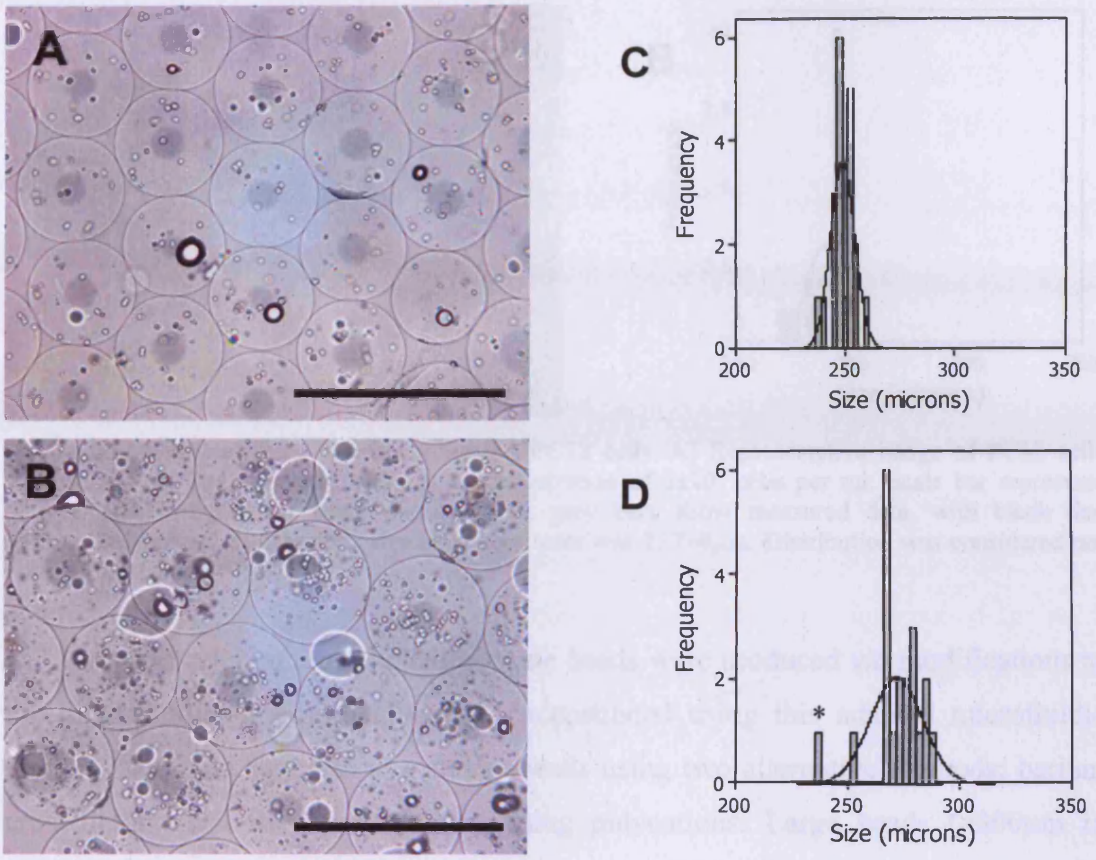

Figure 6.7: Small alginate beads containing HEK293 cells. A) Representative image of HEK293 cells encapsulated in small alginate beads at a concentration of $1x10^7$ cells per ml, B) representative image of HEK293 cells encapsulated in small alginate beads at a concentration of $3x10^7$ cells per ml, C) histogram of beads shown in A; grey bars show measured data, with black line representing normal distribution. Mean bead diameter was 250±5μm. Distribution was considered to be approximately normal (A^2=0.51, $p > 0.05$), D) histogram of beads shown in C; grey bars show measured data, with black line representing normal distribution. Mean bead diameter was 272±12μm. Distribution was considered not normal (A^2=0.73, $p > 0.005$), with an outlier at 236μm, represented by an asterisk (*). Scale bars represent 500 μm

6.2.1.4 PC12 cells encapsulated in small beads

Using chip number 6, as described in Figure 6.5, PC12 cells were successfully encapsulated in small MVM alginate beads. PC12 cells were resuspended in the functional fluid at a concentration of $3x10^7$ cells per ml. Beads were manufactured which contained 47±19 cells (n=30) and were 237±8μm (n=20) in diameter (Figure 6.8). The same concentration of PC12 cells were encapsulated as in the equivalent experiment with HEK293 cells (Section 6.2.1.3). However, fewer cells per bead were observed in encapsulated PC12 beads than in encapsulated HEK293 beads (47±19 compared with 75±15, $t_{58} = 6.64$, $p < 0.001$).

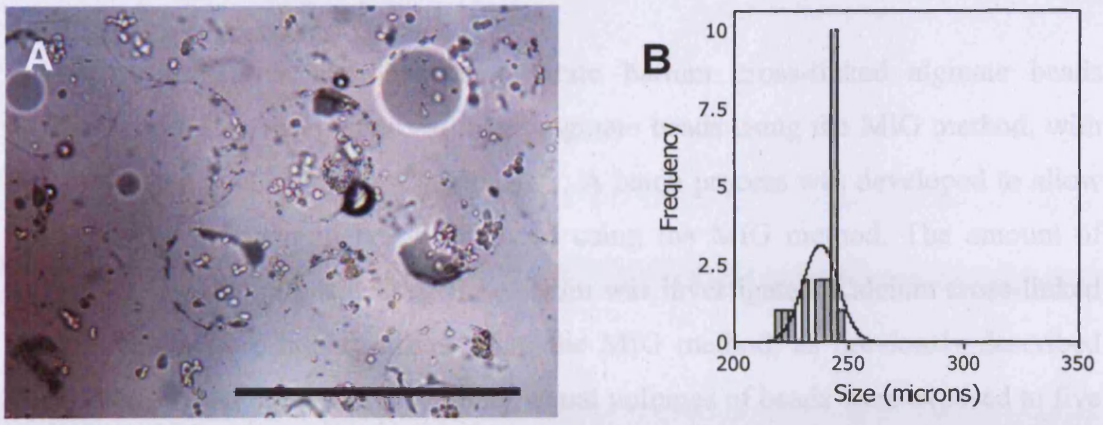

Figure 6.8: Small alginate beads containing PC12 cells. A) Representative image of PC12 cells encapsulated in small alginate beads at a concentration of $3x10^7$ cells per ml. Scale bar represents 500μm. B) Histogram of beads shown in A; grey bars show measured data, with black line representing normal distribution. Mean bead diameter was 237±8μm. Distribution was considered not normal (A^2=1.65, $p < 0.005$)

Small calcium cross-linked alginate beads were produced *via* modifications to the microfluidic process. Cells were encapsulated using this adapted microfluidic method. The next step was to stabilise beads using two alternative methods; barium cross-linking and secondary coating using polycations. Large beads (>300μm in diameter) were used due to better handling capabilities and the ability to carry out viability measurements. Cell viability cannot be measured in beads <300μm in diameter due to problems with manipulating individual beads.

6.2.2 Stabilisation of alginate beads using barium cross-linking

6.2.2.1 Internal barium cross-linking

To produce barium cross-linked alginate beads within a microfluidic system the original MIG method was altered by substituting $BaCO_3$ for $CaCO_3$ as the inert ion source in the functional fluid. Liquid sodium alginate mixtures (2% w/v) containing high concentrations (50-25mM) of $BaCO_3$ were too viscous to introduce into a syringe. The viscosity of a sodium alginate solution (2% w/v) was measured (Section 2.2.4) to be 128mPa·s at 25°C. The viscosity of a sodium alginate solution (2% w/v) containing 50mM $BaCO_3$ was measured (Section 2.2.4) to be 671mPa·s at 25°C. A sodium alginate solution (2% w/v) containing 12.5mM of $BaCO_3$ could be pumped into the MicroPlant™ and onto the chip (Chip number 2, Section 3.3.1). However, segmentation did not occur with regularity and spherical beads were not produced. This method was abandoned due to these technical difficulties.

6.2.2.2 Batch processing

An alternative approach to generate barium cross-linked alginate beads involved producing calcium cross-linked alginate beads using the MIG method, with subsequent ion exchange of Ca^{2+} with Ba^{2+}. A batch process was developed to allow ion exchange to occur in beads produced using the MIG method. The amount of barium required to fully substitute for calcium was investigated. Calcium cross-linked alginate beads were manufactured using the MIG method, as previously described (Section 3.3.3). After extensive washing, equal volumes of beads were exposed to five different concentrations of $BaCl_2$ (20, 10, 5, 2.5 and 1mM dissolved in saline) for 5 minutes. After exposure, excess $BaCl_2$ was washed from the beads; each bead sample was added to a 100μm filter and 1L of water was allowed to flow over them for 20 minutes. Extensive washing allowed excess unbound ions to diffuse out of the bead samples. Alginate beads cross-linked with higher concentrations (>10mM $BaCl_2$) of barium were visually observed to have a more "glassy" appearance when compared with calcium cross-linked alginate beads.

The $BaCl_2$ treated beads and a control sample of untreated calcium cross-linked alginate beads were prepared (Section 2.2.5) and then analysed using atomic absorption spectroscopy to detect amounts of Ca^{2+} and Ba^{2+} present. The concentration of calcium ions present in beads prior to barium treatment was 5.1pmoles/bead (Figure 6.9). Treating beads with 2.5mM $BaCl_2$ reduced the calcium ion concentration to 1.4pmoles/bead. Further addition of Ba^{2+} ions did not decrease the calcium ion concentration. As more $BaCl_2$ was added to the beads, more Ba^{2+} ions were present in the beads, until the maximum concentration of Ba^{2+} detected in beads was 1.2pmoles/bead. The maximum concentration of barium in the bead samples corresponded to 10 and 20mM of $BaCl_2$ added. As barium is extremely toxic to cells, it was decided to utilise 5mM $BaCl_2$ when batch processing beads. The decrease from 10mM to 5mM $BaCl_2$ reduced the amount of barium in the beads from 1.2pmoles/bead to 1.0pmoles/bead, a 17% reduction from the maximum Ba^{2+} concentration.

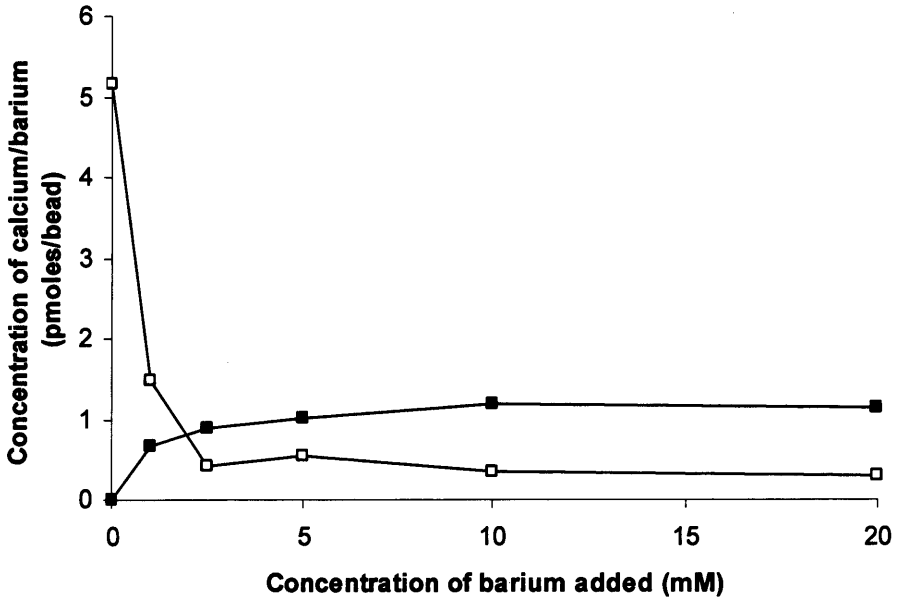

Figure 6.9: Concentration of barium added to bead sample compared to amount of calcium and barium present in bead sample. Open symbols represent calcium concentration, closed symbols represent barium concentration as determined by atomic absorption spectroscopy

Assuming a droplet with diameter 600μm was produced; each droplet has a volume of 113nl and was thus calculated to contain 5.5pmoles of $CaCO_3$, based upon a $CaCO_3$ concentration of 0.05mmoles/ml. The amount of calcium detected in cross-linked beads (5.1pmoles) was similar to the calculated expected value of 5.5pmoles. The exact diameter of droplets produced cannot be measured without high-speed video equipment. Although most of the calcium present within beads is displaced by the addition of barium, an equal amount of barium does not replace the displaced calcium; the amount of barium detected (1.2pmoles) is much lower than the amount of calcium present within beads.

6.2.2.3 Effect of barium on cell viability

As previously stated, barium is toxic to cells at low doses (<10mM). The effect of cross-linking beads with 5mM $BaCl_2$ on HEK293 and PC12 cell viability was investigated.

6.2.2.3 a) Effect of barium on encapsulated HEK viability

Two separate encapsulation experiments were carried out with individual populations of HEK293 cells (as described in Section 4.2.3). Cells were resuspended at a concentration of $1x10^6$ cells per ml in the functional fluid. An hour after encapsulation, each sample of beads was split in half. Batch treatment with 5mM

$BaCl_2$ was carried out on one half (as described in Section 6.2.2.2) and the other half was washed in medium only. Viability of the encapsulated cell populations was observed for 45 days (Figure 6.10) using the adapted trypan blue exclusion method (Section 4.2.1.1).

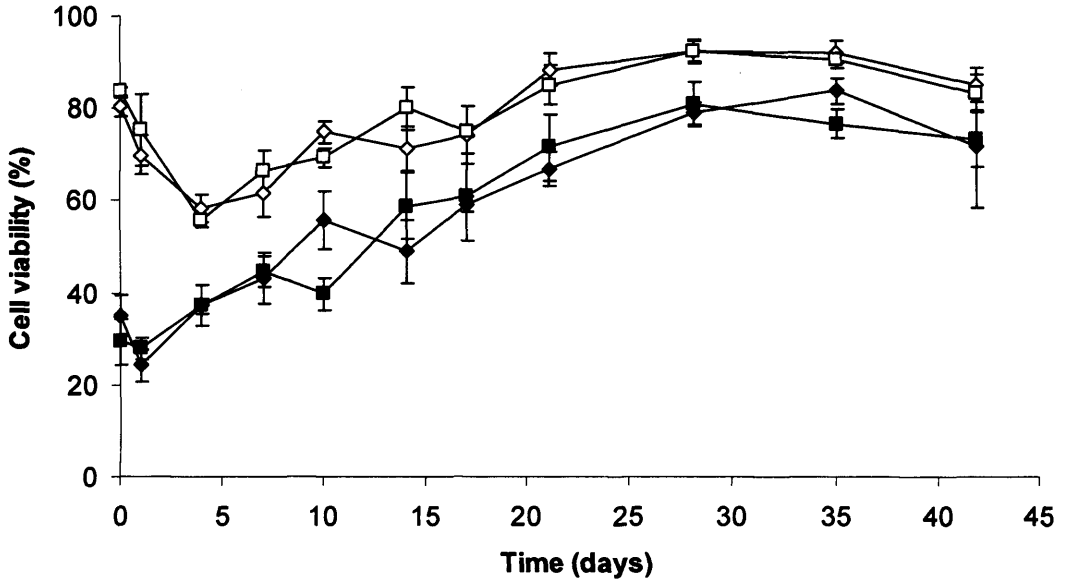

Figure 6.10: Effect of barium exposure on encapsulated HEK293 cell viability. Open symbols represent viability of HEK293 cells encapsulated in calcium cross-linked alginate beads, closed symbols represent viability of HEK cells encapsulated in barium cross-linked alginate beads. Pre-encapsulation viability was 90%. Viability was estimated using the adapted trypan blue method. Error bars show standard error of the mean measured in 4 individual beads

Populations of cells encapsulated in both calcium and barium cross-linked alginate beads were observed to decrease in viability immediately following encapsulation. Cells encapsulated in barium cross-linked alginate beads decreased to 25% viability 1 day after encapsulation, but increased in viability thereafter. Viability of cells encapsulated in calcium cross-linked alginate beads decreased to 55% after 5 days, after which point viability increased. An increase in viability was observed in both bead types until day 30 when viability began to decrease slightly. Cells encapsulated in barium cross-linked alginate beads were observed to be ~20 percentage points lower in viability, between days 7 and 14, than cells encapsulated in calcium cross-linked alginate beads. The difference in viability dropped to ~10 percentage points between days 28 and 42. From day 17 onwards the viability of cells encapsulated in barium cross-linked alginate beads was significantly lower than the

viability of cells encapsulated in calcium cross-linked alginate beads ($F_{1,176} = 36.05$, $p < 0.001$).

6.2.2.3 b) Effect of barium on encapsulated PC12 viability

Three separate encapsulation experiments were carried out with individual populations of PC12 cells (as described in Section 5.2.1). Each batch of cells was resuspended at a concentration of $4x10^7$ cells per ml in the functional fluid. An hour after encapsulation each sample of beads was split in half. Batch treatment with 5mM $BaCl_2$ was carried out on one half (as described in Section 6.2.2.2) and the other half was washed in medium only. Viability was observed for 8 days using adapted trypan blue exclusion method (Section 4.2.1.1). Viability of each of three separate encapsulation experiments is shown (Figure 6.11A), with mean viability also shown for clarity (Figure 6.11B). Viability of cells encapsulated in calcium and barium cross-linked alginate beads was not significantly different ($F_{1,54} = 0.000$, n.s.).

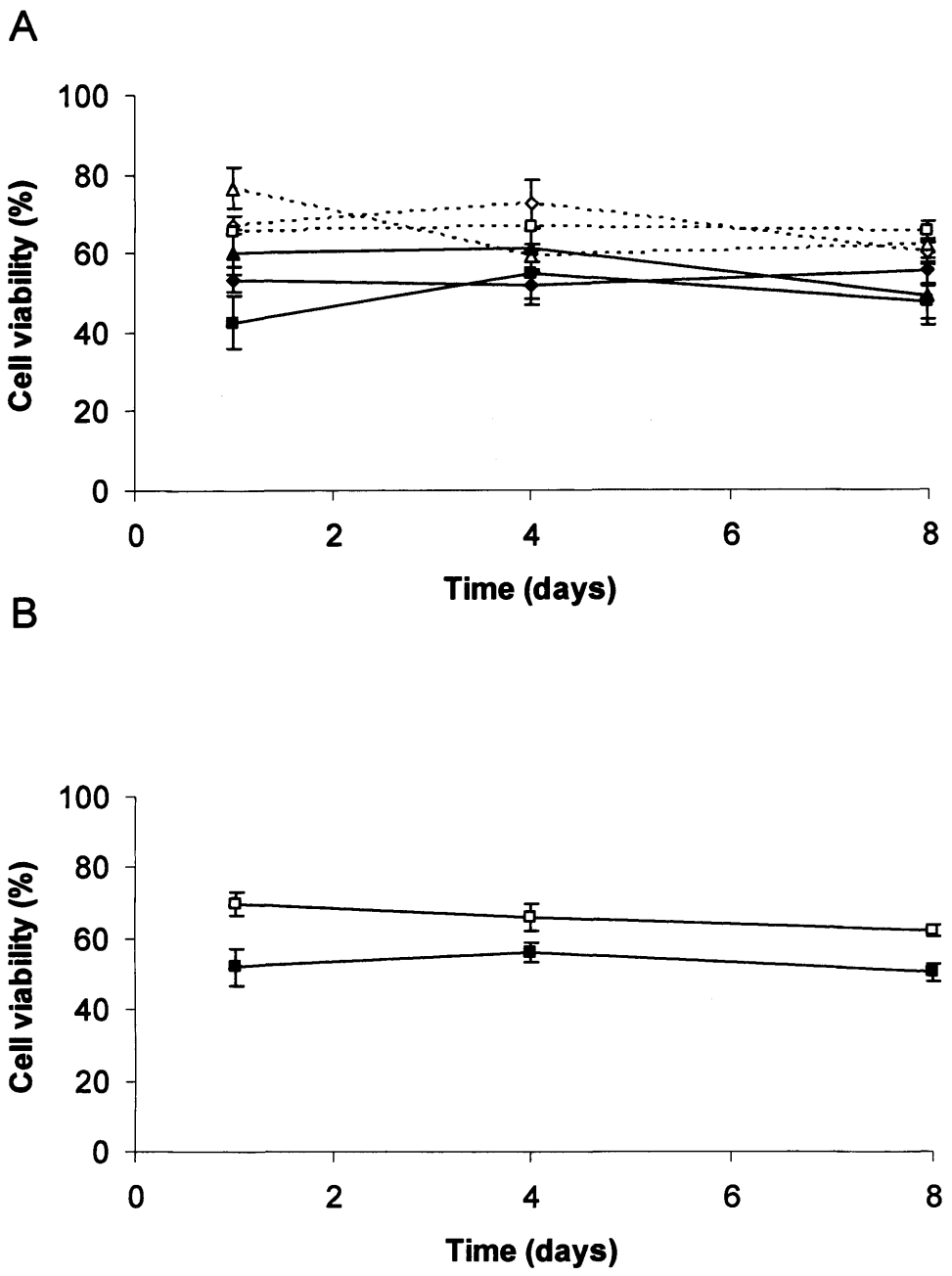

Figure 6.11: Effect of barium exposure on encapsulated PC12 cell viability. A) Viability of PC12 cells, and B) mean viability of PC12 cells encapsulated in alginate beads after treatment with 5mM $BaCl_2$, for each of three replicate encapsulations is shown. Open symbols (with dashed lines in upper panel) represent cells encapsulated in calcium cross-linked alginate beads, closed symbols represent cells encapsulated in barium cross-linked alginate beads. Pre-encapsulation viability was 71% (▲), 74% (■) and 73% (◊). Cell viability was estimated using the adapted trypan blue method. Error bars show standard error of the mean of 3 individual beads from three separate encapsulation experiments

6.2.2.4 Implantation of small calcium and barium cross-linked alginate beads

Previously, small calcium cross-linked alginate beads were produced containing cells (Sections 6.2.1.3 and 6.2.1.4). Cross-linking large alginate beads with barium was shown to have little effect on the therapeutic cell line PC12 (Section

6.2.1.4). Prior to implanting PC12 cells encapsulated in small barium cross-linked alginate beads, initial attempts at implantation were carried out with small barium cross-linked alginate beads minus cells. The ultimate goal was to observe behavioural changes in a rodent model of Parkinson's disease; therefore, beads were required to remain within the striatum for over 6 weeks (Borlongan *et al.*, 2004). An initial time point of 21 days was decided upon to observe beads within the striatum after implantation.

Calcium cross-linked alginate beads were prepared from MVM and MVG alginate using chip number 5 (Figure 6.2). Each bead sample produced was split in half. Batch treatment with 5mM $BaCl_2$ was carried out on one half of each sample (as described in Section 6.2.2.2) and the other half of each sample was washed in medium only. All beads were measured prior to implantation (Section 2.2.3) to ensure bead diameter was <150μm for cannula implantation. Beads were implanted into rat striatum using stereotactic apparatus (Figure 6.12, Section 2.4.2). Beads made of MVM alginate were implanted into two rats and beads made of MVG alginate were implanted into another two rats. In each case calcium cross-linked alginate beads were implanted into the right striatum and barium cross-linked beads were implanted into the left striatum.

An animal from each group was perfused 7 days after implantation. No evidence of any beads was observed in sections of brain tissue prepared (Section 2.4.3) 7 days after implantation (Figure 6.13A and D). The remaining animal from each group was perfused 15 days after implantation. Barium cross-linked alginate beads were observed in sections of brain tissue prepared (Section 2.4.3) 15 days after implantation (Figure 6.13B, C, E and F). MVG beads left a large, well-defined cavity in the brain tissue (Figure 6.13B and E) with some evidence of scar formation around the beads. However, MVM beads appeared to have cells growing around them, with no clearly-defined border around the cavity left by beads (Figure 6.13E and F). No evidence of beads was observed 7 days after implantation; however, barium cross-linked beads were observed 15 days after implantation, hence, there was some uncertainty as to whether beads had been reliably implanted.

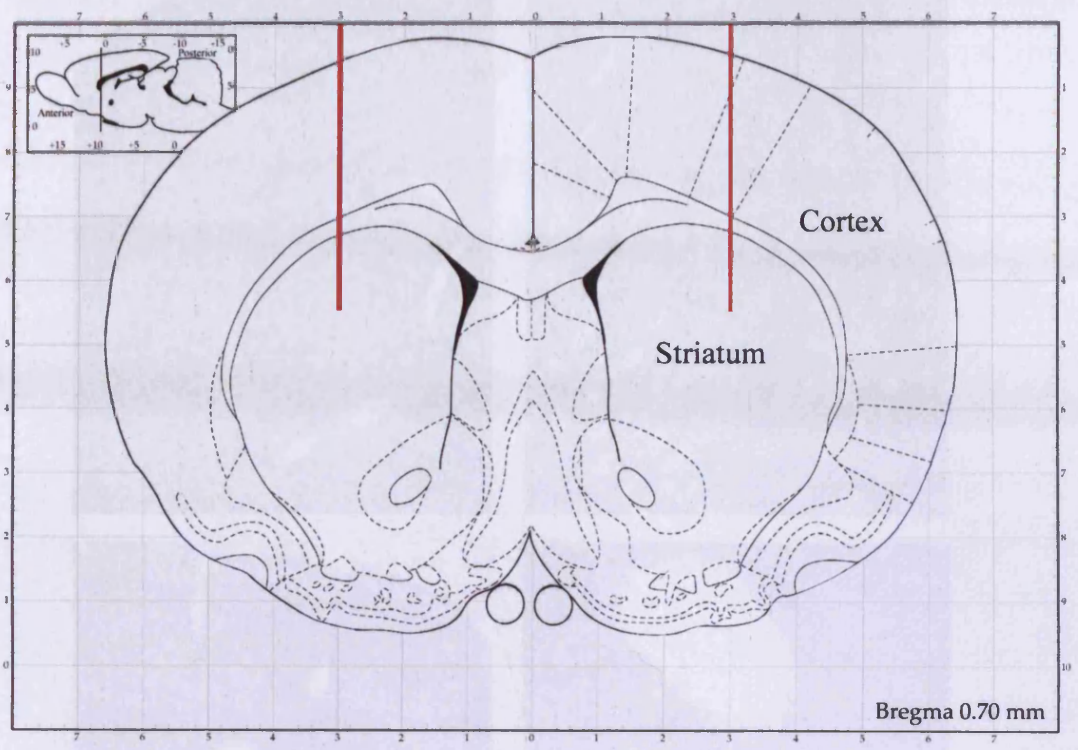

Figure 6.12: Schematic showing sterotactic positions of bead implantation into rat striatum. Red lines indicate position of needle for bead implantation

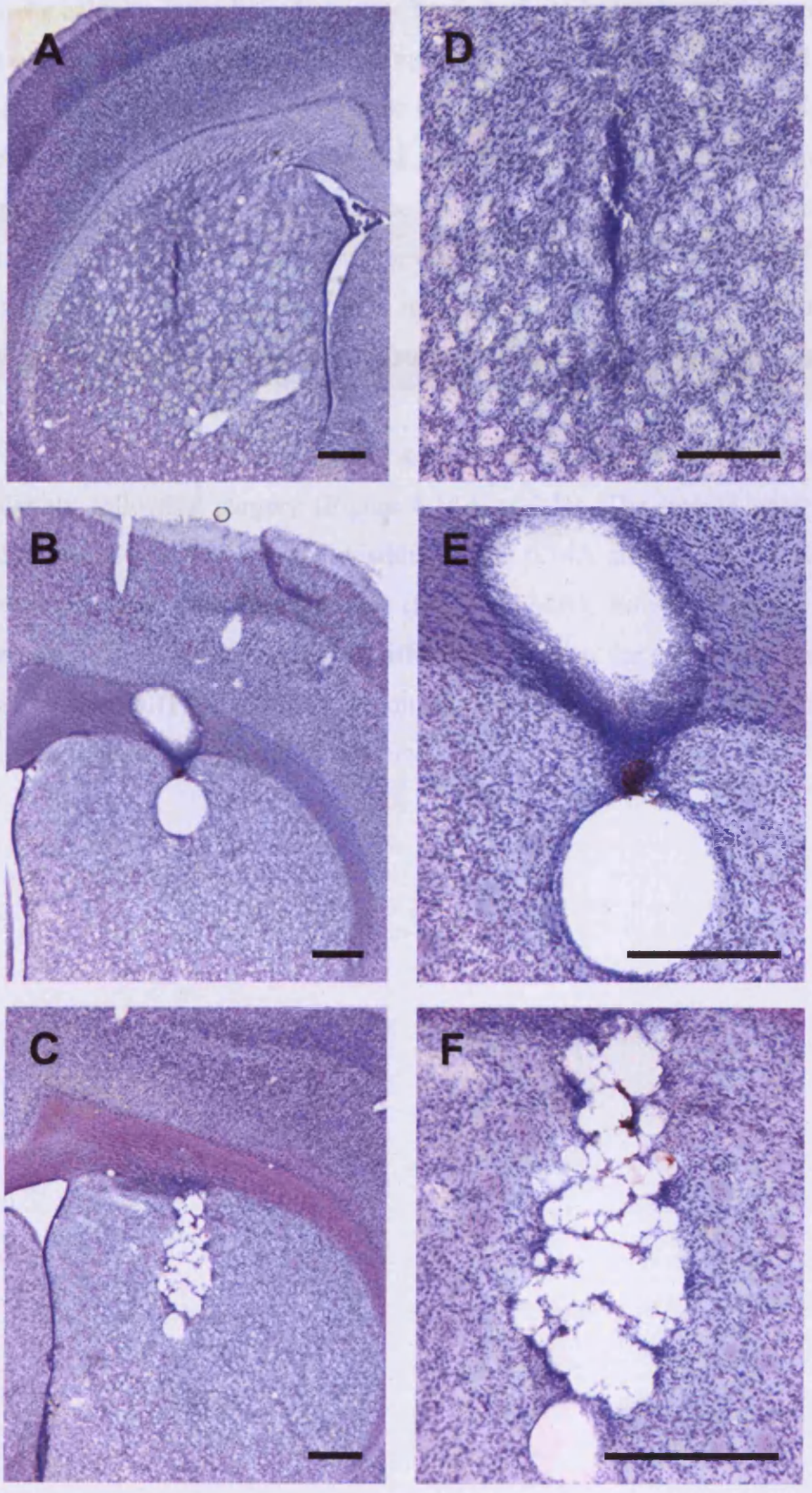

Figure 6.13: Cresyl violet stained sections showing implantation sites of alginate beads. A and D) calcium cross-linked MVM alginate beads 7 days after implantation, B and E) barium cross-linked MVG alginate beads 14 days after implantation, C and F) barium cross-linked MVM alginate beads 14 days after implantation. D, E and F show enlarged versions of A, B and C respectively. Scale bars represent 500μm

As calcium cross-linked alginate beads had not been observed in any sections, it was decided not to continue implanting these beads and to focus instead on barium cross-linked beads. To ensure that beads were being implanted into the striatum, MRI was carried out to visualise implanted beads immediately following implantation. Barium cross-linked MVM alginate beads were implanted into two rats (Section 2.4.2). Control injections of artificial cerebrospinal fluid were carried out on the left hand side of the brain and beads were injected into the right hand side of the brain. MRI was carried out immediately after surgery (Section 2.4.4). One rat was scanned 3 and 15 days after implantation.

A bolus of beads was clearly observable in the striatum of both animals immediately following surgery (Figure 6.14A and D). The needle track associated with the control injection was also visible (Figure 6.14A and D). The beads were still observable 3 days after implantation (Figure 6.14B); however by 15 days after implantation there was no noticeable difference between the control injection and the injection of beads (Figure 6.14C). Upon sectioning and staining (Section 2.4.3) the brain, no evidence of beads could be found.

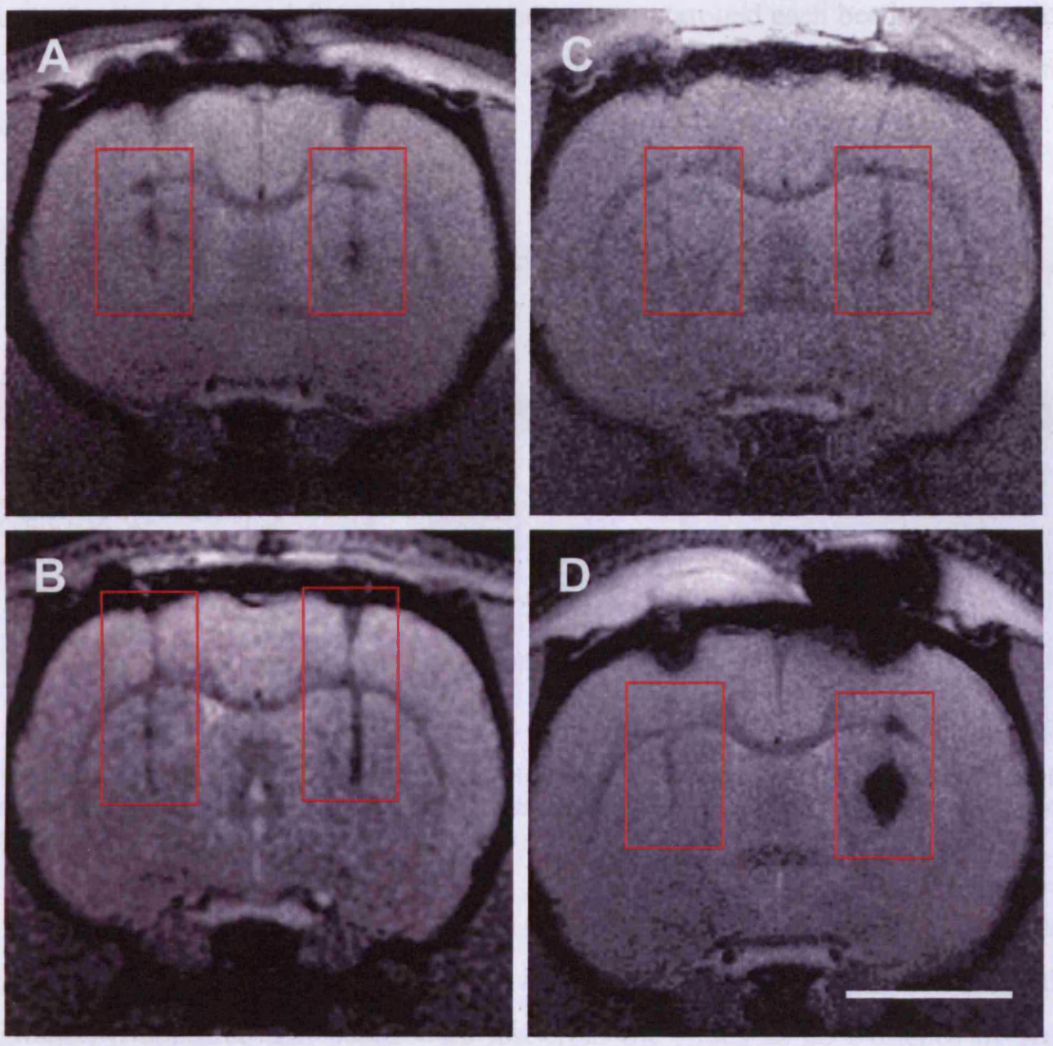

Figure 6.14: MR images of rats' brains after implantation of barium cross-linked MVM alginate beads. A) rat 1, 1 hour after implantation, B) rat 1, 15 days after implantation, C) rat 1, 3 days after implantation and D) rat 2, 1 hour after implantation. Left hand side of brain was injected with artificial cerebral spinal fluid and right hand side was injected with 3µl of barium cross-linked MVM alginate beads. Red boxes highlight areas of implantation. Scale bar represents 0.5cm

Additional implantation experiments were carried out to further investigate the scar formation previously observed upon implantation of MVM and MVG alginate beads (Figure 6.13). The differences in scar formation around the implanted beads observed may have been due to inter-animal differences as the MVM and MVG alginate beads were implanted into separate rats. To investigate inter-animal differences an additional implantation experiment was carried out.

Barium cross-linked MVM beads were implanted into the right striatum of 3 rats. Barium cross-linked MVG beads were implanted into the left striatum of the same 3 rats. A rat was perfused and its brain sectioned 1 week after implantation. Beads were observed in both the left and right striatum (Figure 6.15), no scar

formation was observed, but cells were seen to grow around each bead type. Sections taken from rats perfused 21 and 28 days post-implantation did not show any evidence of beads remaining.

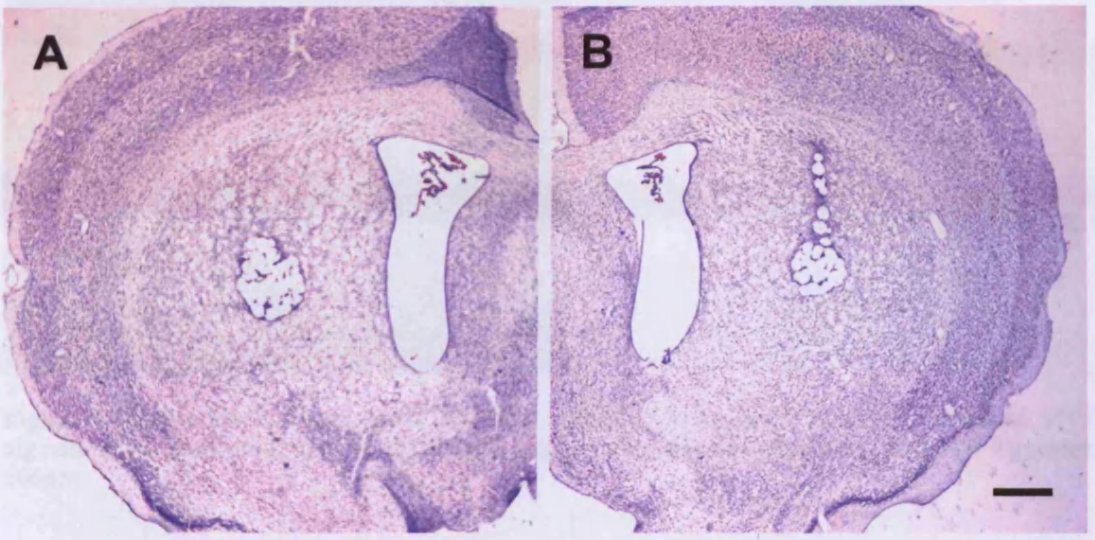

Figure 6.15: Cresyl violet stained sections showing implantation sites of alginate beads. A) Barium cross-linked MVG alginate beads and, B) barium cross-linked MVM alginate beads 7 days after implantation. Scale bar represents 1mm

All sections shown were stained with cresyl violet (Section 2.4.3). Cresyl violet staining requires that slides are agitated in various solutions. During this agitation it appeared that beads were lost from the slides as no evidence of beads remained, but there are clearly voids where they were previously located. Brains were sectioned using a sledge microtome and then collected into PBS. It was thought that the beads may be washed from the sections during this stage. To investigate further, a single brain was sectioned using a cryostat and sections were collected directly onto slides. In this way it was proposed that beads would remain in the sections. To further ensure retention of beads within sections, a wet mounting technique was employed. Slides with sections on were mounted directly with polyvinyl alcohol-1,4-diazabicyclo[2.2.2]octane (PVA-DABCO) without any staining. Many beads were observed to remain in the voids seen in tissue (Figure 6.16).

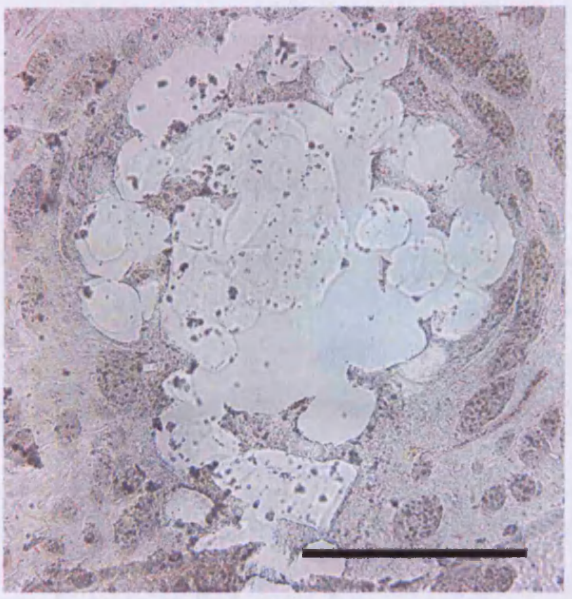

Figure 6.16: Section of brain tissue mounted using PVA-DABCO. Barium cross-linked MVG alginate beads seen in sections of brain tissue taken 7 days after implantation. Scale bar represents 500μm

6.2.2.5 Internal structure of alginate beads produced using the MIG method

As previous groups implanting small alginate beads into rodent brains were able to recover beads 56 days after implantation (Ross *et al.*, 1999), the above result was somewhat unexpected. There is evidence that alginate bead structure has an influence on stability *in vitro*, with homogeneous alginate beads being less stable than non-homogeneous (Thu *et al.*, 1996a). The structure of alginate beads can be elucidated *via* confocal microscopy of beads manufactured using fluorescent alginate (Strand *et al.*, 2003). Alginate beads produced using the MIG method were imaged in this way to reveal their internal structure.

Alginate was labelled with the fluorophore fluoresceinamine, using a procedure adapted from Strand *et al.* (2003, Section 2.2.8). Beads were produced from the fluorescent alginate using the MIG method (Section 4.2.2.3) and visualised using confocal microscopy (Section 2.2.9.1). Images were acquired from the equator of the beads, with an intensity profile being collected across the bead diameter (Figure 6.17). The concentration of alginate across the beads was observed to be homogeneous.

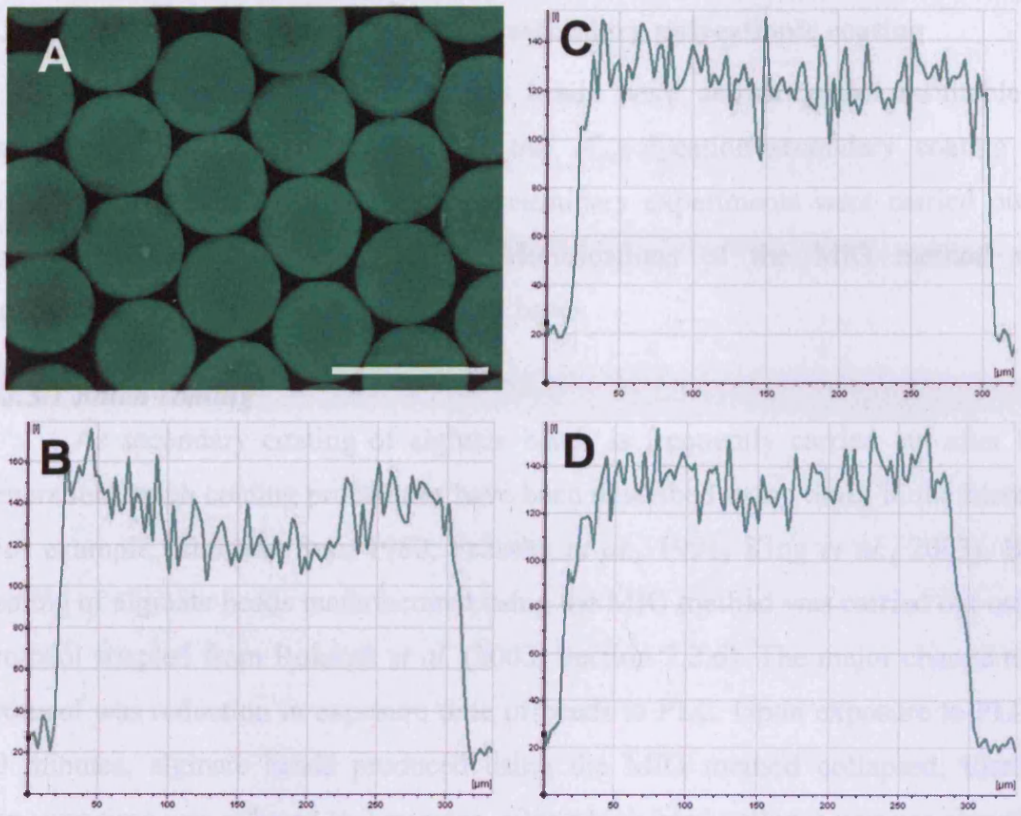

Figure 6.17: Internal structure of alginate beads produced using the MIG method. A) Image taken using confocal microscopy of beads manufactured using fluorescent alginate. B, C and D) Representative micrographs of optical sections taken through the equator of beads shown in A, showing the intensity of fluorescence, across the bead diameter. Scale bar represents 500µm

6.2.3 Stabilisation of alginate beads *via* secondary polycationic coating

As barium cross-linked alginate beads were shown to be unsuitable for implantation into rodent striatum, the use of polycation secondary coating was investigated as an alternative. Again, preliminary experiments were carried out on large (>300μm in diameter) beads. Modifications of the MIG method were subsequently carried out to produce small beads.

6.2.3.1 Batch coating

As secondary coating of alginate beads is frequently carried out after bead generation, batch coating procedures have been described many times in the literature (For example, Lim and Sun, 1980; Fritschy *et al.*, 1991; King *et al.*, 2003). Batch coating of alginate beads manufactured using the MIG method was carried out using a protocol adapted from Rokstad *et al.* (2003, Section 2.2.6). The major change to the protocol was reduction in exposure time of beads to PLL. Upon exposure to PLL for 10 minutes, alginate beads produced using the MIG method collapsed; therefore exposure time was reduced to 7 minutes, after which bead collapse was not observed.

6.2.3.2 Effect of secondary coating procedure on cell viability

In order to establish viability, trypan blue was added to encapsulated cells within PLO- and PLL-coated alginate beads. The coating chemicals employed became stained with trypan blue and, as a consequence, cells could not be observed. In addition, treatment with sodium citrate did not dissolve the PLL- or PLO-coated beads, as an insoluble surface polyplex had been formed between the alginate and polycation (Section 1.8). For these reasons, viability measurements on coated beads were not carried out using trypan blue exclusion.

6.2.3.3 Secondary coating using fluorescent PLL

To investigate whether beads were indeed being coated using the developed method and to observe any possible differences between different bead types, alginate beads were coated using PLL labelled with FITC (PLL-FITC) and imaged using confocal microscopy. Beads produced using the MIG method (internal gelation) and beads produced using an external gelation method were also compared for any differences in PLL binding.

Calcium cross-linked alginate beads were produced using the MIG method (Section 3.3.3). Half of the bead sample was batch treated with $BaCl_2$ to give barium

cross-linked alginate beads (Section 6.2.2.2). Calcium cross-linked alginate beads and barium cross-linked alginate beads were coated with either high MW (30-70 kDa) or low MW (15-30 kDa) PLL-FITC (Section 2.2.6). Calcium cross-linked alginate beads were also produced using an air-assisted droplet break-up method (ADB, Section 2.2.10) and coated with high or low MW PLL-FITC (Section 2.2.6). PLL-FITC was dissolved in 0.3M mannitol solution and washes were carried out in mannitol solution to preserve internal structure (Strand *et al.*, 2003). Images of beads were acquired using confocal scanning laser microscopy (CSLM, Section 2.2.9.1). An intensity profile was collected from bead equators.

Fluorescent signals were collected from all samples of beads prepared (Figure 6.18). The images were all taken at constant laser power, with images being optimised to the dynamic range of the detectors used. During this optimisation process the laser voltage was adjusted for each image taken of different bead samples. As the laser voltage used for each image was different, quantitative comparisons could not be made between samples. Strand *et al.* (2003) were able to measure the thickness of the PLL-FITC layer coating the alginate beads and compare layer thickness between different kinds of beads. As quantitative comparisons of this kind were impossible to make using the data gained during this experiment an alternative approach was used to enable qualitative comparisons to be made. By comparing the laser voltage used for a given image a qualitative estimate of the amount of PLL-FITC present was made (Table 6.2). A lower laser voltage was used to detect larger quantities of PLL-FITC. So, laser voltage is inversely proportional to the amount of PLL-FITC present.

Method of manufacture	Cross-linking ion	MW of PLL	Laser voltage
MIG	Calcium	Low	312.3
MIG	Barium	Low	327.1
ADB	Calcium	Low	283.4
MIG	Calcium	High	414.1
MIG	Barium	High	425.7
ADB	Calcium	High	340.5

Table 6.2: Comparison of bead type with laser voltage required to obtain an image using confocal microscopy. MIG refers to the microfluidic internal gelation method of manufacture, whilst ADB refers to air assisted droplet break-up

From the table above it can be seen that beads produced using the widely used ADB method were more fluorescent than beads produced using the MIG method. Calcium

cross-linked beads were more fluorescent than barium cross-linked beads. Beads coated with low molecular weight PLL-FITC were more fluorescent than beads coated with high molecular weight PLL-FITC. The amount of PLL-FITC present can be summarised as follows:

ADB, calcium cross-linked, coated with low MW PLL > MIG, calcium cross-linked, coated with low MW PLL > MIG, barium cross-linked, coated with low MW PLL > ADB, calcium cross-linked, coated with high MW PLL > MIG, calcium cross-linked, coated with high MW PLL > MIG, barium cross-linked, coated with high MW PLL

Alginate beads produced using the MIG method with subsequent cross-linking with barium and secondary coating with high MW PLL did not survive the process. Many beads were observed to have burst open (Figure 6.18F). As only PLL-FITC was used and not fluorescent alginate as well, it was impossible to visualise the alginate and so it remains unclear as to whether the PLL coating had peeled away from the alginate beads, leaving them intact, or if the alginate chains had destabilised and re-dissolved.

Alginate beads produced using the MIG method with subsequent coating with PLL had a different appearance than any of the other bead types. Beads coated with low MW PLL were observed to have a wrinkled appearance (Figure 6.18C), whereas, beads coated with high MW PLL were observed to be unevenly coated, with areas of intense fluorescence (Figure 6.18D).

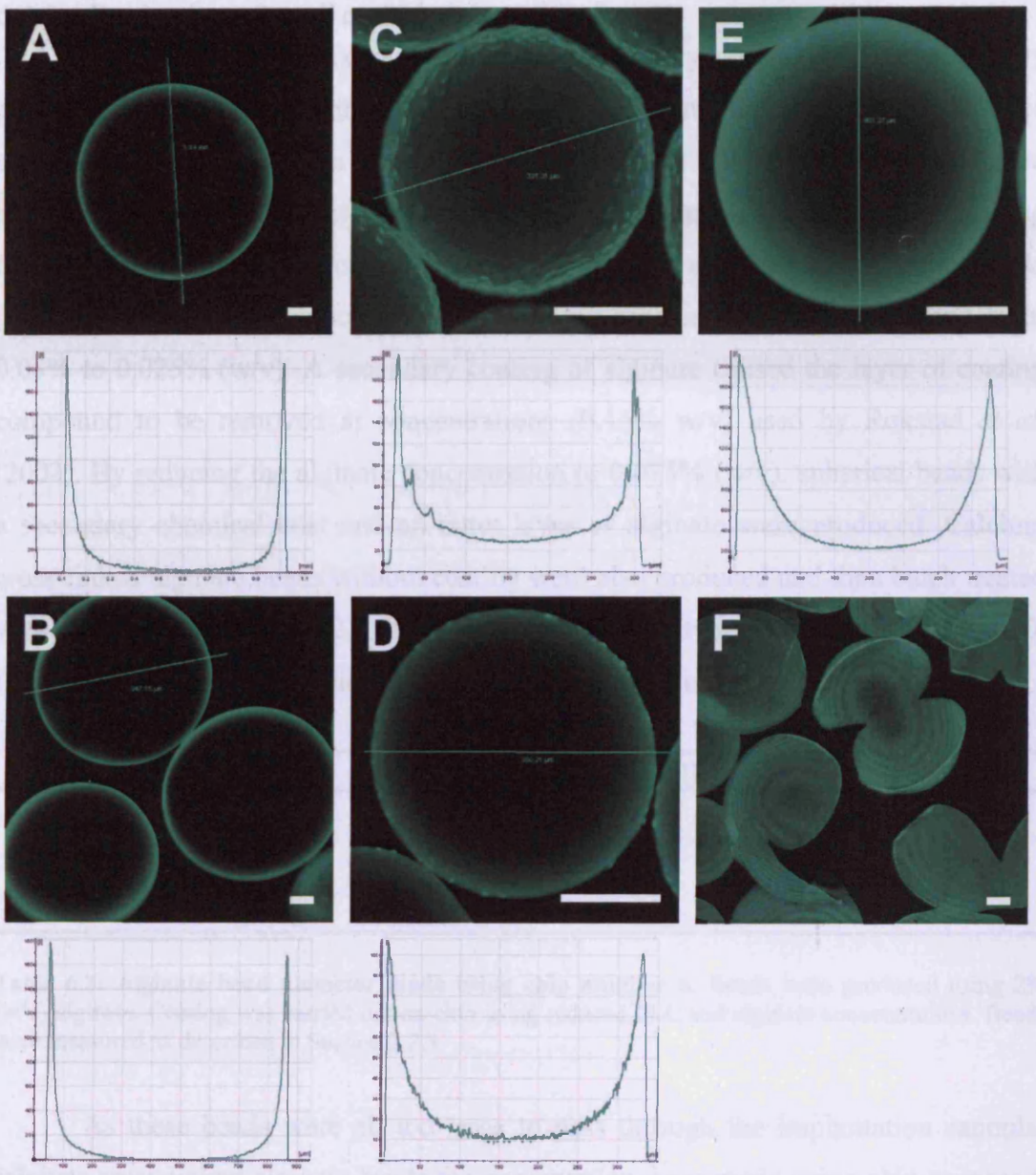

Figure 6.18: Distribution of PLL-FITC in various alginate beads coated. A) ADB generated alginate beads, cross-linked with calcium and coated with high MW fluorescent PLL. B) ADB generated alginate beads, cross-linked with calcium and coated with low MW fluorescent PLL. C) Alginate beads generated using the MIG method, cross-linked with calcium and coated with high MW fluorescent PLL. D) Alginate beads generated using the MIG method, cross-linked with calcium and coated with low MW fluorescent PLL. E) Alginate beads generated using the MIG method, cross-linked with barium and coated with low MW fluorescent PLL. F) Alginate beads generated using the MIG method, cross-linked with barium and coated with high MW fluorescent PLL, gradations present are a scanning artefact. The micrographs are optical sections taken through the equator of beads showing the intensity of the fluorescence emitted across the bead diameter. Scale bars represent 100μm

6.2.3.4 Production of small coated alginate beads

Large alginate beads coated with a secondary polycation layer were previously produced using a batch method (Section 6.2.3.1). An attempt was made to produce small alginate beads with a secondary polycation coat on-chip. The chip designed previously (chip number 6; Figure 6.5), combining small channels with a flushing flow, was used for this purpose. PLL, PLO and chitosan solutions were introduced *via* the flushing flow. The concentration of coating species utilised was reduced from 0.05% to 0.025% (w/v). A secondary coating of alginate caused the layer of coating compound to be removed at concentrations (0.15% w/v) used by Rokstad *et al.* (2003). By reducing the alginate concentration to 0.075% (w/v), spherical beads with a secondary chemical coat and an outer layer of alginate were produced. Calcium cross-linked alginate beads without coating were also produced and then batch treated with $BaCl_2$ (Section 6.2.2.2). Samples from all bead types were measured (n=20, Section 2.2.3). Size distributions are summarised in Table 6.3.

Type of bead	Mean diameter ± SD (μm)	CV (%)
Barium alginate	307±8	2.6
PLL coated alginate	319±37	11.5
PLO coated alginate	319±22	6.8
Chitosan coated alginate	362±13	3.6

Table 6.3: Alginate bead diameter made using chip number 6. Beads were produced using 2% (w/v) alginate. Coating was carried out on-chip using reduced PLL and alginate concentrations. Beads were measured as described in Section 2.2.3

As these beads were all too large to pass through the implantation cannula, calcium cross-linked alginate beads for implantation were made using chip number 5 with subsequent coating carried out using a batch method (Section 2.2.6). Samples from all bead types were measured (n=20, Section 2.2.3). Size distributions are summarised in Table 6.4.

Type of bead	Mean diameter ± SD (μm)	CV (%)
Calcium alginate	134±5	3.7
Barium alginate	130±5	4.1
PLL coated alginate	102±6	6.3
PLO coated alginate	107±5	4.6
Chitosan coated alginate	233±7	2.9

Table 6.4: Alginate bead diameter made using chip number 5 and batch processed. Beads were produced using 2% (w/v) alginate. Coating was carried out using a batch method described in Section 2.2.6. Beads were measured as described in Section 2.2.3

6.2.3.5 Implantation of small coated alginate beads

Implantation of each of the four alginate bead types (Section 6.2.3.4; barium cross-linked and alginate with PLL, PLO and chitosan secondary coat) was carried out. Two groups of rats with three rats in each group were used for this experiment. The first group received barium cross-linked alginate beads in the left hand striatum and chitosan coated alginate beads in the right hand striatum. The second group received PLL coated alginate beads in the left hand striatum and PLO coated alginate beads in the right hand striatum. An animal from each group was perfused and sections were taken of the brain 21 days after implantation. As there was no evidence of any of these beads remaining at this time point, the remaining animals were perfused 10 days later. Again, there was no evidence of any beads remaining in sections prepared from the brains of these animals.

6.3 DISCUSSION

6.3.1 Adaptation of the MIG method to produce small alginate beads

The MIG method was adapted to successfully produce alginate beads below 150μm in diameter. Microfluidic devices are ideally suited to produce alginate droplets below 150μm in diameter and several groups have indeed achieved this (Sugiura *et al.*, 2005; Zhang *et al.*, 2006; Choi *et al.*, 2007; Zhang *et al.*, 2007).

The major advantage to using microfluidic devices as opposed to other emulsion formation methods is that small diameter beads with a narrow size distribution are easily obtainable. For example, Zourob *et al.* (2006) reported standard emulsion formation to produce molecularly imprinted polymer beads (diameter 10μm) with a CV of 67% compared to microfluidic production, which produced beads (diameter 24μm) with a CV of 1.8%. Typically groups utilising microfabricated devices report beads with a CV of less than 2% (Seo *et al.*, 2005; Choi *et al.*, 2007; Zhang *et al.*, 2007). As many properties of alginate beads are dependant upon size, a small size distribution is important to ensure a homologous population of beads which will all respond in the same manner (Strand *et al.*, 2002).

6.3.2 Encapsulating cells in small beads using the MIG method

Cells were successfully encapsulated in small beads produced using the adapted MIG method. However, a higher concentration of cells was needed to allow encapsulation of large numbers of cells. Ross and Chang (2002) also reported the necessity of increasing cell concentration (2.5-fold) to prevent formation of empty capsules. The viability of cells encapsulated in small beads was unchanged as compared to medium sized (500-700μm in diameter) beads, although more cells per unit volume were observed (Ross and Chang, 2002). Addition of cells in a heterogeneous mixture to alginate solutions disrupts segmentation at a microfluidic junction (for example, see Shintaku *et al.*, 2007). The effects of disrupted segmentation are not as noticeable when microfluidic channels are many times larger than cells. However, when channel sizes are decreased to a few times the diameter of a cell, the disruption to segmentation becomes problematic. Beads produced containing cells were observed to be of larger diameter than beads which did not contain cells (Section 6.2.1.3) for this reason. Several groups have also succeeded in encapsulating cells in beads <150μm diameter using microfluidic devices (Sakai *et*

al., 2005; Sugiura *et al.*, 2005; Tan *et al.*, 2006b; Hong *et al.*, 2007; Sugiura *et al.*, 2007; Kim *et al.*, 2009), although none have carried out further investigations into long term viability of cells, stability of beads, suitability for implantation, etc.

6.3.3 Stabilisation using barium cross-linking

Barium cross-linked alginate beads could not be made by adapting the previously described MIG method to utilise $BaCO_3$ as the inert cross-linker. The viscosity of alginate solutions markedly increased upon addition of $BaCO_3$ and satisfactory segmented flow could not be achieved. Capretto *et al.* (2008) recently investigated three microfluidic approaches to producing barium cross-linked alginate beads. In the first method, fluid alginate droplets were formed *via* segmentation with oil and then cross-linked by dropping into a $BaCl_2$ solution, which produced a high proportion of beads with a comet-like appearance. The second method investigated was identical to the one outlined above (Section 6.2.2.1) i.e. internal gelation using $BaCO_3$. The concentrations of $BaCO_3$ tested by Capretto *et al.* were substantially lower (5-10mM) than those tested in this study (50-12.5mM), with the optimum concentration found to be 7.5mM. The third and most successful method investigated was addition of small amounts of $BaCl_2$ to the functional fluid, to increase the viscosity and reduce coalescence of product beads prior to falling into $BaCl_2$. Although barium cross-linked beads were produced using a microfabricated device, cross-linking on-chip was not achieved.

Instead of developing a microfluidic method to produce barium cross-linked alginate beads, a batch method was developed to allow ion exchange of Ca^{2+} for Ba^{2+}. Calcium cross-linked alginate beads were produced using the MIG method and equilibrated in $BaCl_2$ to promote ion exchange. Beads were batch treated with varying concentrations of $BaCl_2$. Ba^{2+} and Ca^{2+} concentrations present in each sample were obtained using atomic absorption spectrometry. The collected data showed that concentrations of $BaCl_2$ higher than 10mM did not increase the amount of Ba^{2+} detected within the batch treated beads. Decreasing the concentration of $BaCl_2$ to 5mM reduced the concentration of Ba^{2+} detected in beads by 17%. This reduction was deemed negligible and 5mM $BaCl_2$ was used in all subsequent experiments. This concentration of barium is below the level found to affect protein biosynthesis (Howell and Tyhurst, 1976) and it was postulated that this amount of barium would not be acutely toxic to cells upon exposure.

The amount of calcium detected by atomic absorption spectrometry in beads produced using the MIG method (5.1pmoles/bead) was extremely similar to the amount of $CaCO_3$ calculated to be present in an alginate droplet (5.5pmoles/droplet). All Ca^{2+} liberated by the reduction in pH is therefore utilised in cross-linking of alginate chains. Ca^{2+} concentration was seen to decrease with increasing Ba^{2+} concentration, indicating ion exchange. However, barium did not replace Ca^{2+} in a 1:1 ratio. The amount of Ba^{2+} present in the beads reached a maximum of 1.2pmoles/bead, whereas the maximum amount of Ca^{2+} present in beads was 5.1pmoles/bead.

The mechanism of ion binding to alginate chains may account for this difference. $CaCO_3$ is present throughout fluid alginate droplets, and so, upon pH decrease, Ca^{2+} ions are liberated in this ordered arrangement. Upon treatment with $BaCl_2$ a concentration gradient of barium is present with no Ba^{2+} inside calcium cross-linked alginate beads and a high surrounding concentration of $BaCl_2$. As barium ions have a larger radius (1.35Å) compared to calcium ions (0.97Å) it has been argued that they are expected to fill a larger space between alginate chains (Al-Musa *et al.*, 1999; Choonara *et al.*, 2008). This tight arrangement is somewhat dubiously argued to limit diffusion of further barium ions into the alginate bead. Barium ions in conventionally produced barium cross-linked alginate beads (i.e. external gelation by dropping into $BaCl_2$) have been shown, using confocal microscopy, to be limited to the outside of the bead (Zimmermann *et al.*, 2003). The present study did not allow the position of barium ions to be visualized, so this theory could not be investigated further. However, this limitation of diffusion is unlikely to occur as alginate gels have a macro-porous structure. Large proteins have been shown to diffuse through an alginate gel (Strand *et al.*, 2002). The likelihood of Ba^{2+} ion binding preventing further diffusion of barium ions to the centre of the bead is small. A more probable explanation for the observed Ba^{2+}/Ca^{2+} inequality is that there are fewer binding sites available for Ba^{2+} than Ca^{2+}. Ca^{2+} and Ba^{2+} differ in charge density and ionic radius. These differences allow Ba^{2+} to bind more strongly to carboxyl groups present in alginate than Ca^{2+} does.

There is evidence that fewer residues are required to cross-link alginate with barium than calcium (Stokke *et al.*, 1991) and that binding of metal ions to alginate depends upon the physical state of the alginate i.e. solution or gelled (Seely and Hart, 1974). Beads used in this experiment were already in a gel state when Ba^{2+} ions were

added. In addition to these explanations, the amount of calcium detected in this experiment was at the lower limit of detection of the spectrometer. A more accurate estimation of the amount of calcium present could be obtained by analysing larger numbers of beads. A more accurate estimate may reveal that more calcium is present than the current experiment indicates.

6.3.3.1 Effect of barium treatment upon encapsulated cell viability

The acute effects of barium exposure *via* the developed batch process on HEK293 and PC12 cells were investigated. HEK293 cells encapsulated in barium cross-linked alginate beads showed a larger decrease in viability than cells encapsulated in calcium cross-linked alginate beads, but recovered more rapidly. HEK293 cells encapsulated in calcium cross-linked alginate beads continued to decrease in viability until day 5, whereas HEK293 cells encapsulated in barium cross-linked alginate beads began to show an increase in viability after day 1.

Barium encapsulated PC12 cell viability did not decrease by more than 20 percentage points at any time point observed. The two later time points showed a 10 percentage point difference between calcium and barium cross-linked alginate beads. The effect of barium treatment upon encapsulated PC12 viability was not statistically significant.

In this study, the long term effects of encapsulation in barium cross-linked alginate beads were investigated for HEK293 cells. Viability of cells encapsulated in barium cross-linked alginate beads was consistently lower than cells encapsulated in calcium cross-linked alginate beads. As discussed in the previous chapter (Section 5.3.2), the microstructure of beads can affect cell growth and proliferation. As alginate chains have a greater affinity for Ba^{2+} than Ca^{2+}, the ionic interactions between alginate chains and Ba^{2+} are stronger than with Ca^{2+}. A more rigid structure prevents cells from growing and forming large aggregations. The long term effects of encapsulation in barium cross-linked alginate beads were not investigated using PC12 cells, due to time constraints.

The most commonly used protocol for the production of barium cross-linked beads utilises small amounts (1mM) of $BaCl_2$ in combination with 50mM $CaCl_2$ as a gelling agent, which has been shown to stabilise alginate beads against swelling (Morch *et al.*, 2006). In addition, barium is not considered toxic at this concentration (Howell and Tyhurst, 1976) and so the effect on viability is not expected to be high.

Even under these relatively benign conditions, HEK293 cells were found to grow significantly slower than in calcium cross-linked alginate beads (Rokstad *et al.*, 2003). Decreased cell growth was proposed to be due to increased gel strength due to stronger cross-links between Ba^{2+} and alginate, although this effect was not observed in other studies with the same cells (Visted *et al.*, 2003). In contrast, encapsulation in alginate beads cross-linked with 20mM barium did not appear to affect any of three cell lines (MDCK epithelial cell, D6 myoblast and 2A50 fibroblasts) investigated in a separate study (Peirone *et al.*, 1998).

6.3.4 Structure of beads produced using the MIG method

Alginate beads produced using the MIG method were observed to have a homogeneous distribution of alginate. Alginate beads cross-linked using internal gelation have previously been found to contain a homogeneous concentration of alginate across a bead (Quong *et al.*, 1998). SEM and confocal microscopy have also shown that beads cross-linked using internal gelation have a looser structure, with larger pores than beads produced using external gelation (Liu *et al.*, 2002). Porosity was also shown to increase in both studies.

Alginate beads produced using the MIG method are likely to have a homogeneous structure for the following two reasons. Firstly, $CaCO_3$ is homogeneously distributed throughout the alginate solution prior to droplet formation, and upon pH reduction, Ca^{2+} is liberated *in situ* throughout the bead. Therefore, a concentration gradient of alginate cannot form under these conditions. Secondly, droplets moving through a microchannel undergo velocity profile mixing, i.e. material from near the wall of the channel is re-circulated into the centre. This recirculation constantly redistributes material within a fluid droplet. Again, a gradient of alginate cannot form under these conditions.

6.3.5 Stability of beads produced using the MIG method

Calcium cross-linked alginate beads produced using the MIG method did not survive washing in phosphate buffered saline (PBS) without Ca^{2+}. Washing alginate beads in buffers which do not contain calcium is know to cause Ca^{2+} to leach from the beads thus destabilising the cross-links (Smidsrod and Skjakbraek, 1990). Barium treatment stabilised alginate beads sufficiently to enable PBS washes. Calcium cross-linked alginate beads are susceptible to phosphate treatment as Ca^{2+} is leached from

the beads, forming calcium phosphate. Many previous studies have found that barium cross-linked alginate beads are more stable than calcium cross-linked ones. Alginate beads cross-linked with 30mM barium remained intact after exposure to distilled water for three hours (Moskalenko *et al.*, 2007). Alginate beads stabilised with 1mM $BaCl_2$ in combination with 50mM $CaCl_2$ were found to be stable using the osmotic pressure test (Section 1.8.1) for 21 days after manufacture, however, addition of cells to the beads led to rapid destabilisation (Rokstad *et al.*, 2002). Non-homogeneous beads were also found to be more stable than beads with a homogeneous distribution of alginate (Rokstad *et al.*, 2003). Although the stability of alginate beads produced using the MIG method was not tested *in vitro*, it is expected that barium cross-linked beads would be more stable than calcium cross-linked beads, and that alginate beads coated with polycations would be more stable than either of these.

6.3.6 Stabilisation using secondary polycationic coating

Preliminary experiments were carried out to coat small beads, produced using the MIG method, with polycations on-chip. Calcium cross-linked alginate beads were produced using the MIG method, and a PLL solution was introduced *via* the flushing flow (Section 5.2.1, Figure 5.3). The concentration of PLL was empirically reduced to 0.025% (w/v)to form spherical beads with a secondary coating layer. The batch coating procedure usually employed utilises twice this concentration (0.05% w/v). The concentration of alginate used for the last layer was also reduced. At alginate concentrations higher than 0.075% (w/v), beads did not survive the coating procedure. Further experiments were not carried out on beads produced using the MicroPlant™ as the beads produced were too large to enter the implantation cannula (>300μm in diameter). Instead the small alginate beads used for implantation were coated using the batch method discussed below. In addition, the batch method proved to be more convenient and reproducible and the results gained were comparable to other studies. There have been no reports of secondary coating being carried out in a microfabricated device; hence, the novel method described here is the first to be reported.

A batch method was adapted from Rokstad *et al.* (2003) to coat beads produced using the MIG method with PLL and PLO. Using fluorescent PLL and confocal microscopy it was possible to show that alginate beads produced using the MIG method were successfully coated using this technique. There was some evidence

that less PLL-FITC bound to beads produced using the MIG method. Previous studies have observed that non-homogeneous beads bind slightly more PLL-FITC than homogeneous alginate beads (Thu *et al.*, 1996b). The observation that more PLL-FITC bound to calcium cross-linked alginate beads than to barium cross-linked alginate beads may be accounted for if less alginate were present at the surface of barium cross-linked beads, although evidence for this was not collected during these experiments.

By optimising the images gained using confocal microscopy, the voltage used to obtain each image was different. Therefore, the images could not be compared as the settings used to obtain each image were different. To gain images which could be analysed to obtain an estimate of the thickness of each coat, which could then be compared to each other, an alternative approach would have to be followed. The use of an internal control, such as commercially available fluorescent polystyrene beads, would allow settings to be kept consistent between samples and would even allow comparison at different time points (personal communication, Anthony Hayes).

The beads produced using the MIG method were smaller than the beads produced using the ADB method. Strand *et al.* observed that smaller (200μm) alginate beads collapsed upon treatment with low concentrations of PLL (0.05% w/v) after 5 minute exposures, whereas larger (500 μm in diameter) beads only occasionally collapsed after prolonged (>10 minutes) exposure to higher concentrations (0.1% w/v) of PLL (Strand *et al.*, 2002). Washing beads in 0.3M mannitol prior to coating with PLL was found to prevent the observed collapse of small beads. This step was not used with the beads produced for implantation, but was used with the beads produced for the experiment utilising fluorescent PLL, as the same group observed that 0.3M mannitol also helps to preserve the non-homogeneous structure of the alginate beads (Strand *et al.*, 2003).

6.3.6.1 Effect of secondary coating on encapsulated cell viability

Exposure to PLL solution is toxic to most cells (Sgouras and Duncan, 1990; Strand *et al.*, 2001), however, the protocol formulated by Lim and Sun (1980) does not appear to affect cell viability or proliferation of encapsulated cells (for example, Rokstad *et al.*, 2002). The problem with PLL coating does not seem to be one of toxicity to encapsulated cells, rather, fibrosis of tissue around implanted APA beads preventing *in vivo* survival longer than several months (De Vos *et al.*, 1993).

Although viability testing was not carried out on cells encapsulated in PLL-coated alginate beads produced during this study, there appears to be no evidence in the literature that the protocol used should be cytotoxic.

6.3.7 Implantation of beads produced using the MIG method

Small alginate beads (<350μm in diameter) coated with PLL have been implanted in various sites; rat epididymal fat pads (Robitaille *et al.*, 1999), rat portal hepatic vein (Leblond *et al.*, 1999) and lateral ventricles of the mouse brain (Ross *et al.*, 1999). All of these studies observed beads to remain intact in the implantation sites, albeit for differing time periods; from 2 weeks (Robitaille *et al.*, 1999) to 16 weeks (Ross *et al.*, 1999). In this study, small alginate beads produced using the MIG method and then cross-linked with barium *via* a batch process were implanted into rat striatum and showed some evidence of remaining 2 weeks after implantation, but not at 21 days. There was no evidence of small alginate beads coated with PLL 21 days after implantation.

Beads produced using the MIG method have been shown to consist of a homogeneous concentration of alginate (Section 6.2.2.5). All of the studies discussed above utilise non-homogeneous beads, which have a higher concentration of alginate at the surface than in the centre. The stability of homogeneous beads is known to be lower than in non-homogeneous beads (Thu *et al.*, 1996a). Smaller beads have a greater surface area to volume ratio than larger beads, thus more surface is available for reactions to take place. Thus, small beads will degrade faster than larger beads. The homogeneity of the beads, coupled with their small size, accounts for the disappearance of small beads produced using the MIG method in a short time period after implantation into rat striatum.

In summary, the MIG method was adapted to enable production of small alginate beads. Using this method cells were also encapsulated in small alginate beads. Barium treatment did not acutely affect encapsulated PC12 cells, but did appear to affect HEK293 cells, both acutely and long term. Although barium treatment appeared to affect the rate of dissolution *via* ion exchange with phosphate solutions, barium cross-linked alginate beads were not stable in a rodent brain for longer than 15 days. Alginate beads produced using the MIG method were found to have a homogeneous concentration of alginate throughout, which appears to adversely affect stability. Secondary coating of alginate beads with polycations was shown to be

possible both on-chip and using a batch method. Less PLL was shown to bind to beads produced using the MIG method, which may account for the fact that coated beads were not observed to have increased stability.

Chapter 7. General Discussion

Cell encapsulation, as a concept, was first discussed in 1964 (Chang) and first used to reverse diabetes in rats in 1980 (Lim and Sun). Since then hundreds of studies have been published which utilise cell encapsulation. Alginate is the most commonly used polymer to encapsulate cells, as it is biocompatible and biodegradable (Orive *et al.*, 2004). In addition, alginate gels can be cross-linked under physiological conditions and the reaction is not harmful to cells (Smidsrod and Skjakbraek, 1990). There are several reasons why cell encapsulation has not become the cure for many diseases that it promised to be. Among these reasons is a major problem with current production methods. Currently, methods for producing encapsulated cells are not reproducible, are only capable of producing small batches of encapsulated cells, and cannot produce beads of small diameter. If these challenges could be addressed, the field of cell encapsulation would move closer to the goal of treating a multitude of diseases.

The aims of this study were to develop and investigate a method to encapsulate viable cells in alginate utilising microfluidic techniques, evaluation of the short and long term impact of this process on cell viability, to validate the encapsulation process with therapeutically relevant cells (PC12) and determine dopamine release. In addition, modification of the microfluidic method developed in the previous steps was required to produce smaller beads suitable for cannula implantation and *in vivo* stability was determined.

At the start of this study there were very few published studies on the use of microfluidic devices to encapsulate cells. A few groups had shown that alginate solutions could be segmented within a microfabricated device to form droplets (Sugiura *et al.*, 2005; Huang *et al.*, 2006) and alginate had been ionically cross-linked on-chip (Braschler *et al.*, 2005), but there was no evidence of both droplet formation and on-chip polymer cross-linking being combined.

During the course of this study, two approaches to cross-link alginate solutions on-chip were investigated; external and internal gelation. External gelation was used to successfully produce alginate beads cross-linked on-chip. Unfortunately, the carrier fluid used was cytotoxic and so this method was unsuitable for encapsulating viable cells. By adapting a method already in use (internal gelation, Poncelet, 2001) for use

with a microfluidic circuit, viable cells were successfully encapsulated. There was some mortality of encapsulated HEK293 cells following encapsulation using this method (Chapter 4). Through minor alterations to the microfluidic internal gelation (MIG) method, therapeutic PC12 cells were successfully encapsulated with less than 20% loss of viability (Chapter 5). PC12 cells were shown to continue to produce dopamine after encapsulation. Dopamine was also able to permeate the encapsulation matrix and be detected outside the beads.

Since the start of this project several groups have successfully produced alginate beads cross-linked on-chip (Huang *et al.*, 2006; Liu *et al.*, 2006; Zhang *et al.*, 2006; Choi *et al.*, 2007; Huang *et al.*, 2007; Shintaku *et al.*, 2007; Tan and Takeuchi, 2007; Zhang *et al.*, 2007; Kim *et al.*, 2009), however, the experiments outlined in this thesis were among the first to be published (Workman *et al.*, 2007; Workman *et al.*, 2008). Attempts have been made to produce alginate beads using methods very similar to those outlined in Chapter 3, with some success (Zhang *et al.*, 2006; Tan and Takeuchi, 2007; Zhang *et al.*, 2007). Although some groups have reported the encapsulation of viable cells using microfabricated devices (Choi *et al.*, 2007; Shintaku *et al.*, 2007; Tan and Takeuchi, 2007; Kim *et al.*, 2009), there have been no studies published which show viability data for periods of more than 7 days for cells encapsulated using these techniques.

The circuits and microfluidic techniques which form this thesis are entirely novel. Not only are these techniques and circuits routinely used by the sponsoring company, Q Chip, other groups working in the field of microfluidics have also taken inspiration from these studies. Several groups have cited the publications originating from this thesis, and have based their work upon them (Kim *et al.*, 2009; Wong *et al.*, 2009).

The goal of the present study was to produce beads capable of implantation into a rodent model of Parkinson's disease. This goal was further sub-divided into two parts; production of beads <200μm in diameter and beads stable *in vivo* for more than 6 weeks.

Production of beads <200μm in diameter is problematic with most currently used techniques (Section 1.10). There is a limit to the size of nozzle which can be reproducibly manufactured and thus the size of beads which can be produced using a nozzle. In addition, although many methods can be scaled-up, this is difficult to do with devices capable of producing smaller bead diameters, as discussed in Section

1.10.3. Droplets with small diameters can be produced using microfluidic circuits by decreasing the size of the channel or increasing the flow rates of the dispersed and continuous phases, without loosing mondispersity.

By manufacturing a circuit composed of smaller channels, beads with diameters of <200μm were produced. Modifications to the processing steps carried out on cells prior to encapsulation allowed cells to be encapsulated in beads <300μm in diameter. These beads were not suitable for implantation as they were too large to fit in the implantation cannula. By further decreasing the size of the microchannels used, cells may be encapsulated in beads <200μm in the future.

Although cells were successfully encapsulated in alginate beads <300μm in diameter using the microfluidic-based method, no viability measurements were carried out due to problems with the viability methods chosen (Chapter 4). It was not possible to count cells in individual beads of diameter ~300μm using the adapted trypan blue method. Further investigations into viability using MTT assay and multiple beads would be beneficial. However, a large number of beads would be required for each time point as MTT is not sensitive enough to detect low cell numbers.

Experiments investigating growth rates of encapsulated PC12 cells and dopamine expression were carried out in large (~350μm diameter) beads (Chapter 5). Although these findings showed that the encapsulation process did not harm cells and that cell numbers could be optimised to find the best growth rate and dopamine expression, it is not known whether these would be similar in small (<200μm diameter) beads. Growth rates and dopamine expression levels would need to be determined for small beads prior to their use in an animal model.

Other groups have successfully implanted alginate beads <200μm in diameter into rats' brains. For example, APA beads were observed to remain intact within lateral ventricles of the brain for 16 weeks (Ross *et al.*, 1999). Calcium cross-linked alginate beads produced using the MIG method were not observed to survive implantation into rats' brains. Barium cross-linked alginate beads were observed to be present within sections of rats' brains 14 days after implantation. Stabilising beads using secondary polycation coating (Chapter 6) did not increase the time which beads were observed to remain intact *in vivo*. Upon further investigation it was found that beads produced using the MIG method had a homogeneous alginate density (Chapter

6). Beads of this type are known to be less stable during *in vitro* testing (Thu *et al.*, 1996a), but no studies appear to have attempted to implant beads of this kind.

Beads produced using the MIG method have an equal density of alginate throughout for two reasons; firstly, $CaCO_3$ is present throughout the droplet and so upon lowering pH Ca^{2+} is released equally throughout the bead and secondly, velocity profile mixing constantly re-circulates material throughout the droplets. These issues appear to be inherent in the production method chosen. There is some evidence that velocity profile mixing can be overcome. Zhang *et al.* have published evidence showing that by using external gelation in combination with a microfluidic device, beads with varying thickness of cross-linked alginate shells can be produced (2006).

Initial attempts to test beads produced using the MIG method for stability using the osmotic pressure test (Van Raamsdonk and Chang, 2001) were not reproducible. Beads produced on different days responded very differently and showed that the method of production and/or post-processing steps (such as washing and coating) were not repeatable. In addition, the failure of one cell encapsulation experiment (Section 4.2.3) out of four also shows that the method is not as repeatable as required. Further work on the reproducibility and repeatability of the method and post-processing steps would need to be carried out before additional information could be collected. Lack of repeatability may also explain the variability observed in the length of time beads remained intact after implantation.

The issue of stability would have to be addressed before more attempts were made to implant beads produced using the MIG method. Optimisation of the secondary coating using polycations and *in vitro* testing of the beads produced using the osmotic pressure test should be carried out. There is evidence that increasing the exposure time of alginate beads to PLL, or increasing the concentration and decreasing the MW of PLL makes alginate beads more resistant to osmotic pressure (Thu *et al.*, 1996a).

Attempts to covalently cross-link alginate beads have succeeded in increasing stability. However, only enzymes (Li *et al.*, 2007; Ortega *et al.*, 2009) and yeast cells (Birnbaum *et al.*, 1981) have been immobilised, possibly due to the toxicity of the processes involved. Improvements to stability without affecting cell viability have been made by covalently linking PLL to a photoactivatable cross-linking molecule. After bead formation, the cross-linking molecule was activated to form a covalent link between the PLL and alginate. Beads formed in this way have proved stable both *in*

vitro and *in vivo* (Dusseault *et al.*, 2005; Dusseault *et al.*, 2008). Investigations into covalent cross-linking or use of co-polymers may result in beads which are more stable and able to be produced using a microfabricated device. Use of microfluidic devices would allow cells to be exposed to toxic chemicals for minimal time periods, thus permitting further use of such chemicals.

Instead of attempting to manipulate the beads produced to make them more stable for implantation, a different use could be investigated for the beads. To see effects in a rodent model of Parkinson's disease encapsulated cells are required to persist for at least 6 weeks (Borlongan *et al.*, 2004). The beads that have been examined so far are not stable for this time period. A model where the therapeutic agent is required for a shorter time period, such as wound repair or vaccination against cancer with granulocyte-macrophage colony-stimulating factor, may be more suited to treatment through use of these beads.

Beads of small diameter can be made using microfluidic circuits. Although the batch size produced using the MIG method is currently 500µl, there is scope for increasing this considerably. Microfluidic circuits can be run in parallel with no loss of production rate. Through use of multiple parallel circuits, Nisisako and Torii (2008) estimated that a device with 128 circuits could produce 320ml of product beads per hour. The use of microfluidic techniques to encapsulate cells has considerable scope and this thesis goes some way towards showing this.

Viable, therapeutic cells were encapsulated in alginate beads and were still able to produce therapeutic agent. Various post-processing steps were introduced on-chip and in this way washing, coating and barium stabilisation of alginate beads has been demonstrated. The beads produced were not stable enough to allow behavioural changes to be observed in a rodent model of Parkinson's disease. However, further work suggested may allow this to be achieved in the future.

Aebischer, P., Tresco, P. A., Winn, S. R., Greene, L. A. and Jaeger, C. B. (1991a). "Long-term cross-species brain transplantation of a polymer-encapsulated dopamine-secreting cell line." Experimental Neurology **111**(3): 269-75.

Aebischer, P., Winn, S. R., Tresco, P. A., Jaeger, C. B. and Greene, L. A. (1991b). "Transplantation of polymer encapsulated neurotransmitter secreting cells: effect of the encapsulation technique." Journal of Biomechanical Engineering, Transactions of the ASME **113**(2): 178-83.

Ahmed, S. A., Gogal, R. M., Jr. and Walsh, J. E. (1994). "A new rapid and simple non-radioactive assay to monitor and determine the proliferation of lymphocytes: an alternative to [3H]thymidine incorporation assay." Journal of Immunological Methods **170**(2): 211-24.

Akers, M. J., Larrimore, D. S. and Morton Guazzo, D. (2002). Parenteral quality control: sterility, pyrogen, particulate, and package integrity testing. New York, Informa Health Care.

Al-Musa, S., Abu Fara, D. and Badwan, A. A. (1999). "Evaluation of parameters involved in preparation and release of drug loaded in crosslinked matrices of alginate." Journal of Controlled Release **57**(3): 223-32.

Aloisi, F. (2001). "Immune function of microglia." Glia **36**(2): 165-79.

Altman, P. L. and Dittmer, D. S. (1974). Biology Data Book Washington D.C., Federation of American Societies for Experimental Biology.

Amaral, K. F., Rogero, M. M., Fock, R. A., Borelli, P. and Gavini, G. (2007). "Cytotoxicity analysis of EDTA and citric acid applied on murine resident macrophages culture." International Endodontic Journal **40**(5): 338-43.

Amici, E., Tetradis-Meris, G., de Torres, C. P. and Jousse, F. (2008). "Alginate gelation in microfluidic channels." Food Hydrocolloids **22**(1): 97-104.

Andlin-Sobocki, P., Jonsson, B., Wittchen, H. U. and Olesen, J. (2005). "Cost of disorders of the brain in Europe." European Journal of Neurology **12 Suppl 1**: 1-27.

Ando, T., Yamazoe, H., Moriyasu, K., Ueda, Y. and Iwata, H. (2007). "Induction of dopamine-releasing cells from primate embryonic stem cells enclosed in agarose microcapsules." Tissue Engineering **13**(10): 2539-47.

Anna, S. L., Bontoux, N. and Stone, H. A. (2003). "Formation of dispersions using "flow focusing" in microchannels." Applied Physics Letters **82**(3): 364-366.

Atencia, J. and Beebe, D. J. (2005). "Controlled microfluidic interfaces." Nature **437**(7059): 648-55.

Baldwin, S. P. and Saltzman, W. M. (2001). "Aggregation enhances catecholamine secretion in cultured cells." Tissue Engineering **7**(2): 179-190.

Barker, C. F. and Billingham, R. E. (1977). "Immunologically privileged sites." Advances in Immunology **25**: 1-54.

Barros, L. F., Castro, J. and Bittner, C. X. (2002). "Ion movements in cell death: from protection to execution." Biological Research **35**(2): 209-14.

Barrow, D. A., Harries, N., Jones, T. G. and Bouris, K. (2002) "Microfluidic Device & Methods for Construction & Application." UK WO/2004/043598.

Barsoum, S. C., Milgram, W., Mackay, W., Coblentz, C., Delaney, K. H., Kwiecien, J. M., Kruth, S. A. and Chang, P. L. (2003). "Delivery of recombinant gene product to canine brain with the use of microencapsulation." Journal of Laboratory and Clinical Medicine **142**(6): 399-413.

Beebe, D. J., Mensing, G. A. and Walker, G. M. (2002). "Physics and applications of microfluidics in biology." Annual Review of Biomedical Engineering **4**: 261-86.

Bencherif, S. A., Srinivasan, A., Sheehan, J. A., Walker, L. M., Gayathri, C., Gil, R., Hollinger, J. O., Matyjaszewski, K. and Washburn, N. R. (2009). "End-group effects on the properties of PEG-co-PGA hydrogels." Acta Biomaterialia **5**(6): 1872-1883.

Bernheimer, H., Birkmayer, W. and Hornykiewicz, O. (1973). "Brain dopamine and the syndromes of Parkinson and Huntington. Clinical, morphological and neurochemical correlations." Journal of the Neurological Sciences **20**(4): 415-455.

Birnbaum, S., Pendleton, R., Larsson, P. O. and Mosbach, K. (1981). "Covalent Stabilization of Alginate Gel for the Entrapment of Living Whole Cells." Biotechnology Letters **3**(8): 393-400.

Blusch, J. H., Patience, C. and Martin, U. (2002). "Pig endogenous retroviruses and xenotransplantation." Xenotransplantation **9**(4): 242-51.

Borlongan, C. V., Skinner, S. J., Geaney, M., Vasconcellos, A. V., Elliott, R. B. and Emerich, D. F. (2004). "Neuroprotection by encapsulated choroid plexus in a rodent model of Huntington's disease." Neuroreport **15**(16): 2521-5.

Borlongan, C. V., Thanos, C. G., Skinner, S. J., Geaney, M. and Emerich, D. F. (2008). "Transplants of encapsulated rat choroid plexus cells exert neuroprotection in a rodent model of Huntington's disease." Cell Transplantation **16**(10): 987-92.

Braccini, I. and Perez, S. (2001). "Molecular basis of C(2+)-induced gelation in alginates and pectins: the egg-box model revisited." Biomacromolecules **2**(4): 1089-96.

Brandenberger, H. and Widmer, F. (1998). "A new multinozzle encapsulation/immobilisation system to produce uniform beads of alginate." Journal of Biotechnology **63**(1): 73-80.

Braschler, T., Johann, R., Heule, M., Metref, L. and Renaud, P. (2005). "Gentle cell trapping and release on a microfluidic chip by in situ alginate hydrogel formation." Lab on a Chip **5**(5): 553-9.

Brendel, M., Hering, B., Schulz, A. and Bretzel, R. (1999). International Islet Tranplant Registry report. Giessen, Germany, University of Giessen: 1-20.

Brody, J. P., Yager, P., Goldstein, R. E. and Austin, R. H. (1996). "Biotechnology at low Reynolds numbers." Biophysical Journal **71**(6): 3430-3441.

Brushett, F. R., Zhou, W. P., Jayashree, R. S. and Kenis, P. J. A. (2009). "Alkaline Microfluidic Hydrogen-Oxygen Fuel Cell as a Cathode Characterization Platform." Journal of the Electrochemical Society **156**(5): B565-B571.

Burek, C. J., Burek, M., Roth, J. and Los, M. (2003). "Calcium induces apoptosis and necrosis in hematopoetic malignant cells: Evidence for caspase-8 dependent and FADD-autonomous pathway." Gene Therapy and Molecular Biology **7**: 173-179.

Cajal, S. R. Y. (1928). Degeneration and regeneration of the nervous system. Oxford, Oxford University Press.

Calafiore, R., Basta, G., Luca, G., Calvitti, M., Calabrese, G., Racanicchi, L., Macchiarulo, G., Mancuso, F., Guido, L. and Brunetti, P. (2004). "Grafts of microencapsulated pancreatic islet cells for the therapy of diabetes mellitus in non-immunosuppressed animals." Biotechnology and Applied Biochemistry **39**(Pt 2): 159-64.

Calafiore, R., Basta, G., Luca, G., Lemmi, A., Montanucci, M. P., Calabrese, G., Racanicchi, L., Mancuso, F. and Brunetti, P. (2006). "Microencapsulated

Pancreatic Islet Allografts Into Nonimmunosuppressed Patients With Type 1 Diabetes: First two cases." Diabetes Care **29**(1): 137-138.

Capretto, L., Mazzitelli, S., Balestra, C., Tosi, A. and Nastruzzi, C. (2008). "Effect of the gelation process on the production of alginate microbeads by microfluidic chip technology." Lab on a Chip **8**(4): 617-21.

Cellesi, F. and Tirelli, N. (2005). "A new process for cell microencapsulation and other biomaterial applications: Thermal gelation and chemical cross-linking in "tandem"." Journal of Materials Science. Materials in Medicine **16**(6): 559-65.

Chabert, M. and Viovy, J. L. (2008). "Microfluidic high-throughput encapsulation and hydrodynamic self-sorting of single cells." Proceedings of the National Academy of Sciences of the United States of America **105**(9): 3191-6.

Chalfie, M., Tu, Y., Euskirchen, G., Ward, W. W. and Prasher, D. C. (1994). "Green fluorescent protein as a marker for gene expression." Science **263**(5148): 802-5.

Chang, T. M. S. (1964). "Semipermeable microcapsules." Science **146**: 524-525.

Chicheportiche, D. and Reach, G. (1988). "In vitro kinetics of insulin release by microencapsulated rat islets: effect of the size of the microcapsules." Diabetologia **31**(1): 54-7.

Chinn, J. A., Horbett, T. A., Ratner, B. D., Schway, M. B., Haque, Y. and Hauschka, S. D. (1989). "Enhancement of serum fibronectin adsorption and the clonal plating efficiencies of Swiss mouse 3T3 fibroblast and MM14 mouse myoblast cells on polymer substrates modified by radiofrequency plasma deposition." Journal of Colloid and Interface Science **127**(1): 67-87.

Choi, B. H., Woo, J. I., Min, B. H. and Park, S. R. (2006). "Low-intensity ultrasound stimulates the viability and matrix gene expression of human articular chondrocytes in alginate bead culture." Journal of Biomedical Materials Research. Part A **79**(4): 858-64.

Choi, C. H., Jung, J. H., Rhee, Y. W., Kim, D. P., Shim, S. E. and Lee, C. S. (2007). "Generation of monodisperse alginate microbeads and in situ encapsulation of cell in microfluidic device." Biomedical Microdevices. **9**(6): 855-62.

Choi, D. W. (1992). "Excitotoxic cell death." Journal of Neurobiology **23**(9): 1261-76.

Choonara, Y. E., Pillay, V., Singh, N., Khan, R. A. and Ndesendo, V. M. K. (2008). "Chemometric, physicomechanical and rheological analysis of the sol-gel dynamics and degree of crosslinking of glycosidic polymers." Biomedical Materials **3**(2).

Christopher, G. F. and Anna, S. L. (2007). "Microfluidic methods for generating continuous droplet streams." Journal of Physics D-Applied Physics **40**: R319-R336.

Clausell-Tormos, J., Lieber, D., Baret, J. C., El-Harrak, A., Miller, O. J., Frenz, L., Blouwolff, J., Humphry, K. J., Koster, S., Duan, H., Holtze, C., Weitz, D. A., Griffiths, A. D. and Merten, C. A. (2008). "Droplet-based microfluidic platforms for the encapsulation and screening of mammalian cells and multicellular organisms." Chemistry & Biology **15**(5): 427-437.

Constantinidis, I., Rask, I., Long, R. C., Jr. and Sambanis, A. (1999). "Effects of alginate composition on the metabolic, secretory, and growth characteristics of entrapped beta TC3 mouse insulinoma cells." Biomaterials **20**(21): 2019-27.

Coward, S. M., Selden, C., Mantalaris, A. and Hodgson, H. J. F. (2005). "Proliferation Rates of HepG2 Cells Encapsulated in Alginate Are Increased in a

Microgravity Environment Compared With Static Cultures." Artificial Organs **29**(2): 152-158.

Cramer, C., Fischer, P. and Windhab, E. J. (2004). "Drop formation in a co-flowing ambient fluid." Chemical Engineering Science **59**: 3045-3058.

Crowley, T. A. and Pizziconi, V. (2005). "Isolation of plasma from whole blood using planar microfilters for lab-on-a-chip applications." Lab on a Chip **5**(9): 922-9.

Darrabie, M. D., Kendall, W. F., Jr. and Opara, E. C. (2005). "Characteristics of Poly-L-Ornithine-coated alginate microcapsules." Biomaterials **26**(34): 6846-52.

Davies, R. H., Palmer, D. D. and Workman, V. L. (2005) "Device and method for the control of chemical processes." UK Application GB0525951.0. 20 December 2005

Davson, H. (1967). Physiology of the Cerebrospinal Fluid. London, J. & A. Churchill, Ltd.

De Geest, B. G., Urbanski, J. P., Thorsen, T., Demeester, J. and De Smedt, S. C. (2005). "Synthesis of monodisperse biodegradable microgels in microfluidic devices." Langmuir **21**(23): 10275-9.

de Vos, P., de Haan, B., Wolters, G. H. and Van Schilfgaarde, R. (1996). "Factors influencing the adequacy of microencapsulation of rat pancreatic islets." Transplantation **62**(7): 888-93.

de Vos, P., de Haan, B. J., Wolters, G. H., Strubbe, J. H. and Van Schilfgaarde, R. (1997). "Improved biocompatibility but limited graft survival after purification of alginate for microencapsulation of pancreatic islets." Diabetologia **40**(3): 262-70.

de Vos, P., Faas, M. M., Strand, B. and Calafiore, R. (2006). "Alginate-based microcapsules for immunoisolation of pancreatic islets." Biomaterials **27**(32): 5603-17.

de Vos, P., Van Straaten, J. F., Nieuwenhuizen, A. G., de Groot, M., Ploeg, R. J., De Haan, B. J. and Van Schilfgaarde, R. (1999). "Why do microencapsulated islet grafts fail in the absence of fibrotic overgrowth?" Diabetes **48**(7): 1381-8.

de Vos, P., Wolters, G. H., Fritschy, W. M. and Van Schilfgaarde, R. (1993). "Obstacles in the application of microencapsulation in islet transplantation." International Journal of Artificial Organs **16**(4): 205-12.

de Vos, P., Wolters, G. H. and van Schilfgaarde, R. (1994). "Possible relationship between fibrotic overgrowth of alginate-polylysine-alginate microencapsulated pancreatic islets and the microcapsule integrity." Transplantation Proceedings **26**(2): 782-3.

Decker, T. and Lohmannmatthes, M. L. (1988). "A Quick and Simple Method for the Quantitation of Lactate-Dehydrogenase Release in Measurements of Cellular Cyto-Toxicity and Tumor Necrosis Factor (Tnf) Activity." Journal of Immunological Methods **115**: 61-69.

Desmangles, A. I., Jordan, O. and Marquis-Weible, F. (2001). "Interfacial photopolymerization of beta-cell clusters: approaches to reduce coating thickness using ionic and lipophilic dyes." Biotechnology and Bioengineering **72**(6): 634-41.

Dusseault, J., Langlois, G., Meunier, M. C., Menard, M., Perreault, C. and Halle, J. P. (2008). "The effect of covalent cross-links between the membrane components of microcapsules on the dissemination of encapsulated malignant cell." Biomaterials **29**(7): 917-924.

Dusseault, J., Leblond, F. A., Robitaille, R., Jourdan, G., Tessier, J., Menard, M., Henley, N. and Halle, J. P. (2005). "Microencapsulation of living cells in

semi-permeable membranes with covalently cross-linked layers." Biomaterials **26**(13): 1515-1522.

Duvivier-Kali, V. F., Omer, A., Lopez-Avalos, M. D., O'Neil, J. J. and Weir, G. C. (2004). "Survival of microencapsulated adult pig islets in mice in spite of an antibody response." American Journal of Transplantation Surgeons **4**(12): 1991-2000.

Edd, J. F., Di Carlo, D., Humphry, K. J., Koster, S., Irimia, D., Weitz, D. A. and Toner, M. (2008). "Controlled encapsulation of single-cells into monodisperse picolitre drops." Lab on a Chip **8**(8): 1262-4.

Ehringer, H. and Hornykiewicz, O. (1998). "Distribution of noradrenaline and dopamine (3-hydroxytyramine) in the human brain and their behavior in diseases of the extrapyramidal system." Parkinsonism Relat Disord **4**(2): 53-7.

Elliott, R. B., Escobar, L., Tan, P. L., Muzina, M., Zwain, S. and Buchanan, C. (2007). "Live encapsulated porcine islets from a type 1 diabetic patient 9.5 yr after xenotransplantation." Xenotransplantation **14**(2): 157-61.

Ezekowitz, R. A., Sim, R. B., Hill, M. and Gordon, S. (1984). "Local opsonization by secreted macrophage complement components. Role of receptors for complement in uptake of zymosan." Journal of Experimental Medicine **159**(1): 244-60.

Fiszman, G. L., Karara, A. L., Finocchiaro, L. M. E. and Glikin, G. C. (2002). "A laboratory scale device for microencapsulation of genetically engineered cells into alginate beads." Electronic Journal of Biotechnology **5**(3).

Folkman, J. and Moscona, A. (1978). "Role of cell shape in growth control." Nature **273**(5661): 345-9.

Freed, C. R., Greene, P. E., Breeze, R. E., Tsai, W. Y., DuMouchel, W., Kao, R., Dillon, S., Winfield, H., Culver, S., Trojanowski, J. Q., Eidelberg, D. and Fahn, S. (2001). "Transplantation of embryonic dopamine neurons for severe Parkinson's disease." New England Journal of Medicine **344**(10): 710-9.

Fritschy, W. M., Wolters, G. H. and van Schilfgaarde, R. (1991). "Effect of alginate-polylysine-alginate microencapsulation on in vitro insulin release from rat pancreatic islets." Diabetes **40**(1): 37-43.

Fundueanu, G., Nastruzzi, C., Carpov, A., Desbrieres, J. and Rinaudo, M. (1999). "Physico-chemical characterization of Ca-alginate microparticles produced with different methods." Biomaterials **20**(15): 1427-1435.

Gansbacher, B. (2002). "Policy statement on the social, ethical and public awareness issues in gene therapy." Journal of Gene Medicine **4**(6): 687-91.

Gaserod, O., Sannes, A. and Skjak-Braek, G. (1999). "Microcapsules of alginate-chitosan. II. A study of capsule stability and permeability." Biomaterials **20**(8): 773-83.

Gaserod, O., Smidsrod, O. and Skjak-Braek, G. (1998). "Microcapsules of alginate-chitosan--I. A quantitative study of the interaction between alginate and chitosan." Biomaterials **19**(20): 1815-25.

Gash, D. M., Notter, M. F., Okawara, S. H., Kraus, A. L. and Joynt, R. J. (1986). "Amitotic neuroblastoma cells used for neural implants in monkeys." Science **233**(4771): 1420-2.

Gentile, F. T., Doherty, E. J., Rein, D. H., Shoichet, M. S. and Winn, S. R. (1995). "Polymer Science for Macroencapsulation of Cells for Central-Nervous-System Transplantation." Reactive Polymers **25**(2-3): 207-227.

Gilman, A. G. (2001). Pharmacological Basis of Therapeutics New York : McGraw-Hill.

Gomez, N., Chen, S. C. and Schmidt, C. E. (2007). "Polarization of hippocampal neurons with competitive surface stimuli: contact guidance cues are preferred over chemical ligands." Journal of the Royal Society Interface **4**(13): 223-233.

Götze, O., Müller-eberhard, H. J. and Frank, J. D. a. H. G. K. (1976). The Alternative Pathway of Complement Activation. Advances in Immunology, Academic Press. **Volume 24:** 1-35.

Greene, L. A. and Rein, G. (1977). "Release, Storage and Uptake of Catecholamines by a Clonal Cell Line of Nerve Growth-Factor (Ngf) Responsive Pheochromocytoma Cells." Brain Research **129**(2): 247-263.

Greene, L. A. and Tischler, A. S. (1976). "Establishment of a noradrenergic clonal line of rat adrenal pheochromocytoma cells which respond to nerve growth factor." Proceedings of the National Academy of Sciences of the United States of America **73**(7): 2424-8.

Haque, T., Chen, H., Ouyang, W., Martoni, C., Lawuyi, B., Urbanska, A. M. and Prakash, S. (2005). "In vitro study of alginate-chitosan microcapsules: an alternative to liver cell transplants for the treatment of liver failure." Biotechnology Letters **27**(5): 317-22.

Hart, P. H., Spencer, L. K., Nikoloutsopoulos, A., Lopez, A. F., Vadas, M. A., McDonald, P. J. and Finlay-Jones, J. J. (1986). "Role of cell surface receptors in the regulation of intracellular killing of bacteria by murine peritoneal exudate neutrophils." Infection and Immunity **52**(1): 245-51.

He, M. Y., Edgar, J. S., Jeffries, G. D. M., Lorenz, R. M., Shelby, J. P. and Chiu, D. T. (2005). "Selective encapsulation of single cells and subcellular organelles into picoliter- and femtoliter-volume droplets." Analytical Chemistry **77**(6): 1539-1544.

Hersel, U., Dahmen, C. and Kessler, H. (2003). "RGD modified polymers: biomaterials for stimulated cell adhesion and beyond." Biomaterials **24**(24): 4385-4415.

Hong, J. S., Shin, S. J., Lee, S., Wong, E. and Cooper-White, J. (2007). "Spherical and cylindrical microencapsulation of living cells using microfluidic devices." Korea-Australia Rheology Journal **19**(3): 157-164.

Howell, S. L. and Tyhurst, M. (1976). "Barium accumulation in rat pancreatic B cells." Journal of Cell Science **22**(2): 455-65.

Huang, K. S., Lai, T. H. and Lin, Y. C. (2006). "Manipulating the generation of Ca-alginate microspheres using microfluidic channels as a carrier of gold nanoparticles." Lab on a Chip **6**(7): 954-7.

Huang, K. S., Lai, T. H. and Lin, Y. C. (2007). "Using a microfluidic chip and internal gelation reaction for monodisperse calcium alginate microparticles generation." Frontiers in Bioscience **12**: 3061-7.

Jaeger, C. B. (1985). "Immunocytochemical study of PC12 cells grafted to the brain of immature rats." Experimental Brain Research **59**(3): 615-24.

Kampf, N. (2002). "The Use of Polymers for Coating of Cells." Polymers for Advanced Technologies **13**: 896-905.

Kelly, G. (1824). "Appearances observed in the dissection of two individuals; death from cold and congestion of the brain." Transactions of the Medical Chirurgical Society Edinburgh **1**: 84-169.

Khattak, S. F., Spatara, M., Roberts, L. and Roberts, S. C. (2006). "Application of colorimetric assays to assess viability, growth and metabolism of hydrogel-encapsulated cells." Biotechnology Letters **28**(17): 1361-70.

Kim, C., Lee, K. S., Kim, Y. E., Lee, K. J., Lee, S. H., Kim, T. S. and Kang, J. Y. (2009). "Rapid exchange of oil-phase in microencapsulation chip to enhance cell viability." Lab on a Chip **9**(9): 1294-1297.

King, A., Sandler, S. and Andersson, A. (2001a). "The effect of host factors and capsule composition on the cellular overgrowth on implanted alginate capsules." Journal of Biomedical Materials Research **57**(3): 374-83.

King, A., Strand, B., Rokstad, A. M., Kulseng, B., Andersson, A., Skjak-Braek, G. and Sandler, S. (2003). "Improvement of the biocompatibility of alginate/poly-L-lysine/alginate microcapsules by the use of epimerized alginate as a coating." Journal of Biomedical Materials Research. Part A **64**(3): 533-9.

King, S. R., Dorian, R. and Storrs, R. W. (2001b). "Requirements for Encapsulation Technology and the Challenges for Transplantation of Islets of Langerhans " Graft **4**(7): 491-499.

Knopf, P. M., Cserr, H. F., Nolan, S. C., Wu, T. Y. and Harling-Berg, C. J. (1995). "Physiology and immunology of lymphatic drainage of interstitial and cerebrospinal fluid from the brain." Neuropathology and Applied Neurobiology **21**(3): 175-80.

Koch, S., Schwinger, C., Kressler, J., Heinzen, C. and Rainov, N. G. (2003). "Alginate encapsulation of genetically engineered mammalian cells: comparison of production devices, methods and microcapsule characteristics." Journal of Microencapsulation **20**(3): 303-16.

Koester, S., Angile, F. E., Duan, H., Agresti, J. J., Wintner, A., Schmitz, C., Rowat, A. C., Merten, C. A., Pisignano, D., Griffiths, A. D. and Weitz, D. A. (2008). "Drop-based microfluidic devices for encapsulation of single cells." Lab on a Chip **8**(7): 1110-1115.

Kordower, J. H., Liu, Y. T., Winn, S. and Emerich, D. F. (1995). "Encapsulated PC12 cell transplants into hemiparkinsonian monkeys: a behavioral, neuroanatomical, and neurochemical analysis." Cell Transplant **4**(2): 155-71.

Kuijlen, J. M., de Haan, B. J., Helfrich, W., de Boer, J. F., Samplonius, D., Mooij, J. J. and de Vos, P. (2006). "The efficacy of alginate encapsulated CHO-K1 single chain-TRAIL producer cells in the treatment of brain tumors." Journal of Neuro-oncology **78**(1): 31-9.

Kulseng, B., B. Thu, Espevik, T. and Skjakbraek, G. (1997). "Alginate polylysine microcapsules as immune barrier: permeability of cytokines and immunoglobulins over the capsule membrane." Cell Transplant **6**(4): 387-94.

Kwack, K. and Lynch, R. G. (2000). "A new non-radioactive method for IL-2 bioassay." Molecules and Cells **10**(5): 575-8.

Lacik, I. (2006). "Polymer chemistry in diabetes treatment by encapsulated islets of Langerhans: Review to 2006." Australian Journal of Chemistry **59**(8): 508-524.

Lahooti, S. and Sefton, M. V. (2000). "Effect of an immobilization matrix and capsule membrane permeability on the viability of encapsulated HEK cells." Biomaterials **21**(10): 987-95.

Lanza, R. P., Kuhtreiber, W. M., Ecker, D., Staruk, J. E. and Chick, W. L. (1995). "Xenotransplantation of porcine and bovine islets without immunosuppression using uncoated alginate microspheres." Transplantation **59**(10): 1377-84.

Larisch, B. C., Poncelet, D., Champagne, C. P. and Neufeld, R. J. (1994). "Microencapsulation of Lactococcus lactis subsp. cremoris." Journal of Microencapsulation **11**(2): 189-95.

Leblond, F. A., Simard, G., Henley, N., Rocheleau, B., Huet, P. M. and Halle, J. P. (1999). "Studies on smaller (approximately 315 microM) microcapsules: IV. Feasibility and safety of intrahepatic implantations of small alginate poly-L-lysine microcapsules." Cell Transplant **8**(3): 327-37.

Legrand, C., Bour, J. M., Jacob, C., Capiaumont, J., Martial, A., Marc, A., Wudtke, M., Kretzmer, G., Demangel, C., Duval, D. and Hache, J. (1992). "Lactate dehydrogenase (LDH) activity of cultured eukaryotic cells as marker of the number of dead cells in the medium." Journal of Biotechnology **25**(3): 231-243.

Lencki, R. W. J., Neufeld, R. J. and Spinney, T. (1989) "Method of producing microspheres." US 4822534.

LeRoux, M. A., Guilak, F. and Setton, L. A. (1999). "Compressive and shear properties of alginate gel: effects of sodium ions and alginate concentration." Journal of Biomedical Materials Research **47**(1): 46-53.

Levitt, M., Spector, S., Sjoerdsma, A. and Udenfriend, S. (1965). "Elucidation of the Rate-Limiting Step in Norepinephrine Biosynthesis in the Perfused Guinea-Pig Heart." Journal of Pharmacology and Experimental Therapeutics **148**: 1-8.

Lewis, G. N. (1923). Valence and the Struture of Molecules. New York, The Chemical Catalogue Company.

Li, T. P., Wang, N., Li, S. H., Zhao, Q. C., Guo, M. and Zhang, C. Y. (2007). "Optimization of covalent immobilization of pectinase on sodium alginate support." Biotechnology Letters **29**(9): 1413-1416.

Lim, F. and Sun, A. M. (1980). "Microencapsulated islets as bioartificial endocrine pancreas." Science **210**(4472): 908-10.

Lindvall, O., Widner, H., Rehncrona, S., Brundin, P., Odin, P., Gustavii, B., Frackowiak, R., Leenders, K. L., Sawle, G., Rothwell, J. C. and et al. (1992). "Transplantation of fetal dopamine neurons in Parkinson's disease: one-year clinical and neurophysiological observations in two patients with putaminal implants." Annals of Neurology **31**(2): 155-65.

Liszewski, M. K., Farries, T. C., Lublin, D. M., Rooney, I. A. and Atkinson, J. P. (1996). "Control of the complement system." Advances in Immunology **61**: 201-83.

Liu, H. W., Ofosu, F. A. and Chang, P. L. (1993). "Expression of human factor IX by microencapsulated recombinant fibroblasts." Human Gene Therapy **4**(3): 291-301.

Liu, K., Ding, H. J., Liu, J., Chen, Y. and Zhao, X. Z. (2006). "Shape-controlled production of biodegradable calcium alginate gel microparticles using a novel microfluidic device." Langmuir **22**(22): 9453-7.

Liu, X. D., Yu, W. Y., Zhang, Y., Xue, W. M., Yu, W. T., Xiong, Y., Ma, X. J., Chen, Y. and Yuan, Q. (2002). "Characterization of structure and diffusion behaviour of Ca-alginate beads prepared with external or internal calcium sources." Journal of Microencapsulation **19**(6): 775-82.

Lombardi, G. and Lechler, R. (1991). "The molecular basis of allorecognition of major histocompatibility complex molecules by T lymphocytes." Annali dell'Istituto Superiore di Sanità **27**(1): 7-14.

Lucas, C. A., Edgar, D. and Thoenen, H. (1979). "Regulation of tyrosine hydroxylase and choline acetyltransferase activities by cell density in the PC12 rat pheochromocytoma clonal cell line." Experimental Cell Research **121**(1): 79-86.

Lundberg, C., Field, P. M., Ajayi, Y. O., Raisman, G. and Bjorklund, A. (1996). "Conditionally immortalized neural progenitor cell lines integrate and differentiate after grafting to the adult rat striatum. A combined autoradiographic and electron microscopic study." Brain Research **737**(1-2): 295-300.

Macknight, A. D. (1988). "Principles of cell volume regulation." Renal Physiology and Biochemistry **11**(3-5): 114-41.

Martinsen, A., Skjak-Braek, G. and Smidsrod, O. (1989). "Alginate as immobilization material: I. Correlation between chemical and physical properties of alginate gel beads." Biotechnology and Bioengineering **33**(1): 79-89.

Martinsen, A., Storro, I. and Skjark-Braek, G. (1992). "Alginate as immobilization material: III. Diffusional properties." Biotechnology and Bioengineering **39**(2): 186-194.

Maruyama, T., Matsushita, H., Uchida, J., Kubota, F., Kamiya, N. and Goto, M. (2004). "Liquid membrane operations in a microfluidic device for selective separation of metal ions." Analytical Chemistry **76**(15): 4495-500.

Mayeux, R. (2003). "Epidemiology of neurodegeneration." Annual Review of Neuroscience **26**: 81-104.

McGuigan, A. P., D. A. Bruzewicz, A. Glavan, M. J. Butte and G. M. Whitesides (2008). "Cell encapsulation in sub-mm sized gel modules using replica molding." PLoS One **3**(5): e2258.

McRae, A., Hjorth, S., Mason, D., Dillon, L. and Tice, T. (1990). "Implantable microencapsulated dopamine (DA): prolonged functional release of DA in denervated striatal tissue." Journal of Neural Transmission Supplement **29**: 207-15.

Mendez, I., Vinuela, A., Astradsson, A., Mukhida, K., Hallett, P., Robertson, H., Tierney, T., Holness, R., Dagher, A., Trojanowski, J. Q. and Isacson, O. (2008). "Dopamine neurons implanted into people with Parkinson's disease survive without pathology for 14 years." Nature Medicine **14**(5): 507-9.

Miyoshi, Y., Date, I., Ohmoto, T. and Iwata, H. (1996). "Histological analysis of microencapsulated dopamine-secreting cells in agarose/poly(styrene sulfonic acid) mixed gel xenotransplanted into the brain." Experimental Neurology **138**(1): 169-75.

Mohamed, H., McCurdy, L. D., Szarowski, D. H., Duva, S., Turner, J. N. and Caggana, M. (2004). "Development of a rare cell fractionation device: application for cancer detection." IEEE Transactions on Nanobioscience **3**(4): 251-6.

Monro, A. (1783). Observations on the structure and function of the nervous system. Edingburgh, Creech & Johnson.

Morch, Y. A., Donati, I., Strand, B. L. and Skjak-Braek, G. (2006). "Effect of Ca2+, Ba2+, and Sr2+ on alginate microbeads." Biomacromolecules **7**(5): 1471-80.

Moskalenko, V., Ulrichs, K., Kerscher, A., Blind, E., Otto, C., Hamelmann, W., Demidchik, Y. and Timm, S. (2007). "Preoperative evaluation of microencapsulated human parathyroid tissue aids selection of the optimal bioartificial graft for human parathyroid allotransplantation." Transplant International **20**(8): 688-96.

Mosmann, T. (1983). "Rapid colorimetric assay for cellular growth and survival: application to proliferation and cytotoxicity assays." Journal of Immunological Methods **65**(1-2): 55-63.

Murphy, K. M., Travers, P. and Walport, M. (2007). Janeway's Immunobiology. London, Garland Science.

Murua, A., de Castro, M., Orive, G., Hernandez, R. M. and Pedraz, J. L. (2007). "In vitro characterization and in vivo functionality of erythropoietin-secreting cells immobilized in alginate-poly-L-lysine-alginate microcapsules." Biomacromolecules **8**(11): 3302-7.

Nedovic, V. and Willaert, R. (2004). Fundamentals of cell immobilisation biotechnology London, Dordrecht.

Nikkhah, G., Olsson, M., Eberhard, J., Bentlage, C., Cunningham, M. G. and Bjorklund, A. (1994). "A microtransplantation approach for cell suspension grafting in the rat Parkinson model: a detailed account of the methodology." Neuroscience **63**(1): 57-72.

Nisisako, T. and Torii, T. (2008). "Microfluidic large-scale integration on a chip for mass production of monodisperse droplets and particles." Lab on a Chip **8**(2): 287-93.

O'Donovan, P., Perrett, C. M., Zhang, X., Montaner, B., Xu, Y. Z., Harwood, C. A., McGregor, J. M., Walker, S. L., Hanaoka, F. and Karran, P. (2005). "Azathioprine and UVA light generate mutagenic oxidative DNA damage." Science **309**(5742): 1871-4.

Ogbonna, J. C., Matsumura, M. and Kataoka, H. (1991). "Effective oxygenation of immobilized cells through reduction in bead diameters: a review." Process Biochemistry **26**(2): 109-121.

Olanow, C. W., Goetz, C. G., Kordower, J. H., Stoessl, A. J., Sossi, V., Brin, M. F., Shannon, K. M., Nauert, G. M., Perl, D. P., Godbold, J. and Freeman, T. B. (2003). "A double-blind controlled trial of bilateral fetal nigral transplantation in Parkinson's disease." Annals of Neurology **54**(3): 403-414.

Olson, L., Backlund, E. O., Ebendal, T., Freedman, R., Hamberger, B., Hansson, P., Hoffer, B., Lindblom, U., Meyerson, B., Stromberg, I. and et al. (1991). "Intraputaminal infusion of nerve growth factor to support adrenal medullary autografts in Parkinson's disease. One-year follow-up of first clinical trial." Archives of Neurology **48**(4): 373-81.

Omer, A., Duvivier-Kali, V., Fernandes, J., Tchipashvili, V., Colton, C. K. and Weir, G. C. (2005). "Long-term normoglycemia in rats receiving transplants with encapsulated islets." Transplantation **79**(1): 52-8.

Orive, G., Hernandez, R. M., Gascon, A. R., Calafiore, R., Chang, T. M., De Vos, P., Hortelano, G., Hunkeler, D., Lacik, I., Shapiro, A. M. and Pedraz, J. L. (2003). "Cell encapsulation: promise and progress." Nature Medicine **9**(1): 104-7.

Orive, G., Hernandez, R. M., Rodriguez Gascon, A., Calafiore, R., Chang, T. M., de Vos, P., Hortelano, G., Hunkeler, D., Lacik, I. and Pedraz, J. L. (2004). "History, challenges and perspectives of cell microencapsulation." Trends in Biotechnology **22**(2): 87-92.

Orive, G., De Castro, M., Kong, H. J., Hernandez, R. M., Ponce, S., Mooney, D. J. and Pedraz, J. L. (2009). "Bioactive cell-hydrogel microcapsules for cell-based drug delivery." J Control Release **135**(3): 203-10.

Ortega, N., Perez-Mateos, M., Pilar, M. C. and Busto, M. D. (2009). "Neutrase Immobilization on Alginate-Glutaraldehyde Beads by Covalent Attachment." Journal of Agricultural and Food Chemistry **57**(1): 109-115.

Palmieri, A., Ley, S. V., Hammond, K., Polyzos, A. and Baxendale, I. R. (2009). "A microfluidic flow chemistry platform for organic synthesis: the Hofmann rearrangement." Tetrahedron Letters **50**(26): 3287-3289.

Parekh, D. B., Katso, R. M., Leslie, N. R., Downes, C. P., Procyk, K. J., Waterfield, M. D. and Parker, P. J. (2000). "Beta1-integrin and PTEN control the phosphorylation of protein kinase C." Biochemical Journal **352 Pt 2**: 425-33.

Park, J. Y., Lim, B. P., Lee, K., Kim, Y. G. and Jo, E. C. (2006). "Scalable production of adeno-associated virus type 2 vectors via suspension transfection." Biotechnology and Bioengineering **94**(3): 416-30.

Park, K. H., Na, K. and Lee, K. C. (2004). "Immobilization of Arg-Gly-Asp (RGD) sequence in sugar containing copolymer for culturing of pheochromocytoma (PC12) cells." Journal of Bioscience and Bioengineering **97**(3): 207-11.

Park, K. H. and Yun, K. (2004). "Immobilization of Arg-Gly-Asp (RGD) sequence in a thermosensitive hydrogel for cell delivery using pheochromocytoma cells (PC12)." Journal of Bioscience and Bioengineering **97**(6): 374-7.

Peirone, M., Ross, C. J., Hortelano, G., Brash, J. L. and Chang, P. L. (1998). "Encapsulation of various recombinant mammalian cell types in different alginate microcapsules." Journal of Biomedical Materials Research **42**(4): 587-96.

Piccini, P., Pavese, N., Hagell, P., Reimer, J., Bjorklund, A., Oertel, W. H., Quinn, N. P., Brooks, D. J. and Lindvall, O. (2005). "Factors affecting the clinical outcome after neural transplantation in Parkinson's disease." Brain **128**(Pt 12): 2977-86.

Polymeropoulos, M. H., Lavedan, C., Leroy, E., Ide, S. E., Dehejia, A., Dutra, A., Pike, B., Root, H., Rubenstein, J., Boyer, R., Stenroos, E. S., Chandrasekharappa, S., Athanassiadou, A., Papapetropoulos, T., Johnson, W. G., Lazzarini, A. M., Duvoisin, R. C., Di Iorio, G., Golbe, L. I. and Nussbaum, R. L. (1997). "Mutation in the alpha-synuclein gene identified in families with Parkinson's disease." Science **276**(5321): 2045-7.

Ponce, S., Orive, G., Hernandez, R., Gascon, A. R., Pedraz, J. L., de Haan, B. J., Faas, M. M., Mathieu, H. J. and de Vos, P. (2006). "Chemistry and the biological response against immunoisolating alginate-polycation capsules of different composition." Biomaterials **27**(28): 4831-9.

Poncelet, D. (2001). "Production of alginate beads by emulsification/internal gelation." Annals of the New York Academy of Sciences **944**: 74-82.

Poncelet, D., Bugarski, B., Amsden, B. G., Zhu, J., Neufeld, R. and Goosen, M. F. A. (1994). "A Parallel-Plate Electrostatic Droplet Generator - Parameters Affecting Microbead Size." Applied Microbiology and Biotechnology **42**(2-3): 251-255.

Poncelet, D., Lencki, R., Beaulieu, C., Halle, J. P., Neufeld, R. J. and Fournier, A. (1992). "Production of alginate beads by emulsification/internal gelation. I. Methodology." Applied Microbiology and Biotechnology **38**(1): 39-45.

Poncelet, D., Poncelet De Smet, B., Beaulieu, C., Huguet, M. L., Fournier, A. and Neufeld, R. J. (1995). "Production of alginate beads by emulsification/internal gelation. II. Physicochemistry." Applied Biochemistry and Biotechnology **43**: 644-650.

Prakash, S. and Bhathena, J. (2008). "Live immobilised cells as new therapeutics." Journal of Drug Delivery Science and Technology **18**(1): 3-14.

Prüβe, U., Fox, B., Kirchhoff, M., Bruske, F., Breford, J. and Vorlop, K.-D. (1998). "The Jet Cutting Method as a new immobilization technique." Biotechnology Techniques **12**(2): 105-108.

Prüße, U., J. Dalluhn, Breford, J. and Vorlop, K. D. (2000). "Production of Spherical Beads by JetCutting." Chemical Engineering & Technology **23**(12): 1105-1110.

Quong, D., Neufeld, R. J., Skjak-Braek, G. and Poncelet, D. (1998). "External versus internal source of calcium during the gelation of alginate beads for DNA encapsulation." Biotechnology and Bioengineering **57**(4): 438-46.

Rang, H., Dale, M., Ritter, J. and Flower, R. (2007). Rang and Dale's Pharmacology. Edinburgh, Churchill Livingstone.

Rayleigh, L. (1879). "On the Capillary Phenomena of Jets." Proceedings of the Royal Society of London (1854-1905) **29**(-1): 71-97.

Remes, A. and Williams, D. F. (1992). "Immune response in biocompatibility." Biomaterials **13**(11): 731-743.

Ribeiro, A. J., Silva, C., Ferreira, D. and Veiga, F. (2005). "Chitosan-reinforced alginate microspheres obtained through the emulsification/internal gelation technique." European journal of pharmaceutical sciences **25**(1): 31-40.

Roberts, T., De Boni, U. and Sefton, M. V. (1996). "Dopamine secretion by PC12 cells microencapsulated in a hydroxyethyl methacrylate--methyl methacrylate copolymer." Biomaterials **17**(3): 267-75.

Robitaille, R., Pariseau, J. F., Leblond, F. A., Lamoureux, M., Lepage, Y. and Halle, J. P. (1999). "Studies on small (<350 microm) alginate-poly-L-lysine microcapsules. III. Biocompatibility Of smaller versus standard microcapsules." Journal of Biomedical Materials Research **44**(1): 116-20.

Rokstad, A. M., Donati, I., Borgogna, M., Oberholzer, J., Strand, B. L., Espevik, T. and Skjak-Braek, G. (2006). "Cell-compatible covalently reinforced beads obtained from a chemoenzymatically engineered alginate." Biomaterials **27**(27): 4726-4737.

Rokstad, A. M., Holtan, S., Strand, B., Steinkjer, B., Ryan, L., Kulseng, B., Skjak-Braek, G. and Espevik, T. (2002). "Microencapsulation of cells producing therapeutic proteins: optimizing cell growth and secretion." Cell Transplantation **11**(4): 313-24.

Rokstad, A. M., Strand, B., Rian, K., Steinkjer, B., Kulseng, B., Skjak-Braek, G. and Espevik, T. (2003). "Evaluation of different types of alginate microcapsules as bioreactors for producing endostatin." Cell Transplantation **12**(4): 351-64.

Rollan, A., McCormack, D., McHale, L., McCormack, H. and McHale, A. P. (1996). "A rapid in situ, colorimetric assay for the determination of mammalian cell viability in alginate-immobilized and encapsulated systems." Bioprocess and Biosystems Engineering **15**(1): 47-49.

Ross, C. J. and Chang, P. L. (2002). "Development of small alginate microcapsules for recombinant gene product delivery to the rodent brain." Journal of Biomaterials Science Polymer Edition **13**(8): 953-62.

Ross, C. J., Ralph, M. and Chang, P. L. (1999). "Delivery of recombinant gene products to the central nervous system with nonautologous cells in alginate microcapsules." Human Gene Therapy **10**(1): 49-59.

Rubin, L. L. and Staddon, J. M. (1999). "The cell biology of the blood-brain barrier." Annual Review of Neuroscience **22**: 11-28.

Sakai, S., Kawabata, K., Ono, T., Ijima, H. and Kawakami, K. (2005). "Development of mammalian cell-enclosing subsieve-size agarose capsules (<100 microm) for cell therapy." Biomaterials **26**(23): 4786-92.

Saphire, E. O., Parren, P. W., Pantophlet, R., Zwick, M. B., Morris, G. M., Rudd, P. M., Dwek, R. A., Stanfield, R. L., Burton, D. R. and Wilson, I. A. (2001).

"Crystal structure of a neutralizing human IGG against HIV-1: a template for vaccine design." Science **293**(5532): 1155-9.

Schwarz, E. C., Wissenbach, U., Niemeyer, B. A., Strauß, B., Philipp, S. E., Flockerzi, V. and Hoth, M. (2006). "TRPV6 potentiates calcium-dependent cell proliferation." Cell Calcium **39**(2): 163-173.

Schwinger, C., Koch, S., Jahnz, U., Wittlich, P., Rainov, N. G. and Kressler, J. (2002). "High throughput encapsulation of murine fibroblasts in alginate using the JetCutter technology." Journal of Microencapsulation **19**(3): 273-80.

Seely, G. R. and Hart, R. L. (1974). "The binding of alkaline earth metal ions to alginate." Macromolecules **7**(5): 706-10.

Sefton, M. V., Dawson, R. M., Broughton, R. L., Blysnink, J. and Sugamori, M. E. (1987). "Microencapsulation of Mammalian cells in a water-insoluble polyacrylate by coextrusion and interfacial precipitation." Biotechnology and Bioengineering **29**(9): 1135-1143.

Seifert, D. B. and Phillips, J. A. (1997). "Production of small, monodispersed alginate beads for cell immobilization." Biotechnology Progress **13**(5): 562-568.

Selden, C., Shariat, A., McCloskey, P., Ryder, T., Roberts, E. and Hodgson, H. (1999). "Three-dimensional in vitro cell culture leads to a marked upregulation of cell function in human hepatocyte cell lines - an important tool for the development of a bioartificial liver machine." Bioartificial Organs Ii: Technology, Medicine, and Materials **875**: 353-363.

Seo, M., Nie, Z., Xu, S., Mok, M., Lewis, P. C., Graham, R. and Kumacheva, E. (2005). "Continuous microfluidic reactors for polymer particles." Langmuir **21**(25): 11614-22.

Serp, D., Cantana, E., Heinzen, C., Stockar, U. v. and Marison, I. (2000). "Characterization of an Encapsulation Device for the Production of Monodisperse Alginate Beads for Cell Immobilization." Biotechnology and Bioengineering **70**(1): 41-53.

Sgouras, D. and Duncan, R. (1990). "Methods for the evaluation of biocompatibility of soluble synthetic polymers which have potential for biomedical use: 1 — Use of the tetrazolium-based colorimetric assay (MTT) as a preliminary screen for evaluation of in vitro cytotoxicity." Journal of Materials Science. Materials in Medicine **1**(2): 61-68.

Shi, C. M. and Cheng, T. M. (2004). "Differentiation of dermis-derived multipotent cells into insulin-producing pancreatic cells in vitro." World Journal of Gastroenterology **10**(17): 2550-2.

Shinohara, K., Yokoyama, Y., Torii, T. and Okamoto, K. (2008). "Between microdroplets and microfluidics: Unbreakable liquid/liquid interfaces at a junction of hydrophilic microchannels." Applied Physics Letters **93**(3): 3.

Shintaku, H., Kuwabara, T., Kawano, S., Suzuki, T., Kanno, I. and Kotera, H. (2007). "Micro cell encapsulation and its hydrogel-beads production using microfluidic device." Microsystem Technologies **13**(8): 951-958.

Silva, C. M., Ribeiro, A. J., Figueiredo, M., Ferreira, D. and Veiga, F. (2005). "Microencapsulation of hemoglobin in chitosan-coated alginate microspheres prepared by emulsification/internal gelation." AAPS Journal **7**(4): E903-13.

Sim, R. B. and Tsiftsoglou, S. A. (2004). "Proteases of the complement system." Biochemical Society Transactions **32**(Pt 1): 21-7.

Sinden, J., Stevanato, L. and Miljan, E. (2007) "Conditionally-immortalised Pancreatic Cells." UK Application PCT/GB2006/004103 05/10/2007

Skjakbraek, G., Grasdalen, H. and Smidsrod, O. (1989). "Inhomogeneous Polysaccharide Ionic Gels." Carbohydrate Polymers **10**(1): 31-54.

Sladowski, D., Steer, S. J., Clothier, R. H. and Balls, M. (1993). "An improved MTT assay." Journal of Immunological Methods **157**(1-2): 203-207.

Smidsrod, O. (1974). "Molecular basis for some physical properties of alginates in the gel state." Faraday Discussions of the Chemical Society **57**(1): 263-274.

Smidsrod, O. and Skjakbraek, G. (1990). "Alginate as Immobilization Matrix for Cells." Trends in Biotechnology **8**(3): 71-78.

Song, H., Tice, J. D. and Ismagilov, R. F. (2003). "A microfluidic system for controlling reaction networks in time." Angewandte Chemie (International ed. in English) **42**(7): 768-72.

Soon-Shiong, P., Feldman, E., Nelson, R., Komtebedde, J., Smidsrod, O., Skjak-Braek, G., Espevik, T., Heintz, R. and Lee, M. (1992). "Successful reversal of spontaneous diabetes in dogs by intraperitoneal microencapsulated islets." Transplantation **54**(5): 769-74.

Soon-Shiong, P., Heintz, R. E., Merideth, N., Yao, Q. X., Yao, Z., Zheng, T., Murphy, M., Moloney, M. K., Schmehl, M., Harris, M. and et al. (1994). "Insulin independence in a type 1 diabetic patient after encapsulated islet transplantation." Lancet **343**(8903): 950-1.

Stabler, C., Wilks, K., Sambanis, A. and Constantinidis, I. (2001). "The effects of alginate composition on encapsulated betaTC3 cells." Biomaterials **22**(11): 1301-10.

Steiner, L. A. and Andrews, P. J. (2006). "Monitoring the injured brain: ICP and CBF." British Journal of Anaesthesia **97**(1): 26-38.

Stevens, M. G. and Olsen, S. C. (1993). "Comparative analysis of using MTT and XTT in colorimetric assays for quantitating bovine neutrophil bactericidal activity." Journal of Immunological Methods **157**(1-2): 225-231.

Stokke, B. T., Smidsrod, O., Bruheim, P. and Skjakbraek, G. (1991). "Distribution of Uronate Residues in Alginate Chains in Relation to Alginate Gelling Properties." Macromolecules **24**(16): 4637-4645.

Stone, H. A., Stroock, A. D. and Ajdari, A. (2004). "Engineering flows in small devices: Microfluidics toward a lab-on-a-chip." Annual Review of Fluid Mechanics **36**: 381-411.

Strand, B. L., Gaserod, O., Kulseng, B., Espevik, T. and Skjak-Baek, G. (2002). "Alginate-polylysine-alginate microcapsules: effect of size reduction on capsule properties." Journal of Microencapsulation **19**(5): 615-30.

Strand, B. L., Morch, Y. A., Espevik, T. and Skjak-Braek, G. (2003). "Visualization of alginate-poly-L-lysine-alginate microcapsules by confocal laser scanning microscopy." Biotechnology and Bioengineering **82**(4): 386-94.

Strand, B. L., Ryan, T. L., In't Veld, P., Kulseng, B., Rokstad, A. M., Skjak-Brek, G. and Espevik, T. (2001). "Poly-L-Lysine induces fibrosis on alginate microcapsules via the induction of cytokines." Cell Transplant **10**(3): 263-75.

Strober, W. (2001). "Trypan blue exclusion test of cell viability." Current Protocols in Immunology **Appendix 3**: Appendix 3B.

Sugiura, S., Nakajima, M., Iwamoto, S. and Seki, M. (2001). "Interfacial Tension Driven Monodispersed Droplet Formation from Microfabricated Channel Array." Langmuir **17**(18): 5562-5566.

Sugiura, S., Oda, T., Aoyagi, Y., Matsuo, R., Enomoto, T., Matsumoto, K., Nakamura, T., Satake, M., Ochiai, A., Ohkohchi, N. and Nakajima, M. (2007).

"Microfabricated airflow nozzle for microencapsulation of living cells into 150 micrometer microcapsules." Biomedical Microdevices **9**(1): 91-9.

Sugiura, S., Oda, T., Izumida, Y., Aoyagi, Y., Satake, M., Ochiai, A., Ohkohchi, N. and Nakajima, M. (2005). "Size control of calcium alginate beads containing living cells using micro-nozzle array." Biomaterials **26**(16): 3327-31.

Sun, Y., Ma, X., Zhou, D., Vacek, I. and Sun, A. M. (1996). "Normalization of diabetes in spontaneously diabetic cynomologus monkeys by xenografts of microencapsulated porcine islets without immunosuppression." The Journal of Clinical Investigation **98**(6): 1417-22.

Surmeian, M., Slyadnev, M. N., Hisamoto, H., Hibara, A., Uchiyama, K. and Kitamori, T. (2002). "Three-layer flow membrane system on a microchip for investigation of molecular transport." Analytical Chemistry **74**(9): 2014-20.

Tada, H., Shiho, O., Kuroshima, K.-i., Koyama, M. and Tsukamoto, K. (1986). "An improved colorimetric assay for interleukin 2." Journal of Immunological Methods **93**(2): 157-165.

Tagalakis, A. D., Diakonov, I. A., Graham, I. R., Heald, K. A., Harris, J. D., Mulcahy, J. V., Dickson, G. and Owen, J. S. (2005). "Apolipoprotein E delivery by peritoneal implantation of encapsulated recombinant cells improves the hyperlipidaemic profile in apoE-deficient mice." Biochimica et Biophysica Acta **1686 3**: 190-9.

Tam, S. K., Dusseault, J., Polizu, S., Menard, M., Halle, J. P. and Yahia, L. (2005). "Physicochemical model of alginate-poly-L-lysine microcapsules defined at the micrometric/nanometric scale using ATR-FTIR, XPS, and ToF-SIMS." Biomaterials **26**(34): 6950-61.

Tan, J., Xu, J. H., Li, S. W. and Luo, G. S. (2008). "Drop dispenser in a cross-junction microfluidic device: Scaling and mechanism of break-up." Chemical Engineering Journal **136**(2-3): 306-311.

Tan, W. H. and Takeuchi, S. (2007). "Monodisperse alginate hydrogel microbeads for cell encapsulation." Advanced Materials **19**(18): 2696-2701.

Tan, Y. C., Hettiarachchi, K., Siu, M. and Pan, Y. P. (2006a). "Controlled microfluidic encapsulation of cells, proteins, and microbeads in lipid vesicles." Journal of the American Chemical Society **128**(17): 5656-5658.

Tan, Y.-C., Cristini, V. and Lee, A. P. (2006b). "Monodispersed microfluidic droplet generation by shear focusing microfluidic device." Sensors and Actuators B: Chemical **114**(1): 350-356.

Taylor, C. J., Bolton, E. M., Pocock, S., Sharples, L. D., Pedersen, R. A. and Bradley, J. A. (2005). "Banking on human embryonic stem cells: estimating the number of donor cell lines needed for HLA matching." Lancet **366**(9502): 2019-2025.

Taylor, M. S., Daniels, A. U., Andriano, K. P. and Heller, J. (1994). "Six bioabsorbable polymers: in vitro acute toxicity of accumulated degradation products." Journal of Applied Biomaterials **5**(2): 151-7.

Teramura, Y. and Iwata, H. (2009). "Islet encapsulation with living cells for improvement of biocompatibility." Biomaterials **30**(12): 2270-2275.

Thanos, C. G., Bintz, B. E. and Emerich, D. F. (2007). "Stability of alginate-polyornithine microcapsules is profoundly dependent on the site of transplantation." Journal of Biomedical Materials Research. Part A **81**(1): 1-11.

Thorsen, T., Roberts, R. W., Arnold, F. H. and Quake, S. R. (2001). "Dynamic pattern formation in a vesicle-generating microfluidic device." Physical Review Letters **86**(18): 4163-6.

Thu, B., Bruheim, P., Espevik, T., Smidsrød, O., Soon-Shiong, P. and Skjåk-Bræk, G. (1996a). "Alginate polycation microcapsules : I. Interaction between alginate and polycation." Biomaterials **17**(10): 1031-1040.

Thu, B., Bruheim, P., Espevik, T., Smidsrod, O., Soon-Shiong, P. and Skjak-Braek, G. (1996b). "Alginate polycation microcapsules. II. Some functional properties." Biomaterials **17**(11): 1069-79.

Torres, E. M., Meldrum, A., Kirik, D. and Dunnett, S. B. (2006). "An investigation of the problem of two-layered immunohistochemical staining in paraformaldehyde fixed sections." Journal of Neuroscience Methods **158**(1): 64-74.

Torres, E. M., Monville, C., Lowenstein, P. R., Castro, M. G. and Dunnett, S. B. (2005). "Delivery of sonic hedgehog or glial derived neurotrophic factor to dopamine-rich grafts in a rat model of Parkinson's disease using adenoviral vectors Increased yield of dopamine cells is dependent on embryonic donor age." Brain Research Bulletin **68**(1-2): 31-41.

Uludag, H., Babensee, J. E., Roberts, T., Kharlip, L., Horvath, V. and Sefton, M. V. (1993). "Controlled release of dopamine, insulin and other agents from microencapsulated cells." Journal of Controlled Release **24**(1-3): 3-11.

Uludag, H., De Vos, P. and Tresco, P. A. (2000). "Technology of mammalian cell encapsulation." Advanced Drug Delivery Reviews **42**(1-2): 29-64.

Uludag, H. and Sefton, M. V. (1993). "Microencapsulated human hepatoma (HepG2) cells: In vitro growth and protein release." Journal of Biomedical Materials Research **27**(10): 1213-1224.

Um, E., Lee, D.-S., Pyo, H.-B. and Park, J.-K. (2008). "Continuous generation of hydrogel beads and encapsulation of biological materials using a microfluidic droplet-merging channel." Microfluidics and Nanofluidics **5**(4): 541-549.

Valdes-Gonzalez, R. A., Dorantes, L. M., Garibay, G. N., Bracho-Blanchet, E., Mendez, A. J., Davila-Perez, R., Elliott, R. B., Teran, L. and White, D. J. (2005). "Xenotransplantation of porcine neonatal islets of Langerhans and Sertoli cells: a 4-year study." European Journal of Endocrinology **153**(3): 419-27.

Van Den Eeden, S. K., Tanner, C. M., Bernstein, A. L., Fross, R. D., Leimpeter, A., Bloch, D. A. and Nelson, L. M. (2003). "Incidence of Parkinson's disease: variation by age, gender, and race/ethnicity." American Journal of Epidemiology **157**(11): 1015-22.

Van Raamsdonk, J. M. and Chang, P. L. (2001). "Osmotic pressure test: a simple, quantitative method to assess the mechanical stability of alginate microcapsules." Journal of Biomedical Materials Research **54**(2): 264-71.

VanDelinder, V. and Groisman, A. (2006). "Separation of plasma from whole human blood in a continuous cross-flow in a molded microfluidic device." Analytical Chemistry **78**(11): 3765-71.

VanDelinder, V. and Groisman, A. (2007). "Perfusion in microfluidic cross-flow: separation of white blood cells from whole blood and exchange of medium in a continuous flow." Analytical Chemistry **79**(5): 2023-30.

Vandenbossche, G. M., Bracke, M. E., Cuvelier, C. A., Bortier, H. E., Mareel, M. M. and Remon, J. P. (1993). "Host reaction against empty alginate-polylysine microcapsules. Influence of preparation procedure." Journal of Pharmacy and Pharmacology **45**(2): 115-20.

Veng, L. M., Bjugstad, K. B., Freed, C. R., Marrack, P., Clarkson, E. D., Bell, K. P., Hutt, C. and Zawada, W. M. (2002). "Xenografts of MHC-deficient mouse

embryonic mesencephalon improve behavioral recovery in hemiparkinsonian rats." Cell Transplant **11**(1): 5-16.

Visted, T., Furmanek, T., Sakariassen, P., Foegler, W. B., Sim, K., Westphal, H., Bjerkvig, R. and Lund-Johansen, M. (2003). "Prospects for delivery of recombinant angiostatin by cell-encapsulation therapy." Human Gene Therapy **14**(15): 1429-40.

Wee, S. and Gombotz, W. R. (1998). "Protein release from alginate matrices." Advanced Drug Delivery Reviews **31**(3): 267-285.

Wickremaratchi, M. M., Perera, D., O'Loghlen, C., Sastry, D., Morgan, E., Jones, A., Edwards, P., Robertson, N. P., Butler, C., Morris, H. R. and Ben-Shlomo, Y. (2009). "Prevalence and age of onset of Parkinson's disease in Cardiff: a community based cross sectional study and meta-analysis." Journal of Neurology Neurosurgery & Psychiatry **80**(7): 805-7.

Wild, S., Roglic, G., Green, A., Sicree, R. and King, H. (2004). "Global prevalence of diabetes: estimates for the year 2000 and projections for 2030." Diabetes Care **27**(5): 1047-53.

Williams, D. F. (1987). Definitions in biomaterials. Progress in biomedical engineering. D. F. Williams. Amsterdam, Elsevier.

Winkler, C., Kirik, D. and Bjorklund, A. (2005). "Cell transplantation in Parkinson's disease: how can we make it work?" Trends in Neurosciences **28**(2): 86-92.

Winn, S. R., Tresco, P. A., Zielinski, B., Greene, L. A., Jaeger, C. B. and Aebischer, P. (1991). "Behavioral recovery following intrastriatal implantation of microencapsulated PC12 cells." Experimental Neurology **113**(3): 322-9.

Wong, E. H., E. Rondeau, P. Schuetz and J. Cooper-White (2009). "A microfluidic-based method for the transfer of biopolymer particles from an oil phase to an aqueous phase." Lab Chip **9**(17): 2582-90.

Workman, V. L., Dunnett, S. B., Kille, P. and Palmer, D. D. (2007). "Microfluidic chip-based synthesis of alginate microspheres for encapsulation of immortalized human cells." Biomicrofluidics **1**(1): 014105.

Workman, V. L., Dunnett, S. B., Kille, P. and Palmer, D. D. (2008). "On-Chip Alginate Microencapsulation of Functional Cells." Macromolecular Rapid Communications **29**(2): 165-170.

Yang, C. H., Huang, K. S. and Chang, J. Y. (2007). "Manufacturing monodisperse chitosan microparticles containing ampicillin using a microchannel chip." Biomedical Microdevices **9**(2): 253-9.

Yeh, C.-H., Zhao, Q., Lee, S.-J. and Lin, Y.-C. (2009). "Using a T-junction microfluidic chip for monodisperse calcium alginate microparticles and encapsulation of nanoparticles." Sensors and Actuators A: Physical **151**(2): 231-236.

Yi, X., Sun, X. and Zhang, Y. (2004). "Effects of osmotic pressure on recombinant BHK cell growth and von willebrand factor (vWF) expression." Process Biochemistry **39**(11): 1817-1823.

Yu, L., Shen, Z., Mo, J., Dong, X., Qin, J. and Lin, B. (2007). "Microfluidic chip-based cell electrophoresis with multipoint laser-induced fluorescence detection system." Electrophoresis **28**(24): 4741-7.

Zeng, Y., Ricordi, C., Lendoire, J., Carroll, P. B., Alejandro, R., Bereiter, D. R., Tzakis, A. and Starzl, T. E. (1993). "The effect of prednisone on pancreatic islet autografts in dogs." Surgery **113**(1): 98-102.

Zhang, H., Tumarkin, E., Peerani, R., Nie, Z., Sullan, R. M., Walker, G. C. and Kumacheva, E. (2006). "Microfluidic production of biopolymer microcapsules

with controlled morphology." Journal of the American Chemical Society **128**(37): 12205-10.

Zhang, H., Tumarkin, E., Sullan, R. M. A., Walker, G. C. and Kumacheva, E. (2007). "Exploring Microfluidic Routes to Microgels of Biological Polymers." Macromolecular Rapid Communications **28**(5): 527-538.

Zhang, X. (1999). "Dynamics of drop formation in viscous flows." Chemical Engineering Science **54**(12): 1759-1774.

Zhao, D. S., Roy, B., McCormick, M. T., Kuhr, W. G. and Brazill, S. A. (2003). "Rapid fabrication of a poly(dimethylsiloxane) microfluidic capillary gel electrophoresis system utilizing high precision machining." Lab on a Chip **3**(2): 93-9.

Zhou, Y., Sun, T., Chan, M., Zhang, J., Han, Z., Wang, X., Toh, Y., Chen, J. P. and Yu, H. (2005). "Scalable encapsulation of hepatocytes by electrostatic spraying." Journal of Biotechnology **117**(1): 99-109.

Zielinski, B. A. and Aebischer, P. (1994). "Chitosan as a Matrix for Mammalian-Cell Encapsulation." Biomaterials **15**(13): 1049-1056.

Zimmermann, H., Hillgartner, M., Manz, B., Feilen, P., Brunnenmeier, F., Leinfelder, U., Weber, M., Cramer, H., Schneider, S., Hendrich, C., Volke, F. and Zimmermann, U. (2003). "Fabrication of homogeneously cross-linked, functional alginate microcapsules validated by NMR-, CLSM- and AFM-imaging." Biomaterials **24**(12): 2083-96.

Zimmermann, H., Zimmermann, D., Reuss, R., Feilen, P. J., Manz, B., Katsen, A., Weber, M., Ihmig, F. R., Ehrhart, F., Gessner, P., Behringer, M., Steinbach, A., Wegner, L. H., Sukhorukov, V. L., Vasquez, J. A., Schneider, S., Weber, M. M., Volke, F., Wolf, R. and Zimmermann, U. (2005). "Towards a medically approved technology for alginate-based microcapsules allowing long-term immunoisolated transplantation." Journal of Materials Science. Materials in Medicine **16**(6): 491-501.

Zourob, M., Mohr, S., Mayes, A. G., Macaskill, A., Perez-Moral, N., Fielden, P. R. and Goddard, N. J. (2006). "A micro-reactor for preparing uniform molecularly imprinted polymer beads." Lab on a Chip **6**(2): 296-301.

Appendix 1 – Circuit diagrams

All chips are shown actual size.

Chip number 1

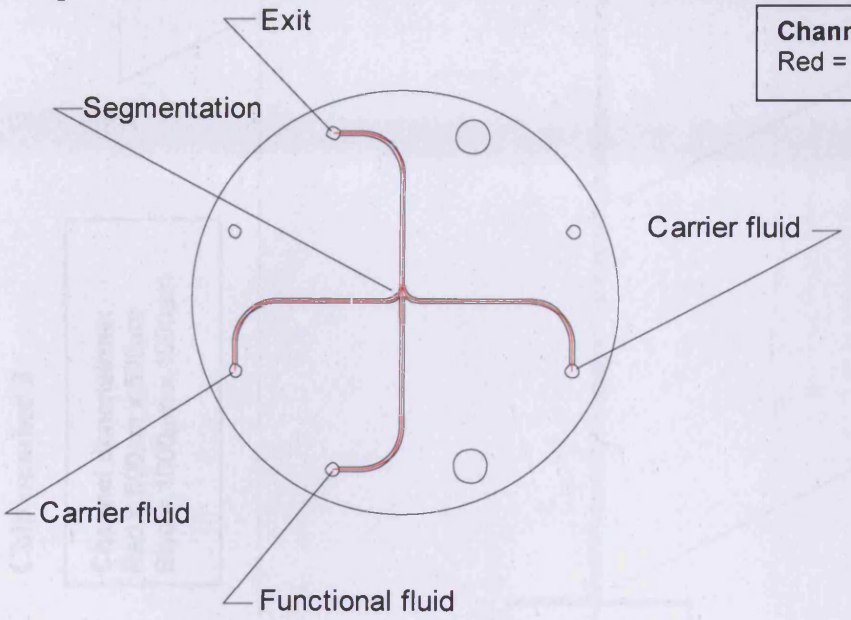

Channel dimensions:
Red = 500µm x 500µm

Chip number 2

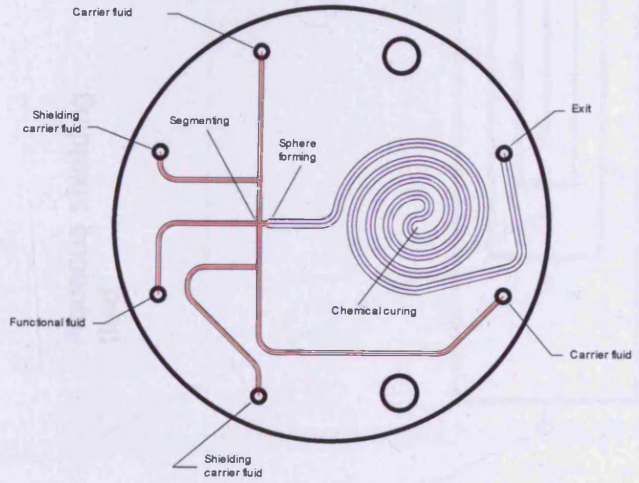

Channel dimensions:
Red = 500µm x 500µm
Blue = 1000µm x 1000µm

Chip number 3

Channel dimensions:
Red = 500μm x 500μm
Blue = 1000μm x 1000μm

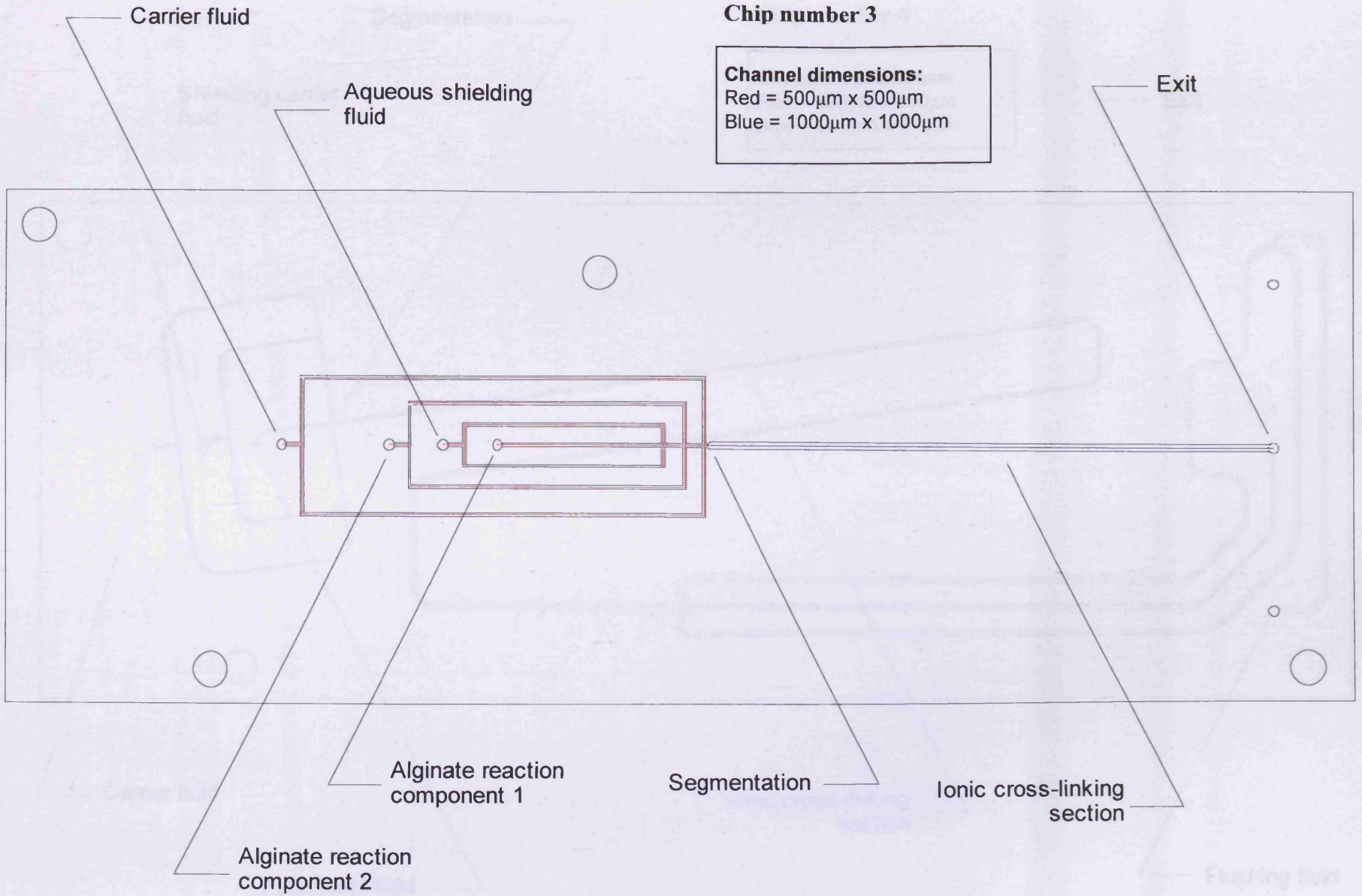

Chip number 4

Channel dimensions:
Red = 300μm x 300μm
Blue = 600μm x 600μm

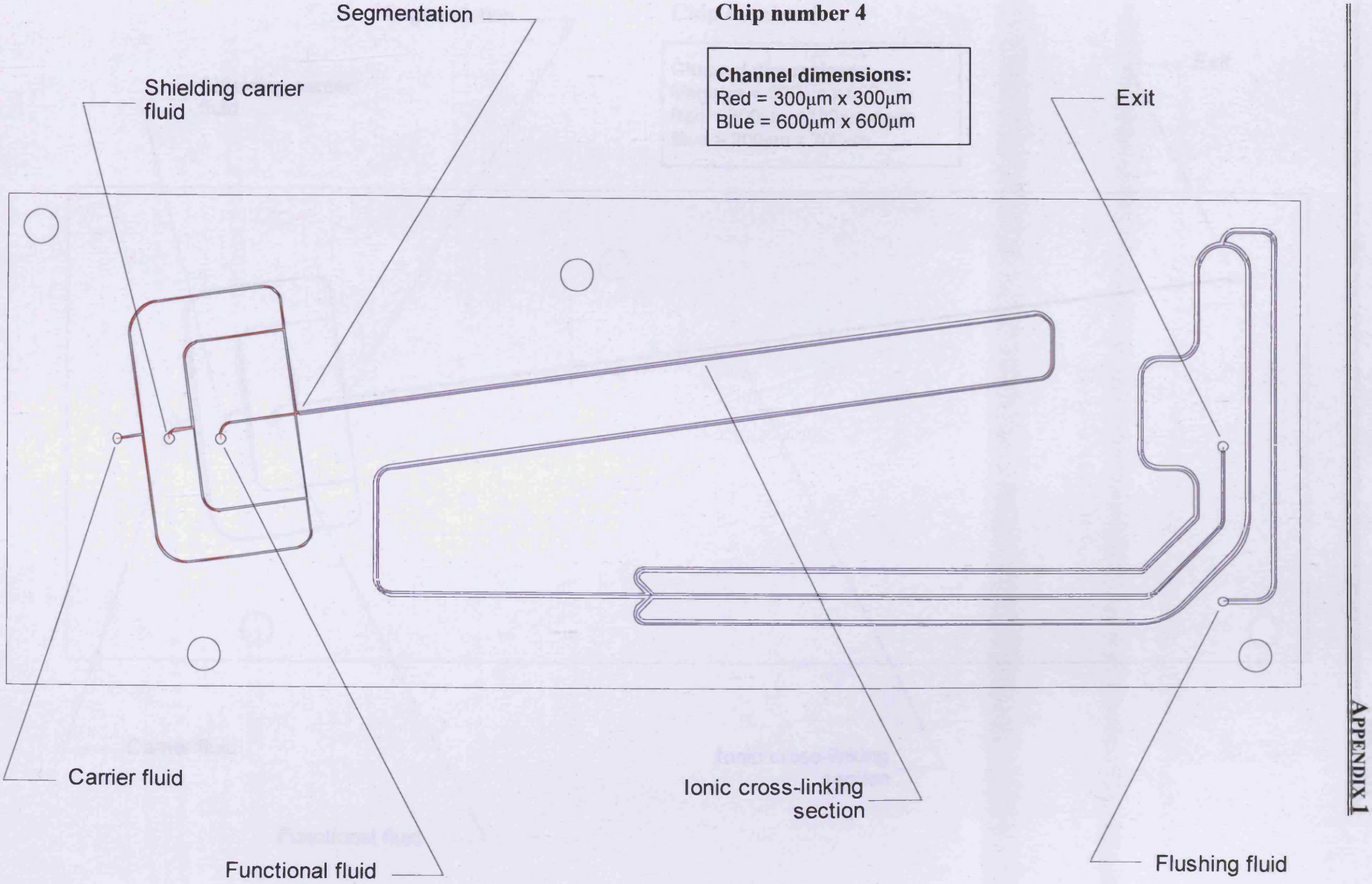

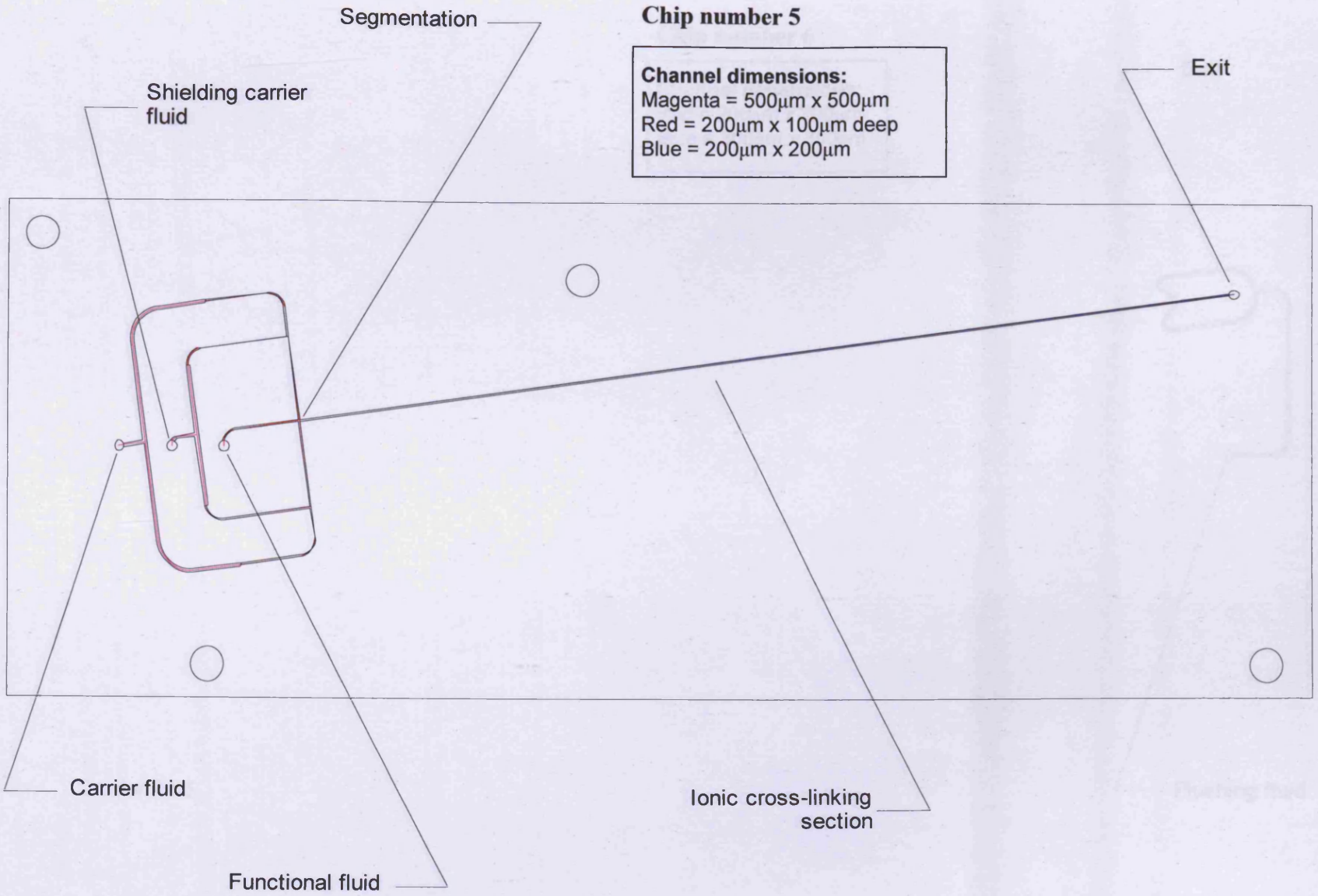
Chip number 5
Channel dimensions:
Magenta = 500μm x 500μm
Red = 200μm x 100μm deep
Blue = 200μm x 200μm
Segmentation
Shielding carrier fluid
Exit
Carrier fluid
Functional fluid
Ionic cross-linking section

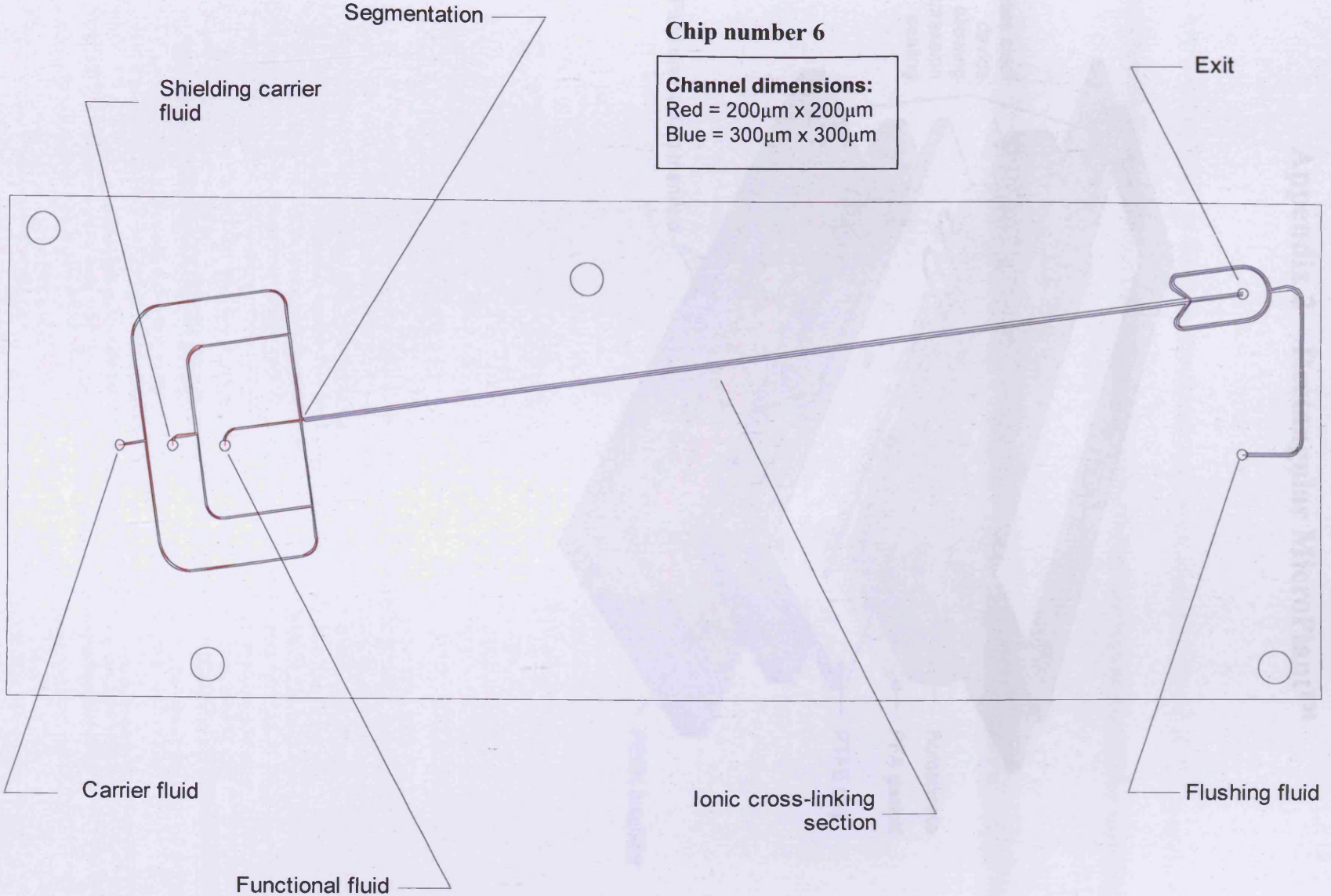
Segmentation
Chip number 6
Channel dimensions:
Red = 200μm x 200μm
Blue = 300μm x 300μm
Exit
Shielding carrier fluid
Carrier fluid
Functional fluid
Ionic cross-linking section
Flushing fluid

Appendix 2 – Rectangular MicroPlant™

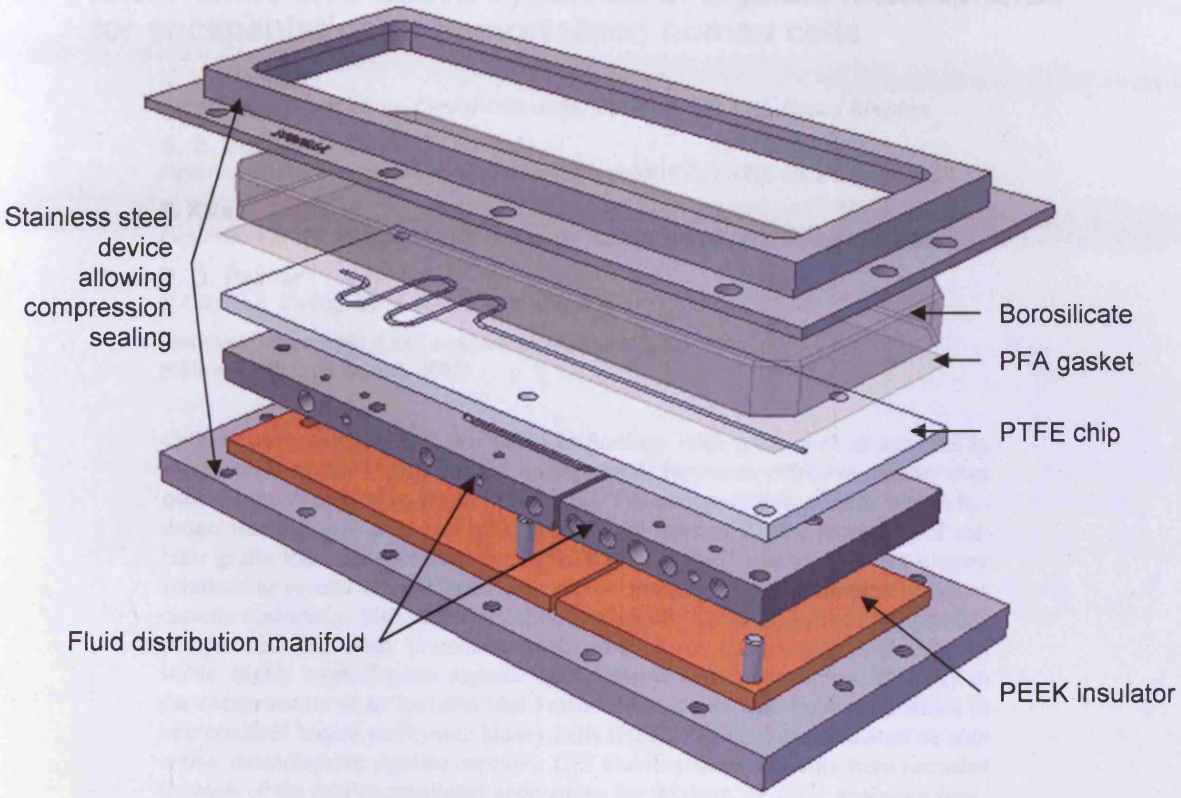

BIOMICROFLUIDICS 1, 014105 (2007)

Microfluidic chip-based synthesis of alginate microspheres for encapsulation of immortalized human cells

V. L. Workman
Department of Biosciences, Cardiff University, Cardiff, CF10 3XQ, United Kingdom

S. B. Dunnett
Department of Biosciences, Cardiff University, Cardiff, CF10 3XQ, United Kingdom

P. Kille
Department of Biosciences, Cardiff University, Cardiff, CF10 3XQ, United Kingdom

D. D. Palmer[a)]
Q Chip Ltd., Cardiff, CF14 4UJ, United Kingdom

(Received 7 November 2006; accepted 14 December 2006;
published online 25 January 2007)

Cellular transplantation is a promising technology with great clinical potential in regenerative medicine and disease management. However, effective control over patient immunological response is essential. The encapsulation of cells within hydrogel microspheres is an increasingly prevalent method for the protection of cellular grafts from immune rejection. Microfluidic "chip" reactors present elegant solutions to several capsule generation issues, including the requirement for intercapsule uniformity, high reproducibility, and sterile, good manufacturing practice compliance. This study presents a novel method for the *on-chip* production of stable, highly monodisperse alginate microspheres and demonstrates its utility in the encapsulation of an immortalized human-derived cell line. Four populations of immortalized human embryonic kidney cells (HEK293) were encapsulated *on chip* within monodisperse alginate capsules. Cell viability measurements were recorded for each of the four encapsulated populations for 90 days. © *2007 American Institute of Physics.* [DOI: 10.1063/1.2431860]

I. INTRODUCTION

The term "cell therapy" is now widely used to describe the process of transplanting nonautologous cells for therapeutic purposes. The scope of cellular therapy continues to broaden, and now extends into many areas of regenerative medicine, involving stem cells,[1] bone augmentation,[2] neuron stimulation,[3] and artificial skin.[4] The implantation of stable, allogeneic or xenogeneic cells, which are engineered to continually secrete functional molecules, is a highly promising approach to disease treatment. The simplest and most widely investigated approach to date has been the encapsulation of cells within cross-linked natural polysaccharide hydrogels such as alginate (a linear block copolymer of *D*-mannuronic acid and *L*-guluronic acid). Calcium-linked alginate hydrogels have been extensively tried and tested, and in many cases have given promising results in immuno-isolation in animals.[5,6]

The prospect of long-term therapies for diseases such as Type I diabetes has attracted widespread interest. The World Health Organization (WHO) estimates that more than 180 million people worldwide suffer from diabetes, and this number is predicted to more than double by 2030.[7] The National Diabetes Information Clearinghouse estimates that diabetes costs $132 billion in the United States alone every year. The prospect of replacement of insulin-producing pancreatic

[a)]Corresponding author. Tel+44 29 20682092; Fax +44 29 20751380; Electronic mail: dan.palmer@q-chip.com

islet beta cells has been described as "the ultimate treatment for Type I diabetes."[8] Clearly, the market for cell therapy is massive. Recently, the first clinical trials in nonimmunosuppressed human patients were undertaken.[9] Preliminary data shows that two patients responded to Ca-alginate encapsulated islet grafts, although exogenous insulin was only decreased and not withdrawn completely.

There are many reasons why this considerable potential has not (yet) been fully realized, only some of which are discussed here. Cell-containing microspheres are often of a large diameter (>500 μm), with a broad size distribution. This means that nutrient diffusion to the center of the microspheres becomes an issue,[10] and standardization of cell number per microsphere is difficult. There is also an inability to produce clinical-scale volumes of cell-containing microspheres. Good manufacturing practice (GMP) compliance becomes paramount when producing microspheres for use in clinical applications.

In response to this, the use of microfluidics is ideally suited to production of cell-containing microspheres. Linear emulsions can easily be produced in a sealed microenvironment, utilizing the phenomenon of segmented flow.[11] The diameter of the product microspheres can be accurately controlled, with size distributions of <1% coefficient of variance. Microfluidic devices containing flow-focusing junctions have previously been used as effective droplet generation systems. However, in most reports, alginate droplets thus formed are crosslinked off-chip, falling from the microfluidic chip into a setting bath of calcium ions.[12] Using such an approach, both standardization and sterility are difficult to achieve. Zhang *et al.*[13] have succeeded in curing alginate droplets *in situ*, in a microfluidic device, using undecanol as a solvent for calcium ions. This methodology was used to demonstrate the encapsulation of polystyrene microbeads. However, cells were not encapsulated using this device. A method similar to that of Zhang *et al.* was previously employed in our laboratory, where a solution of calcium cyclohexanebutyrate was dissolved in octanol. Solid alginate microspheres were successfully produced via this method (unpublished observations).

The primary objective of this work is to simplify and further develop the encapsulation and immunoisolation of live, therapeutically-active cells. It is therefore clear that the encapsulation process should not have any detrimental effect on the cellular payload. In our preliminary studies, aliphatic alcohols such as octanol were found to have an extremely cytotoxic effect on cultured human embryonic kidney cells (HEK293) and primary murine hepatocytes. This encapsulation method was therefore abandoned. In this article we will report the successful encapsulation of cells using an internal gelation method adapted for a microfluidic reactor.

II. MATERIALS AND METHODS

A. Microsphere formation

The microfluidic device consists of a 316 stainless steel manifold into which high performance liquid chromatography fluid connectors are introduced equatorially. Vertical through holes were sealed with nitrile rubber O rings, allowing fluid to flow to the top surface of a virgin polytetrafluoroethylene (PTFE) disc (50×3 mm) located on the manifold. A circular polyfluoroalkoxy polymer film gasket was placed in between the PTFE chip and a borosilicate glass disc (50×5 mm) cover. A 316 stainless steel clamping piece was bolted to the fluidic manifold, allowing the entire laminated assembly to be compression sealed. Microfluidic channels were machined into PTFE discs (Polyflon, Staffordshire, UK) using a Computer Numerical Controlled milling machine (Roland, Swansea, UK). A series of microfluidic "chips" was produced with varying channel dimensions. In one example, the fluidic input channels were of the dimension 500 μm^2, opening out to 1000 μm^2 in the sphere forming channel. This cross-sectional ratio (1:4) was conserved throughout the scalar series of fluidic chips.

Fluids were introduced into the microfluidic circuit using syringe drivers (KD Scientific—Linton Instrumentation, Norfolk, UK). In all cell encapsulation experiments, the stainless steel rig, glass, gasket, fittings, and PTFE chip were autoclaved and then air dried in an oven at 50 °C. Syringe drivers were cleaned with bactericidal wipes before being placed in a Class II hood to maintain sterility. All experiments were carried out in a Class II hood.

Nanocrystalline precipitated $CaCO_3$, with an average particle size of 70 nm (donated by Speciality Minerals, Birmingham, UK) was suspended in either water or D-MEM/F12 medium (Invitrogen, Paisley, UK) at a concentration of 0.5% (w/v). Pronova UP MVM alginate (NovaMatrix™, Drammen, Norway) was added to the $CaCO_3$ suspension at a final concentration of 2% (w/v). The carrier phase contained sunflower oil (Statfold, Staffordshire, UK) and sunflower oil containing 0.5% acetic acid (v/v; Sigma, Dorset, UK). All cell encapsulation experiments used the human embryonic kidney cell line HEK 293 (American Type Culture Collection CRL-1573). These were resuspended in the alginate/$CaCO_3$ mixture at a concentration of 1×10^6 cells/ml.

B. Cell culture

HEK293 cells and cell-containing microspheres were cultured in complete medium consisting of Dulbecco's modified Eagle medium (Invitrogen, Paisley, UK) with 10% fetal bovine serum (Autogen Bioclear, Wiltshire, UK) in an atmosphere of 5% CO_2/95% air at 37 °C. Cells were dissociated using 0.02% (w/v) trypsin/0.05% (w/v) EDTA in PBS (Invitrogen, Paisley, UK).

C. Size measurement

Microsphere radii were measured using a light microscope (Motic, Suffolk, UK) with an attached camera. The coefficient of variance was calculated as the standard deviation of the derived diameters of microspheres as a percentage of mean diameter.

D. Viability measurement

Direct cell counts of individual microspheres were carried out using an adapted trypan blue exclusion method. Individual microspheres were placed on a haemocytometer and all excess medium removed. Alginate microspheres were dissolved by addition of 55 mM sodium citrate (Sigma, Dorset, UK). Cell viability (%) was subsequently determined by trypan blue exclusion.

E. Confocal microscopy

The viability of encapsulated cells was determined using live/dead viability/cytotoxicity kit for mammalian cells (Molecular Probes), according to the manufacturer's instructions. Briefly, the gels were incubated in 1 mL of Hank's buffered salt solution containing 2 μM calcein stain and 4 μM of ethidium homodimer-1 for 15 min at room temperature in the dark. Subsequently, the distribution of red (dead) and green (live) cells was visualized using a fluorescent microscope (Leica DM6000B upright microscope) at 20×.

III. RESULTS

A. Microfluidic method for microsphere formation

The heterogeneous process, first developed by Poncelet *et al.*,[14] involving an insoluble calcium salt ($CaCO_3$), was considered to be the most applicable to a microfluidic flow reaction.

A mixture of nanocrystalline calcium carbonate and sodium alginate solution was used as the *functional phase* in the microfluidic reaction. Alginate droplets containing $CaCO_3$ were produced *via* segmentation with an immiscible hydrocarbon. Acetic acid in the reactive carrier phase reacted immediately with the immobile crystals of calcium carbonate (present at the interface between the droplets' surface and the organic phase), producing Ca^{2+}, H_2O, and CO_2. The free Ca^{2+} ions were sequestered by the dissolved alginate chains and produced the desired ionotropic hydrogel.

The reaction between H^+ and calcium carbonate in the aqueous phase is fast, and resulted in rapid Ca^{2+} release and subsequent gelation. In the microfluidic device, the first point of contact for these two reagents is the junction. Consequently, as an aqueous fluid packet began to emerge from the junction, its interface immediately underwent reaction and crosslinking. As a result, a thin hydrogel skin formed across the junction (Fig. 1). The presence of this hydrogel solid caused the

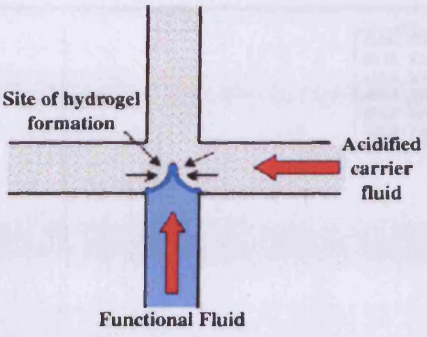

FIG. 1. Schematic showing immediate interfacial hydrogel formation in a crossroads fluidic junction. The calcium carbonate in the functional fluid (shown in blue) reacts rapidly with the acidified oil. The Ca^{2+} ions thus released a form of solid hydrogel at the junction.

fluid flows to decelerate, and quickly produced further solid masses of alginate gel within the microfluidic channel. These eventually occluded the channel, thereby terminating the microsphere synthesis experiment.

B. Shielded segmented flow

To remedy the problem of immediate gelation, it was postulated that a two-component laminar flow could be used as the *carrier phase* stream. At the micron scale, turbulent fluid flow, which is responsible for fluid mixing, is constrained and indeed replaced by laminar flow. Under these conditions, fluids move in planes and with the exception of slow interfacial diffusion, do not undergo mixing. Therefore, it is possible to create a laminar flow of two *miscible* liquids, and maintain separation of the two for some considerable time.

The microfluidic device and junction was enhanced to include an additional fluid flow, into which pure sunflower oil was introduced. Hence, the carrier phase can be thought of as a reactive stream of acidified sunflower oil, containing a *stripe* of inert, unmodified sunflower oil; hereafter referred to as the *shielding flow* (Fig. 2). The two-phase laminar flows were created at microfluidic T-junctions, and approached the aqueous alginate mixture from either side, at an angle of 90°. The fluid flows were oriented such that the nonreactive shielding flows contacted the aqueous alginate flow at the junction. However, the acidified sunflower oil did not come into contact with the emerging aqueous droplets at the junction. This is pictorially demonstrated in Fig. 2(b).

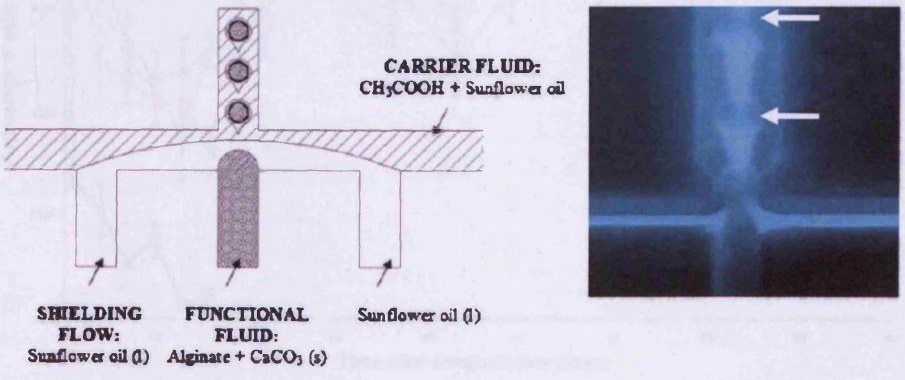

FIG. 2. (a) Schematic showing microfluidic shielding junction with fluid inputs. Laminar streams of sunflower oil and acidified sunflower oil are shown. (b) A negative image of the shielding flow junction. The shielding flow is dyed in blue for ease of visualization. Beads are highlighted with arrows.

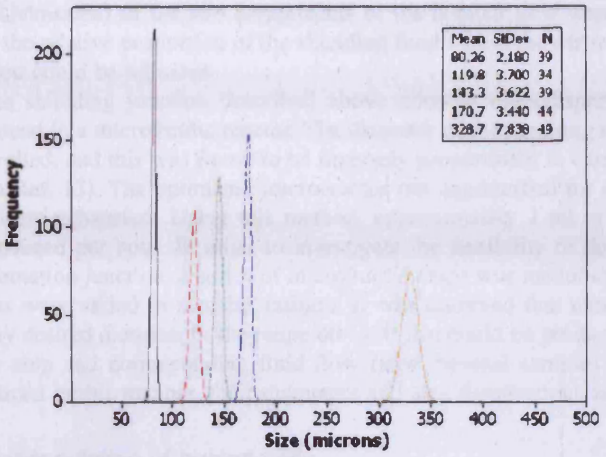

FIG. 3. Graphical representation of 5 alginate microsphere populations showing size distribution. A separate microfluidic chip and optimized flow rates were used to produce each sample.

This modification allowed the problem of immediate gelation at the junction to be overcome. The emerging droplets were insulated from the acidified fraction of the carrier phase by a layer of the shielding fluid [colored blue in Fig. 2(b)]. Spherical droplets of the alginate mixture were successfully generated at the junction, and these proceeded through the reactor channel. As the droplets were carried through the circuit, the shielding layer that surrounds them became gradually acidified, as protons diffused from the acidic surroundings. The eventual reaction between calcium carbonate and H^+ was seen to be slower and more controllable, since the relative flow rates (and

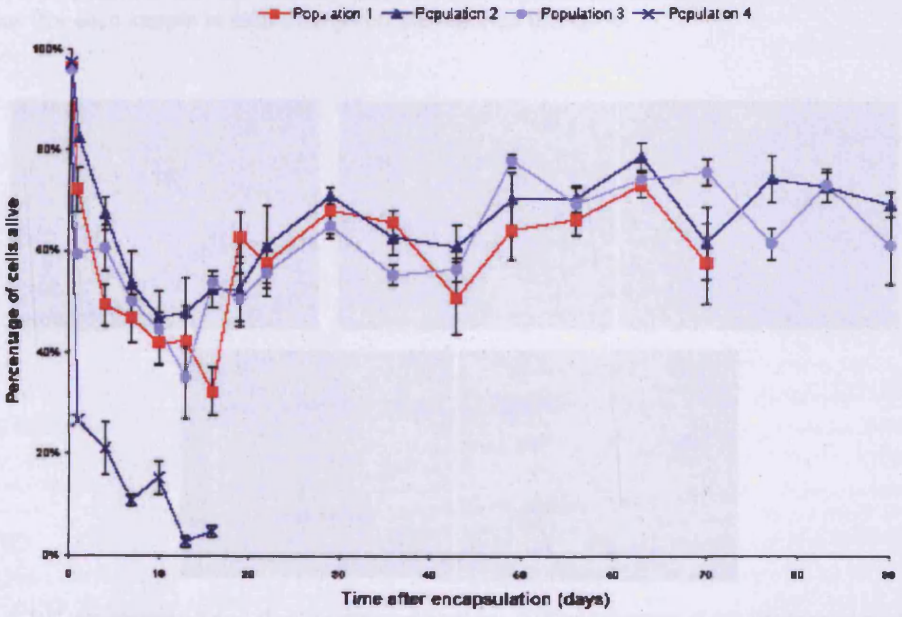

FIG. 4. Percentage cell viability measured using an adapted trypan blue method, as described in Sec. II D. Note that the increase in cell viability is concomitant with observing cell clusters. Error bars show standard error for four replicates.

consequently the thicknesses) of the two components of the laminar flow were entirely variable. Hence, by varying the relative proportion of the shielding fluid within the carrier phase, the rate of microsphere gelation could be adjusted.

The use of the shielding junction described above allowed monodisperse alginate microspheres to be produced in a microfluidic reactor. The diameter of the resulting microspheres could be accurately controlled, and this was found to be inversely proportional to carrier phase flow rate (in agreement with Ref. 13). The optimized microreactor ran unperturbed for several hours, until the feed syringes were exhausted. Using this method, approximately 1 ml of monodisperse microspheres was produced per hour. In order to investigate the flexibility of the chemical method and shielded segmentation junction, a series of microfluidic chips was manufactured, in which the channel dimensions were varied in a scalar fashion. It was observed that monodisperse alginate microspheres of any desired diameter in the range 80–400 μm could be produced by selecting the appropriate fluidic chip and corresponding fluid flow rates. Several samples of alginate microspheres were produced in this manner, their diameters and size distributions are shown in Fig. 3.

C. Microfluidic encapsulation of human cells

The microfluidic procedure for alginate microsphere synthesis described above was further adapted to enable the encapsulation of cellular material. The functional fluid formulation was modified to include the cell growth-medium D-MEM/F12. Four separate populations of HEK-293 cells were dissociated to form single-cell suspensions. Four samples of monodisperse alginate microspheres were obtained, containing approximately one hundred HEK293 cells, randomly distributed throughout each sphere. Approximately 500 μl of microspheres were produced for each population of cells. Using a modified trypan blue exclusion assay, the viability of each sample of encapsulated cells was quantified. Cell viability was measured at several time points, beginning immediately after the dissociation step (time point zero). The alginate capsules were seen to be stable in the cell growth medium and remained intact through numerous manipulations during medium changes. Weekly viability measurements were taken over the next 12 weeks. Over this time the viability of the encapsulated cells continued to increase. After 12 weeks no more cell capsules remained, and the viability measurement experiment was terminated. Live/dead cell ratios (for each sample at each time point) are reported in Fig. 4.

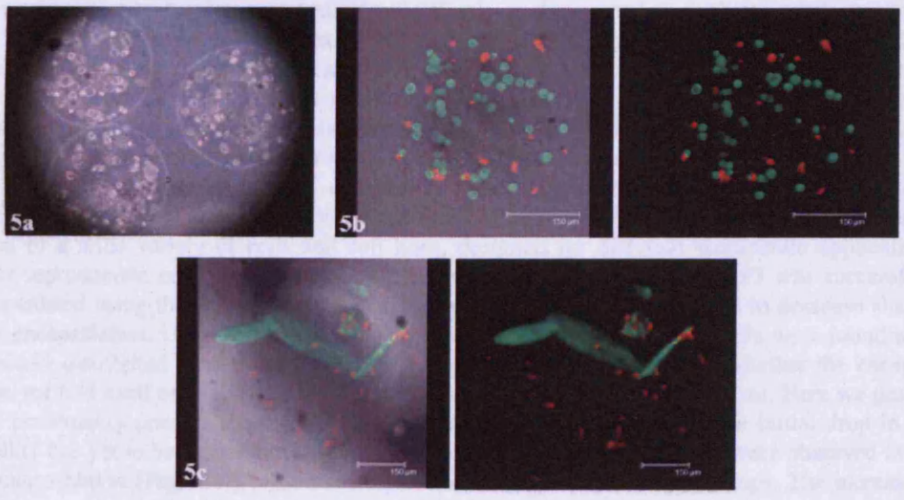

FIG. 5. (a) Light microscope image of cell-containing microspheres. (b) Confocal images of cell-containing microspheres stained with live/dead stains (24 h post encapsulation). (c) Confocal images of cell-containing microspheres stained with live/dead stains (14 days post encapsulation showing cell clusters. Live cells are stained green, and dead cells are stained red).

In addition to trypan blue viability readings, confocal microscopy using live/dead staining was carried out. Cells were seen to be randomly distributed through the microspheres 24 h after encapsulation [see Figs. 5(a) and 5(b)]. After 14 days of encapsulation, cells were observed in clusters. When observed using confocal microscopy, cell clusters were seen to be alive, while individual cells appeared dead [Fig. 5(c)]. Between one and four cell clusters of variable size were observed per microsphere.

IV. DISCUSSION

The interfacial reaction between $CaCO_3$ and H^+ is immediate, producing Ca^{2+}, CO_2, and water. In a solution of sodium alginate, Ca^{2+} ions (liberated upon acidification) are immediately chelated by alginate molecules to form the widely accepted helical "eggbox" structures.[15] This ionic crosslinking produces solid hydrogel, which has been widely used in cell encapsulation and immunoisolation experiments.[5,6,16] The "internal" gelation method was adapted to suit a microfluidic flow reactor, as described above. However, it became immediately clear that the rapid, uncontrolled cross-linking (and therefore gel-forming) reaction at the emerging interface of a droplet caused problems at the fluidic junction. The presence of solid hydrogel at the junction greatly affects the surface properties of the PTFE microfluidic chip, which is intrinsically hydrophobic. The hydrophilic nature of the hydrogel solid causes the aqueous flow stream to be attracted to the surface, thereby disrupting the segmented flow conditions and precluding the formation of droplets.

It was postulated that the gelation reaction could in effect be "postponed" if the aqueous droplets were formed in the absence of H^+, and exposed a moment later to the acidified immiscible phase. Previously, microfluidic laminar flows have been used to create such chemical gradients and to perform liquid-liquid extractions.[17–19] These reported experiments involve combinations of miscible fluids or stratified flows containing an immiscible "membrane" flow. By introducing an unreactive laminar stream into the carrier fluid a diffusion barrier was created, which served to delay the interfacial reaction.

The "shielded" segmented flow described above was designed, and proved to be effective in this application. As the aqueous droplet emerges from the fluidic junction, it meets only the nonreactive portion of the carrier phase. Hence, the droplet elution is not hindered by the formation of thin hydrogel film as before. Diffusion of H^+ within the laminar oil flow begins to occur post segmentation, and thus the reaction of calcium carbonate with H^+ is more gradual. This allows the aqueous droplets to crosslink more slowly as they travel through the microchannel.

As described above, it is imperative that the capsule-forming reaction is compatible with the survival and growth conditions for a cellular payload. In order to limit the possible deleterious effect of H^+ and Ca^{2+} on cells, the minimum concentrations of glacial acetic acid and calcium carbonate required to induce the cross-linking reaction were identified. Using these conditions, the microfluidic flow reaction produced stable, extremely monodisperse alginate microspheres.

HEK293 was used as a model cell line in these experiments due to its high growth rate, hardiness, and ease of transformation. In the future, this novel method could allow the encapsulation of a wide variety of cells and cell lines, designed for different therapeutic applications, under reproducible and sterile conditions. The immortalized cell-line HEK293 was successfully encapsulated using the described method. Initially, viability of cells was seen to decrease sharply after encapsulation. Upon investigation (using confocal microscopy), dead cells were found to be randomly distributed throughout the microspheres [Fig. 5(a)]. It is unclear whether the encapsulation method itself or a lack of cell-cell interactions is the cause of this decrease. Here we present only preliminary results, and further work into investigating the cause of the initial drop in cell viability has yet to be carried out. After approximately 14 days, cell clusters were observed inside the microspheres [Fig. 5(b)], with a corresponding increase in viability readings. The increase in viability was in direct relation to the appearance of cell clusters. It is proposed that cells in close contact at encapsulation are able to proliferate to form the cell clusters observed. Viability (live/dead cell ratio) stabilized at 70% after a month and this was seen to continue, until no microspheres remained (at three months post encapsulation).

Similar results were observed for three of the four replicate encapsulated populations. By contrast, the fourth population exhibited markedly reduced viability 24 h post encapsulation. The cell viability continued to decrease, relative to the other three populations, until at 15 days after encapsulation, all encapsulated cells were dead. Cells encapsulated in this population were not observed to form cell clusters. We have not established a satisfactory explanation for the failure of this one batch, but it is noteworthy that the fate of each batch could be determined within 24 h of production, which will be an important factor in quality control for any therapeutic application.

In the context of cell encapsulation, the ingress of nutrients and oxygen toward the center of a sphere is extremely important. Hence, porosity and sphere size are factors in determining optimum conditions for cells contained within a hydrogel matrix. Larger alginate microspheres (500–2000 μm) can easily be generated via standard droplet generation techniques such as air-jet break-up.[20,21] However, in our experience it is significantly more difficult to produce spheres with a diameter of <400 μm using these conventional methods. By virtue of having decreased diffusion paths, beads with smaller diameter are arguably more effective in averting cell hypoxia.[10] Using microfluidic devices with the shielded segmented flow junction described, we can now reliably synthesize monodisperse samples of alginate microspheres in the range 80–400 μm.

An important issue for the development of cell therapies toward clinical trial application, will be the need to develop GMP-compliant methods for the production, manipulation, and validation of encapsulated cells.[7] Few existing droplet-generation protocols are sufficiently well developed to enable the reproducible production of cell capsules under GMP conditions. Microfluidic devices are intrinsically "sealed environments"; and this will likely prove to be a significant advantage in the attainment of GMP standards. Furthermore, the microfluidic device described here is entirely constructed from "generally regarded as safe" materials.

In the context of microsphere production, the output from a single-circuit microfluidic reactor is typically in the range of 1–20 ml/h (depending *inter alia* on reactive-fluid flow-rates and microsphere diameter). Pharmaceutical and life-science applications are likely to require tens or hundreds of liters of microsphere products for effective clinical trials. Clearly, it would be an extremely laborious task to produce these quantities of microspheres from such a single-circuit microreactor. Indeed, a single-circuit microfluidic device as described here is suitable primarily for the production of much smaller sample volumes for analysis and proof-of-principle studies. If microfluidic devices are to advance and add further value to the encapsulation of live cells, further work toward scaling-up and increasing production volumes must be performed. It is highly likely that this could be achieved via the development of GMP-compliant multicircuit-array devices.

ACKNOWLEDGMENTS

The study was funded in part by the commercial sponsorship of Q Chip Ltd. The authors are also grateful to the Welsh Assembly Government and EPSRC for their support and CASE award (0500 1359). The authors thank the Q Chip technical team for their assistance and advice concerning microreactor design. Q Chip holds patent rights to design of the microfluidic device. D.D.P. is fully employed by Q Chip; V.L.W. receives a CASE studentship part funded by Q Chip; S.B.D. is an academic consultant and member of the scientific advisory board of Q Chip; P.K. is an academic supervisor at Cardiff University School of Biosciences.

[1] X. Wang, W. Wang, J. Ma, X. Guo, X. Yu, and X. Ma, Biotechnol. Prog. **22**, 791 (2006).
[2] J. C. Pound, D. W. Green, J. B. Chaudhuri, S. Mann, H. I. Roach, and R. O. Oreffo, Tissue Eng. **12**, 2789 (2006).
[3] K. Moriyasu, H. Yamazoe, and H. Iwata, J. Biomed. Mater. Res. **77**, 136 (2006).
[4] Z. H. Hu, S. Z. Chen, Y. Jin, Y. Xiong, W. Wang, X. J. Ma, and M. Song, Singapore Med. J. **47**, 504 (2006).
[5] R. Calafiore, G. Basta, G. Luca, M. Calvitti, G. Calabrese, L. Racanicchi, G. Macchiarulo, F. Mancuso, L. Guido, and P. Brunetti, Biotechnol. Appl. Biochem. **39**, 159 (2004).
[6] A. Omer, V. Duvivier-Kali, J. Fernandes, V. Tchipashvili, C. K. Colton, and G. C. Weir, Transplantation **79**, 52 (2005).
[7] The prevention of diabetes and its complications, WHO Review 2006.
[8] C. M. Shi and T. M. Cheng, World J. Gastroenterol. **10**, 2550 (2004).
[9] R. Calafiore, G. Basta, G. Luca, A. Lemmi, M. P. Montanucci, G. Calabrese, L. Racanicchi, F. Mancuso, and P. Brunetti, Diabetes Care **29**, 137 (2006).
[10] J. C. Ogbonna, M. Matsumura, and H. Kataoka, Process Biochem. (Oxford, U.K.) **26**, 109 (1991).

[11] M. Joanicot and A. Ajdari, Science **309**, 887 (2005).
[12] K. S. Huang, T. H. Lai, and Y. C. Lin, Lab Chip **6**, 954 (2006).
[13] H. Zhang, E. Tumarkin, R. Peerani, Z. Nie, R. M. Sullan, G. C. Walker, and E. Kumacheva, J. Am. Chem. Soc. **128**, 12205 (2006).
[14] D. Poncelet, R. Lencki, C. Beaulieu, J. P. Halle, and R. J. Neufeld, Appl. Microbiol. Biotechnol. **38**, 39 (1992).
[15] I. Braccini and S. Perez, Biomacromolecules **2**, 1089 (2001).
[16] Y. Gao, H. C. Jiang, J. Xu, S. H. Pan, and Y. D. Li, Transplant. Proc. **37**, 4589 (2005).
[17] M. Surmeian, M. N. Slyadnev, H. Hisamoto, A. Hibara, K. Uchiyama, and T. Kitamori, Anal. Chem. **74**, 2014 (2002).
[18] T. Maruyama, H. Matsushita, J. Uchida, F. Kubota, N. Kamiya, and M. Goto, Anal. Chem. **76**, 4495 (2004).
[19] J. Atencia and D. J. Beebe, Nature (London) **437**, 648 (2005).
[20] G. L. Fiszman, A. L. Karara, L. M. E. Finocchiaro, and G. C. Glikin, Electronic Journal of Biotechnology (2002), available at: http://www.ejbiotechnology.info/content/vol5/issue3/full/5/
[21] S. Koch, C. Schwinger, J. Kressler, C. Heinzen, and N. G. Rainov, J. Microencapsul. **20**, 303 (2003).

Macromolecular Journals

Macromolecular Rapid Communications

On-Chip Alginate Microencapsulation of Functional Cells

Victoria L. Workman, Stephen B. Dunnett, Peter Kille, Daniel D. Palmer*

We report the use of a PTFE-based microfluidic device for the encapsulation of living, therapeutically-active cells within monodisperse alginate microspheres. We present a novel microfluidic platform and a flexible experimental method for the production of alginate microspheres. Cell lines HEK293, U-2 OS and PC12 were separately encapsulated using this method, with minimal loss of cell viability.

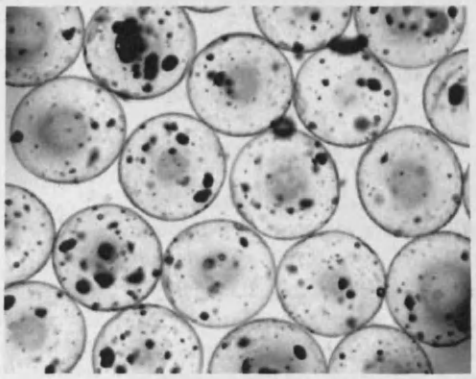

Introduction

Polymer encapsulation is now an accepted route into cellular therapies via implantation of therapeutically-active allogeneic and xenogeneic cells. Continual expression of functional molecules in vivo by an engineered cell line offers a particularly powerful and sustainable strategy for stable, long-term drug-delivery. The forty-year push[1,2] toward a stable, fully immuno-isolating, porous polymer membrane by academic and commercial research groups is indicative of the perceived therapeutic potential of this technology.[3,4] Numerous methods for generating polymer microspheres have been used in the encapsulation of functional cells.[5–10] Among these, micro-electro-mechanical systems (MEMS) and microfluidic device technologies are perhaps the most promising for developing scaleable, GMP-compliant platforms for the production of monodisperse cell-containing microspheres.

The use of flow-focusing fluidic junctions for creating segmented flows of immiscible fluids is now well established.[11–15] Numerous organic liquids have been shown to be effective continuous phases for the production of stable linear emulsions of aqueous solutions. A flow-focusing junction enables the droplet size of a dispersed phase to be precisely controlled, and is therefore highly suitable for the generation of droplets of alginate solutions.[16]

We have previously reported the difficulties in introducing divalent cations to a linear emulsion of alginate droplets in a cell-friendly manner.[17] We have also reported a novel feature of our microfluidic devices, termed "shielded flow" (Figure 1), that enables us successfully to produce such microspheres via an adaptation of Poncelet's internal gelation method.[17,18]

Two other groups have recently reported the synthesis of alginate microspheres via similar microfluidics-based droplet generation methods, utilising PDMA (Polydimethylsiloxane) microfluidic devices containing flow-focussing fluidic junctions. Zhang et al.[19] have developed

V. L. Workman, S. B. Dunnett, P. Kille
Department of Biosciences, Cardiff University, Cardiff, CF10 3XQ, UK
D. D. Palmer
Q-Chip Ltd, Cardiff, CF14 4UJ, UK
Fax: +44 29 2075 1380; E-mail: dan.palmer@q-chip.com

DOI: 10.1002/marc.200700641

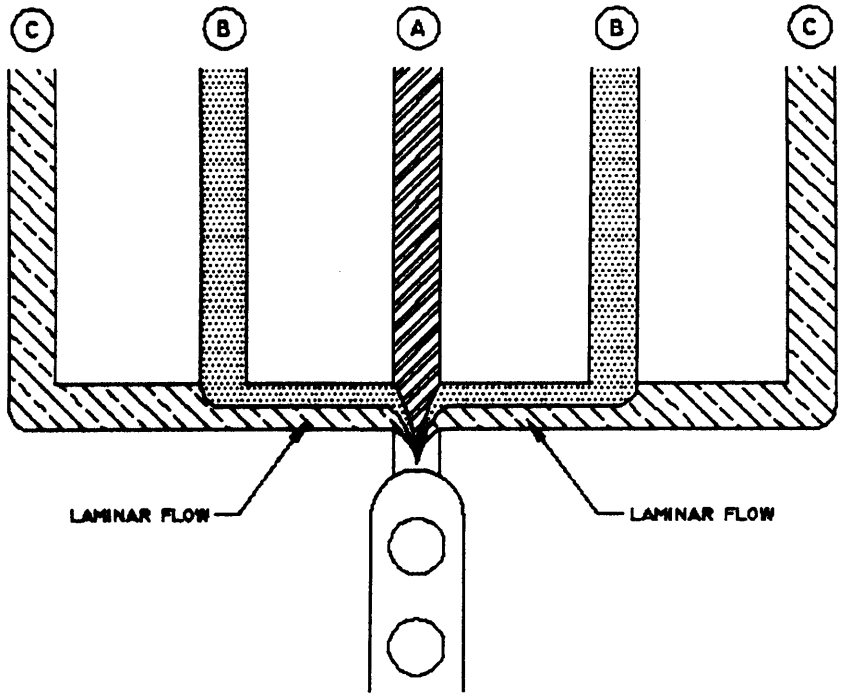

Figure 1. A representation of the shielded junction employed to generate alginate microspheres. Aqueous sodium alginate mixed with $CaCO_3$ and cells is introduced into the central channel (A). Sunflower oil mixed with acetic acid is supplied to the outermost channels (C). Sunflower oil is supplied to the intermediate channels (B) to act as a shield preventing the alginate solution from coming into contact with the acidified oil flow. Between channels B and A the two oils flow in a laminar fashion, with minimal diffusion of H^+ into the protective sunflower oil. After droplet formation at the junction, H^+ diffuses into the alginate droplet, thus liberating Ca^{2+} from $CaCO_3$, which causes gelation of the alginate. Channels prior to the junction are 500 μm^2, after the junction channels are 1 000 μm^2.

a microfluidic method for cross-linking alginate droplets on-chip by suspending calcium acetate in the continuous phase. Calcium acetate dissolves upon contact with the surface of the aqueous alginate-containing dispersed phase, inducing ionotropic cross-linking to produce externally gelled microspheres. Zhang and co-workers[19] report some difficulties in adapting Poncelet's method for internal gelation emulsification, involving an aqueous suspension of calcium carbonate and an acid-containing continuous phase, to their microfluidic platform. We have overcome these difficulties and in this communication demonstrate reproducible capsule synthesis using this method.

Huang et al. report a stable segmented flow system comprising an alginate-calcium carbonate dispersed phase and an inert continuous phase.[20] This microfluidic device enabled the generation of droplets, which were subsequently crosslinked off chip in an acid-containing setting bath. Neither group have reported the successful use of a microfluidic device for the encapsulation of living cells within product microspheres. Here we present the use of such a system for the encapsulation of three cell lines.

Experimental Part

Materials

Cell culture media and supplements for HEK293 and PC12 cells were purchased from Invitrogen, Paisley, UK. Sera were purchased from Autogen Bioclear, UK. Media and supplements for U-2 OS cells were purchased from Sigma, UK. Nanocrystalline precipitated $CaCO_3$ (average particle size 70 nm) was donated by Speciality Minerals, UK. Pronova UP MVM and MVG alginate was obtained from NovaMatrix™, Norway. All other chemicals were purchased from Sigma, UK and used as supplied.

Methods

Microfluidic Device

The microfluidic device consisted of a circular 316 stainless steel manifold into which HPLC fluid connectors were introduced equatorially. Vertical through holes were sealed with nitrile rubber O-rings, allowing fluid to flow to the top surface of a virgin PTFE disc (50 mm diameter ×3 mm; Polyflon, UK) located on the manifold. A circular PFA gasket was placed in between the PTFE chip and a borosilicate glass disc (50 mm diameter ×5 mm) cover. A 316 stainless steel clamping piece was bolted to the fluidic manifold, allowing the entire laminated assembly to be compression sealed. A microfluidic "chip" was produced by machining microfluidic channels into a PTFE disc using a Computer Numerical Controlled milling machine (Roland, UK). The fluidic input channels were of dimension 500 μm^2, opening out to 1 000 μm^2 in the sphere forming channel.

Cell Culture

HEK293 cells (American Type Culture Collection, CRL-1573) were maintained in Dulbecco's modified Eagle medium (DMEM) supplemented with 10% fetal bovine serum and penicillin-streptomycin. G1S Cell Cycle Phase Marker cell line (U-2 OS cells exhibiting stable expression of a Green Fluorescent Protein sensor) was maintained in McCoy's 5A medium containing 10% fetal calf serum, 2×10^{-3} M L-glutamine, 500 $\mu g \cdot ml^{-1}$ G418 and 100 units $\cdot ml^{-1}$ penicillin/100 $\mu g \cdot ml^{-1}$ streptomycin. PC12 cells (ATCC,

Macromol. Rapid Commun. **2008**, *29*, 165–170

DOI: 10.1002/marc.200700641

CRL-1721, a gift from Dr. Jack Ham at the Centre for Endocrine and Diabetes Sciences, Cardiff University, UK) were grown in DMEM supplemented with 5% fetal calf serum, 10% heat-inactivated horse serum and penicillin-streptomycin.

Cell Encapsulation

All cell encapsulation experiments were carried out in a Class II hood to ensure sterility.

All cell types were dissociated using 0.02 wt.-% trypsin/0.05 wt.-% EDTA in PBS and resuspended at a concentration of 1×10^6 cells $\cdot$ ml^{-1} in 2.0 wt.-% MVM alginate containing 0.5 wt.-% calcium carbonate (w/v) in DMEM medium.

Fluids were introduced into the microfluidic circuit using syringe drivers (KD Scientific, Linton Instrumentation, UK). The functional phase contained cells, alginate and $CaCO_3$. The continuous phase was a two-component laminar flow consisting of pure sunflower oil flowing alongside oil with 0.3 vol.-% acetic acid. Oil flow = 10 ml $\cdot$ h^{-1}, acidified oil flow = 25 ml $\cdot$ h^{-1} and functional phase = 1 ml $\cdot$ h^{-1}.

Viability Measurement

Direct cell counts of individual microspheres were carried out using an adapted trypan blue exclusion method. Microspheres were placed on a haemocytometer and excess medium removed. Microspheres were dissolved by addition of 55×10^{-3} M sodium citrate. Cell viability (%) was subsequently determined by trypan blue exclusion.

Confocal Microscopy

The viability of encapsulated cells was determined using LIVE/DEAD viability/cytotoxicity kit for mammalian cells (Invitrogen, UK), according to the manufacturers' instructions. Briefly, the microspheres were incubated in 1 mL of HBSS containing 2×10^{-6} M calcein stain and 4×10^{-6} M of ethidium homodimer-1 for 15 min at room temperature in the dark. Subsequently, the distribution of red (dead) and green (live) cells was visualized using a fluorescent microscope (Leica DM6000B upright microscope) at $\times$20 magnification.

Results and Discussion

As stated by Zhang et al., rapid gelation occurred at a microfluidic crossroad junction. To bypass this problem, calcium levels were reduced. This allowed droplet formation but cross-linker concentrations were insufficient for solid gel microspheres to be collected.[19] As we have previously described, our novel shielded junction (Figure 1) allows alginate droplet formation to occur without immediate gelation,[17] whilst H^+ diffusion and subsequent cross-linking occurs further down the channel. The alginate microspheres formed can be collected in oil or medium on exiting the reactor.

Contact with chemicals detrimental to cells should obviously be minimised during the encapsulation process. For the method presented here, calcium carbonate and glacial acetic acid are used to crosslink alginate droplets within a sunflower oil continuous phase. Previous cytotoxicity testing showed samples of alginate, calcium carbonate and sunflower oil to be non-toxic to the HEK293 cell-line after 4 h incubation, whilst 0.75 vol.-% acetic acid was found to kill 50% of HEK cells after 5 min (unpublished data).

In contrast to Zhang et al., a $CaCO_3$ concentration of 0.5 wt.-% was used, compared to 0.1–0.25 wt.-%.[19] Problems with fluid flow or aggregation of solid $CaCO_3$, in either the feed-tubing or the microfluidic channels, were not observed. A lower concentration of acetic acid was utilised: 0.3 vol.-% compared with 5–25 wt.-%.[19] By reducing acetic acid levels and exposure time of cells to acid (from 5 min to 30 s) a 20% increase in cell viability was observed.

The aforementioned experimental conditions were applicable to 2.0 wt.-% solutions of MVM alginate. However, 2.0 wt.-% MVG alginate solutions (with higher guluronic acid content) could also be manipulated within the microfluidic device to produce solid microspheres. At identical fluid flow rates, an increased concentration of $CaCO_3$ (1.0 wt.-%) was required to induce complete cross-linking. A comparison of the effects of guluronic acid content on encapsulated cell survival is currently underway.

The use of PDMS as a substrate for microfluidic devices is now commonplace, due in part to its favourable hydrophobic properties, its relatively low cost and standardisation of the soft-lithography technique. However, disadvantages of this material lead us to propose PTFE (Teflon)-based microfluidic devices to be more suitable for the future development of 3D hydrogel-cell capsules.

Synthesising a microfluidic device via the multi-stage soft-lithography, PDMS casting, oven-curing and plasma cleaning process has been reported to take a minimum of 8 h.[21] By using PTFE as a starting material for our microfluidic chip synthesis, the multi-step lithography process is avoided, and substituted by a single, automated micro-machining operation. This method allows microfluidic features consisting of microchannels with diameters of 100 μm or greater to be produced. Typically, a microfluidic device of this kind, containing multiple parallel circuits may be produced within sixty minutes.

By avoiding a permanently sealed cover, a compression-sealed PTFE device may be dismantled, cleaned and reassembled as required. This is particularly useful in cases of accidental failure (e.g., channel blockage due to unwanted gelation), allowing rapid recovery during testing and optimisation of conditions.

Three cell lines have been encapsulated using the presented method: HEK293, U-2 OS and PC12. When grown as an adherent culture HEK293 cells exhibit epithelial qualities. In addition HEK293 cells have been successfully adapted for growth in suspension.[22,23] U-2 OS cells are derived from a bone carcinoma and also exhibit epithelial adherent morphology. The U-2 OS cell line used for this study stably expresses a Green Fluorescent Protein sensor that is used to indicate the cell cycle status of each individual cell. PC12 cells are derived from a rat pheochromocytoma.[24] This cell-line secretes clinically useful catecholamines, including dopamine and norepinephrine.

All three cell types were successfully encapsulated and maintained initial viability over at least 4 days (Figure 2), demonstrating that this procedure is not acutely lethal to the cell types tested. PC12 cells had lower viability after harvesting from tissue culture flasks, which was not altered by the encapsulation process. In contrast, although U-2 OS and HEK293 cells had higher post harvest viability compared to PC12, after encapsulation the number of viable cells decreased by approximately 20% for both cell lines. This may be due to increased susceptibility of these cells types to the acidic conditions employed during encapsulation. During cytotoxicity testing PC12 cells showed a 10% decrease in viability after 5 min exposure to 0.3 vol.-% acetic acid, compared to a 50% reduction in viability for HEK293 cells (data not shown).

After encapsulation, U-2 OS and HEK293 cells were randomly distributed throughout their microspheres (Figure 3A,C). After 5 d these cells began to form clusters. Live/Dead staining was employed and images were taken via confocal microscopy as illustrated after 21 d (Figure 3B,D).

HEK293 cells have previously been observed to form clusters that eventually fill microspheres, causing them to disintegrate.[25,26] Between one and four cell clusters were seen to form within any one microsphere (Figure 3D) varying in size and shape. Some were spherical with a diameter estimated between 75 and 100 μm, more commonly; cigar-shaped clusters of length 100 to 350 μm were formed.

Although U-2 OS cells also formed clusters, they showed different features to those formed by HEK293 cells. U-2 OS cell clusters were smaller than HEK293 cell clusters, typically 75 μm in diameter. These smaller clusters took 21 d to form, slower than the 7 d for HEK293 clusters. By day 21, only cells that had formed clusters near the periphery of a microsphere were observed to be alive (Figure 3B). To our knowledge, this cell type has not previously been encapsulated.

Unlike U-2 OS and HEK293 cells, PC12 cells grow in small clumps, which adhere poorly to plastic substrates. Upon harvesting, cell clumps were triturated as much as possible, but each microsphere contained at least one clump of PC12 cells upon synthesis (Figure 3E and 4). In contrast to U-2 OS and HEK293 cells, PC12 cells did not increase in number after encapsulation (Figure 3F). PC12 cells encapsulated in hydroxyethyl methacrylate-methyl methacrylate copolymer after an initial decrease exhibited a quiescent period from day 7 to day 21, followed by an increase in viability of the surviving cells from day 21 to day 28.[27]

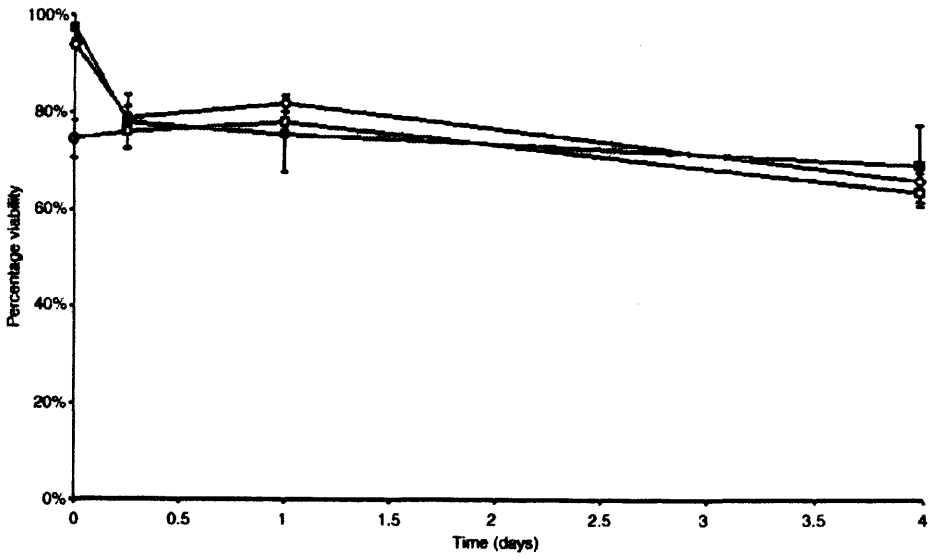

Figure 2. Viability, estimated using trypan blue exclusion, of different cell types encapsulated within alginate microspheres. Results are presented as mean values of quadruplicate beads ± Standard Error. Although HEK293 (■) and U-2 OS (◇) cells show higher viability after harvesting than PC12 (□) cells, no drop in viability is observed after PC12 cells are encapsulated.

Conclusion

Previous examples of PDMS microfluidic devices have been shown to be useful only in the production of inert alginate spheres. By

Macromol. Rapid Commun. **2008**, *29*, 165–170

DOI: 10.1002/marc.200700641

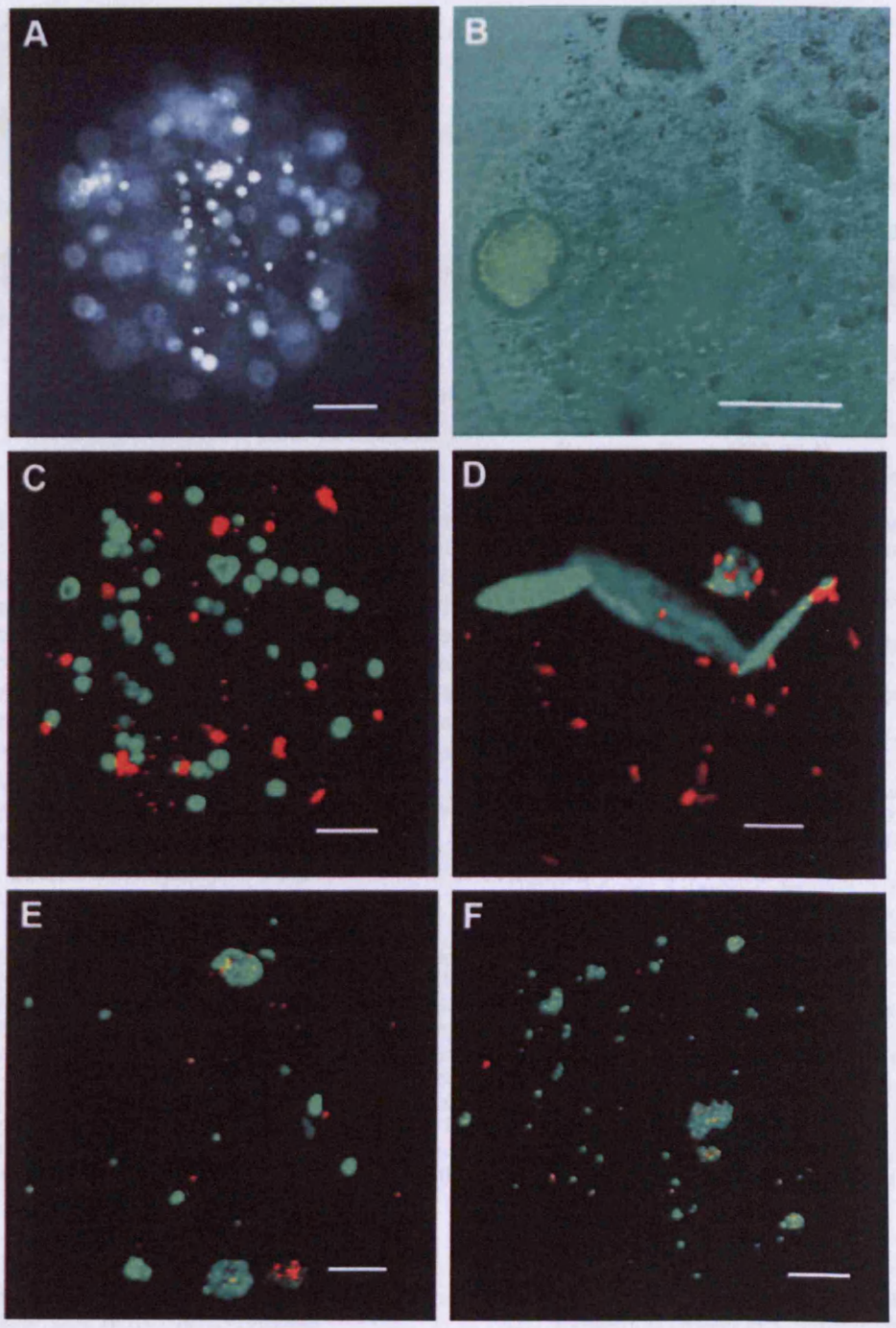

Figure 3. Images showing distribution of live and dead cells within alginate microcapsules 1 d (A, C, E) and 21 d (B, D, F) after encapsulation. A, B) U-2 OS cells encapsulated within alginate microcapsules, showing endogenous GFP expression. C-F) Confocal images of encapsulated cells stained with Live/Dead dyes. Green fluorescence is emitted from the intracellular esterase-converted calcein in live cells whereas red fluorescence is emitted from ethidium homodimer present in dead cells. C, D) HEK293 cells and E, F) PC12 cells encapsulated within alginate microspheres. Scale bar is 100 μm.

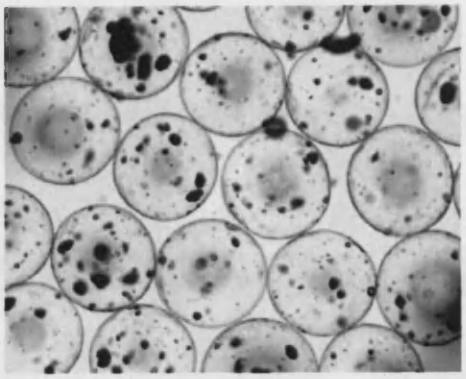

Figure 4. Light microscope image of encapsulated PC12 cells, showing small cell clumps present after encapsulation.

combining an adapted bulk emulsion process with a novel PTFE microfluidic production device, we have successfully encapsulated three different cell lines on-chip. Alginate samples consisting of both high and medium concentrations of guluronic acid have been shown to be suitable for the micro-reaction process. Crucially, the present method has been shown to have minimal effect on the viability of encapsulated cells during and post processing. We are now seeking to optimise encapsulation of the PC12 cell-line to produce monodisperse stable samples of dopamine-producing cell-capsules for evaluation in neurodegenerative disease models.

Acknowledgements: The study was funded in part by sponsorship from *Q-Chip Ltd.* We are also grateful to the *Welsh Assembly Government* and *EPSRC* for their support and *CASE* award (0500 1359). We thank Dr. *Anthony Hayes* of the *Confocal Microscopy Unit* at *Cardiff School of Biosciences* for assistance with imaging microscopy and Dr *Jack Ham, Centre for Endocrine and Diabetes Sciences, Cardiff University,* for the kind gift of PC12 cells. U-2 OS cell cycle phase marker cell line was kindly provided by *GE Healthcare,* The Maynard Center, Forest Farm, Whitchurch, Cardiff, CF14 7YT. *Q-Chip* holds patent rights to design of the microfluidic device.

Received: September 5, 2007; Revised: October 4, 2007; Accepted: October 10, 2007; DOI: 10.1002/marc.200700641

Keywords: alginate; biomaterials; cellular therapy; microencapsulation; microfluidics

[1] T. M. Chang, *Nat. Rev. Drug Discovery* **2005**, *4*, 221.
[2] T. M. S. Chang, *Science* **1964**, *146*, 524.
[3] O. Hauser, E. Prieschl-Grassauer, B. Salmons, *Curr. Opin. Mol. Ther.* **2004**, *6*, 412.
[4] G. Orive, A. R. Gascon, R. M. Hernandez, M. Igartua, J. Luis Pedraz, *Trends Pharmacol. Sci.* **2003**, *24*, 207.
[5] F. Cellesi, N. Tirelli, *J. Mater. Sci. -Mater. Med.* **2005**, *16*, 559.
[6] G. L. Fiszman, A. L. Karara, L. M. E. Finocchiaro, G. C. Glikin, *EJB Electr. J. Biotechnol.* **2002**, 5.
[7] T. I. Klokk, J. E. Melvik, *J. Microencapsulation* **2002**, *19*, 415.
[8] S. Koch, C. Schwinger, J. Kressler, C. Heinzen, N. G. Rainov, *J. Microencapsulation* **2003**, *20*, 303.
[9] D. Serp, E. Cantana, C. Heinzen, U. v. Stockar, I. Marison, *Biotechnol. Bioeng.* **2000**, *70*, 41.
[10] B. C. Larisch, D. Poncelet, C. P. Champagne, R. J. Neufeld, *J. Microencapsulation* **1994**, *11*, 189.
[11] L. Martin-Banderas, M. Flores-Mosquera, P. Riesco-Chueca, A. Rodriguez-Gil, A. Cebolla, S. Chavez, A. M. Ganan-Calvo, *Small* **2005**, *1*, 688.
[12] S. L. Anna, N. Bontoux, H. A. Stone, *Appl. Phys. Lett.* **2003**, *82*, 364.
[13] S. H. Huang, W. H. Tan, F. G. Tseng, S. Takeuchi, *J. Micromech. Microeng.* **2006**, *16*, 2336.
[14] L. Yobas, S. Martens, W. L. Ong, N. Ranganathan, *Lab on a Chip* **2006**, *6*, 1073.
[15] T. Thorsen, R. W. Roberts, F. H. Arnold, S. R. Quake, *Phys. Rev. Lett.* **2001**, *86*, 4163.
[16] H. Shintaku, T. Kuwabara, S. Kawano, T. Suzuki, I. Kanno, H. Kotera, *Microsyst. Technol.* **2007**, *13*, 951.
[17] V. L. Workman, S. B. Dunnett, P. Kille, D. D. Palmer, *Biomicrofluidics* **2007**, *1*, 014105.
[18] D. Poncelet, R. Lencki, C. Beaulieu, J. P. Halle, R. J. Neufeld, A. Fournier, *Appl. Microbiol. Biotechnol.* **1992**, *38*, 39.
[19] H. Zhang, E. Tumarkin, R. M. A. Sullan, G. C. Walker, E. Kumacheva, *Macromol. Rapid Commun.* **2007**, *28*, 527.
[20] K. S. Huang, T. H. Lai, Y. C. Lin, *Lab on a Chip* **2006**, *6*, 954.
[21] D. S. Zhao, B. Roy, M. T. McCormick, W. G. Kuhr, S. A. Brazill, *Lab on a Chip* **2003**, *3*, 93.
[22] D. B. Parekh, R. M. Katso, N. R. Leslie, C. P. Downes, K. J. Procyk, M. D. Waterfield, P. J. Parker, *Biochem. J.* **2000**, *352*, 425.
[23] J. Y. Park, B. P. Lim, K. Lee, Y. G. Kim, E. C. Jo, *Biotechnol. Bioeng.* **2006**, *94*, 416.
[24] L. A. Greene, A. S. Tischler, *Proceedings of the National Academy of Sciences of the United States of America* **1976**, *73*, 2424.
[25] A. M. Rokstad, S. Holtan, B. Strand, B. Steinkjer, L. Ryan, B. Kulseng, G. Skjak-Braek, T. Espevik, *Cell Transplant.* **2002**, *11*, 313.
[26] A. M. Rokstad, B. Strand, K. Rian, B. Steinkjer, B. Kulseng, G. Skjak-Braek, T. Espevik, *Cell Transplant.* **2003**, *12*, 351.
[27] T. Roberts, U. De Boni, M. V. Sefton, *Biomaterials* **1996**, *17*, 267.

Macromol. Rapid Commun. **2008**, *29*, 165–170

Macromolecular Journals

DOI: 10.1002/marc.200700641